The Dissertation Committee for Sheryl Lynn Wiskur Certifies that this is the approved version of the following dissertation:

Boronic Acid and Guanidinium Based Synthetic Receptors: New Applications in Differential Sensing

Committee:

_____

Eric V. Anslyn, Supervisor

_____

Brent L. Iverson

_____

Philip D. Magnus

_____

Jason B. Shear

_____

Charles B. Mullins

Boronic Acid and Guanidinium Based Synthetic Receptors: New Applications in Differential Sensing

by

Sheryl Lynn Wiskur, B. S.

Dissertation

Presented to the Faculty of the Graduate School of

The University of Texas at Austin

in Partial Fulfillment

of the Requirements

for the Degree of

Doctor of Philosophy

The University of Texas at Austin

May, 2003

Dedication

I would like to dedicate this to my family and friends

who have given me so much love and support.

Thank you.

Acknowledgements

It has been a long and difficult road getting this far in my education, but I could not have done it alone. There are many people that have helped me along the way with their love and support including family, friends, and teachers.

First and most importantly, I would like to acknowledge my mom and dad. Thank you for always being there for me. You have given me so much over the years, with encouragement, love, and financial support. (How much do I owe now?) I hope to one day follow in your footsteps as a parent.

As for Keith, I could not have asked for a better big brother. You have always watched out for me and let me tag along on many adventures. Thank you. I'm glad you now have Pam to watch over you.

I never could have made it through graduate school without the great friends I met here at UT. Thank you Mary Jane, Theo, Suzy, and John, for laughing with me, letting me cry on your shoulders, and just being my friends. You will always mean a lot to me.

Finally, thank you Eric for believing in me, even when I didn't believe in myself. I have learned so much from you, I hope that I continue to use this knowledge and make you proud.

Boronic Acid and Guanidinium Based Synthetic Receptors: New Applications in Differential Sensing

Publication No._____

Sheryl Lynn Wiskur, Ph. D.

The University of Texas at Austin, 2003

Supervisor: Eric V. Anslyn

In the field of supramolecular chemistry a common goal is to design a receptor that is highly selective for a targeted analyte. While this is a worthwhile goal, many of these synthetic receptors are less selective than their natural counterparts such as enzymes or antibodies. Many aspects of the work shown herein demonstrate that these less selective synthetic receptors are still useful chemosensors. Just as Nature utilizes differential receptors in our sense of taste and smell, synthetic sensor arrays can be developed to achieve similar results.

Chapter 1 is an overview of the development of a sensor. It begins with the aspects of binding carboxylates and diols, specifically by guanidiniums and boronic acids. Next, signaling motifs of a sensor are discussed, leading to the advantages of using an indicator displacement assay. Finally, differential sensors

are discussed, introducing the idea of incorporating non-selective synthetic sensors for the detection of multiple analytes with the use of pattern recognition.

Chapter 2 discusses the use of non-selective synthetic receptors in a number of sensing schemes. First a receptor was used to bind a class of age related analytes found in scotch whiskies. A correlation was found between the age of the scotch and the sensing ensemble's response to the beverage. In another sensing application, a high degree of selectivity was achieved by using two receptors and two indicators together in solution. Due to the differential response of the receptors to the indicators and the guests, the simultaneous quantification of tartrate and malate was achieved with the aid of pattern recognition. Finally, initial efforts were put forth for incorporating the receptor into a differential sensing array by immobilizing the receptor on a solid support. The selectivity of the receptor was investigated, showing that the receptor still had a higher affinity for tartrate over malate.

Chapter 3 investigated the thermodynamics of guanidiniums and boronic acids binding carboxylates and diols, respectively. Four hosts were investigated with a variety of guests. The association constants were determined through UV/vis analysis, while the entropy and enthalpy were determined with isothermal titration calorimetry. The binding of boronic acids to more than just aliphatic diols was also investigated.

Chapter 4 discussed the development of new sensor for catechol containing analytes. The sensor's design is based on iron binding siderophores.

The iron is both the binding site and the signaling motif for the sensor. Upon addition of catechol guests, a signal modulation did occur.

Table of Contents

List of Tables

List of Figures

List of Schemes

Chapter 1: Introduction and Background

1.0   INTRODUCTION

One goal of supramolecular chemistry is to selectively bind a target molecule by the rational design of a synthetic receptor.[1] The targets often include guests such as saccharides,[2] natural products,[3-5] metals,[6,7] and ions.[8-10] The ultimate goal is to achieve the selectivity and affinity of natural receptors such as enzymes and antibodies. Some excellent selectivities can indeed be achieved with synthetic systems.[4,5,7,8,11,12] Although this is a very worthwhile endeavor that our group[13-18] and many others are pursuing,[3,4,9,19] it is still true that the relative simplicity of synthetic receptors render most of these less selective than their natural counterparts. However, this lack of selectivity can, for some applications, still be very useful, as Nature has proven in a sensing method for multiple analytes. Our sense of taste is achieved through the combination of differential or non-specific receptors and pattern recognition. Detection of complex mixtures of analytes can be obtained through the use of sensors designed to bind classes of analytes instead of designing sensors for each analyte. The fingerprint of the data obtained can then be deciphered with pattern recognition to determine the composition of the mixture.   To mimic Nature through the development of differential sensors, there first must be an understanding of molecular recognition

and single analyte detection. Sensor arrays can then be developed as a powerful tool for multi-analyte detection.

1.1   MOLECULAR RECOGNITION

Supramolecular chemistry is a field that was designed to study the events of natural processes such as an enzyme binding a substrate. Model compounds are synthesized that are much simpler than their natural counterparts and their interactions with various guest molecules are investigated. The first macromolecules were crown ethers and cryptands, which were determined to bind metal cations. That was over forty years ago. Since then, the field has undergone extensive growth and chemists have obtained a wealth of knowledge from this research. Many receptors have been explored and many guests have been targeted. These guests include saccharides, natural products, metals, ions, and biomolecules.

The nature of these host/guest interactions comes from a concept termed molecular recognition. This is the study of two molecules and the specific nature of their interactions. In other words, the forces that allow two molecules to interact or bind are investigated, such as an enzyme binding a substrate in the active site. This is generally accomplished through non-covalent interactions. To understand molecular recognition, a basic knowledge of the properties of molecular interactions, or the forces that are responsible for attraction must be understood. The most important ones are ion pairing, hydrogen bonding, van der

Waals attractions, and metal-ligand interactions. Many of these non-covalent interactions are a part of biological processes and structure, where several interactions are used in collaboration to complete the job. For example, the structure and stability of proteins rely on hydrogen bonding between the carbonyl and the N-H groups in the polypeptide backbone, electrostatic interactions between charged groups, and hydrophobic interactions of neutral non-polar amino acids. Generally, host/guest complexes also rely on a combination of these forces to obtain tight associations.

The binding of a guest to a receptor or host is dependent on many factors. These include the size and shape of the host and guest, whether the binding site is complementary, and what the solvent is. All of these aspects should be considered in the design of a receptor. Again, many of the ideas are derived from natural systems such as enzymes. For example, the functional groups in enzyme binding pockets are known to be cooperative due to the preorganization of the cavity. The exclusion of water from the cavity also plays a role in many enzyme active sites, derived from the use of hydrophobic amino acids in key positions.

1.2 PREORGANIZATION OF THE SCAFFOLD

The selectivity and affinity of synthetic hosts are commonly altered by carefully choosing a scaffold upon which to append binding moieties to create a binding pocket. A pocket that is complimentary in size and shape to the guest will improve the selectivity.[20-22] With regards to the affinity, higher binding

3

constants are commonly achieved by preorganizing the functional groups at the binding site.[20-22] Cram stated "the more highly hosts and guests are preorganized for binding and low solvation prior to their complexation, the more stable will be their complexes."[20]

The ability of crown ethers to bind alkali and alkali earth metals was first discovered by C. J. Pederson.[22] This discovery came about with the observation that compound **1.1**, the first of many crown ethers, became soluble in methanol upon the addition of sodium hydroxide. Since the crown ether had no acidic groups this seemed like a strange phenomenon. Soon Pederson realized that the increased solubility was not due to the base, but due to the sodium salt. In fact, any sodium salt such as sodium chloride also increased the solubility. It was later discovered that the crown ether was complexing the cation through interactions between the positive charge of the cation and the negative dipole charges on the oxygens. The crown ethers were soon termed phase transfer catalysts, due to their ability to catalyze solid to liquid transfers. In order to easily name the crowns, Pedersen invented a system of shorthand. Compound **1.1** was named dibenzo-18-crown-6, where the eighteen refers to the number of atoms in the ring and the six refers to the number of heteroatoms. Upon further studies of different sized macrocycles, it was determined that each cation had an optimum sized crown or host. Sodium prefers crowns between 15-crown-5 and 18-crown-6, while potassium is bound best by 18-crown-6. Cesium prefers a little larger macrocycle, such as 18-crown-6 or 21-crown-7. Sandwich type complexes tend

to form when the crown and the cation are not the ideal size for one another. The term sandwich refers to two crowns binding one cation.
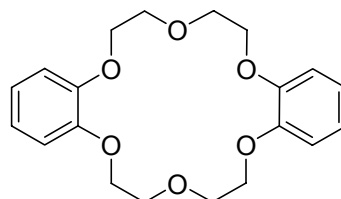
1.1

Strong complexation of the cation based on preorganization of the crown ether was used as the basis to further supramolecular chemistry with the development of cryptands by Lehn[23] and cavitands by Cram.[24] Both systems rely on the importance of the preorganization of the host and the binding through non-covalent forces. Over the years, many different preorganized scaffolds have been designed and utilized in host/guest chemistry with great success, some of which will be discussed later in the chapter.

1.3 SOLVENT EFFECTS

Many aspects of the design of the receptor need to be considered, but external factors must also be contemplated, such as solvent. Unlike biological systems, synthetic receptors can take advantage of varying the solvent systems to modify or enhance intermolecular interactions, such as hydrogen bonding or charge pairing.[15,25,26] Such interactions can be enhanced by replacing solvents such as water and methanol with non-hydrogen bonding solvents such as DMSO

or chloroform, that have lower dielectric constants. Even subtle differences such as increasing the methanol concentration in an aqueous solution can enhance charge pairing interactions. Therefore, the affinity constants can be tuned to work in a desired concentration range.

Hamilton and coworkers investigated the role of the solvent in host/guest association,[27] specifically the recognition of dicarboxylates by bis-guanidinium receptors. They studied the association and thermodynamics of binding of **1.2** with **1.3** in increasingly competitive solvents, starting with dimethyl sulfoxide (DMSO) then moving to methanol and finally adding water. The association constants were determined to decrease upon introduction of higher concentrations of the stronger hydrogen bonding solvent, resulting in an increased solvation of both host and guest. The association constant was determined to be near 55,000 M^{-1} in DMSO with a dramatic decrease to 230 M^{-1} in 50% water in methanol.

1.2   **1.3**
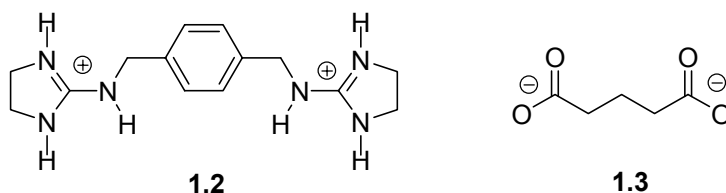
1.4   MOLECULAR RECOGNITION OF CARBOXYLATES

In designing a receptor, functional groups must be incorporated that are complementary to the functional groups on the guest that is being targeted. In our group, many of these guests are comprised of anionic groups such as

carboxylates. There are numerous examples of receptors or sensors that have been developed for this purpose. Anions such as carboxylates are often bound to synthetic receptors via hydrogen bonding or charge pairing interactions, where ammonium and guanidinium[28] groups are commonly used at the binding pocket. The most favorable binding motifs of carboxylates/carboxylic acids are shown in Eq. 1.1. Ammonium groups have a high localization of charge,[29] but their geometry is not as conducive for hydrogen bonding to carboxylates (Eq. 1.1A). The charge pairing interactions of guanidinium groups are more diffuse, but they also have a more favorable geometry for binding carboxylates and remain protonated over a higher pH range (Eq. 1.1B).[30] Neutral binding sites are also

Eq. 1.1

X = O or S
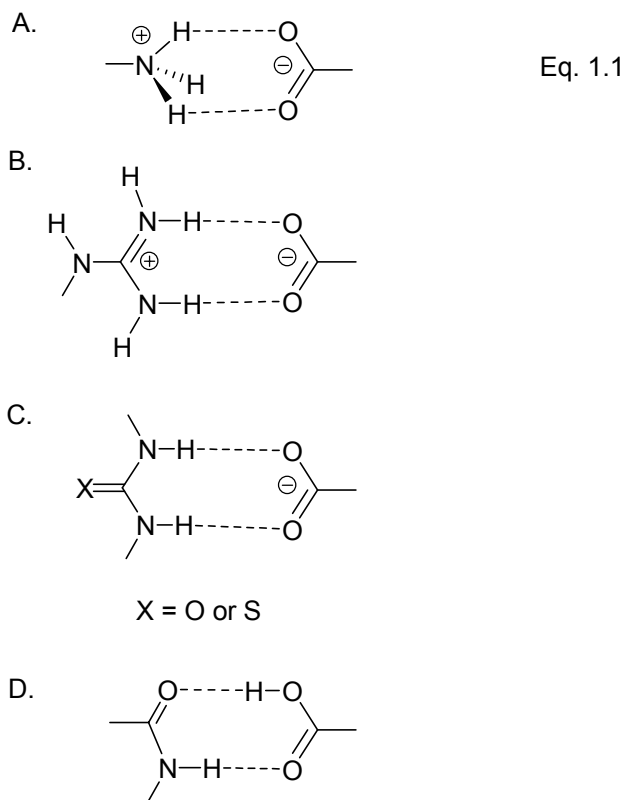
used, such as ureas, thioureas, and amides.[28] Although they lack the electrostatic component, they have been shown to form strong associations with carboxylates through bidentate hydrogen bonding motifs (Eq. 1.1C and D).

1.4.1 Ammoniums

The interaction of polyammonium salts with carboxylates was studied by Kimura and coworkers.[31] They synthesized a series of polyammonium macrocycles **1.4-1.6**, and found that at neutral pH they were triply protonated. All three macrocycles formed complexes with the tris-carboxylate analyte citrate. Association constants of 55-1000 M^{-1} were obtained where the host with the larger ring had the strongest association. The macrocycles **1.5** and **1.6** were also shown to bind bis-carboxylates that had short linkages between the carboxylates, such as succinate and malonate, but the binding constants were decreased in relation to citrate. Longer bis-carboxylates such as glutarate and aspartate did not bind. When a similar host was studied that was acyclic, binding of all the guests was negligible showing that the preorganization of the amines in the cavity enhances binding.

| **1.4** | **1.5** | **1.6** |

8
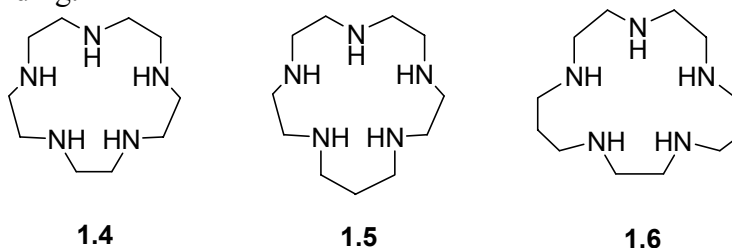
1.4.2 Ureas, Thioureas, and Amides

Strong associations can be achieved between carboxylates and receptors that contain ureas, thioureas, or amide binding sites. Without the electrostatic component, the studies are generally done in non protic solvents such as dimethyl sulfoxide or chloroform to enhance hydrogen bonding. Morán and coworkers developed a receptor for carboxylates[32] that is composed of two chromenones linked by a urea. The host binds through hydrogen bonding from a combination of urea and amide hydrogens. Receptor **1.7** bound benzoic acid in DMSO through four hydrogen bonds (Scheme 1.1) to achieve an association constant of 1.5×10^4 M^{-1} (^{1}H NMR). In a similar receptor which lacked one of the chromenones, binding was greatly reduced even though only one hydrogen bond was removed. The association constant was determined to be 20 M^{-1} in DMSO.

Scheme 1.1

1.7
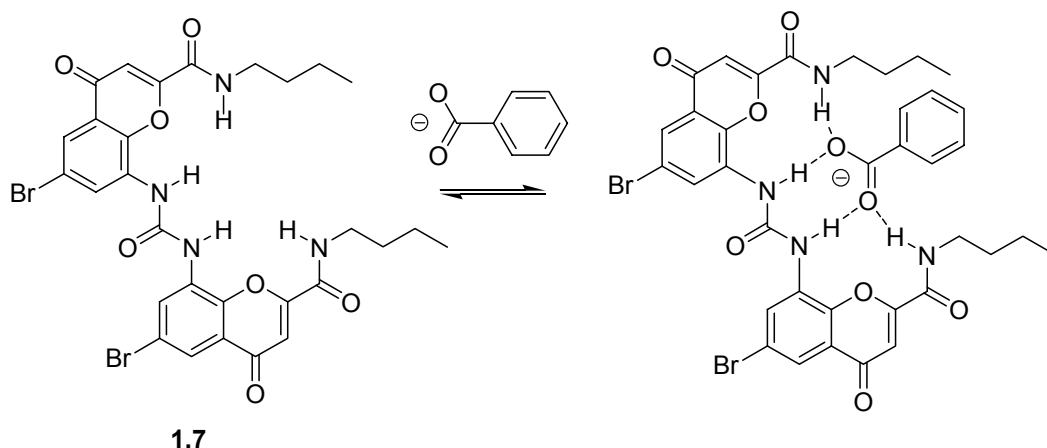
CPK models suggested that the urea carbonyl was twisted out of the plane of the chromenone ring due to steric hinderance of a hydrogen on the aromatic ring with the carbonyl. This may have prevented the formation of linear hydrogen bonds compared to the added rigidity of making four hydrogen bonds in **1.7**.

1.4.3 Guanidiniums

Schmidtchen and co-workers have extensively studied the thermodynamics of anion recognition by guanidiniums.[33] They have studied the role of solvent, counter anions, and the functionality around the binding site.[34] The study of the association of bicyclic guanidinium structure **1.8** with benzoic acid was done by isothermal titration calorimetry (ITC) to determine the counter anion's effect on binding. The binding constant of **1.8** to the carboxylate was greatly affected by the guanidinium's counter ion in acetonitrile. The larger binding constants came from the larger, less hydrogen-bonding anions. Both enthalpy and entropy were determined to be favorable. Smaller anions resulted in an increase in entropy, due to more solvent molecules being released from the binding site. The exothermic component also decreased with a decrease in the counter anion size, indicating that the anion was competing with the guest for the guanidinium.
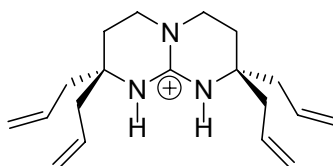
1.8

Hamilton[27,35] has also performed research into the thermodynamics of guanidinium/carboxylate interactions. In one study, the binding of tetrabutylammonium acetate to a series of guanidinium derivatives was investigated by ITC. [25] The association of the bicyclic guanidinium (**1.9**) with acetate had a reasonable affinity in DMSO, but the presence of the methyl groups in **1.10** and **1.11** completely inhibited binding, as found by ITC and ^{1}H NMR, showing the importance of hydrogen bonding for complexation. The thermodynamic data showed that the guanidinium/carboxylate interaction was favorable with the binding being exothermic, with positive entropy. Therefore, the binding was attributed predominately to hydrogen bonding interactions, and the affinities were again reduced when the counter ion was changed from iodide or tetraphenyl borate to chloride.
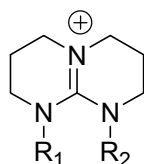
1.9 R$_1$=H, R$_2$=H
1.10 R$_1$=CH$_3$, R$_2$=H
1.11 R$_1$=CH$_3$, R$_2$=CH$_3$

1.5   MOLECULAR RECOGNITION OF DIOLS

As for the binding of diols, there have been a variety of studies aimed at targeting this functional group, primarily concerned with sugar recognition.[36]

Carbohydrates are one of the most abundant organic molecules found in Nature. Their functions are numerous including energy, structure, and intercellular communication. For example, ribofuranosides are a vital component of RNA and ATP, while cell surface oligosaccharides are involved in cell-recognition processes. The understanding of the molecular recognition of sugars is an important investigation that many supramolecular chemists are pursuing. There have been numerous receptors and sensors developed for the binding of saccharides. Many of these receptors were designed to form neutral hydrogen bonds with sugar molecules, since they possess more hydrogen-bonding functional groups per carbon atom, than any other natural product.

1.5.1 Hydrogen Bonding Receptors in Organic Solvents

Some artificial receptors are designed to form neutral hydrogen bonds to the hydroxyl groups of the sugar with amide NH or alcohol groups, patterned after protein/carbohydrate interactions. In biotic binding clefts, water is generally excluded in order to eliminate competing hydrogen bonds; therefore, artificial receptors are generally studied in aprotic solvents to achieve the same effect. Polypyridine-macrocyclic receptors were designed for the binding of glucopyranosides by Inouye and coworkers.[37] Amides as well as pyridines were incorporated in the receptor for hydrogen bonding to the saccharides. Receptor **1.12** was determined to have an affinity with *n*-octyl β-(D)-glucopyranoside of 170 M^{-1} (^{1}H NMR, $CDCl_3$). It was theorized that the low affinity of the acyclic

system resulted from the loss of energy through rotation about the pyridine-pyridine axis to bind to the saccharide. Therefore the macrocyclic receptor **1.13** was synthesized to create a preorganized cavity. The resulting complexes were determined to have an association constant near 5600 M^{-1} for glucopyranoside, with selectivity over galatopyranoside. The selectivity is obtained due to the difference of one hydroxyl group between the sugars (axial versus equatorial). Glucopyranoside is able to efficiently make more hydrogen bonds when bound than the galatopyranoside with its one axial hydroxyl group.

1.12   **1.13**
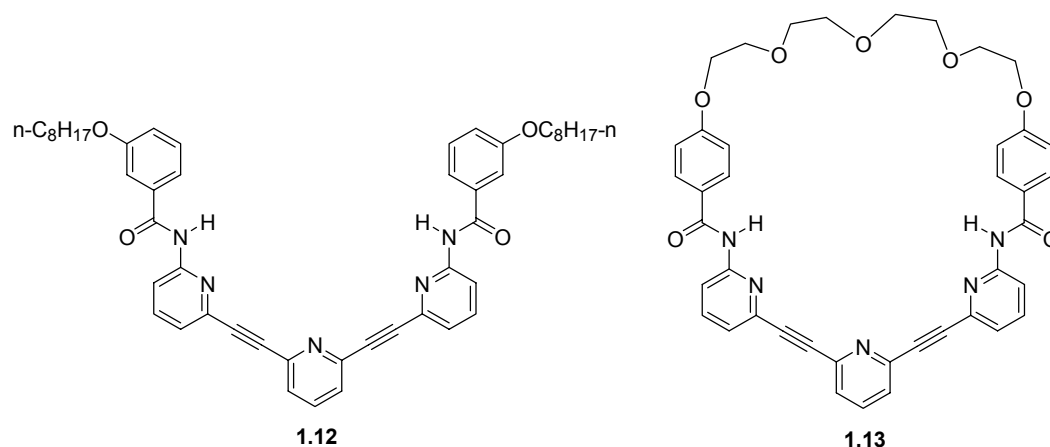
1.5.2   Saccharide Binding Receptors in Water

There is also an interest in binding diols, or mainly saccharides, in water. The reason monosaccharides are so difficult to bind in water is because the receptor must exclude water from its binding pocket in order to bind its guest. Yet saccharides resemble a water cluster due to the large number of hydroxyl

13

groups making it difficult for the receptor to distinguish between the saccharide and the water. Binding of monosaccharides in water has been accomplished, but very low association constants are generally the result; therefore many others have targeted functionalized substrates that are easier to bind such as saccharides with hydrophobic surfaces.[36,38] One successful system that bound unfunctionalized saccharides in water was synthesized by Kral, Schmidtchen, and coworkers.[39] The macrocyclic porphyrin compound **1.14** was designed to sandwich saccharides between the two hydrophobic porphyrins, with the tertiary amides assisting with the formation of hydrogen bonds. Association constants were determined by UV/visible titrations and **1.14** was determined to have the strongest affinity for maltotriose (5.5×10^4 M^{-1}), a trisaccharide of glucose. The affinities decrease with the di- and monosaccharides, but were still respectable in water. For example, glucose bound with an affinity of 1.3×10^3 M^{-1} while a disaccharide such as lactose had an affinity of 2.8×10^4 M^{-1}. It was suggested that the high association constants were derived from the complementarity of the host and guest in regards to the hydrophobic and hydrophilic portions of each.
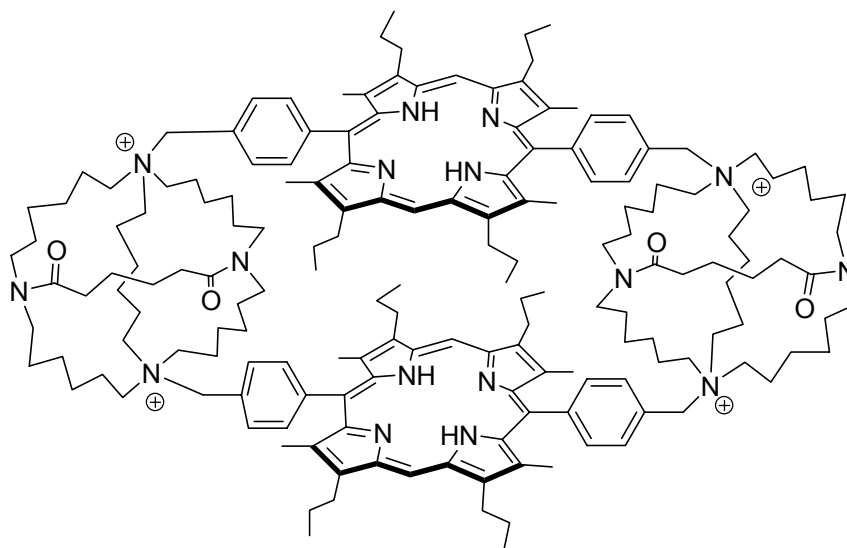
1.14

1.5.3 Boronic Acids

Molecular recognition has traditionally been focused on the use of non-covalent bonding interactions for the study of host/guest interactions, such as hydrogen bonding and charge pairing discussed previously. More recently, the use of covalent interactions has been explored in this area. The use of boronic acids has helped to advance the molecular recognition of sugars in aqueous media, by forming reversible covalent linkages to 1, 2- and 1, 3-diols (Scheme 1.2, **B** going to **D**). Due to their ability to form boronate esters,[40] they have been extensively studied for the binding of saccharides, and are routinely incorporated into synthetic receptors.[41,42] The formation of the boronate ester is faster when the boron is tetrahedral, which happens at high pH. Scheme 1.2 shows the equilibrium of phenylboronic acid with a diol in aqueous media. At low pH, the

15

Scheme 1.2
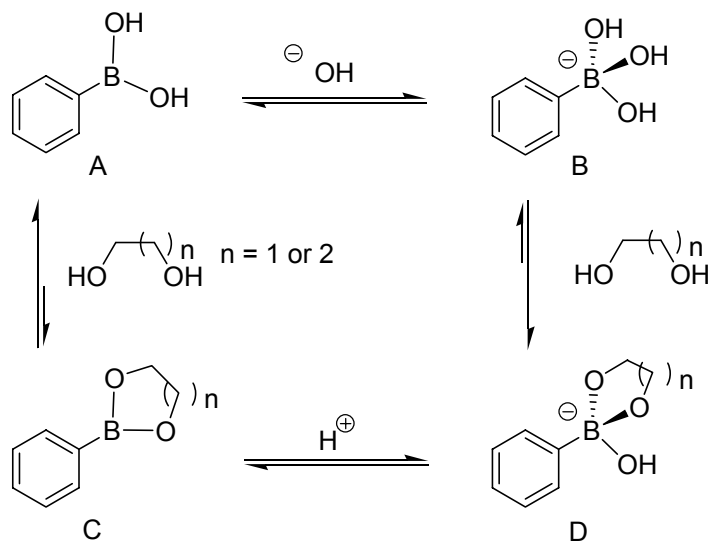
boronic acid is trigonal planar (**A**), therefore upon an increase in pH, the boron becomes tetrahedral (**B**) as the water that is coordinated to the boron's empty p orbital is deprotonated ($pK_a = 8.8$).[43] Addition of a diol results in the formation of a boronate ester (**D**) which in turn enhances the Lewis acidity of the boron. This increase in Lewis acidity results in a lowering of the pK_a of the bound water.[42] When the pH is lowered below the pK_a of the boronate ester, the boron again becomes trigonal planar (**C**) where the hybridization of the boron is no longer conducive for binding, resulting in a shift in equilibrium to **A**.

A fluorescent sensor of saccharides developed by Czarnik and coworkers helps to illustrate the increased Lewis acidity of the boronic acid upon complexation of a diol. Fluorescent-pH titrations of **1.15** were performed varying the amount of fructose present from 0-100 mM. When the boron is tetrahedral, the fluorescence is quenched, resulting in a decrease in signal, which happens at

high pH. Yet, in the presence of increasing amounts of fructose, the quenching occurrs at lower and lower pH values, indicating that the tetrahedral boron was forming. It was found that the pK_a of the water bound to the boronate ester was 5.9 in the presence of fructose compared to 8.8 of the uncomplexed boronic acid. An association constant of 270 M^{-1} was determined, by the titration of fructose into a solution of **1.15** in water at pH 7.4, where the greatest signal modulation occurred.
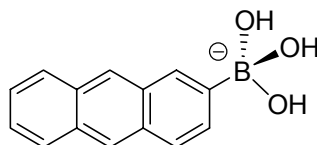
1.15

Wang and coworkers have studied the interactions of boronic acids and diols in detail,[44] using phenyl boronic acid and Alizarin Red S as a fluorescent reporter. They have studied buffer effects, pH effects, and overall affinities of phenyl boronic acid for different diols, showing that many common beliefs may actually be misperceptions. For example, it has been stated in the literature that binding constants of these systems are buffer-independent.[45] This work shows that the binding constant is dependent on the type of buffer, and in the case of phosphate, the concentration as well. It is also shown that phenyl boronic acid has a stronger affinity for catechol than other 1,2-alkane diols, and all of their binding constants were pH dependent.

Since it is not always desirable to work at high pH, Wulff[46] demonstrated a method of binding diols at neutral pH. His discovery came about while he was investigating new binding sites for affinity chromatography of diols, alcohols, and amines. Polymers were available that bound diols with the tetrahedral boron discussed above, but some of the targeted analytes were labile in basic solutions. Wulff discovered that a tertiary amine adjacent to the boron allows for the formation of boronate esters (**G**) at neutral pH. The pK_a of the ammonium **E** was determined to be 5.2, which allows for a boron-nitrogen complexation between the lone pair of the nitrogen and the empty *p* orbital of the boron. This results in formation of a tetrahedral boron (**F**) at neutral pH with efficient boronate ester formation, also at neutral pH (Scheme 1.3).

Scheme 1.3
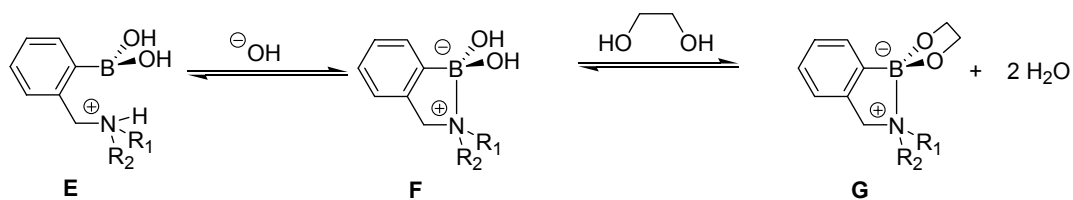
Shinkai and coworkers have done extensive research into the binding and selectivity of sugars with the amine complexed boronic acids. The fluorescent photoinduced electron transfer (PET) (Section 1.6.1) sensor **1.16**,[47] which has only one boronic acid for complexing saccharides, was determined to be selective for fructose. Yet, when a second boronic acid is incorporated into the scaffold, the host (**1.17**) now shows a preference for glucose.[48] This shows that the spatial

18

orientation of the binding moieties has a significant affect on determining the selectivity of the receptor.
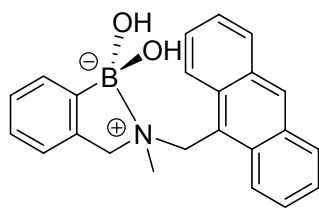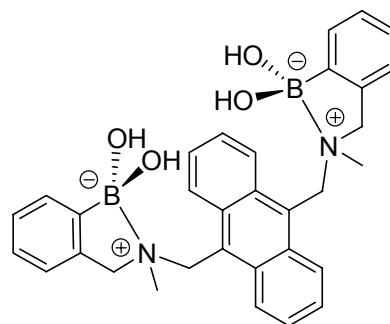
1.16   1.17

1.6   DEVELOPMENT OF A SENSOR

So far, the development of receptors for molecular recognition has only been discussed. In order to detect analytes, a way to signal their presence needs to be incorporated. Since many analytes of interest do not include their own chromophore or fluorophore, and detecting them without chemical modification is preferred, the development of receptors into sensors needs to be investigated. A sensor is a device that upon a specific interaction yields a measurable response. Many scientists in the past have viewed sensors as macroscopic devices such as pH meters, where all the components are contained within one device. Yet, there are others that consider engineered molecules as sensors or chemosensors. In order to make a useful chemosensor, a compound must contain a "binding site" and a "signaling site," such as a chromophore, fluorophore, or redox active center.

Further, a mechanism to communicate between them must exist.[49] For the most part, these synthetic sensors possess covalent links between the fluorophore or chromophore and the binding site. Traditionally, when an analyte associates with the binding site, a microenvironment modulation occurs that perturbs the properties of the signaling site (Scheme 1.4). From changes in the spectroscopic or redox properties, binding constants and stoichiometries can be obtained.[50] With organic structures, absorbance or fluorescence changes are commonly observed. A change in signal upon binding can result from PET,[51,52] charge transfer, fluorescence resonance energy transfer (FRET),[53] or simple microenvironment changes such as those that arise from changes in local ionic strength or pH.

Scheme 1.4
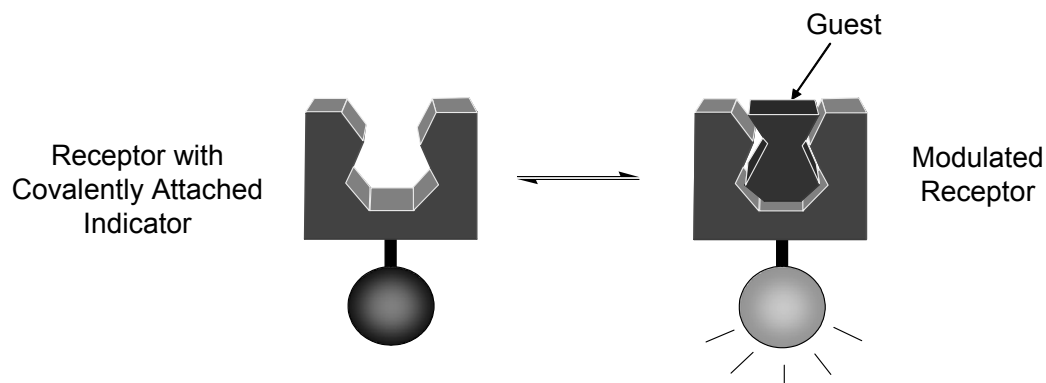
Colorimetric versus fluorimetric signaling both have distinct advantages and disadvantages. Colorimetric has the advantage of being detectable by the

naked eye, such as a color change, or the appearance or disappearance of color. For example, the pH indicator phenolphthalein switches between colorless and pink at the appropriate concentration of protons. The disadvantages for colorimetric versus fluorescence are that higher concentrations of receptor and analyte are needed to obtain accurate absorbance measurements. Fluorescence has the advantage of being more sensitive, due to the low background, and therefore lower concentrations of analyte can be detected. The problems associated with fluorescence are photobleaching of the fluorophore, stability of the fluorophore, and sensitivity to the solution environment including pH, polarity, and temperature.

1.6.1   Photoinduced Electron Transfer (PET)

Photoinduced electron transfer (PET)[52] is a method of signaling for a sensor that is like a switch, the fluorescence is either "on" or "off." This generally entails a fluorophore-spacer-receptor system, where the binding event triggers the switch. A popular example of this utilizes the fluorophore with an adjacent amine. In the absence of an analyte, the lone pair of the amine quenches the fluorescence of the fluorophore through PET. Upon binding of an analyte, the lone pair is no longer available for electron transfer due to association with the analyte and thus the fluorescence is regenerated. This form of signaling, where the sensor is "off" and the analyte switches the fluorescence "on," is powerful in relation to the reverse method. The difference is the background when the sensor

is uncomplexed. The "off-on" method essentially starts at zero and grows in intensity, while the "on-off" situation already has a strong signal and the presence of analyte just decreases the signal. A large number of sensors have been constructed based upon this principle.[47,49,54]

There has been a large development of PET sensors over the years for a variety of different analytes, with cations being one group of targets. Sensor **1.18** was developed for the selective detection of lithium.[55] The amino-crown binding site quenches the fluorescence of the naphthalenes, until the addition of lithium switches the fluorescence on due to the lone pairs of the amine complexing the cation, resulting in a PET lithium cation sensor. In non aqueous systems, **1.18** had a high selectivity for lithium over other cations such as sodium, potassium, calcium, and magnesium.

1.18
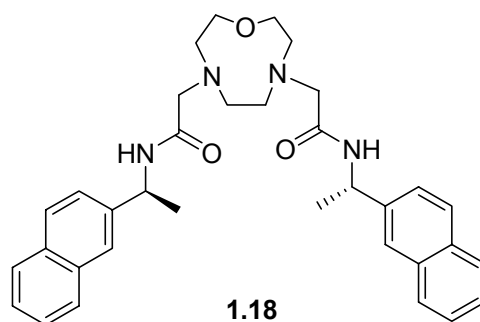
1.6.2 Fluorescence Resonance Energy Transfer (FRET)

Another method of signaling that can be incorporated into sensors is a technique termed fluorescence resonance energy transfer (FRET).[56] The

22

principles of this technique have been widely used in biochemical settings and it involves the use of two fluorophores. The FRET pair has overlapping excitation and emission bands so that energy can be exchanged between them. When radiation is absorbed by one fluorophore (the donor), in theory it could emit a photon, but when the second fluorophore is near, it transfers its energy to the second molecule or the acceptor. This molecule subsequently fluoresces, resulting in a large shift in excitation versus emission wavelengths. The efficiency of the transfer is greatly affected by the distance between the two fluorophores. Therefore, when they are separated, FRET no longer occurs, and the excitation of the acceptor results in straight emission, with no transfer of energy.

James and coworkers developed a bis-boronic acid, bis-fluorophore receptor (**1.19**) that was selective for saccharides.[57] Phenanthrene and pyrene were chosen as the donor and acceptor respectively since the emission wavelength of phenanthrene overlaps with the excitation wavelength of pyrene for fluorescence energy transfer in the excited state. Excimer emission was observed with **1.19** free in solution due to π-π stacking. Upon titration of **1.19** with different saccharides, FRET emission was viewed with an increase in fluorescence at 417 nm, the emission wavelength of pyrene through the excitation of phenanthrene (299 nm). The excimer emission also decreased upon addition of the saccharides. It was determined that **1.19** had the strongest affinity for glucose relative to galactose and fructose, by a factor of two. Due to the relative intensities of the host/guest complexes, it was determined that the energy transfer

from donor to acceptor is more efficient in the rigid **1.19**/glucose complex relative to the more flexible **1.19**/fructose complex.

1.19
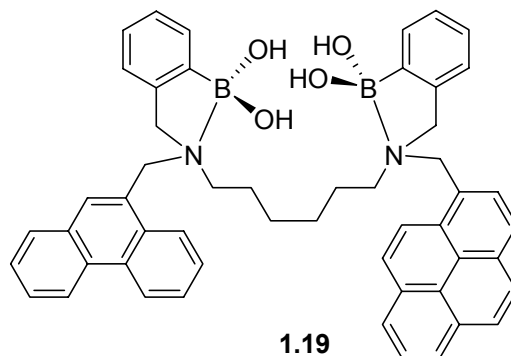
1.6.3   pH

Another common method of indicating binding is the use of an indicator that is sensitive to changes in pH. A frequently used indicator that is used to detect changes in pH is phenolphthalein. When the indicator is protonated, it is colorless, but in solutions that are above a pH of 8 or 9, the solution becomes pink. Incorporating a signaling site like this with a binding site allows for detection of microenvironment changes upon complexation of an analyte.

An example of a sensor that uses a pH sensitive indicator to modulate absorbance upon complexation with a guest is **1.20**, an alizarin yellow-modified β-cyclodextrin (β-CD).[58] The cyclodextrin receptor is known to form inclusion complexes with organic guests in aqueous media.[59] In order to create a chemosensor for such entities, alizarin yellow, a pH indicator,[60] was covalently attached to a β-CD through an ethylenediamine linkage. In solution, the indicator

is partially incorporated within the CD cavity, protecting it from the aqueous environment. Upon inclusion of a guest such as 1-adamantanol (**1.21**), the indicator is displaced from the cavity and the pK_a values are shifted. This causes a change in the protonation state of the alizarin yellow and hence a change in the absorption spectrum. This example highlights a sensor with a fundamentally different signaling mechanism than sensors based upon PET. A displacement occurs that leads to a signal modulation, due to a change in protonation state of a pH indicator. In this kind of general scheme, one may ask, "why have any covalent attachment between the receptor and the reporter?" By eliminating several synthetic steps, the creation of chemosensors would then be more facile.

1.20   **1.21**
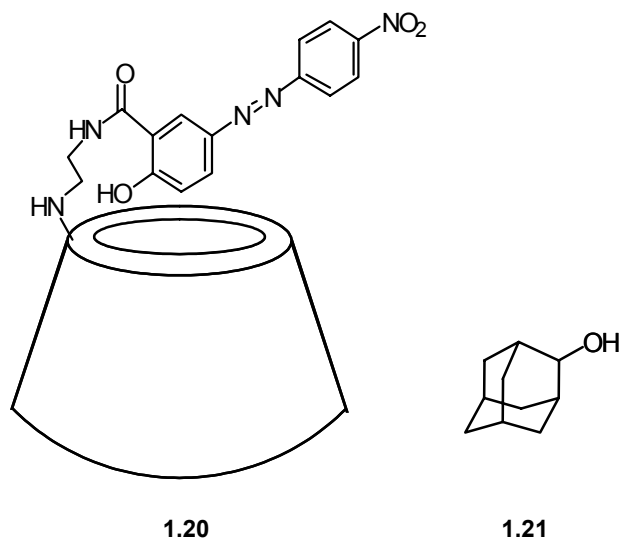
1.6.4 Dye Displacement Assay

An alternative method to a covalently attached chromophore or fluorophore is a competition between the indicator and the analyte for the binding pocket. This signaling mechanism is well precedented for the determination of association constants,[61] and works in a similar manner to many antibody-based biosensors in competitive immunoassays.[62] A solution containing the unlabeled antigen is added to the antibody receptor, which is associated with a tagged antigen. Upon displacement of the tagged antigen a signal modulation is observed. Although the method is easy and convenient, it has seen relatively little incorporation in the molecular recognition/supramolecular community. For the synthetic receptors, an indicator is displaced from the binding pocket upon addition of an analyte, causing a signal modulation (Scheme 1.5). This type of signaling protocol can be applied to most synthetic receptors. There are several

Scheme 1.5
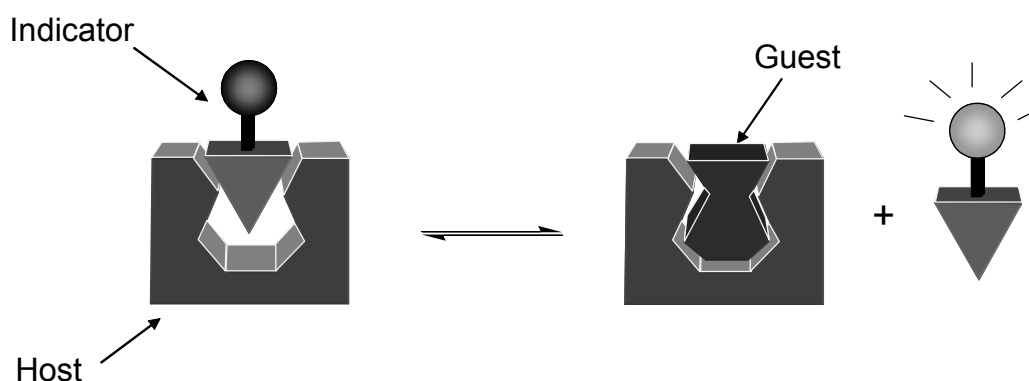
advantages to this method of signaling: 1) since the receptor is not covalently attached to the indicator, it is possible to change indicators at will, 2) no extra covalent bond architecture is required in the synthesis, allowing one to focus on the design of the host first, and choose an indicator later, and 3) it works well in both aqueous and organic solvents, and therefore one can tune the solvent system to obtain the desired K_a values of the indicator and analyte. The major disadvantage of this technique is that it is not amenable to imaging, such as tissue or whole cells, because the indicator is present everywhere in solution, not just isolated to the receptor.

1.6.4.1 Acetylcholine Sensors

Prior to our exploitation of this technique, few examples were found in the literature. One example was reported by Inouye[12] for the detection of acetylcholine (**1.22**) (Scheme 1.6). The resorcinal based calixarene **1.23** forms inclusion complexes with alkyl ammonium cations in an alkaline media through electrostatic and/or cation-π interactions. The indicator chosen was a pyrene-modified *N*-alkylpyridinium cation (**1.24**). When **1.24** was bound in the cavity of **1.23**, its orange fluorescence was quenched through PET from the anionic oxygen of **1.23**. Upon addition of **1.22** to the solution, a competition for the binding cavity occurred that led to the release of the fluorophore and the regeneration of fluorescence.

Scheme 1.6
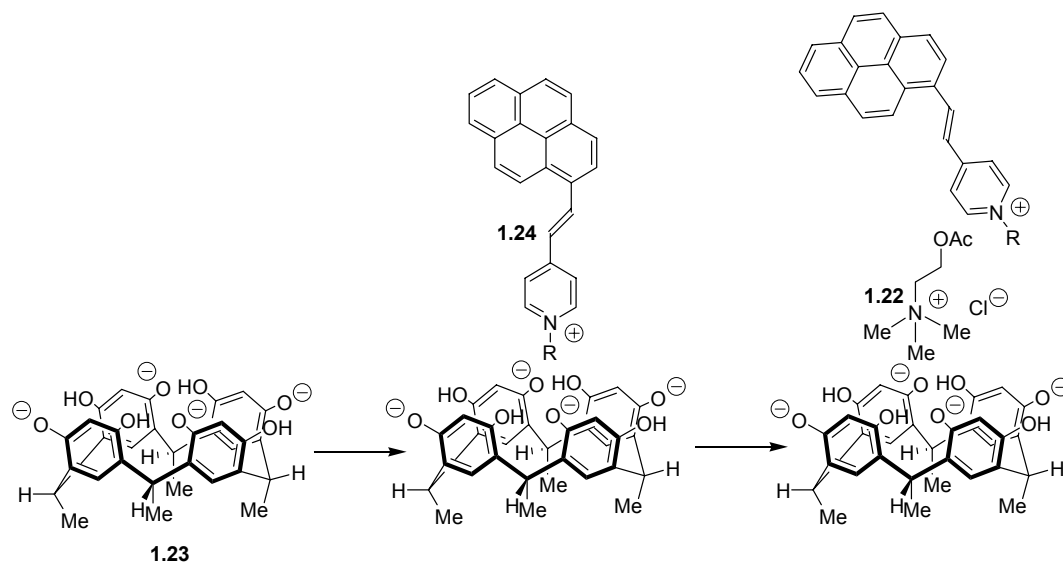
Inouye's system required strongly basic conditions to deprotonate four of the hydroxyl groups of **1.23**, which caused problems such as nucleophilic attack on the pyridinium and degradation of the acetylcholine. This prompted Shinkai[63] to investigate a way to monitor the presence of acetylcholine in a neutral environment. Calix[*n*]arene-*p*-sulfonates (*n* = 4 or 6) were chosen as the receptors (**1.25**) since they have a lower pK_a value making them anionic at neutral pH, and also form inclusion complexes with cationic guests through electrostatic and/or cation-π interactions. The fluorescence of **1.24** was quenched upon inclusion in this cavity, and was regenerated upon addition of **1.22**. Since these first few examples, other groups are beginning to exploit this signaling method.[64]

1.25
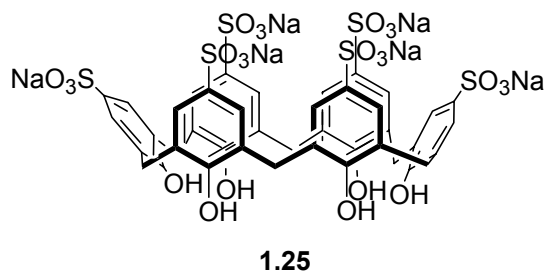
1.6.4.2 Citrate Sensor

Using an indicator displacement assay, our group developed a chemosensor for citrate (Scheme 1.7). The sensor consisted of an ensemble of the host molecule **1.26** and the indicator 5-carboxyfluorescein (**1.27**).[65] It was anticipated that this competition assay would be able to signal the presence of citrate in highly competitive media.

The design of **1.26** focused on a 1,3,5-trisubstituted-2,4,6-triethylbenzene scaffold incorporating three guanidinium recognition units. The six substituents point alternately up and down around the ring, thereby preorganizing the guanidinium binding sites on one face of the aromatic ring.[66] When the binding of citrate to a host lacking the ethyl groups was compared to **1.26**, the binding affinity dropped by a factor of two.[14] Since ammonium and guanidinium functionalities are commonly used for binding anions in aqueous media,[67,68] the two were contrasted to determine selectivity. The tris-guanidinium receptor was nearly three-fold better than the tris-ammonium receptor for binding citrate in water as determined by ^{1}H NMR.

29

Scheme 1.7
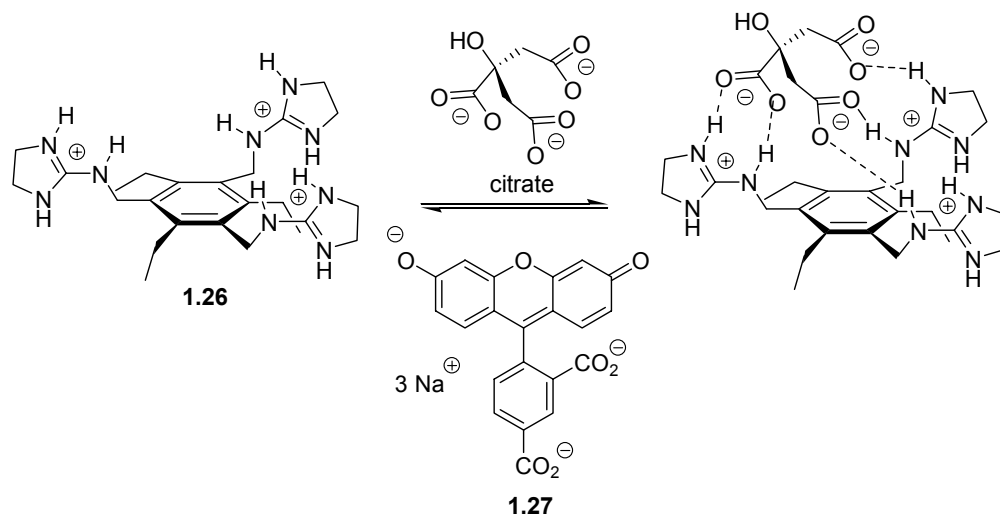
The fluorescent indicator **1.27** was chosen due to its similar characteristics to citrate (tris-anionic) and the fact that it is a pH indicator.[69]   Since the absorbance and fluorescence intensities of **1.27** are sensitive to changes in pH, it was expected that small microenvironment differences such as the binding cavity of **1.26** would induce these pH changes. Upon addition of **1.26** to a solution of **1.27** in a solvent mixture of methanol and water, the absorbance increased at λ_{max} 498 nm (Figure 1.1A) as more of the indicator became bound, inducing a microenvironment change. This was the expected modulation. The indicator is more highly ionized when bound in the cavity of **1.26**, which is associated with an increase in absorbance and emission intensity. When citrate was added to the solution of **1.26** and **1.27**, the absorbance decreased (Figure 1.1B) as **1.27** was displaced from the binding pocket. A binding constant of 2.9×10^5 M^{-1} was determined for **1.26**-citrate by UV/visible spectroscopy.[50]

30
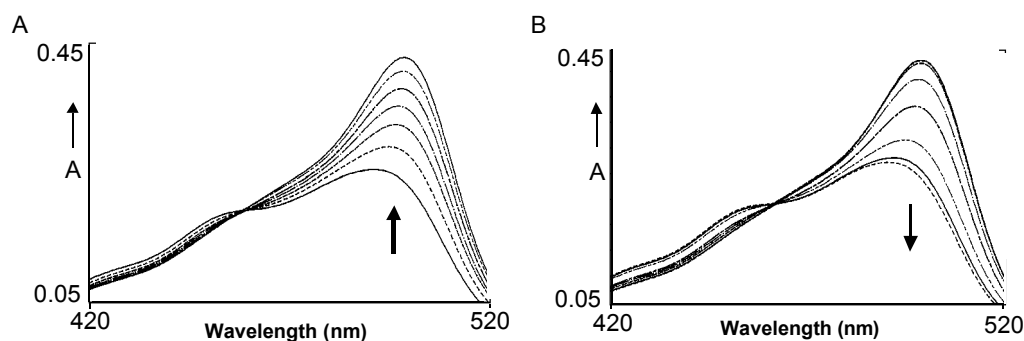
FIGURE 1.1. UV/VIS SPECTRUM FOR CITRATE SENSING ENSEMBLE. (A) The absorbance was measured as **1.26** was added to a solution of **1.27** at constant concentration. (B) The absorbance was measured as citrate was added to a solution of **1.26** and **1.27** at constant concentrations (25% water in methanol (v/v), 5 mM HEPES, pH 7.4).

Upon testing different solvent systems, a ratio of 25% water in methanol at a pH of 7.4 (4-(2-hydroxyethyl)-1-piperazineethanesulfonic acid (HEPES) buffer) was chosen. A stipulation in picking a buffer is that it should not inhibit the binding of the analyte. HEPES was the buffer of choice due to its low association with guanidiniums. When the buffer was changed from one containing sulfonate groups to phosphate groups, the complexation between citrate and **1.26** was inhibited due to buffer interference. Methanol was used in the solutions to increase the host's affinity for both citrate and **1.27**. By changing the solvent system, the association constants of the indicator or analyte to host can be tuned to be able to work in the desired concentration range of the analyte. When the solvent was changed from water to 3:1 methanol:water, the binding constant increased approximately an order of magnitude. Finally, the pH was

31

adjusted within range of the pK_a of **1.27** to increase the sensitivity to microenvironment changes.

Calibration curves were generated for citrate under the same solution conditions discussed above. Figure 1.2A shows a decrease in absorbance at 498 nm as the concentration of citrate is increased. Figure 1.2B displays the selectivity of **1.26** for citrate by examination of emission calibration curves at 525 nm. Addition of di- and mono-carboxylates such as succinate and acetate respectively, results in little or no fluorescence change. The same result is achieved when the analytes are simple salts or sugars.
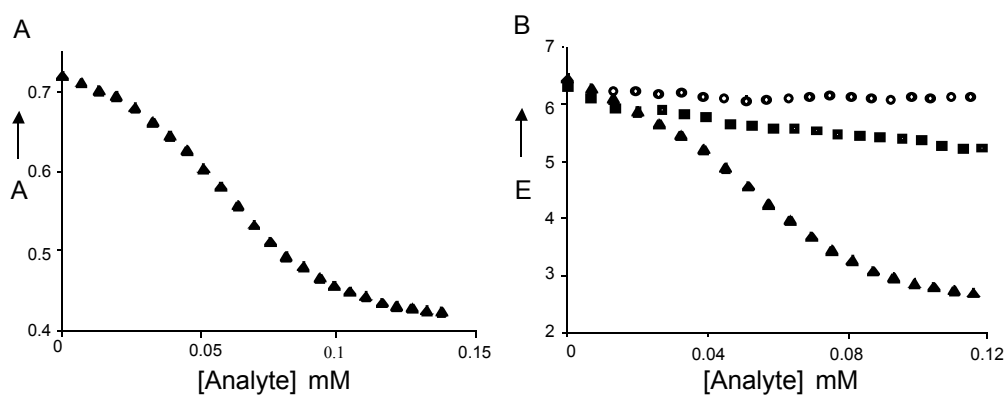
FIGURE 1.2. **CALIBRATION CURVES FOR CITRATE SENSING ENSEMBLE** (A) UV/Vis calibration curve of citrate at λ = 498 nm. (B) Fluorescence emission calibration curve for citrate (▲), succinate (■), and acetate (●). Excitation at λ = 490 nm and emission at λ = 525 nm (25% water in methanol (v/v), 5 mM HEPES, pH 7.4).

Once the selectivity of the chemosensor was determined, its ability to detect citrate in a highly competitive media was tested. The sensing ensemble **1.26-1.27** was used to assay the concentration of citrate in beverages such as soft

drinks and sports drinks. Table 1.1 depicts these results from colorimetric and fluorescent analysis as compared to NMR titrations as a control. Regardless of the highly competitive media, the assay performed with good agreement across the three methods.

TABLE 1.1. ANALYSIS OF CITRATE CONCENTRATION (MM) IN BEVERAGES determined by NMR and competition assay **1.26-1.27** by absorbance and fluorescence.

	by NMR	**1.26** plus **1.27**, absorbance [mM]	**1.26** plus **1.27**, emission [mM]
citrate model solution		30.3	29.9
orange juice	43.1	44.1	44.7
Gatorade	16.0	15.1	15.1
Powerade	12.4	11.1	11.3
All Sport	7.4	7.1	8.1
Mountain Dew	8.0	5.5	5.4
tonic water	21.0	21.2	20.8
Coca Cola	0	0	<0.5
Diet Coke	<0.2	<0.4	<0.7

1.6.4.3 Glucose-6-phophate Sensor

Using the same basic principle, a sensing ensemble was designed to signal the presence of glucose-6-phosphate (**1.28**). To achieve selectivity, a receptor needed to be designed that incorporated binding sites with an affinity for diols and anions in water. Boronic acids are known to rapidly and reversibly form boronate esters with 1,2- and 1,3-diols in basic aqueous media (Section 1.5.3).[40] Thus, the glucose-6-phosphate receptor **1.29** incorporates three *m*-aminomethyl benzene boronic acids as the binding sites on the 1,3,5-trisubstituted-2,4,6-triethylbenzene scaffold.[70] The boronic acids are in a position to form cyclic boronate esters with the hydroxyls of glucose-6-phosphate, while the ammoniums were incorporated to coordinate with the phosphate through charge pairing interactions. It is worth noting that the kinetics of the boronate ester formation is fast in a basic environment when the boron is tetrahedral. These studies were done near neutral pH where the boron is planar (sp^2). Even though the assay was not under optimal conditions, with a slow rate of exchange, binding was still feasible.

1.28   **1.29**
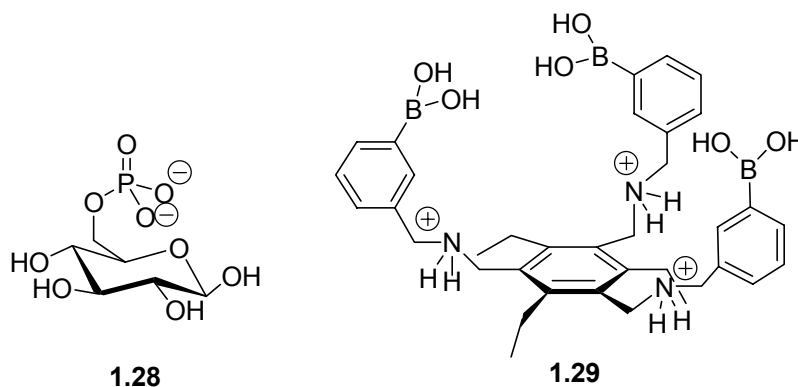
Binding studies were performed using ^{31}P NMR and UV/visible spectroscopy in a solvent system of 70% methanol in water. A 1:1 binding stoichiometry was determined using ^{31}P NMR. Using this data, the host was found to have a binding constant for glucose-6-phosphate of 1.6×10^3 M^{-1}. With UV/visible spectroscopy, a competition assay was employed to signal binding. Once again, 5-carboxyfluorescein (**1.27**) was chosen as the indicator. Since the indicator's absorbance and fluorescence is sensitive to small pH changes, upon binding to **1.29** it was expected to behave in a similar fashion to the previous sensing ensemble. Indeed, upon addition of **1.29** to a solution of **1.27**, the absorbance increases at 494 nm (Figure 1.3A) as more of the indicator becomes bound to the host. As **1.28** is added to a solution of **1.27** and **1.29**, the absorbance decreases (Figure 1.3B) as more of the indicator is displaced from the binding pocket by **1.28**. Using this data, the binding constant between **1.28** and **1.29** was determined to be 2.2×10^3 M^{-1} (by UV/Vis), similar to the value determined using ^{31}P NMR. Testing similar analytes, there was no detectable change in the sensing ensemble's absorbance upon addition of glucose or sodium phosphate. However, the overall spectral response is relatively small, and is not likely practical. Yet, we have discovered ways to improve upon low signal response, as shown in a sensing ensemble for IP$_3$.
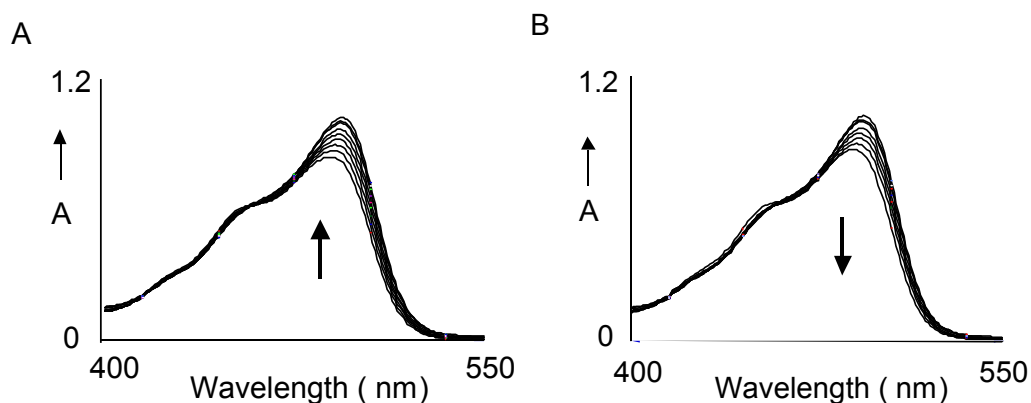
FIGURE 1.3. UV/V IS SPECTRUM FOR GLUCOSE-6-PHOSPHATE SENSING ENSEMBLE (70% methanol in water (v/v), 40 mM HEPES, pH 7.4). (A) Absorbance increase as **1.29** was added to a solution of **1.27** at constant concentration. (B) Absorbance decrease as **1.28** was added to a solution of **1.27** and **1.29** at constant concentration.

1.6.4.4 IP₃ Sensor

The next receptor was designed due to an interest in being able to detect inositol-1,4,5-trisphosphate (IP$_3$), a polyanionic secondary messenger, by utilizing capillary electrophoresis (CE) during cellular processes.[71] In this regard, a sensor needed to be developed that can signal the presence of very low concentrations of IP$_3$. In the development of a sensor with an affinity constant appropriate for so sensitive an application, the binding of anions in aqueous media needed to be further analyzed. Guanidiniums were chosen as binding sites due to their high affinity for not only carboxylates, but phosphates as well. [67] Further, several guanidiniums were required and needed to be preorganized to complement IP$_3$.

As a result, the cleft-like receptor **1.30** consists of four units of the 1,3,5-trisubstituted-2,4,6-triethylbenzenes with one acting as the base and the other three surrounding it as substituents linked via amines.[15] The six guanidinium binding sites were expected to be oriented toward the center of the cavity through steric gearing.

IP₃   1.30
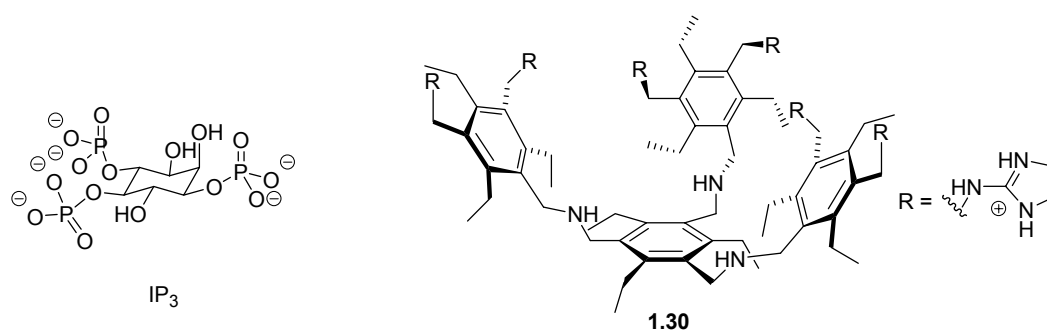
A 1:1 binding stoichiometry was determined for IP₃ with **1.30** using ^{1}H NMR. Fluorescence spectroscopy was chosen for the binding studies of nanomolar concentrations of IP₃, due to the sensitivity of the technique. The signaling motif again employed a competition assay with 5-carboxyfluorescein (**1.27**) as the indicator. In water, as with the previous glucose-6-phosphate studies, little intensity and wavelength shift upon indicator binding was observed. A switch between fluorescent and non-fluorescent forms upon binding would increase the sensitivity of the sensor. To achieve this, binding studies were done in methanol, where **1.27** preferred the non-fluorescent lactonized form, which is generated when the carboxylate undergoes an intramolecular conjugate addition to the quinoid structure, thereby disrupting the conjugation. It was expected that the positive microenvironment of the host would cause the ring to reopen, thereby returning **1.27** to the fluorescent form. Indeed, Figure 1.4A shows the

37

regeneration of fluorescence at 530 nm upon addition of **1.30** to the solution as more of the indicator becomes bound to the host. When IP$_3$ is incrementally added to an ensemble of **1.27** and **1.30**, the fluorescence decreases (Figure 1.4B) as the indicator is displaced from the binding cavity and the cyclized form dominates. The binding constant between IP$_3$ and **1.30** was determined to be 1.0×10^8 M^{-1}. It was found that IP$_3$ in methanol could be detected at the 2 nM range with the sensing ensemble **1.27** and **1.30** in the absence of any competing analytes. At this detection level it is feasible that the intracellular concentration of IP$_3$ can be determined with the assistance of CE.
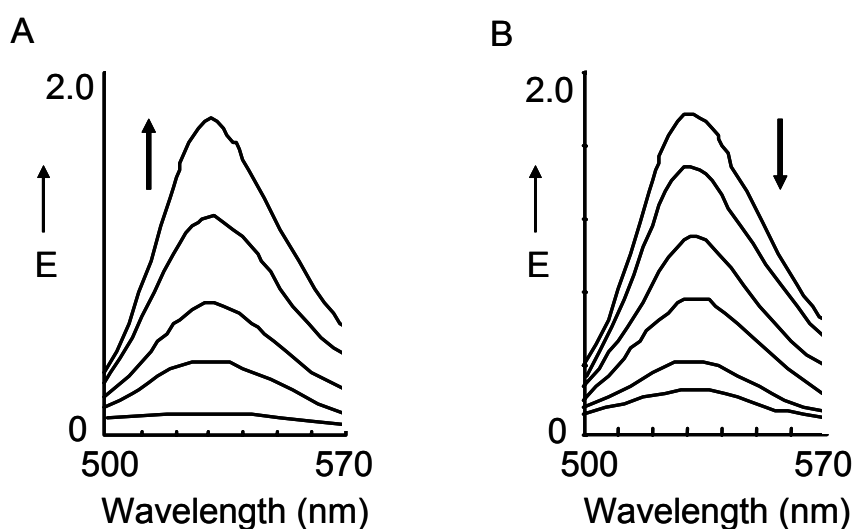
FIGURE 1.4. FLUORESCENCE SPECTRUM FOR IP$_3$ SENSING ENSEMBLE. (A) Increase in fluorescence intensity as incremental amounts of **1.30** are added to a solution of **1.27**. (B) Decrease in fluorescence intensity as IP$_3$ is incrementally added to a solution of **1.30** and **1.27**. Excitation is at 450 nm (100% methanol, 10 mM HEPES buffer, pH 7.4).

1.6.4.5 Non-Aqueous Indicator Displacement

All of the assays presented thus far have used 5-carboxyfluorescein as the indicator where either fluorescence or absorbance intensity modulations can be monitored in response to the presence of analyte. In this manner, the indicator is used to signal analytes it was never designed to signal. To further generalize this method, it was shown that inorganic ions such as nitrate could be targeted as guests. Nature uses amides in proteins to complex anions such as sulfates and phosphates.[72] The receptor designed for the complexation of nitrate was an amide-linked C_3-symmetric bicyclic cyclophane (**1.31**).[18] It was shown that the amide hydrogens complex as neutral hydrogen bond donors to the anion's π-systems. Our receptor consists of two molecules of the 1,3,5-tris-aminomethyl-2,4,6-triethylbenzene as the base and the cap. The two are linked by the formation of 2,6-pyridine diamides, where the six amide hydrogens converge into the center of the cavity.

1.31

1.32

1.33
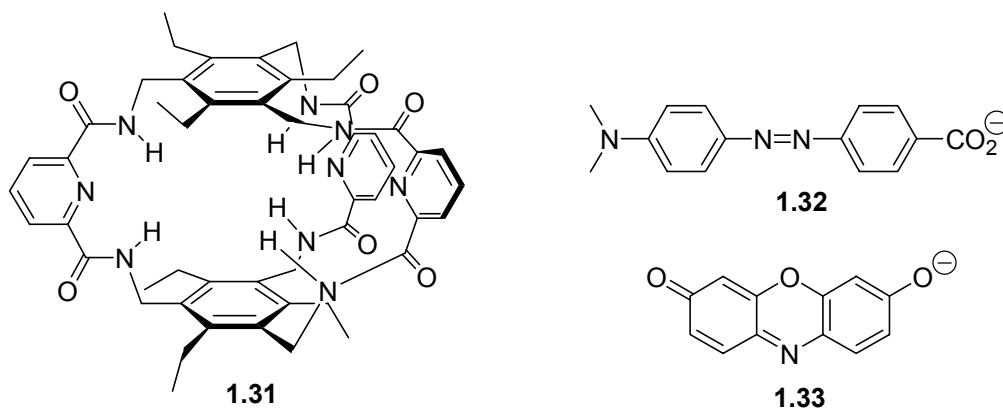
In order to complete the chemosensor, the pH indicators methyl red (**1.32**) and resorufin (**1.33**) were chosen.[16] It was expected that the anionic dyes would bind in the cavity causing a change in their absorbance. Upon addition of an appropriate analyte, the dyes would be displaced from the cavity resulting in a change in absorbance associated with the dye free in solution. Indeed, upon addition of **1.31** to a solution of **1.32** or **1.33,** the absorbance spectrum of the indicators changed. The formation of the complex **1.31**-**1.32** resulted in a decrease in absorbance at 575 nm (Figure 1.5A). An increase in absorbance occurred at 495 nm when the complex **1.31**-**1.33** was formed (Figure 1.5B). When neutral methyl red was tested for complexation with **1.31** the spectrum showed no change, indicating that an anion is needed for complexation.
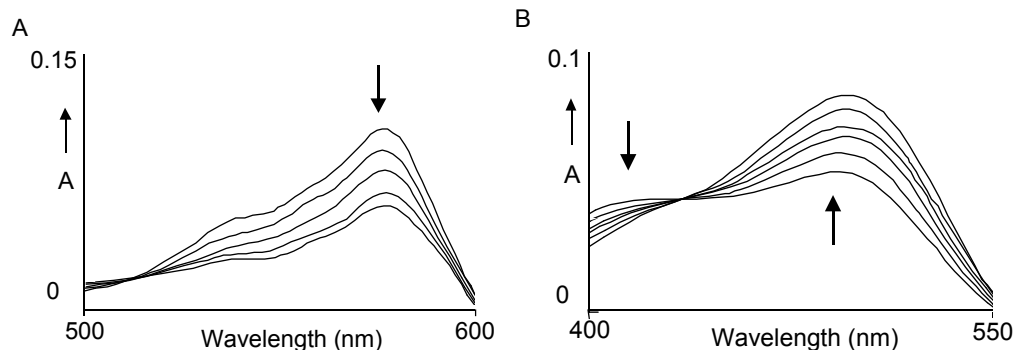
FIGURE 1.5. **UV/VIS SPECTRUM OF (A) RESORUFIN AND (B) METHYL RED** at constant concentrations as **1.31** is added (50% methanol in dichloromethane (v/v)).

The formation of a complex between **1.31** and **1.33** is inhibited in the presence of nitrate. Figure 1.6A shows the absorbance changes of **1.33** at 576 nm

40

upon the addition of various analytes. The host **1.31** shows selectivity for nitrate over other anionic guests such as bromine and perchlorate in 50% (v/v) methanol in dichloromethane. The association constant between **1.31** and nitrate was determined to be 380 M^{-1} by UV/Vis spectroscopy when using **1.33** as the indicator. When indicator **1.32** in 75% (v/v) acetonitrile in dichloromethane is used, higher bonding constants were anticipated due to a lower dielectric media and the absence of competing hydrogen bonds. Figure 1.6B shows the absorbance changes of **1.32** at 423 nm in the presence of **1.31** with varying concentrations of anions. Again, **1.31** is found to be selective for nitrate over other anions with a binding constant for **1.31** to nitrate of 500 M^{-1}. The
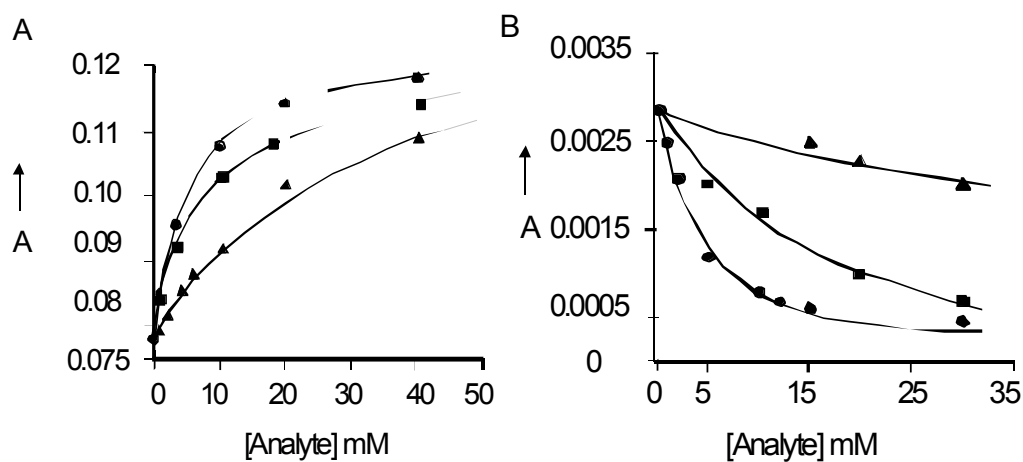
FIGURE 1.6. **UV/VIS CALIBRATION CURVES FOR NITRATE SENSING ENSEMBLE** (A) the sensing ensemble **1.31** and **1.33** at 576 nm upon addition of analytes: NO3- (●), Br- (■), and ClO4- (▲) (50 % methanol in dichloromethane (v/v)). (B) the sensing ensemble **1.31** and **1.32** at 423 nm upon addition of analytes: NO3- (●), Br- (■), and ClO4- (▲) (25% acetonitrile in dichloromethane (v/v)). The counter cations are sodium and tetrabutylammonium for the two different solvent systems respectively.

41

development of this chemosensor shows that the competition assay is applicable in an organic solvent system, and the sensing ensemble is not limited to one indicator.

1.6.4.6 Tartrate/Malate Sensing Ensemble

The next example discusses the result of a sensor that was designed to be selective for a particular analyte (tartrate), yet it also had a similar affinity for a very structurally similar analyte (malate). The assay for tartrate was developed using a colorimetric indicator. The host was designed to bind tartrate, which is a common natural product found in grape derived beverages such as wine and juice.[13] Since tartrate is comprised of two carboxylates and a diol functionality, complimentary binding sites needed to be chosen accordingly. From what we learned in the use of the previously described hosts, two guanidiniums and a boronic acid were chosen as the recognition moieties in host **1.34**, and the same hexa-substituted benzene scaffold was used. The boronic acid coordination chemistry used here is different from that of **1.29**, because the amino methyl group is now ortho to the boronic acid instead of meta. We previously noted that the kinetics of the boronate ester formation is fast when the boronic acid is tetrahedral due to the lone pair of the adjacent amine donating into the empty *p*-orbital of the boron.

tartrate   malate   **1.34**   **1.35**
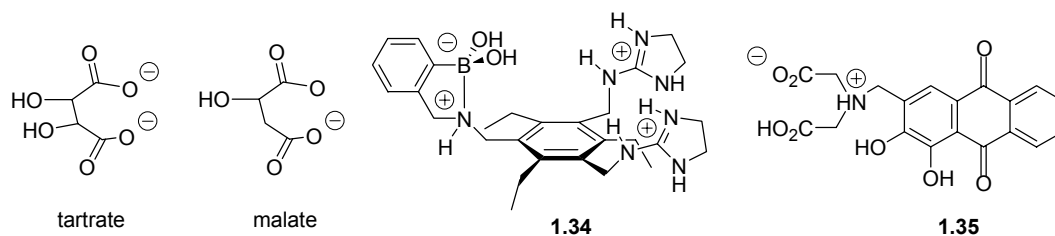
The chosen chromophore, alizarin complexone (**1.35**), possesses similar functionalities to tartrate, and is used as an indicator for the determination of pH, fluoride ions, and some rare-earth metals.[73,74] It was expected that **1.35** bound to **1.34** would have a different "protonation state" than **1.35** free in solution. Indeed, Figure 1.8A shows that upon incremental addition of **1.34** to a solution of **1.35** in a methanol/water mixture the absorbance at 525 nm decreases as the absorbance at 450 nm increases, which is indicative of a color change from burgundy to
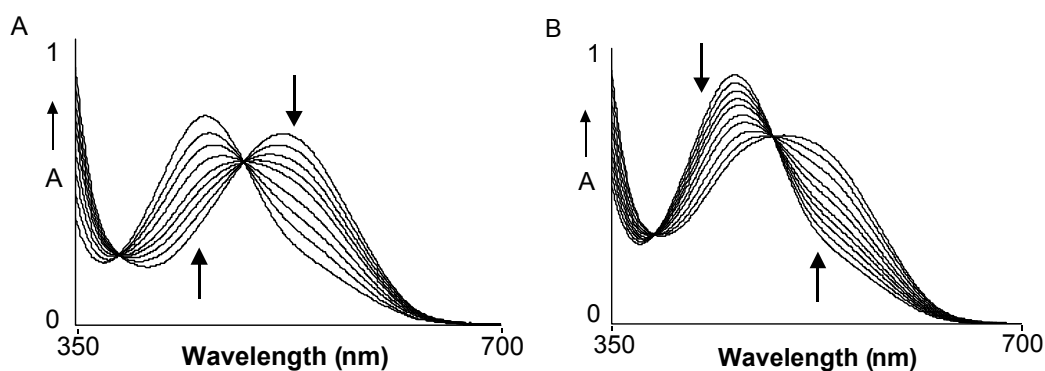
FIGURE 1.8. TARTRATE/MALATE COMPETITION ASSAY. UV/Vis spectrum of **1.35** (75% methanol in water (v/v), 10 mM HEPES, pH 7.4). (A) Absorbance decrease at λ = 525 nm and increase at λ = 450 nm as **1.34** is added to a solution of **1.35** at constant concentration. (B) Absorbance decrease at λ = 450 nm and increase at λ = 525 nm as tartrate is added to a solution of **1.34** and **1.35** at constant concentration.

43

yellow. This is one of the first indicators discussed, where there was a large color change upon addition of the receptor. When tartrate is added to a solution of **1.34** and **1.35** under the same conditions, the absorbance change is reversed with an increase at 525 nm and decrease at 450 nm (Figure 1.8B). A binding constant of $5.5 \times 10^4 \text{ M}^{-1}$ between tartrate and **1.34** was determined by UV/Vis spectroscopy.

Other possible competing analytes were tested with the sensing ensemble using UV/Vis spectroscopy, including: ascorbate, malate, succinate, lactate, and glucose. Figure 1.9 depicts the calibration curves that were generated in these studies. The sensing ensemble **1.34** – **1.35** was selective for tartrate over sugars and mono- and bis-carboxylates, including lactate, with the exception of malate
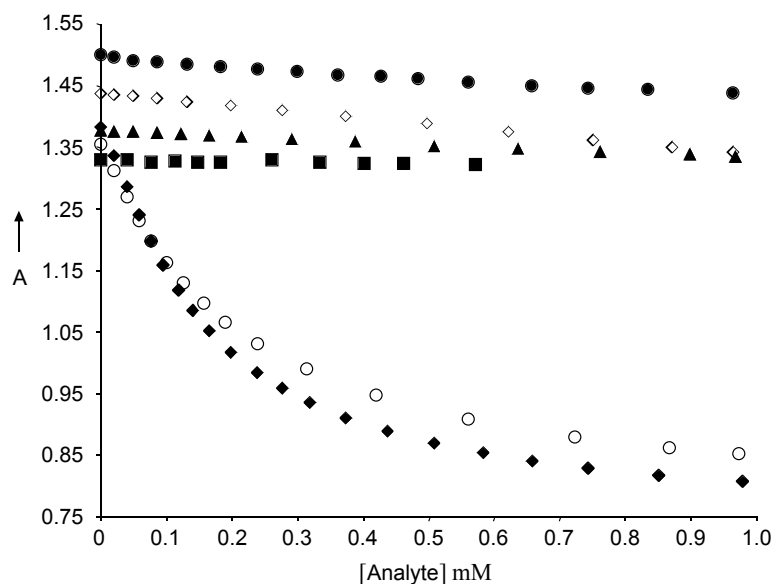
FIGURE 1.9. UV/VIS CALIBRATION CURVES FOR TARTRATE/MALATE SENSING ENSEMBLE at 450 nm for **1.34** and **1.35** upon addition of the analytes: tartrate (♦), malate (O), ascorbate (◇), succinate (▲), glucose (■), and lactate (●) (75% methanol in water (v/v), 10 mM HEPES, pH 7.4).

(4.8 x 10^4 M^{-1}). Since, tartrate and malate are very structurally similar in which they only differ by one hydroxyl, the result was **1.34** had similar affinity constants for both analytes. The similarity in affinity constants can be seen in the response given by the sensing ensemble in the calibration curves.

With the calibration curves in hand, various beverages were analyzed for their total concentration of tartrate and malate. Wines and grape juices were tested with **1.34** and **1.35**, and the values obtained were in good agreement with values independently determined by NMR (Table 1.2). In summary, even though the colorimetric sensing ensemble was designed to be selective for one analyte, it demonstrated a similar affinity for two very structurally similar analytes. Yet one

TABLE 1.2. TARTRATE AND MALATE CONCENTRATIONS IN GRAPE DERIVED BEVERAGES determined by both NMR and colorimetric assay.

	NMR [mM]	**1.34 + 1.35** UV-Vis [mM]
Tartaric acid model solution	51.2	50.2
Ernest & Julio Gallo Sauvignon Blanc	35.6	32.9
Ste. Genevieve Chardonnay	34.1	36.3
Henri Marchant Spumante	26.5	24.9
Talus Merlot	19.5	20.3
Santa Cruz Organic White Grape Juice	43.7	42.3
Welch's Grape Juice	69.4	71.3

goal of supramolecular chemistry is to develop receptors that have high selectivity. Therefore, one might question the utility of this sensing ensemble. In the end, the sensor was able to quantify both analytes simultaneously in grape derived beverages. Due to its ability to bind a "class of analytes" one might envision this sensor as a differential receptor that could be effective in a sensor array.

1.7   MULTIPLE ANALYTE SENSOR

At the beginning of this chapter, it was discussed that supramolecular chemists strive to develop synthetic receptors that have high affinities and selectivities, yet due to their inherent simplicity, many fall short of this goal. Yet, in some instances, this lack of selectivity can make these systems desirable, especially in the area of multi-component sensing, as shown above. In order to simultaneously detect multiple analytes in a solution, many different sensors are needed. A selective sensor can be developed for each analyte, but depending on the number of analytes that are being quantified, that can be an arduous task. A more practical approach would be the development of sensors that sense for classes of analytes, similar to Nature's approach to taste and smell. Fewer sensors are needed due to the cross-talk that is displayed for a particular analyte eliciting a response from many receptors at once. This idea is portrayed in Figure 1.10, where the response is shown from a six component sensor array upon addition of analyte A and B, respectively. From the example shown, analyte A received a
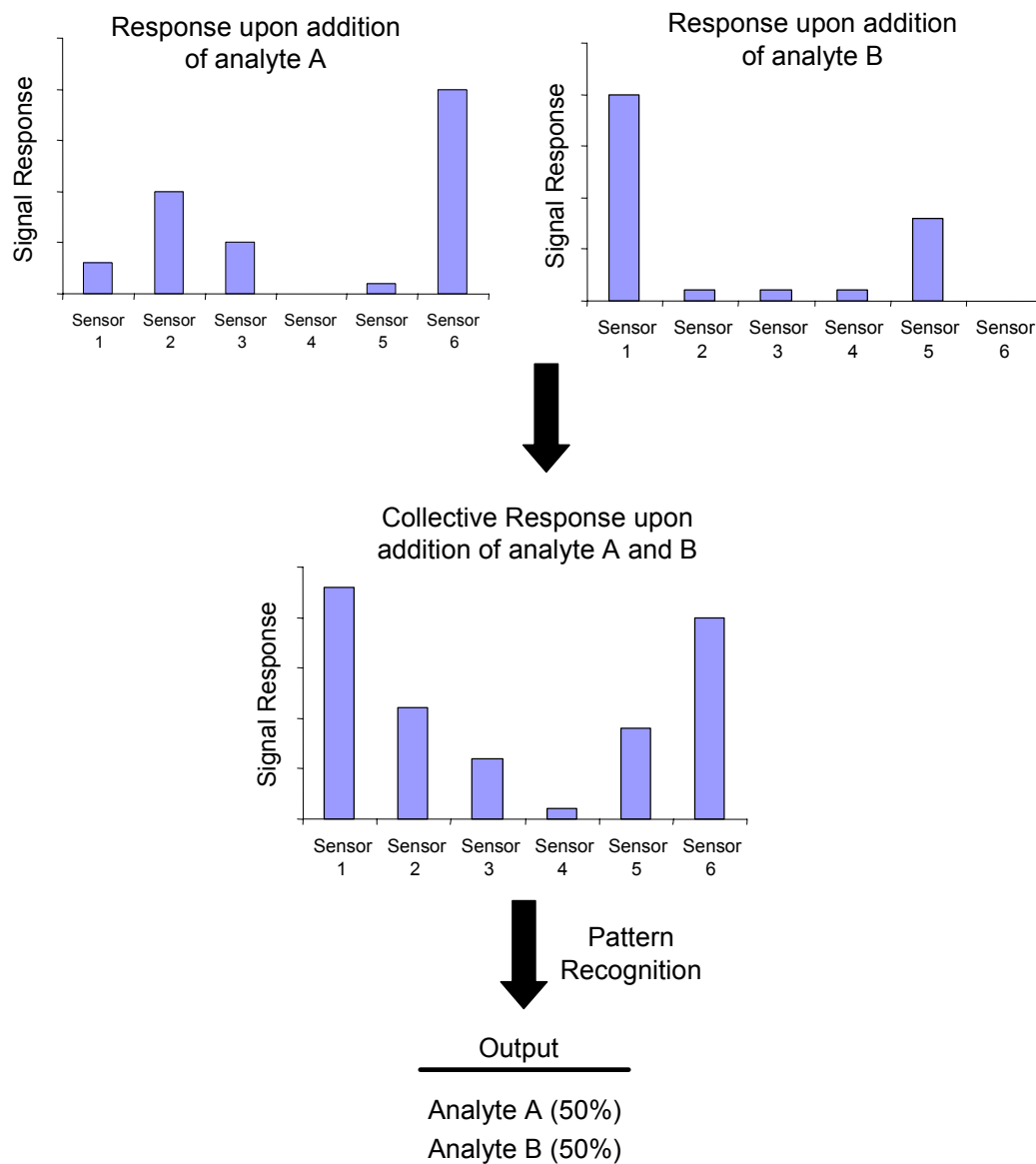
FIGURE 1.10. A REPRESENTATION OF A SENSOR ARRAY where only one factor is being looked such as one wavelength for absorbance. The top two graphs represent the response obtained from the sensors upon addition of analytes A and B separately. The bottom graph is the collective response from the array upon addition of both analytes. Pattern recognition would be used to determine the composition of the mixture.

strong response from sensor 6, with smaller responses from sensors 1, 2, and 3, while sensors 4 and 5 offer essentially no response. Of the same six sensors, only 1 and 5 gave a response upon addition of analyte B. The pattern from each analyte of interest was collected, such that upon addition of both analytes pattern recognition programs used the collective response to determine the composition of the sample. This example only looks at one factor, for example looking at only one wavelength out of entire UV/visible spectrum. The addition of more responses from more "wavelengths" results in a very powerful tool for sensing.

1.7.1   Nature's Multi-Analyte Sensor

Of the five mammalian senses, vision, hearing, touch, smell, and taste, the first three are physical senses based on forces such as sound waves, light waves, etc. The other two, taste and smell, are often referred to as the lower senses, and are based on our response to chemical stimuli resulting in Nature's sensor array.[75]

Over the years the number of primary tastes has been disputed and at one point even included "tastes" such as fatty, astringent, sharp, and nauseous. Wund eventually would narrow it down to only sweet, sour, salty, and bitter.[75] Even with only four primary tastes, mixing these components in different combinations create unique tastes, much like the mixing of the primary colors.

Taste or gustation is a result of chemical interactions or molecular recognition events on the surface of the tongue through "taste buds," shaped like and named for an unopened flower.[76] The concept of taste receptors has been

around since the time of Aristotle, but taste buds were first identified in the mid nineteenth century by Leydig. Schultze (1863) proposed the idea that they were chemosensory structures.[76] Taste buds exhibit selectivity for a particular taste and are clustered in different regions of the tongue in depressions called taste pores according to their selectivity. The tip of the tongue is where salt is sensed, the sides nearest the tip is sweet, further back on the sides is sour, and across the back of the tongue seems to have the greatest sensitivity for bitterness. The center of the tongue appears to be insensitive to all taste. When chemical stimuli enter the taste pores, the epithelial cells within the taste buds respond to the stimuli and activate nerves.[76] Sweetness results from sugar, sugar derivatives, sweet amino acids like most D-amino acids, and some simple salts (beryllium and lead). Bitterness is thought to be a safety mechanism against poisons by being directly related to the gag reflux and is attributed to a diverse amount of stimuli including, hydrophobic amino acids, basic heterogeneous compounds, divalent salts, and some peptides.[77] Sour is dependent on the acidity of the food, while saltiness stems from halide salts such as sodium chloride.[78] Due to the diverse types of stimuli for one particular taste, multiple receptors are required. Yet there it would be impossible to have a specific receptor for each stimuli that can be eaten. This is where the idea of differential receptors is applied. The receptors have selectivities for classes of analytes where each receptor has a different affinity for a particular stimulus. The response of each of these receptors is combined to create a pattern that is specific for a certain taste. This pattern can be stored in the

brain so that the same taste can be identified upon future exposure. This pattern may also be used to classify similar tastes as pleasant or unpleasing.

1.7.2   Synthetic Multi-Component Sensor Arrays

To mimic the sense of taste, we need to have the ability to detect single or multiple analytes through a collection of specific or general sensors utilizing a signaling scheme and pattern recognition. An array of sensors is compiled and a specific pattern emerges for each stimuli and mixture of stimuli that is tested. This pattern can then be stored in a computer to create a library of "tastes" to be utilized for future recognition.   One approach uses poly-(ethylene glycol)-polystyrene (PEG-PS) resin beads with a variety of covalently attached chemical sensors to mimic taste buds (Figure 1.11A)[79]. These sensors were selective for individual analytes, but not specific in their recognition ability. These derivatized beads were placed in micromachined wells (Figure 1.11B) in silicon wafers to immobilize the beads.[80] A 3 x 3 array was used to detect a variety of analytes at once. A charge-coupled device (CCD) was used to determine the absorption properties of the beads, and the red, green, and blue (RGB) light intensities were studied for each individual bead upon addition of analyte. Of the four sensors chosen, one was specific and three were nonspecific. Each was compared to a control, which consisted of a resin bead where the amines were acetylated. The

A.   B.
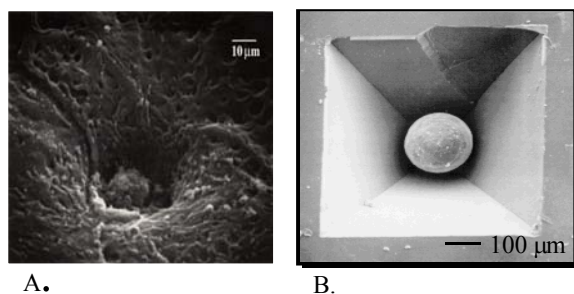
FIGURE 1.11. NATURAL AND SYNTHETIC "TASTE BUD" (A) A rat fungiform papilla as seen by a scanning electron microscope (SEM).[83] (B) An SEM image of a micromachined silicon well, with a bead immobilized in it.

sensors included fluorescein as a pH indicator,[81] *o*-cresolphthalein complexone for detection of Ca^{2+} and pH,[82] alizarin complexone for Ce^{3+}, Ca^{2+}, and pH,[74] and a boronic acid with a resorufin-derivatized galactose associated with it to indicate the presence of simple sugars.

Proof of concept for the detection of Ca^{2+} using 0.1 M $Ca(NO_3)_2$ at various pH values is shown in Figure 1.12. The CCD array analyzed the change in transmitted light as the beads responded to calcium and pH. Experiments were also performed with cerium ($Ce(NO_3)_3$), a combination of cerium and calcium, and the simple sugar fructose. *o*-Cresolphthalein indicated the presence of calcium at a pH of 11.4 by a purple color. In the absence of calcium ion, the purple color was not observed until pH 12.5. Fluorescein was used as a pH sensor, changing from light yellow to orange at a pH around 6. Alizarin complexone was used for multiple roles, including a pH sensor were the beads were yellow at a pH less than 4.5, orange/red from pH 4.5-10, and a deep purple when the pH was higher than 11.5. When cerium was present, the change from

51

yellow to orange/red occurred at a lower pH. The same effect was also observed for calcium, but the color change was not as dramatic. When fructose is added to the resorufin-β-D-galactopyranoside boronic acid complex, the bead changes from dark orange to yellow as the tagged sugar is displaced from the boronic acid and washed away due to the higher binding affinity of fructose. There was also a slight sensitivity to pH that was recorded by the CCD showing an increase in the absorbance of red light. These studies show that it is possible to detect multiple analytes at once, by analysis of the RGB patterns.
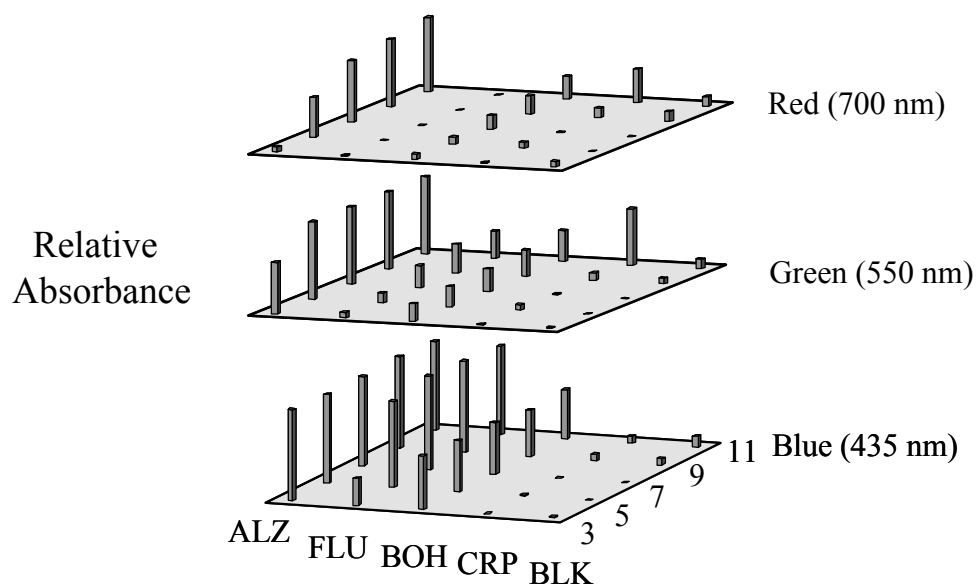
FIGURE 1.12. RGB PATTERNS FOR ELECTRONIC TONGUE. A series of bar graphs showing the color attenuation that was recorded by the CCD as the sensors were exposed to calcium at various pHs. (ALZ = alizarin complexone, FLU = fluorescein, BOH = boronic acid/galactose/resorufin, CRP = *o*-cresolphthalein complexone, BLK = blank)

A cross-reactive sensor array was developed with Nature's own enzymes by Walt and coworkers.[84] The sensor array was developed to determine the presence of a series of esters, through the use of esterase enzymes which catalyze the hydrolysis of esters to carboxylic acids. While some enzymes have a high specificity for their substrates, others have overlapping specificities such that they are class reactive. The assay was performed in a microtiter plate, and the reaction kinetics was monitored by fluorescence, with the presence of fluorescein. The indicator is sensitive to changes in pH, such that the fluorescence was altered as more of the carboxylic acid was produced. Twenty-three esters were tested in the array, which ranged from simple aliphatic to multi-functional esters. The esterases varied in specificity such that the presence of each ester created a fingerprint of fluorescent responses that was used as a training set for pattern recognition. Principle component analysis (PCA) was used to analyze the data. The pattern recognition program is widely used to reveal simpler patterns within complex data sets. In this experiment, approximately twenty amino acids were correctly identified in solution by themselves and in mixtures. Even though it was determined that complex mixtures of esters would be difficult to determine, the system helped to demonstrate the utility of using the combination of differential sensors and pattern recognition for sensing applications.

1.7.3 Support Bound Single Analyte Sensing

Now that the technology is in place to form sensor arrays, the immobilization of synthetic receptors on solid supports needs to be investigated. In the Anslyn group, a library of support bound single analyte chemosensors was designed to be selective for ATP.[17] This sensor takes advantage of a rationally designed core while utilizing combinatorial methods in the development of the recognition moieties. A preorganized cavity was formed using the 1,3,5-trisubstituted-2,4,6-triethylbenzene scaffold mentioned previously. One of the substituents consisted of lysine/urea linkage to Tentagel resin. The remaining substituents were identical tripeptide chains extending from guanidinium linkages to the base **1.36**.[85] The fluorophore 5-carboxyfluorescein was attached to the N-terminus of the peptide chains while 7-diethylaminocoumarin-3-carboxylic acid was attached to the lysine side chain. It was expected that binding could then be signaled by some perturbation of the fluorescence resonance energy transfer (FRET) between the two fluorophores.

54
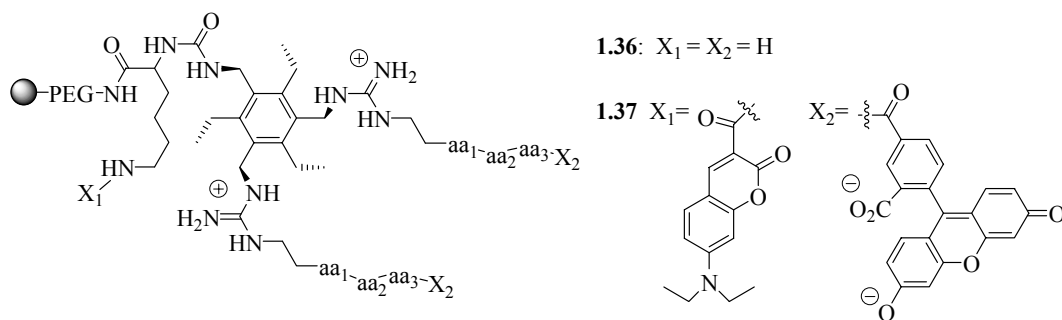
A library was generated and then screened against the desired analyte, ATP, to determine the most selective receptors. The host without the fluorophores (**1.36**) was used to screen the library. A fluorescently labeled N-methylanthraniloyl-ATP (MANT-ATP, 0.25 mM) was used to select the strongest binding members of the library (HEPES buffer 10 mM, pH 7.1).[86] Illumination of the beads at 366 nm allowed for a range of fluorescent intensities to be viewed. Several of the highly fluorescent and nonfluorescent beads were removed and sequenced to determine which peptide chains were active and inactive (Table 1.3). Three highly fluorescent "hits" and one nonfluorescent "miss" were resynthesized with the fluorophores as in **1.37**.

The randomly chosen "hit" and "miss" beads were sandwiched between two layers of gold mesh on a glass slide to create a mono layer which could be studied using a standard fluorimeter to determine their ATP signaling ability. As expected, the "miss" exhibited no fluorescence modulation upon excitation of either fluorophore when exposed to ATP. Upon excitation of fluorescein all but one "hit" (Thr-Val-Asp) exhibited fluorescence modulation, however no change in the extent of FRET was observed. A large spectral change was observed with ATP and the Ser-Tyr-Ser sensor to yield a binding constant of $3.4 \times 10^3 \, M^{-1}$ (Figure 1.12). The fluorescence modulation may be due to an increase in the positive microenvironment around the fluorescein upon binding of the ATP. The potentially competing analytes AMP and GTP were also tested with this sensor due to their similarity in structure to ATP. Selectivity for ATP over AMP suggests the importance of the guanidinium binding. Similarly, the specificity

over GTP indicates the tripeptide arms create specificity for nucleotide bases. This demonstrates that a selective resin bound chemosensor can be created through combinatorial methods.

TABLE 1.3. SEQUENCING RESULTS OF SELECT MEMBERS OF LIBRARY. The peptide chains in bold were resynthesized, incorporating the fluorophores.

Active Beads	Inactive Beads
Thr-Val-Asp	**His-Phe-Gly**
Asp-Ala-Asp	Ser-Ala-Asp
Ser-Tyr-Ser	Trp-Asn-Glu
Asp-His-Asp	Thr-Phe-Ser
Met-Thr-His	
Glu-Pro-Thr	
His-Ala-Asp	
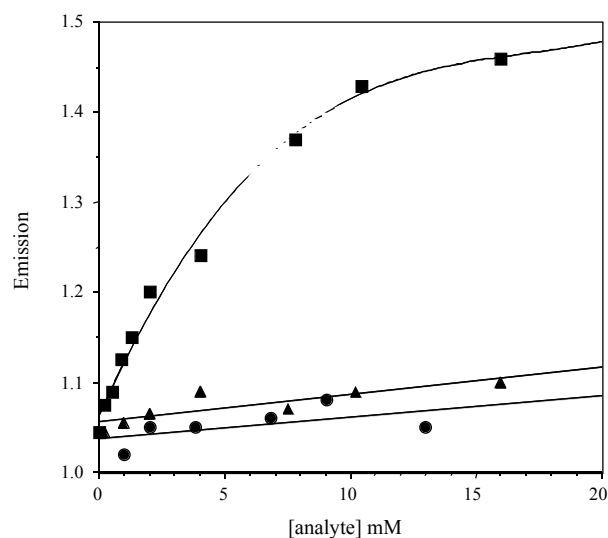
FIGURE 1.12. BINDING ISOTHERMS FOR THE SER-TYR-SER 1.37 when combined with ■ = ATP, ▲ = AMP, and ● = GTP. (200 mM HEPES buffer, pH 7.4)

1.8 SUMMARY

The study of molecular recognition and the development of single analyte sensors has led to the ability to simultaneously analyze for several components in a complex solution. Instead of developing sensors that have high selectivity and specificity, perhaps a new frontier might be the development of sensors that are responsive to classes of analytes. The creation of a pattern, or fingerprint, resulting from the response of several of these differential sensors allows for the determination and potential quantification of these analytes using pattern recognition protocols. The fact that the molecular recognition events are taking place in parallel allows for "cross-talk" or non-specific receptors to be used. A

57

library can be created out of the patterns obtained, to be used for future analysis of unknown solutions.

The next few chapters help to show how many of these concepts and ideas can be applied. From investigating sensors that are selective for classes of analytes to using multiple sensors and pattern recognition for analyte quantification. These advances help to show that synthetic receptors can make useful differential sensors, and work is shown how they will be incorporated into sensor arrays. An investigation of the thermodynamics of boronic acid and guanidinium binding is also discussed. The binding of four boronic acid/guanidinium hosts with various combinations of diol/carboxylate guests are studied by UV/visible titrations and isothermal titration calorimetry and the cooperativity is looked at. Finally, a new sensing method for catechol containing compounds is investigated, that resembled iron binding siderophores.

1.9 REFERENCES

(1)   Antonisse, M. M. G.; Reinhoudt, D. N. Neutral Anion Receptors: Design and Application. *Chem. Commun.* **1998**, 443-448; Beer, P. D.; Gale, P. A. Anion Recognition and Sensing: The State of the Art and Future Perspectives. *Angew. Chem., Int. Ed.* **2001***, 40*, 486-516; Reichenback-Klinke, R.; Konig, B. Metal Complexes of Azacrown Ethers in Molecular Recognition and Catalysis. *J. Chem. Soc., Dalton Trans.* **2002**, 121-130; Linton, B.; Hamilton, A. D. Formation of Artificial Receptors by Metal-Templated Self Assembly. *Chem. Rev.* **1997***, 97*, 1669-1680; Sanders, J. K. M. Adventures in Molecular Recognition. The Ins and Outs of Templating. *Pure Appl. Chem.* **2000***, 72*, 2265-2274; Schmidtchen, F. P.; Berger, M. Artificial Organic Host Molecules for Anions. *Chem. Rev.* **1997***, 97*, 1609-1646; Schneider, H.-J. Mechanisms of Molecular Recognition: Investigations of Organic Host-Guest Complexes. *Angew. Chem., Int. Ed.* **1991***, 30*, 1417-1436; Snowden, T. S.; Anslyn, E. V. Anion Recognition: Synthetic Receptors for Anions and Their Application in Sensors. *Curr. Opin. Chem. Biol.* **1999***, 3*, 740-746.

(2)   Lewis, P. T.; Davis, C. J.; Cabell, L. A.; He, M.; Read, M. W.; McCarroll, M. E.; Strongin, R. M. Visual sensing of saccharides promoted by resorcinol condensation products. *Org. Lett.* **2000***, 2*, 589-592; Inouye, M.; Chiba, J.; Nakazumi, H. Glucopyranoside Recognition by Polypyridine-Macrocyclic Receptors Possessing a Wide Cavity with a Flexible Linkage. *J. Org. Chem.* **1999***, 64*, 8170-8176; Inouye, M.; Miyake, T.; Furusyo, M.; Nakazumi, H. Molecular Recognition of .beta.-Ribofuranosides by Synthetic Polypyridine-Macrocyclic Receptors. *J. Am. Chem. Soc.* **1995***, 117*, 12416-12425.

(3)   Breslow, R.; Zhang, B. Cholesterol Recognition and Binding by Cyclodextrin Dimers. *J. Am. Chem. Soc.* **1996***, 118*, 8495-8496; Zimmerman, S. C.; Zeng, Z. Improved binding of adenine by a synthetic receptor. *J. Org. Chem.* **1990***, 55*, 4789-4791.

(4)   Bell, T. W.; Hou, Z. A Hydrogen-Bonding Receptor that Binds Urea with High Affinity. *Angew. Chem., Int. Ed.* **1997***, 36*, 1536-1538.

(5)   Bell, T. W.; Hou, Z.; Luo, Y.; Drew, M. G. B.; Chapoteau, E.; Czech, B. P.; Kumar, A. Detection of Creatinine by a Designed Receptor. *Science* **1995***, 269*, 671-674.

(6)   Bell, T. W.; Cragg, P. J.; Firestone, A.; Kwok, A. D. I.; Liu, J.; Ludwig, R.; Sodoma, A. Molecular Architecture 2. Synthesis and Metal Complexation of Heptacyclic Terpyridyl Molecular Clefts. *J. Org. Chem.* **1998**, *63*, 2232-2243; Unob, F.; Asfari, Z.; Vicens, J. An anthracene-based fluorescent sensor for transition metal ions derived from calix[4]arene. *Tetrahedron Lett.* **1998**, *39*, 2951-2954.

(7)   Hirano, T.; Kikuchi, K.; Urano, Y.; Higuchi, T.; Nagano, T. Highly Zinc-Selective Fluorescent Sensor Molecules Suitable for Biological Applications. *J. Am. Chem. Soc.* **2000**, *122*, 12399-12400.

(8)   Chin, J.; Walsdorff, C.; Stranix, B.; Oh, J.; Chung, H. J.; Park, S.-M.; Kim, K. A Rational Approach to Selective Recognition of NH4+ over K+. *Angew. Chem., Int. Ed.* **1999**, *38*, 2756-2759.

(9)   Davis, A. P.; Gilmer, J. F.; Perry, J. J. A steroid-based cryptand for halide anions. *Angew. Chem., Int. Ed.* **1996**, *35*, 1312-1315; Amendola, V.; Bastianello, E.; Fabbrizzi, L.; Mangano, C.; Pallavicini, P.; Perotti, A.; Lanfredi, A. M.; Ugozzoli, F. Halide-ion encapsulation by a flexible dicopper(II) bis-tren cryptate. *Angew. Chem., Int. Ed.* **2000**, *39*, 2917-2920.

(10)   Sebo, L.; Schweizer, B.; Diederich, F. Cleft-type diamidinium receptors for dicarboxylate binding in protic solvents. *Helv. Chim. Acta* **2000**, *83*, 80-92.

(11)   Cheng, Y.; Suenaga, T.; Still, W. C. Sequence-Selective Peptide Binding with a Peptido-A,B-trans-steroidal Receptor Selected from an Encoded Combinatorial Receptor Library. *J. Am. Chem. Soc.* **1996**, *118*, 1813-1814; Haino, T.; Rudkevich, D. M.; Shivanyuk, A.; Rissanen, K.; Rebek, J. J. Induced-Fit Molecular Recognition with Water-Soluble Cavitands. *Chem. Eur. J.* **2000**, *6*, 3797-3805; James, T. D.; Sandanayake, K. R. A. S.; Shinkai, S. Chiral discrimination of monosaccharides using a fluorescent molecular sensor. *Nature* **1995**, *374*, 345-347.

(12)   Inouye, M.; Hashimoto, K.; Isagawa, K. Nondestructive Detection of Acetylcholine in Protic Media: Artificial-Signaling Acetylcholine Receptors. *J. Am. Chem. Soc.* **1994**, *116*, 5517-5518.

(13)   Lavigne, J. J.; Anslyn, E. V. Teaching old indicators new tricks: a colorimetric chemosensing ensemble for tartrate/malate in beverages. *Angew. Chem., Int. Ed.* **1999**, *38*, 3666-3669.

(14)   Metzger, A.; Lynch, V. M.; Anslyn, E. V. A synthetic receptor selective
         for citrate. *Angew. Chem., Int. Ed.* **1997***, 36*, 862-865.

(15)   Niikura, K.; Metzger, A.; Anslyn, E. V. Chemosensor Ensemble with
         Selectivity for Inositol-Trisphosphate. *J. Am. Chem. Soc.* **1998***, 120*, 8533-
         8534.

(16)   Niikura, K.; Bisson, A. P.; Anslyn, E. V. Optical sensing of inorganic
         anions employing a synthetic receptor and ionic colorimetric dyes. *J.
         Chem. Soc., Perkin Trans. 2* **1999***,* 1111-1114.

(17)   Schneider, S. E.; O'Neil, S. N.; Anslyn, E. V. Coupling Rational Design
         with Libraries Leads to the Production of an ATP Selective Chemosensor.
         J. Am. Chem. Soc. **2000***, 122*, 542-543.

(18)   Bisson, A. P.; Lynch, V. M.; Monahan, M.-K. C.; Anslyn, E. V.
         Recognition of anions through NH-.pi. hydrogen bonds in a bicyclic
         cyclophane- selectivity for nitrate. *Angew. Chem., Int. Ed.* **1997***, 36*, 2340-
         2342.

(19)   Fujimoto, T.; Shimizu, C.; Hayashida, O.; Aoyama, Y. Solution-to-
         Surface Molecular-Delivery System Using a Macrocyclic Sugar Cluster.
         Sugar-Directed Adsorption of Guests in Water on Polar Solid Surfaces. *J.
         Am. Chem. Soc.* **1997***, 119*, 6676-6677; Goodman, M. S.; Jubian, V.;
         Linton, B.; Hamilton, A. D. A Combinatorial Library Approach to
         Artificial Receptor Design. *J. Am. Chem. Soc.* **1995***, 117*, 11610-11611;
         Choi, K.; Hamilton, A. D. Selective Anion Binding by a Macrocycle with
         Convergent Hydrogen Bonding Functionality. *J. Am. Chem. Soc.* **2001***,
         123*, 2456 - 2457.

(20)   Cram, D. J. The Design of Molecular Hosts, Guests, and Their
         Complexes. *Science* **1988***, 240*, 760-767.

(21)   Lehn, J. M. Supramolecular Chemistry-Scope and Perspectives: Molecules
         - Supermolecules - Molecular Devices. *J. Incl. Phenom.* **1988***, 6*, 351-396.

(22)   Pedersen, C. J. The Discovery of Crown Ethers. *Science* **1988***, 241*, 536-
         540.

(23)   Lehn, J.-M. Cryptates: The Chemistry of Macropolycyclic Inclusion
         Complexes. *Acc. Chem. Res.* **1978***, 11*, 49-57.

(24)   Cram, D. J. Cavitands: Organic Hosts with Enforced Cavities. *Science* **1983***, 219*, 1177-1183.

(25)   Linton, B.; Hamilton, A. D. Calorimetric investigation of guanidinium-carboxylate interactions. *Tetrahedron* **1999***, 55*, 6027-6038.

(26)   Sebo, L.; Schweizer, B.; Diederich, F. Cleft-type diamidinium receptors for dicarboxylate binding in protic solvents. *Helv. Chim. Acta* **2000***, 83*, 80-92.

(27)   Linton, B. R.; Goodman, M. S.; Fan, E.; Van Arman, S. A.; Hamilton, A. D. Thermodynamic Aspects of Dicarboxylate Recognition by Simple Artificial Receptors. *J. Org. Chem.* **2001***, 66*, 7313-7319.

(28)   Fitzmaurice, R. J.; Kyne, G. M.; Douheret, D.; Kilburn, J. D. Synthetic receptors for carboxylic acids and carboxylates. *J. Chem. Soc., Perkin Trans. 1* **2002**, 841-864.

(29)   Dietrich, B.; Fyles, D. L.; Fyles, T. M.; Lehn, J. M. Anion coordination chemistry: polyguanidinium salts as anion complexons. *Helv. Chim. Acta* **1979***, 62*, 2763-2787.

(30)   Hannon, C. L.; Anslyn, E. V. The guanidinium group: its biological role and synthetic analogs. *Bioorg. Chem. Front.* **1993***, 3*, 193-255.

(31)   Kimura, E.; Sakonaka, A.; Yatsunami, T.; Kodama, M. Macromonocyclic polyamines as specific receptors for tricarboxylate-cycle anions. *J. Am. Chem. Soc.* **1981***, 103*.

(32)   Raposo, C.; Mussons, M. L.; Caballero, M. C.; Morán, J. R. Readily Available Chromenone Receptors for Carboxylates. *Tetrahedron Lett.* **1994***, 35*, 3409-3410.

(33)   Berger, M.; Schmidtchen, F. P. Zwitterionic Guanidinium Compounds Serve as Electroneutral Anion Hosts. *J. Am. Chem. Soc.* **1999***, 121*, 9986-9993; Berger, M.; Schmidtchen, F. P. The binding of sulfate anions by guanidinium receptors is entropy-driven. *Angew. Chem., Int. Ed.* **1998***, 37*, 2694-2696; Metzger, A.; Gloe, K.; Stephan, H.; Schmidtchen, F. P. Molecular Recognition and Phase Transfer of Underivatized Amino Acids by a Foldable Artificial Host. *J. Org. Chem.* **1996***, 61*, 2051-2055; Schiessl, P.; Schmidtchen, F. P. Abiotic molecular recognition of dicarboxylic anions in methanol. *Tetrahedron Lett.* **1993***, 34*, 2449-2452.

(34)   Haj-Zaroubi, M.; Mitzel, N. W.; Schmidtchen, F. P. Communications: The rational design of anion host compounds: An exercise in subtle energetics. *Angew. Chem., Int. Ed.* **2002***, 41*, 104-107.

(35)   Sukharevsky, A. P.; Read, I.; Linton, B.; Hamilton, A. D.; Waldeck, D. H. Experimental Measurements of Low-Frequency Intermolecular Host-Guest Dynamics. *J. Phy. Chem. B* **1998***, 102*, 5394-5403.

(36)   Davis, A. P.; Wareham, R. S. Carbohydrate Recognition through Noncovalent Interactions: A Challenge for Biomimetic and Supramolecular Chemistry. *Angew. Chem., Int. Ed.* **1999***, 38*, 2978-2996.

(37)   Inouye, M.; Chiba, J.; Nakazumi, H. Glucopyranoside Recognition by Polypyridine-Macrocyclic Receptors Possessing a Wide Cavity with a Flexible Linkage. *J. Org. Chem.* **1999***, 64*, 8170-8176.

(38)   Coteron, J. M.; Vicent, C.; Bosso, C.; Penades, S. Glycophanes, cyclodextrin-cyclophane hybrid receptors for apolar binding in aqueous solutions. A stereoselective carbohydrate-carbohydrate interaction in water. *J. Am. Chem. Soc.* **1993***, 115*, 10066-10076; Hubbard, R. D.; Horner, S. R.; Miller, B. L. Highly substituted ter-cyclopentanes as receptors for lipid A. *J. Am. Chem. Soc.* **2001***, 123*, 5810-5811.

(39)   Kral, V.; Rusin, O.; Schmidtchen, F. P. Novel Porphyrin-Cryptand Cyclic Systems: Receptors for Saccharide Recognition in Water. *Org. Lett.* **2001***, 3*, 873-876.

(40)   Lorand, J. P.; Edwards, J. O. Polyol complexes and structure of the benzeneboronate ion. *J. Org. Chem.* **1959***, 24*, 769-774.

(41)   Norrild, J. C.; Eggert, H. Boronic acids as fructose sensors. Structure determination of the complexes involved using 1JCC coupling constants. *J. Chem. Soc., Perkin Trans. 2* **1996**, 2583-2588; Sandanayake, K. R. A.; Shinkai, S. Novel molecular sensors for saccharides based on the interaction of boronic acid and amines: saccharide sensing in neutral water. *J. Chem. Soc., Chem. Commun.* **1994**, 1083-1084; Deetz, M. J.; Smith, B. D. Heteroditopic ruthenium(II) bipyridyl receptor with adjacent saccharide and phosphate binding sites. *Tetrahedron Lett.* **1998***, 39*, 6841-6844; Ward, C. J.; Ashton, P. R.; James, T. D.; Patel, P. A molecular colour sensor for monosaccharides. *Chem. Commun.* **2000**, 229-230; Springsteen, G.; Wang, B. Alizarin Red S. as a general optical reporter for studying the binding of boronic acids with carbohydrates. *Chem. Commun.* **2001**, 1608-1609.

(42) Yoon, J.; Czarnik, A. W. Fluorescent Chemosensors of Carbohydrates. A Means of Chemically Communicating the Binding of Polyols in Water Based on Chelation-Enhanced Quenching. *J. Am. Chem. Soc.* **1992***, 114*, 5874-5875.

(43) Nakatani, H.; Morita, T.; Hiromi, K. Substituent Effect on the Elementary Processes of the Interaction between Several Benzeneboronic Acids and Substilisin BPN. *Biochim. Biophys. Acta* **1978***, 525*, 423-428; Juillard, J.; Geugue, N. C. R. Sur La Dissociation de Quelques Acides Arylboriques en Solvants Mixtes Eau-Methanol. *Acad. Paris C* **1967***, 264*, 259-261.

(44) Springsteen, G.; Wang, B. A detailed examination of boronic acid-diol complexation. *Tetrahedron* **2002***, 58*, 5291-5300.

(45) Conner, J. M.; Bulgrin, V. C. Equilibriums between borate ion and some polyols in aqueous solution. *J. Inorg. Nucl. Chem.* **1967***, 29*, 1953-1961.

(46) Wulff, G. Selective binding to polymers via covalent bonds. The construction of chiral cavities as specific receptor sites. *Pure Appl. Chem.* **1982***, 54*, 2093-2102.

(47) James, T. D.; Sandanayake, K. R. A. S.; Shinkai, S. Novel photoinduced electron-transfer sensor for saccharides based on the interaction of boronic acid and amine. *J. Chem. Soc., Chem. Commun.* **1994**, 477-478.

(48) James, T. D.; Sandanayake, K. R. A. S.; Iguchi, R.; Shinkai, S. Novel Saccharide-Photoinduced Electron Transfer Sensors Based on the Interaction of Boronic Acid and Amine. *J. Am. Chem. Soc.* **1995***, 117*, 8982-8987.

(49) Czarnik, A. W. Chemical Communication in Water using Fluorescent Chemosensors. *Acc. Chem. Res.* **1994***, 27*, 302-308.

(50) Connors, K. A. *Binding Constants, The Measurement of Molecular Stability*; Wiley: New York, 1987.

(51) Bissell, R. A.; de Silva, A. P.; Gunaratne, H. Q. N.; Lynch, P. L. M.; Maguire, G. E. M.; McCoy, C. P.; Sandanayake, K. R. A. S. Fluorescent PET (Photoinduced Electron Transfer) Sensors. *Top. Curr. Chem.* **1993***, 168*, 223-264; Czarnik, A. W. Supramolecular Chemistry, Fluorescence, and Sensing. *Fluorescent Chemosensors for Ion and Molecule Recognition*; American Chemical Society: Washington, D. C., 1993.

(52)   de Silva, A. P.; Gunaratne, H. Q. N.; Gunnlaugsson, T.; Huxley, A. J. M.; McCoy, C. P.; Rademacher, J. T.; Rice, T. E. Signaling Recognition Events with Fluorescent Sensors and Switches. *Chem. Rev.* **1997**, *97*, 1515-1566; Bissell, R. A.; de Silva, A. P.; Gunaratne, H. Q. N.; Lynch, P. L. M.; Maguire, G. E. M.; Sandanayake, K. R. A. S. Molecular Fluorescent Signaling with 'Fluor-Spacer-Receptor' Systems: Approaches to Sensing and Switching Devices via Supramolecular Photophysics. *Chem. Soc. Rev.* **1992**, *21*, 187-195.

(53)   Lakowicz, J. R. *Principles of Fluorescence Spectroscopy*; Plenum Press: New York, 1983.

(54)   Wang, W.; Springsteen, G.; Gao, S.; Wang, B. The First Fluorescent Sensor for Boronic Acids and Boric Acids with Sensitivity at Sub-Micromolar Concentrations. *Chem. Commun.* **2000**, 1283-1284.

(55)   Gunnlaugsson, T.; Bichell, B.; Nolan, C. A novel fluorescent photoinduced electron transfer (PET) sensor for lithium. *Tetrahedron Lett.* **2002**, *43*, 4989-4992.

(56)   Ueyama, H.; Takagi, M.; Takenaka, S. A Novel Potassium Sensing in Aqueous Media with a Synthetic Oligonucleotide Derivative. Fluorescence Resonance Energy Transfer Associated with Guanine Quartet-Potassium Ion Complex Formation. *J. Am. Chem. Soc.* **2002**, *124*, ASAP; Takakusa, H.; Kikuchi, K.; Urano, Y.; Sakamoto, S.; Yamaguchi, K.; Nagano, T. Design and Synthesis of an Enzyme-Cleavable Sensor Molecule for Phosphodiesterase Activity Based on Fluorescence Resonance Energy Transfer. *J. Am. Chem. Soc.* **2002**, *124*, 1653-1657.

(57)   Arimori, S.; Bell, M. L.; Oh, C. S.; James, T. D. A Modular Fluorescence Intramolecular Energy Transfer Saccharide Sensor. *Org. Lett.* **2002**, *4*, 4249-4251.

(58)   Aoyagi, T.; Nakamura, A.; Ikeda, H.; Ikeda, T.; Mihara, H.; Ueno, A. Alizarin Yellow-Modified -Cyclodextrin as a Guest-Responsive Absorption Change Sensor. *Anal. Chem.* **1997**, *69*, 659-663.

(59)   Easton, C. J.; Lincoln, S. F. *Modified Cyclodextrins, Scaffolds and Templates for Supramolecular Chemistry*; Imperial College Press: London, 1999; Szejtli, J. *Cyclodextrins and Their Inclusion Complexes*; Akadémiai Kiadó: Budapest, 1982; Wenz, G. Cyclodextrins as Building Blocks for Supramolecular Structures and Functional Units. *Angew. Chem., Int. Ed.* **1994**, *33*, 803-822.

(60) Gonzalez, A. G.; Herrador, M. A.; Asuero, A. G. Acid-Base Behavior of Some Substituted Azo Dyes in Aqueous N,N-dimethylformamide Mixtures. *Anal. Chim. Acta* **1991***, 246*, 429-434; Issa, I. M.; Issa, R. M.; Temerk, Y. M.; Mahmoud, M. R. Reduction of Azo-Compounds-I. Polarographic Behavior of Some 4-Hydroxy-monoazo Compounds at the Dropping Mercury Electrode. *Electrochim. Acta* **1973***, 18*, 139-144.

(61) Klotz, I. M. Spectrophotometric Investigations of the Interactions of Proteins with Organic Anions. *J. Am. Chem. Soc.* **1946***, 68*, 2299-2304; Ohyoshi, E. Spectrophotometric Study of Complexation Equilibria Involving a Metal and Colored and Buffer Ligands by the Competitive Effect of the Two Ligands. *Anal. Chem.* **1985***, 57*, 446-448; Klotz, I. M.; Triwush, H.; Walker, F. M. The Binding of Organic Ions by Proteins. Competition Phenomena and Denaturation Effects. *J. Am. Chem. Soc.* **1948***, 70*, 2935-2941.

(62) Perry, M. J. The Role of Monoclonal Antibodies in the Advancement of Immunoassay Technology. *Monoclonal Antibodies: Principles and Applications*; Wiley-Liss: New York, 1995; pp 107-120.

(63) Koh, K. N.; Araki, K.; Ikeda, A.; Otsuka, H.; Shinkai, S. Reinvestigation of Calixarene-Based Artificial-Signaling Acetylcholine Receptors Useful in Neutral Aqueous (Water/Methanol) Solution. *J. Am. Chem. Soc.* **1996***, 118*, 755-758.

(64) Fabrizzi, L.; Leone, A.; Taglietti, A. A Chemosensing Ensemble for Selective Carbonate Detection in Water Based on Metal-Ligand Interactions. *Angew. Chem., Int. Ed.* **2001***, 40*, 3066-3069; Gale, P. A.; Twyman, L. J.; Handlin, C. I.; Sessler, J. L. A Colourimetric Calix[4]pyrrole-4-nitrophenolate Based Anion Sensor. *Chem. Commun.* **1999**, 1851-1852.

(65) Metzger, A.; Anslyn, E. V. A chemosensor for citrate in beverages. *Angew. Chem., Int. Ed.* **1998***, 37*, 649-652.

(66) Iverson, D. J.; Hunter, G.; Blount, J. F.; Damewood, J. R.; Mislow, K. Static and Dynamic Stereochemistry of Hexaethylbenzene and of Its Tricarbonylchromium, Tricarbonylmolybdenum, and Dicarbonyl(triphenylphosphine)chromium Complexes. *J. Am. Chem. Soc.* **1981***, 103*, 6073-6083; Kilway, K. V.; Siegel, J. S. Effects of Transition-Metal Complexation on the Stereodynamics of Persubstituted Arenes. Evidence for Steric Complementarity between Arene and Metal Tripod. *J. Am. Chem. Soc.* **1992***, 114*, 255-261.

(67) Dietrich, B.; Fyles, D. L.; Fyles, T. M.; Lehn, J.-M. Anion Coordination Chemistry: Polyguanidinium Salts as Anion Complexones. *Helv. Chim. Acta* **1979***, 62*, 2763-2787.

(68) Dietrich, B.; Fyles, T. M.; Lehn, J.-M.; Pease, L. G.; Fyles, D. L. Anion Receptor Molecules. Synthesis and Some Anion Binding Properties of Macrocyclic Guanidinium Salts. *J. Chem. Soc., Chem. Commun.* **1978**, 934-936.

(69) Bramhall, J.; Hofmann, J.; DeGuzman, R.; Montestruque, S.; Schell, R. Temperature Dependence of Membrane Ion Conductance Analyzed by Using the Amphiphilic Anion 5/6-Carboxyfluorescein. *Biochem.* **1987***, 26*, 6330-6340; Graber, M. L.; DiLillo, D. C.; Friedman, B. L.; Pastoriza-Munoz, E. Characteristics of Fluoroprobes for Measuring Intracellular pH. *Anal. Biochem* **1986***, 156*, 202-212.

(70) Cabell, L. A.; Monahan, M.-K.; Anslyn, E. V. A competition assay for determining glucose-6-phosphate concentration with a Tris-boronic acid receptor. *Tetrahedron Lett.* **1999***, 40*, 7753-7756.

(71) Potter, B. V. L.; Lampe, D. Chemistry of Inositol Lipid Mediated Cellular Signaling. *Angew. Chem., Int. Ed.* **1995***, 34*, 1933-1972; Berridge, M. J. Inositol Trisphosphate and Calcium Signaling. *Nature* **1993***, 361*, 315-325.

(72) Leucke, H.; Quiocho, F. A. High Specificity of a Phosphate Transport Protein Determined by Hydrogen Bonds. *Nature* **1990***, 347*, 402-406; Pflugrath, J. W.; Quiocho, F. A. Sulphate Sequestered in the Sulphate-Binding Protein of Salmonella Typhimurium is Bound Solely by Hydrogen Bonds. *Nature* **1985***, 314*, 257-260.

(73) Leonard, M. A.; West, T. S. Chelating Reactions of 1,2-Dihydroxyanthraquinon-3-ylmethyl-amine-N,N-diacetic Acid with Metal Cations in Aqueous Media. *J. Chem. Soc., Dalton Trans.* **1960**, 4477-4485.

(74) Belcher, R.; Leonard, M. A.; West, T. S. The Preparation and Analytical Properties of N,N-Di(carboxy-methyl)aminomethyl Derivatives of Some Hydroxyanthraquinones. *J. Chem. Soc.* **1958**, 2390-2393.

(75) Shallenberger, R. S. *Taste Chemistry*; Blankie Academic and Professional: London, 1993; pp Chapter 1.

(76)   Miller, I. J., Jr. Anatomy of the Peripheral Taste System. In *Handbook of Olfaction and Gustation*; Doty, R. L. Ed.; Marcel Dekker: New York, 1995; pp 521-547.

(77)   Margolskee, R. F. Receptor Mechanisms in Gustation. In *Handbook of Olfaction and Gustation*; Doty, R. L. Ed.; Marcel Dekker: New York, 1995; pp 575-595.

(78)   Mierson, S. Transduction of Taste Stimuli by Receptor Cells in the Gustatory System. In *Handbook of Olfaction and Gustation*; Doty, R. L. Ed.; Marcel Dekker: New York, 1995; pp 597-610.

(79)   Lavigne, J. J.; Savoy, S.; Clevenger, M. B.; Ritchie, J. E.; McDoniel, B.; Yoo, S.-J.; Anslyn, E. V.; McDevitt, J. T.; Shear, J. B.; Neikirk, D. Solution-Based Analysis of Multiple Analytes by a Sensor Array: Toward the Development of an \"Electronic Tongue\". *J. Am. Chem. Soc.* **1998**, *120*, 6429-6430.

(80)   Yoo, S.-J.; Lavigne, J. J.; Savoy, S.; McDoniel, J. B.; Anslyn, E. V.; McDevitt, J. T.; Neikirk, D. P.; Shear, J. B. Micromachined storage wells for chemical sensing beads in an "artificial tongue". *SPIEs Micromachining and Microfabrication 1996 Symposium: Micromachined Devices and Components III*, 1997.

(81)   Kessler, G.; Wolfman, M. An Automated Procedure for the Simultaneous Determination of Calcium and Phosphorus. *Clin. Chem.* **1964**, *10*, 686-703.

(82)   Ray Sakar, B. C.; Chauhan, U. P. S. A New Method for Determining Micro Quantities of Calcium in Biological Materials. *Anal. Biochem.* **1967**, *20*, 155-166.

(83)   Spielman, A. I.; Brand, J. G.; Kare, M. R. *Encycl. Human Biol.*, 1991; 527.

(84)   Schauer, C. L.; Steemers, F. J.; Walt, D. R. A Cross-Reactive, Class Selective Enzymatic Array Assay. *J. Am. Chem. Soc.* **2001**, *123*, 9443-9444.

(85)   Furka, A.; Sebestyên, F.; Asgedom, M.; Dibó, G. General method for rapid synthesis of multicomponent peptide mixtures. *Int. J. Peptide Protein Res.* **1991**, *37*, 487-493.

(86)   Hiratsuka, T., 7442, 496 New ribose-modified fluorescent analogs of adenine and guanine nucleotides available as substrates for various enzymes. *Biochem. Biophys. Acta.* **1983**, *742*, 496-508.

Chapter 2: Teaching Old Receptors New Tricks

2.0 INTRODUCTION

In chapter one, the use of selective versus non-selective receptors was discussed. The point was made that many supramolecular chemists strive to design and synthesize selective receptors that rival the affinity and selectivity of natural receptors such as antibodies or enzymes.[1] While many research groups have had partial success in this endeavor,[2] including our own,[3,4] synthetic receptors are inherently much simpler than their biological counterparts. Therefore, due to this simplicity, they are generally less selective than natural receptors and it is difficult to obtain a high degree of selectivity for complex guests. However, this lack of selectivity can, for some applications, make synthetic receptors more desirable than natural ones. For example, receptors with selectivities for classes of analytes can be used in differential sensor arrays, creating powerful diagnostic tools.

The development of receptor **2.1** illustrates how a receptor that lacked a certain degree of selectivity, can still be a useful chemical sensor.[5] The receptor was designed to be selective for gallate, a tris-hydroxy benzoic acid derivative. When binding studies were performed, it was determined that the receptor was actually selective for a class of analytes similar to gallate.

2.1   gallate
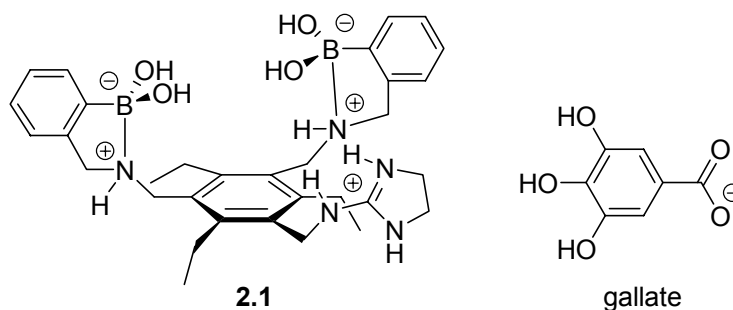
This chapter goes on to discuss the development of a highly selective sensing ensemble which was created through the use of multiple synthetic receptors in solution. Two hosts were chosen that had differential responses to tartrate and malate and to the two indicators that were selected. The simultaneous detection of tartrate and malate was determined through the use of pattern recognition using neural network analysis. The results demonstrate the achievement of a highly selective sensing ensemble through the use of differential receptors which resulted in determination of two structurally similar analytes.

Finally, the incorporation of an analog of receptor **2.1** into a differential sensor array platform will be discussed. Receptor **2.1** was incorporated onto a solid phase resin for incorporation into the array platform. It was found that the receptor was still selective for tartrate over malate. This was all done in preparation of incorporating an enzyme sensing assay into the array, creating a differential sensing platform.

2.1 DEVELOPMENT OF 2.1

2.1.1 Design

The design of receptor **2.1** is based on a scaffold that induces preorganization of the binding sites. The scaffold was again the 1,3,5-trisubstituted-2,4,6-triethylbenzene unit, where the groups attached to the methylene groups alternate up and down around the ring, allowing the binding sites to be sterically preorganized on one face of the benzene ring.[6] This steric gearing has been shown to enhance binding in earlier work, where decreased binding was observed with a similar receptor lacking the ethyl groups (Section 1.6.4.2, compound **1.26**).[4]

The binding sites chosen were designed to target the guest gallate and other similar analytes. Gallate contains a 3,4,5-trihydroxy phenyl group and a carboxylate. Therefore, two phenyl boronic acids with *o*-aminomethyl groups and a guanidinium imbedded in an aminoimidazoline group were incorporated into the design to bind the diols and the carboxylate, respectively. As discussed in Chapter 1 (Section 1.5.3), the boronic acids form reversible, covalent bonds with 1,2- and 1,3-diols in aqueous media[7] making them desirable binding sites in sensors for saccharides and other related analytes. Guanidiniums are known to bind carboxylates through charge pairing and hydrogen bonding interactions (Chapter 1, Section 1.4.3).[8] The proposed binding motif of gallate and **2.1** can be seen in Figure 2.1.
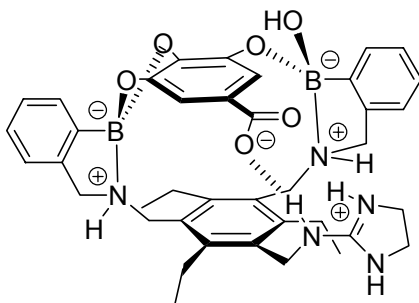
FIGURE 2.1. PROPOSED BINDING MOTIF OF 2.1 AND GALLATE. The carboxylate should charge pair with the guanidinium, while boronate esters are formed between the boronic acids and the catechol functionalities.

2.1.2 Synthesis

The synthesis of receptor **2.1** began with electrophilic aromatic substitution on the commercially available 1,3,5-triethylbenzene (**2.2**) with paraformaldehyde in refluxing acetic acid and hydrobromic acid (Scheme 2.1).[4] The bis-bromo methylene substituted product (**2.3**) was first isolated, and subjected to substitution conditions again with paraformaldehyde, potassium bromide, and sulfuric acid refluxing, to obtain the tris bromomethyl substituted product **2.4**. The yield was rather low over the two step procedure. This product was taken on to the tris azide compound (**2.5**) through nucleophilic displacement of the bromides with azides in near quanitative yields.

Scheme 2.1
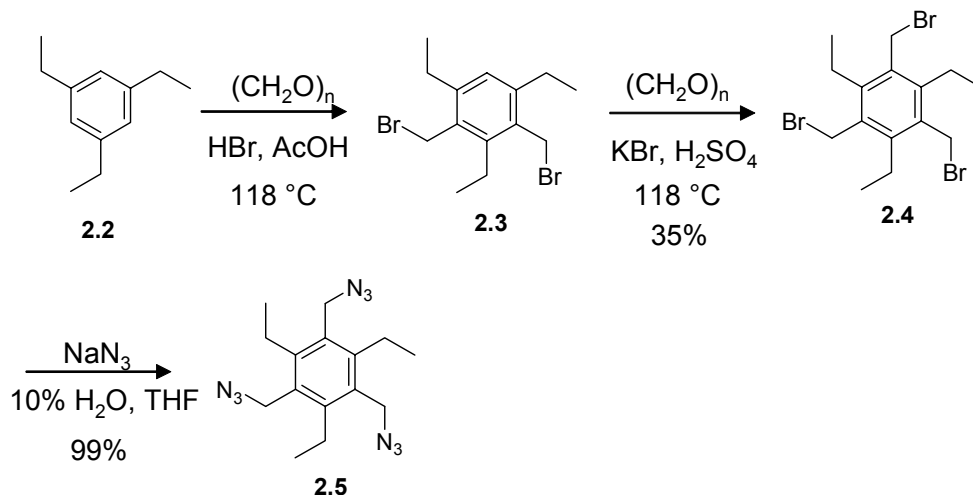
The synthetic route shown in Scheme 2.1 to obtain product **2.5** had been proven to work over the years, but there were a few problems associated with it. To obtain the tris halogenated product, the synthesis was performed over two steps, and the resulting yield was rather low. The formation of **2.5** also needed improvement, not due to low yields, but due to the dangerous use of water with the sodium azide. Through the work of Dr. Robert Hanes, the synthetic route shown in Scheme 2.2 was developed.[9] The tris chloro product (**2.6**) was now the target through electrophilic aromatic substitution using chloromethylmethyl ether and tin tetrachloride. The reaction proceeded well, resulting in yields in the high seventies. High yields were still obtained for the nucleophilic displacement with sodium azide even though the solvent was changed from water/THF mixtures to DMF.

Scheme 2.2
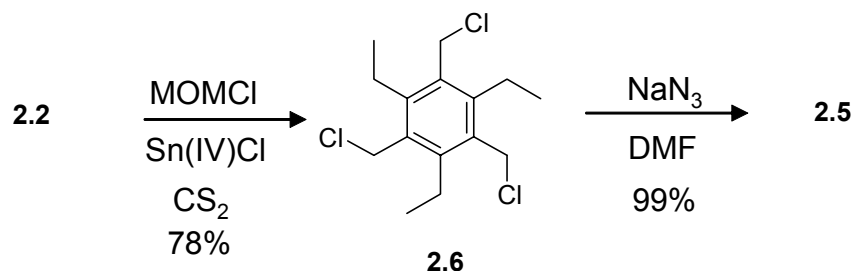
Subsequent reduction of the azides of **2.5** with triphenylphosphine and water through a Staudinger reduction[10] resulted in compound **2.7**. In order to put boronic acids and a guanidinium on the scaffold, two of the nitrogens needed to be protected. The protecting group chosen was the *t*-butyl carbamate or the BOC group. The addition of di-*t*-butyl dicarbonate to **2.7**, resulted in a statistical mixture of four different products, that ranged from the tris protected amine to the tris free amine. The bis-BOC protected compound **2.8** was the product desired, which was obtained in 28% yield.

Scheme 2.3
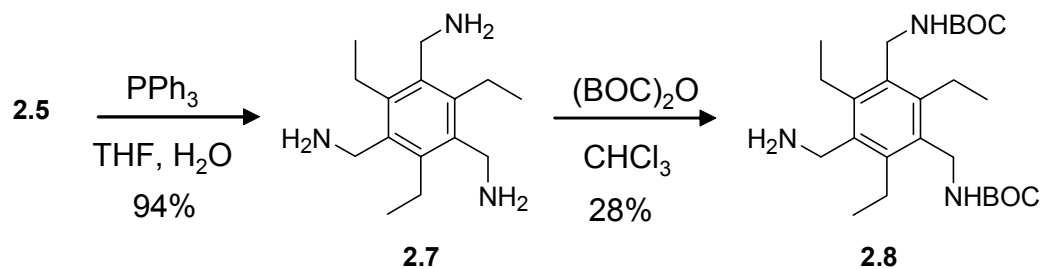
The next step was to incorporate the guanidinium binding site. The acetic acid salt of **2.8** and free based 2-methylthio-2-imidazoline (**2.9**) were ground together, placed in a conical vial, and heated to 80 °C for three days. This solid melt resulted in compound **2.10** in only 37 percent yield. The removal of the BOC protecting groups was accomplished with trifluoroacetic acid, and the counter ions were exchanged to acetates to give **2.11**.

Scheme 2.4
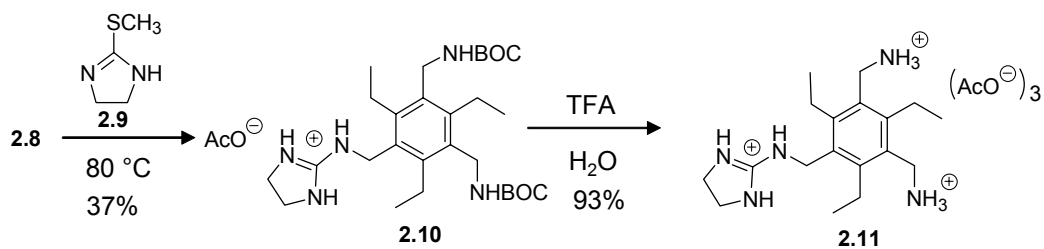
Due to the difficulty in purifying a water soluble compound through reverse phase chromatography, and the low yields in obtaining **2.10**, a new route of obtaining the guanidinium was pursued (Scheme 2.5). This new route coupled

Scheme 2.5

76
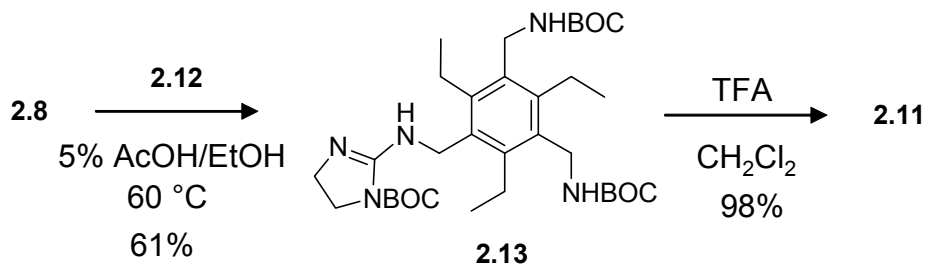
the free amine of bis-BOC protected **2.8** with an N-BOC protected imidazoline derivative (**2.12**), which was synthesized through a BOC protection of 2-methylthio-2-imidazoline hydroiodide (Scheme 2.6).[11] The coupling produced

Scheme 2.6
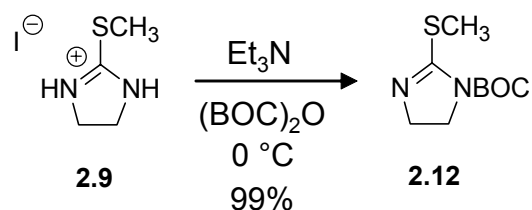
the BOC protected guanidine **2.13** more efficiently, and purification was more facile than in the guanidinium formation. Deprotection of all three BOC groups of **2.13** was accomplished with trifluoroacetic acid to give **2.11** in near quantitative yields. The anions were all exchanged to acetates to determine the protonation state of **2.11**. The final step to obtain **2.1** was a reductive amination with 2-formylbenzene boronic acid (**2.14**) and **2.11** (Scheme 2.7).

Scheme 2.7
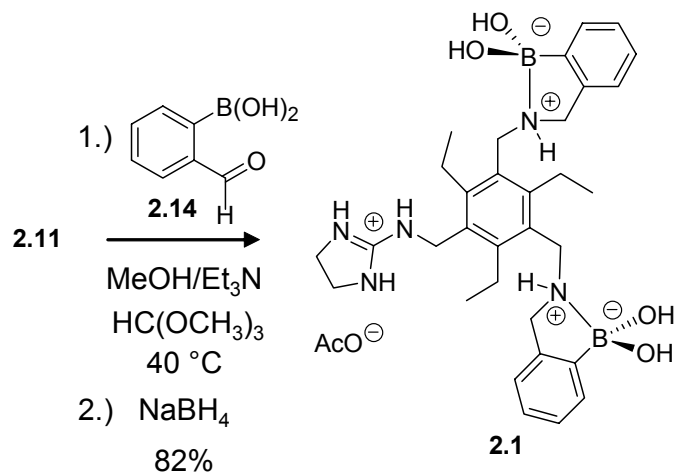
2.2   INVESTIGATION INTO THE AMINE ADJACENT TO THE BORONIC ACID

The binding of boronic acids with alkane diols was discussed in Chapter 1 (Section 1.5.3). The formation of boronate esters is facile in basic aqueous media when the boron is tetrahedral. Wulff[7] discovered that the incorporation of an amine adjacent to the boronic acid forms an sp^3 boron at or near neutral pH, due to the intramolecular coordination of the amine with the boron. This boron-nitrogen interaction raises the boronic acid's pK_a from near nine[12] to near twelve, and can lower the pK_a of a tertiary ammonium ion from around nine to near five. Many boronic acid receptors exist that incorporate an adjacent tertiary amine. The intramolecular coordination between a tertiary amine and a boronic acid not only improves the kinetics of exchange, but can also be used to modulate photoinduced electron transfer (PET), leading to a sensing application. For

78

example, Shinkai's sugar sensor **2.15** is a boronic acid linked to an anthracene moiety *via* a proximal tertiary amine.[13] The amine is able to quench the receptor's fluorescence through PET, even though it is involved in the boron-nitrogen interaction. Upon complexation with a sugar, the fluorescence of the anthracene is regenerated as the formation of the boronate ester increases the Lewis acidity of the boron, decreasing the PET.
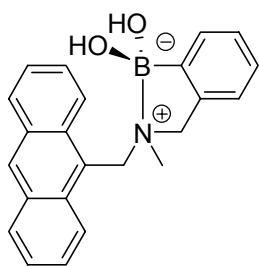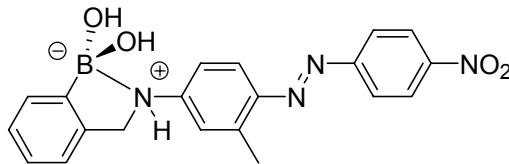
2.15   **2.16**

Recently, a secondary amine has been used in a non-fluorescent boronic acid sensor. James and coworkers synthesized a colorimetric sensor (**2.16**) for saccharides.[14] The host was generated by covalently attaching an azo dye to a phenyl boronic acid through a proximal secondary amine. The use of an aniline nitrogen gave a color change due to deprotonation upon sugar complexation.

Due to the incorporation of a secondary amine adjacent to a boronic acid in receptor **2.1** and other receptors from the Anslyn group such as **1.34** (Section 1.6.4.6) and **2.17**,[15,16] the structure of the amine needed to be investigated. In these receptors, dye displacement strategies were used to signal the presence of guests[17] as compared to the covalently attached signaling moieties of **2.15** and **2.16**. In our systems, the role of the secondary amine is both structural and

electronic, preorganizing the cavity and enhancing the kinetics of exchange, respectively.

1.34   **2.17**
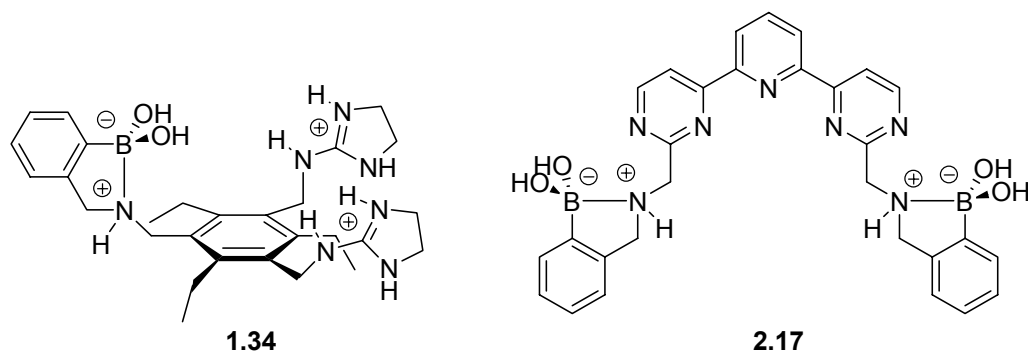
While several examples exist which locate tertiary amines adjacent to boronic acids for sensing applications, few are available that incorporate secondary amines. The utility of this latter combination raises questions pertaining to the pK_a of the secondary ammonium ion relative to its tertiary counterpart (i.e. the strength of the B-N interaction at neutral pH) as well as the geometry found at the boron and nitrogen centers with varying pH.

To address the questions concerning pK_as, model compounds **2.18** and **2.19** were synthesized. With these compounds, there are several equilibria to consider. The first pK_a is undoubtedly deprotonation of the ammonium ion in **2.18a** (Scheme 2.8A). The second pK_a can be attributed to either another

2.18   **2.19**
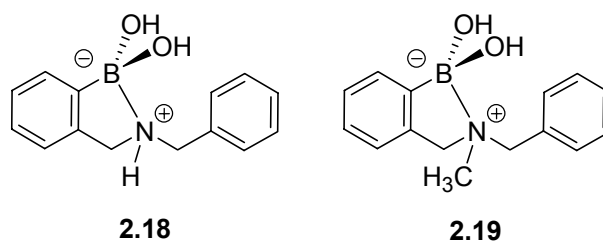
deprotonation of the amine (**2.18b** to **2.18d**) or coordination of hydroxide to the boronic acid (**2.18b** to **2.18c**). We expected that the pK_a of the amine **2.18b** should be above that of an alkyl ammonium since the

Scheme 2.8

A

2.18 a   2.18 b   2.18 c

2.18 d   2.18 e

B

2.19 a   2.19 b   2.19 c
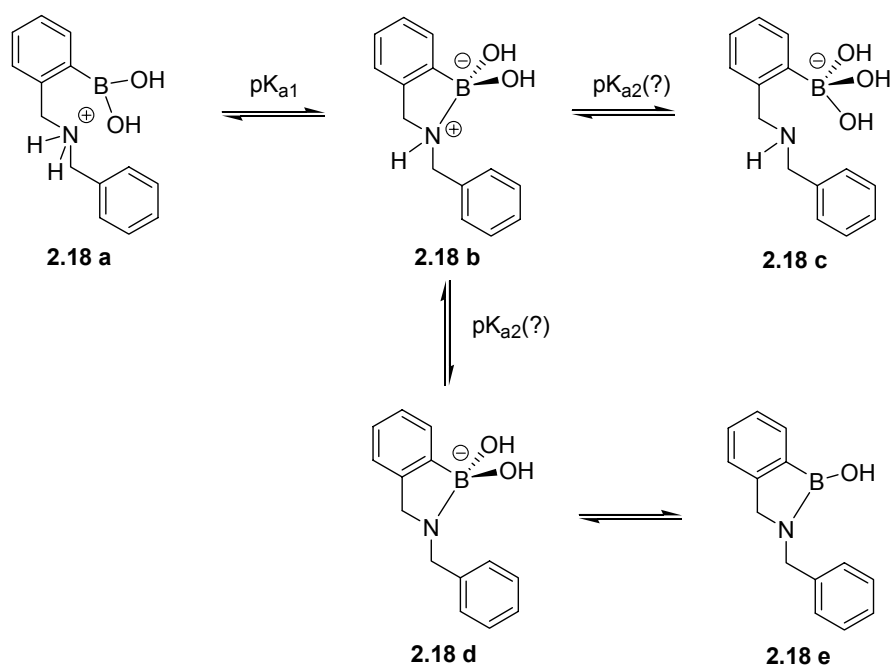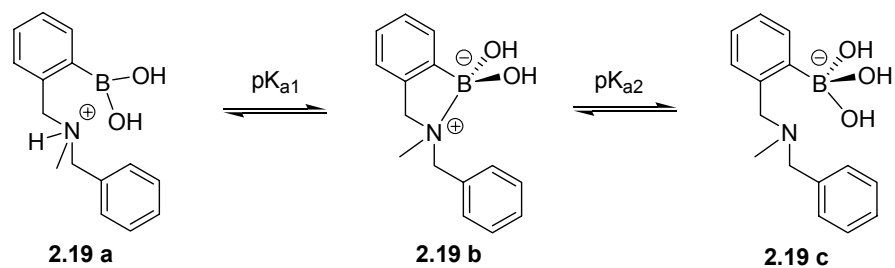
lone pair has no ability to delocalize and is near a negative charge, yet this needed to be confirmed. If the second deprotonation is of the amine, this could lead to hydroxide elimination to give **2.18e**, which can be found under dehydrating conditions.[18] This would not be evident in a potentiometric titration since it is formally the elimination of water, although it would be evident in a ^{11}B NMR spectrum, where changes in the hybridization of the boron are reflected in its chemical shift. Importantly, if **2.18e** does dominate at neutral pH, it would not be as effective for binding diols in sensing applications as is a tertiary amine analog.

The equilibria available to the analogous tertiary model (**2.19**) is much simpler (Scheme 2.8B). Deprotonation of the ammonium ion (**2.19a** to **2.19b**) and coordination of hydroxide (**2.19b** to **2.19c**) can be assigned to the first and second pK_a, respectively.[7] Given the equilibria presented in Scheme 2.8, potentiometric titrations were performed and ^{11}B NMR versus pH studies were done on **2.18** and **2.19** to probe the pK_a values and the geometries at boron as a function of pH.

2.2.1   Synthesis of Model Compounds

Secondary model **2.18** was prepared in one step through a reductive amination between benzyl amine and 2-formylbenzene boronic acid (**2.14**) (Scheme 2.9) to afford the product in high yield. Tertiary model **2.19** was prepared (Scheme 2.10) in a similar procedure to Shinkai's[13,19] approach by

Scheme 2.9
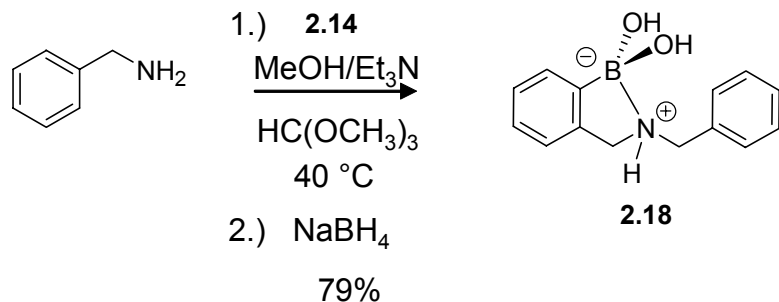
protecting the boronic acid of 2-methylbenzene boronic acid (**2.20**) with neopentyl glycol to obtain essentially 100% protected boronic acid (**2.21**) as a clear oil. The methyl group was then brominated to obtain **2.22**, where the low yield of 31% resulted from over bromination and difficulty in product purification.

Scheme 2.10
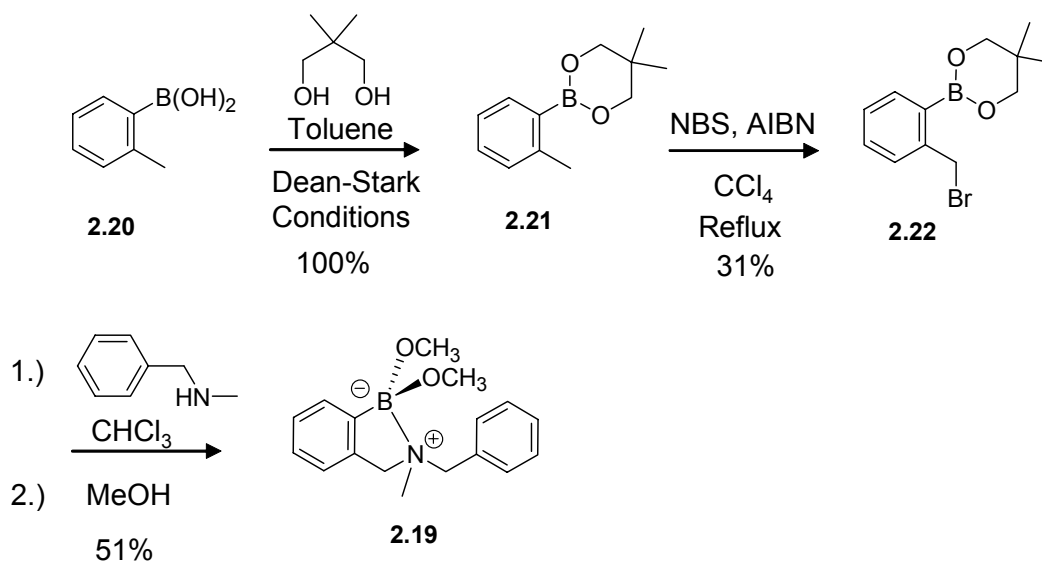
Subsequently the bromine was displaced through nucleophilic substitution by *N*-methyl benzylamine. The boronic acid was deprotected by hydrolysis on silica gel and eluted with methanol to obtain **2.19** with a yield of 50%.[20]

2.2.2   pH Titrations

Potentiometric titrations were performed to determine the first pK_a values associated with **2.18a** and **2.19a**. These values were obtained with the help of Dr. James W. Canary at New York University and his graduate student Yu Hung Chiu. The pK_a of an ammonium generally ranges between 9 and 10, but a boronic acid adjacent to an ammonium will lower that significantly. The titration curves for both models are shown in Figure 2.2 and the equilibrium constants were determined with Martell's program BEST.[21] From these curves, a pK_a of 5.7 was found for **2.19a**, which is comparable to the known value of 5.2 for a dimethyl ammonium ion adjacent to a boronic acid.[7] The titration of the secondary model **2.18a** produced a value of 5.3 for its pK_a. Hence, the pK_a values determined from the potentiometric titrations of **2.18a** and **2.19b** are quite similar.[22]
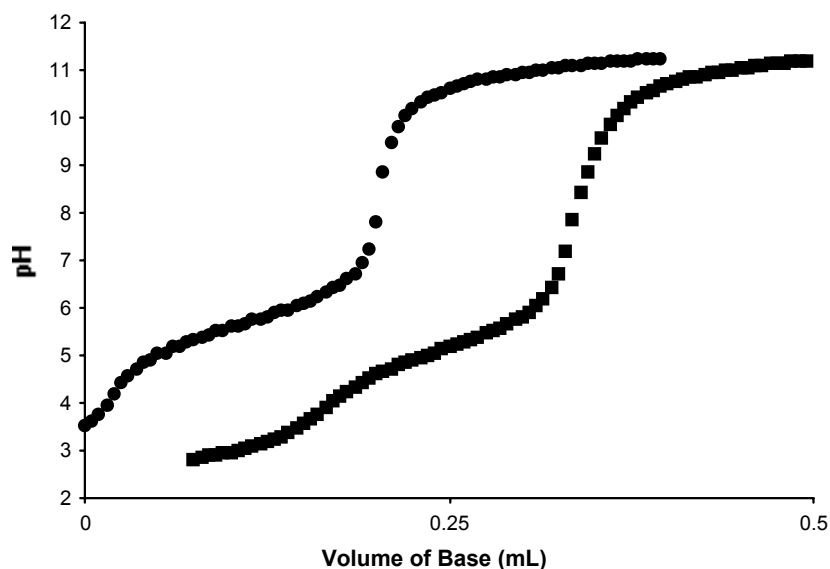
FIGURE 2.2. PH PROFILE OF 2.18 (■) AND 2.19 (●) upon addition of base. (0.15 M NaCl in water, 0.1 M NaOH, and 4.5 mM (initial) **2.18** and **2.19**) The titration of **2.18** started with a higher concentration of acid and the first few data points were excluded.

2.2.3 ^{11}B NMR Investigations

In an effort to better understand the geometry at boron, the ^{11}B NMR spectra of **2.18** and **2.19** were recorded as a function of pH (Figure 2.3).[23] It is known that changes in hydridization of boron can be seen in changes of the chemical shift of ^{11}B NMR spectra. When boron is tetrahedral, its chemical shift is upfield from that of the trigonal planar geometry, where pure sp^3 and sp^2 are approximately 0 and 30 ppm respectively.[24] In our studies, both compounds **2.18** and **2.19** showed shifts from approximately 30 to 10 ppm as the pH was raised.

85

This indicates that the boron centers in both the secondary and the tertiary model compounds are trigonal planar at low pH and upon increasing the pH they become tetrahedral, with pK_a values of 5.2 and 5.8 respectively. These values are in agreement with those determined by potentiometric titrations. Further, at neutral pH the chemical shifts found for **2.18** and **2.19** are near identical. Since we are confident in the assignment of form **2.19b** at neutral pH for the tertiary model, it indicates that the proper form for the secondary counterpart is **2.18b** at this pH. This data therefore signifies that the dominant forms of the secondary and tertiary compounds near neutral pH are **2.18b** and **2.19b** respectively.
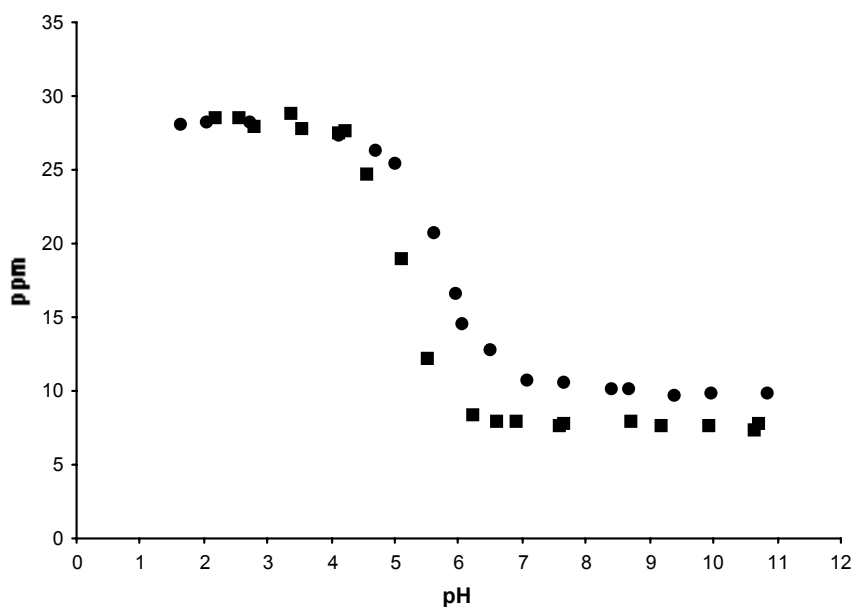
FIGURE 2.3. ¹¹**B NMR CHEMICAL SHIFTS OF MODEL COMPOUNDS 2.18 (■) AND 2.19 (●)** with increasing pH. (10% d$_4$-methanol in water, 40 mM **2.18** and **2.19**, 40 mM NaCl) Referenced to Et$_2$O•BF$_3$ in toluene as zero.

2.2.4   Crystal Structures

To further investigate the geometry of the boron center of **2.18** near neutral pH, a crystal structure was obtained. Crystallographic quality crystals were grown from pure methanol (Figure 2.4). As can be seen, the nitrogen has added into the boron, making the boron tetrahedral, and more conducive to binding. The protonation state of the nitrogen can also be seen, where the hydrogen on the nitrogen is still present,[25] allowing the secondary nitrogen and the boron to form a zwitterionic complex, with a B-N bond length of approximately 1.665 Å.[26]
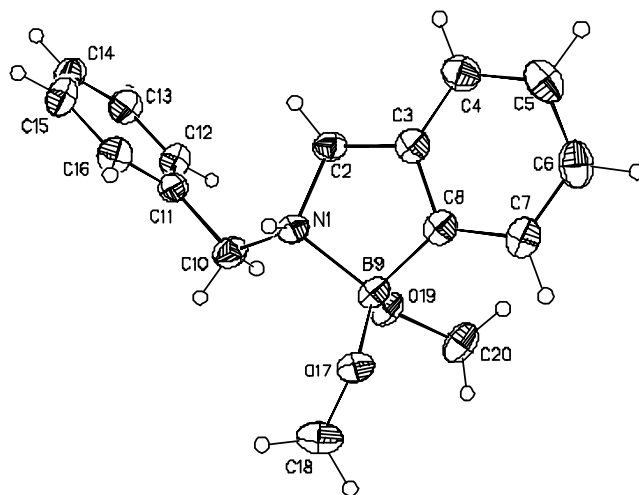
FIGURE 2.4. CRYSTAL STRUCTURE OF 2.18 showing the atom labeling scheme. Displacement ellipsoids are scaled to the 50% probability level.

As further evidence, Hassan Ait-Haddou obtained a crystal structure of the polyaza compound **2.17** (Figure 2.5). Importantly, the boron is tetrahedral, as is the coordinated nitrogen, and the B-N bond lengths are about 1.669 Å.[27] ^{11}B NMR of the crystals provide a chemical shift of 9.4 ppm, consistent with our assignment of form **2.18b** at neutral pH.
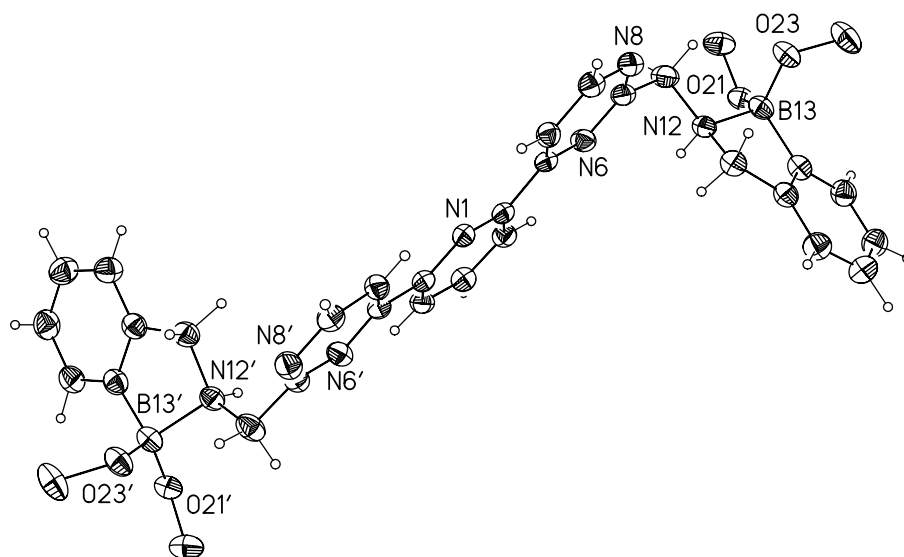
FIGURE 2.5. **CRYSTAL STRUCTURE OF 2.17** showing a partial atom labeling scheme. Thermal ellipsoids are scaled to the 50% probability level. Hydrogen atoms shown are drawn to an arbitrary scale. The molecule lies on a crystallographic two-fold rotation axis bisecting the pyridine ring and passing through N1. Atoms with labels appended by ' are related by -x, y, 1/2 - z. The protons on the amines were located and refined in the crystal structure.

In conclusion, it was determined that the pK_a values of secondary ammoniums adjacent to boronic acids are comparable to the analogous tertiary amines. Further, at neutral pH, form **2.18b** dominates. Therefore, secondary amines can be used to coordinate boronic acids for sensor applications with geometries appropriate for the complexation of 1,2- and 1,3-diols, as is routinely done with tertiary amines. Undoubtedly there will be a difference in the extent of PET between a tertiary and secondary amine that can be exploited for sensor applications,[28] but the use of secondary and tertiary amines are essentially the same with regards to complexation geometry and pH dependence.

2.3   BINDING TARGETS OF RECEPTOR 2.1

As was discussed earlier, receptor **2.1** was designed to bind gallate, a tris hydroxy benzoic acid derivative. This analyte is found in scotch whiskies along with other similar analytes due to the aging process. Fine scotch whiskies are required to age for a period of time in oak barrels or casks before they are ready for consumption. This aging process is known to affect the flavor and color of the beverage through extraction of phenolic acids from the wood.[29,30] Some examples are ellagic acid, protocatechuic acid, cafeic acid, and gallic acid (shown below). The amount of gallic acid present in scotch whiskey is considered to be an indication of age, since it is generated through the hydrolysis of tannins over time.[30] However, the concentration of these other "gallate-like" compounds can also act as an indicator of the age of the scotch whiskey. Other factors that

determine the concentration of gallic acid and analogs incorporated into the spirit depend on the type of wood, how many times the casks have been used, and what they were used for. Therefore, the exact level of any specific compound can only be roughly related to age. Yet, gallate is currently the compound most often quantified.

gallic acid

3,4-dihydroxybenzoic acid

caffeic acid

4-hydroxycinnamic acid

ellagic acid
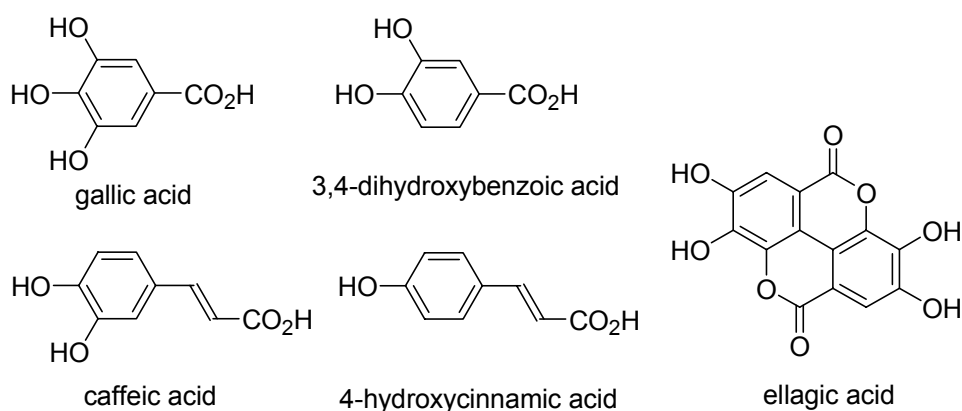
2.3.1 Choosing the Indicator for the Sensing Ensemble

In order to perform binding studies with receptor **2.1**, a way to signal binding needed to be incorporated. The method chosen for receptor **2.1** was an indicator displacement assay. As you recall from Chapter 1 (Section 1.6.4), an indicator is associated with the host, and upon addition of an analyte, the indicator is displaced from the cavity causing a signal modulation. It was expected that the microenvironment change upon binding the indicator to the host would cause a change in its absorbance in a manner similar to increasing the pH, since the positive microenvironment of the binding pocket was expected to lower the pK_a

of the phenol of the indicators. A few different indicators with similar functionalities to gallate were investigated to determine which one would work the best. Figure 2.6 shows the structures of the indicators and the UV/visible spectrum upon addition of increasing amounts of **2.1**. The three shown are alizarin complexone (**1.35**), bromopyrogallol red (**2.23**), and pyrocatechol violet (**2.24**). Other indicators that were examined were alizarin yellow, pyrogallol red, Evan's blue, alizarin, bromochlorophenol blue, and bromocresol purple. All of them except pyrogallol red essentially exhibited no response upon addition of **2.1**. Pyrogallol red was not used because it decomposed easily.

Alizarin complexone is used for the determination of pH, fluoride ions, and some rare-earth metals[31] and was used as the signaling indicator with the tartrate/malate sensing ensemble in Chapter 1 (Section 1.6.4.6).[16] It was chosen to try with **2.1** due to its similar functionalities to gallate, since **1.35** also possesses carboxylates and hydroxy phenyl groups. Upon addition of **2.1** to a solution of **1.35** (0.18 mM) in 75% methanol in water (v/v), the maroon indicator solution turned yellow as the indicator became bound in the binding pocket of the receptor (Figure 2.6A).

Bromopyrogallol red is also a pH indicator that is used in the spectrophotometric determination of various metals such as yttrium and cerium.[32] The presence of catechols for binding to the boronic acids, as well as a sulfonate for charge pairing with the guanidinium, made it a good indicator to investigate with **2.1**. Upon formation of a complex between **2.23** (0.02 mM) and **2.1**, the

absorbance of the indicator decreases at 570 nm (Figure 2.6B) resulting in a change in color from purple to pink.

A.

B.

C.
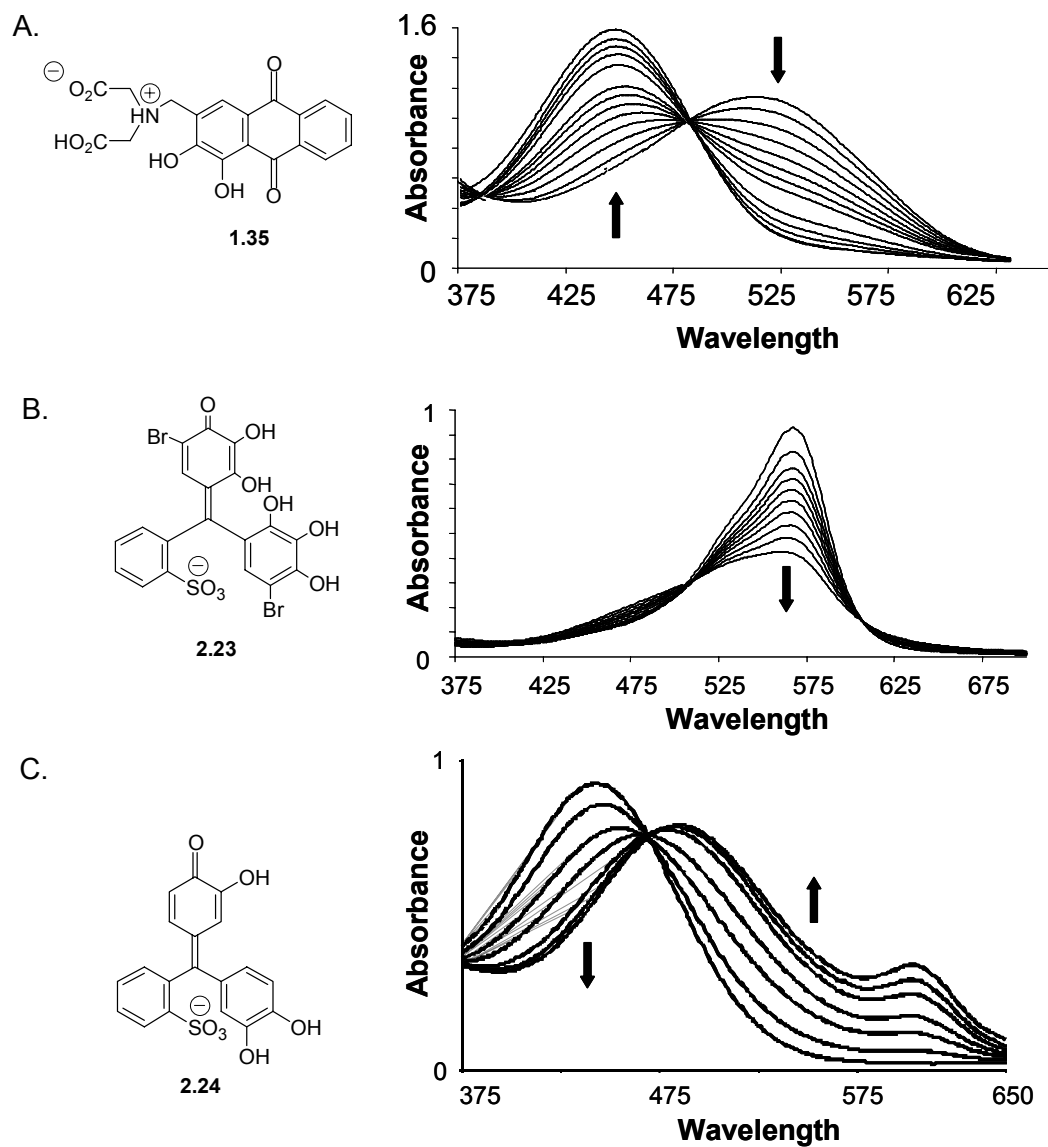
FIGURE 2.6. UV/VIS SPECTRUM OF INDICATORS TESTED WITH RECEPTOR 2.1. A. Alizarin Complexone (**1.35**) B. Bromopyrogallol Red (**2.23**) C. Pyrocatechol Violet (**2.24**) (10 mM HEPES buffer, 75% methanol in water, pH 7.4).

Finally, pyrocatechol violet, a colorimetric indicator commonly used for the determination of tin and bismuth,[33] was also explored, for the same reasons **2.23** was chosen. Figure 2.6C shows the absorbance changes associated with **2.24** (0.06 mM) upon complexation with receptor **2.1**. The free indicator is yellow at pH 7.4 in 75% methanol in water and upon binding **2.1** the color changes to maroon which resulted in the λ_{max} absorbance shifts from 442 nm to 488 nm. Next, the binding affinities of each of these ensembles were investigated.

2.3.2 Determination of Binding Affinities between Indicators and 2.1

The data for each of the above titrations was fit with a 1:1 binding algorithm,[34] but only one example will be discussed here, the interaction of **2.1** and **2.24**. The binding of **2.1** and **2.24** was defined through Eq. 2.1, where I = indicator and L = host. Absorbance is defined with Beer's law, and through a

$$I + L \rightarrow IL \qquad \qquad \text{Eq. 2.1}$$
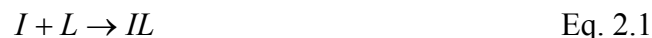
derivation of equations using the mass balance equations of indicator and ligand and the equilibrium constants, the free ligand (L_i) can be calculated using the quadratic equation (Eq. 2.2), where I_t is the total indicator concentration, K_1 represents the binding constant, and L_t refers to the total ligand concentration.

$$K_1[L_i]^2 + (1 - K_1[L_t] + K_1[I_t])[L_i] - [L_t] = 0 \qquad \text{Eq. 2.2}$$

The free ligand concentration is then used in the final binding isotherm (Eq. 2.3).

$$\frac{\Delta A}{b} = \frac{\Delta \varepsilon K_1[L_i][I_t]}{1 + K_1[L_i]} \qquad \text{Eq. 2.3}$$

The calculated delta absorbance and the actual delta absorbance were plotted against the concentration of host. The binding constant (K_1) and the delta molar absorptivity ($\Delta \varepsilon$) were iterated until the best fit of the data was obtained (Figure 2.7). This gave a binding constant of 6.2 x 10^4 M^{-1} in 75% methanol in water (v/v) at pH 7.4 for **2.1** and **2.24**. The association constant of **2.1** to **1.35** was
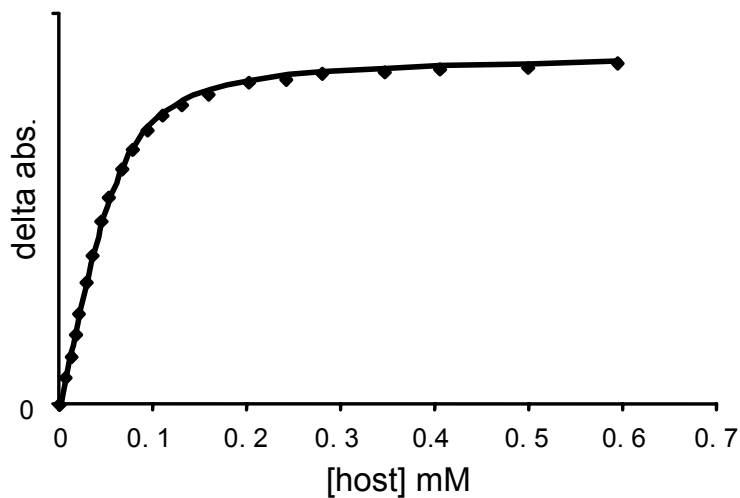
FIGURE 2.7. **UV/VIS STUDY FOR ASSOCIATION OF 2.1 AND 2.24** The curve fitting analysis of the binding of **2.1** and **2.24** using a 1:1 binding algorithm. The data was taken at 510 nm (75% methanol in water (v/v), 10 mM HEPES, pH 7.4).

determined to be 9.0 x 10^4 M^{-1}, while the affinity between **2.1** and **2.23** was calculated to be 5.3 x 10^4 M^{-1}. Pyrocatechol violet was the indicator that was chosen out of the three. The binding of **1.35** to **2.1** was investigated because it was known to work before, yet we were looking for a new indicator. Pyrocatechol violet was chosen over bromopyrogallol red because a color change was more desirable than just an intensity decrease, which is essentially all that **2.23** displayed.

The absorbance of pyrocatechol violet was investigated at a variety of different pH values (Figure 2.8). Between pH 1 and 7, the indicator is yellow in solution. Upon further deprotonation, the indicator becomes purple. When **2.24**
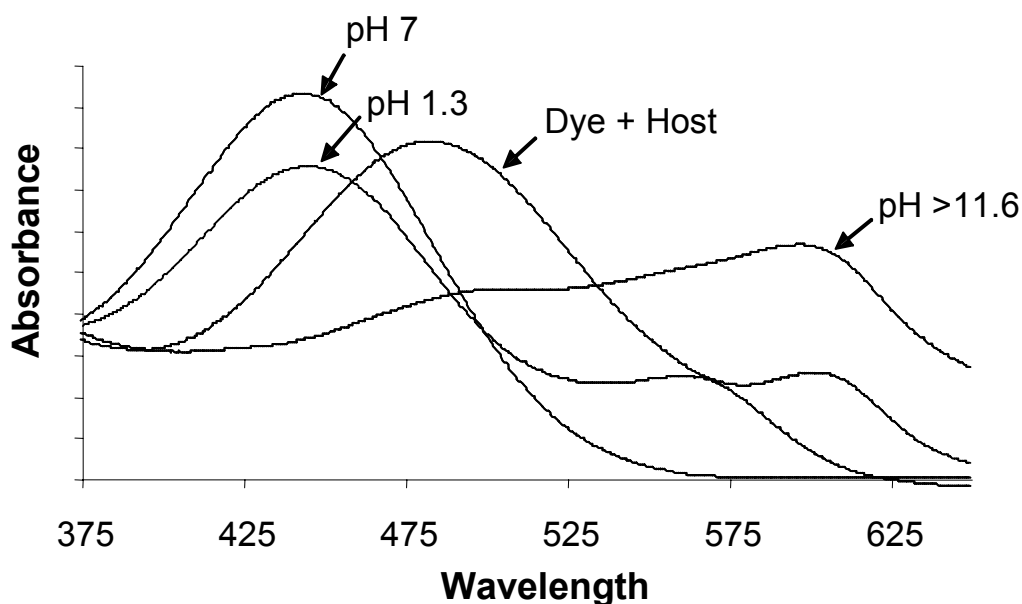
FIGURE 2.8. THE ABSORBANCE OF PYROCATECHOL VIOLET AT DIFFERENT PH VALUES. Pyrocatechol violet is yellow at low pH and becomes blue/violet at high pH. The absorbance of the dye/host complex (**2.1**/**2.24**) shifts toward the absorbance at higher pH.

95

is complexed by **2.1** it displays a maroon color, which is in between the absorbances at pH 7 and near 12, suggesting that when the indicator is bound, the change in microenvironment is similar to an increase in pH.

2.3.3 Determining Analyte Binding Constants with the Competition Assay

A competition assay is the next step to determine the binding constant of the guests to **2.1**. All the assays work in a similar manner, but only one specific example will be discussed here. Upon addition of gallate to a solution of **2.1** and **2.24** at constant concentration and pH (Figure 2.9), the absorbance spectra shifted
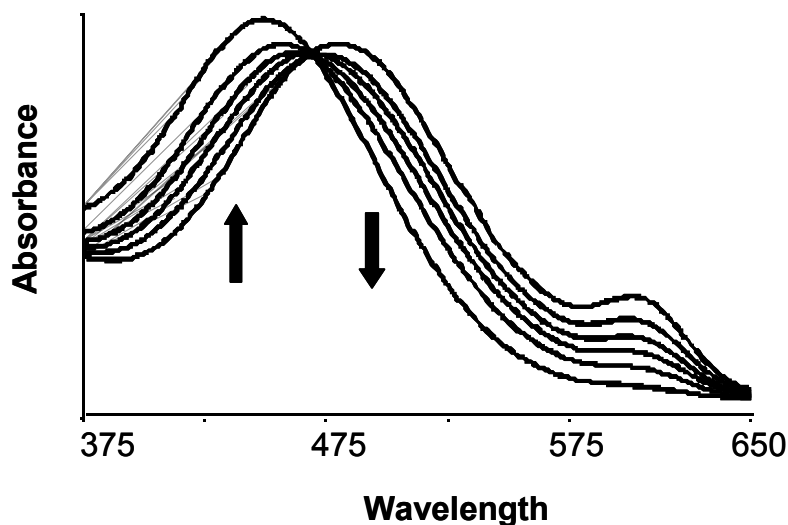
FIGURE 2.9. UV/VIS SPECTRUM OF COMPETITION ASSAY. The absorbance of the sensing ensemble **2.24**-**2.1** upon addition of increasing amounts of gallate. The absorbance decreases at $\lambda = 488$ nm and increases at $\lambda = 442$ nm is a result of the indicator being displaced back into solution. Both **2.1** and **2.24** are at constant concentration. (10 mM HEPES, 75% methanol in water, pH 7.4)

96

back towards 442 nm, as the indicator was displaced from the cavity. The determination of the binding constant is more complicated than the indicator/receptor association because the equilibria between the guest (S) and the indicator host complex (IL) now exists (Eq. 2.4), along with the equilibria from Eq. 2.1.[34]

$$IL + S \rightarrow SL + I \qquad\qquad \text{Eq. 2.4}$$

For a graphical approach to determining a binding constant between gallate and **2.1** (K_{11}), the mass balance equations and the equilibrium constants were used to derive the equations defined by P (Eq. 2.5) and Q (Eq. 2.6).[34] Q is termed the indicator ratio, and can be obtained through the absorbances of the free (A_I) and bound indicator (A_{IL}). These two equations are then used to derive Eq. 2.7, which defines the equation of a line (y=mx+b), where y is $[S_t]/P$, x is Q, b is 1, and the

$$P = \frac{K_{11}[S_t]}{K_1 Q + K_{11}} \qquad\qquad \text{Eq. 2.5}$$

$$Q = \frac{A - A_{IL}}{A_I - A} \qquad\qquad \text{Eq. 2.6}$$

$$\frac{[S_t]}{P} = \frac{K_1}{K_{11}} Q + 1 \qquad\qquad \text{Eq. 2.7}$$

slope is the ratio of the binding constant of **2.1**-**2.24** (K_1) over **2.1**-gallate (K_{11}). The data was subsequently fit by varying the value of A_{IL} until the Y-intercept was 1 (Figure 2.10), and K_{11} was determined to be $1.0 \times 10^4 \text{ M}^{-1}$.
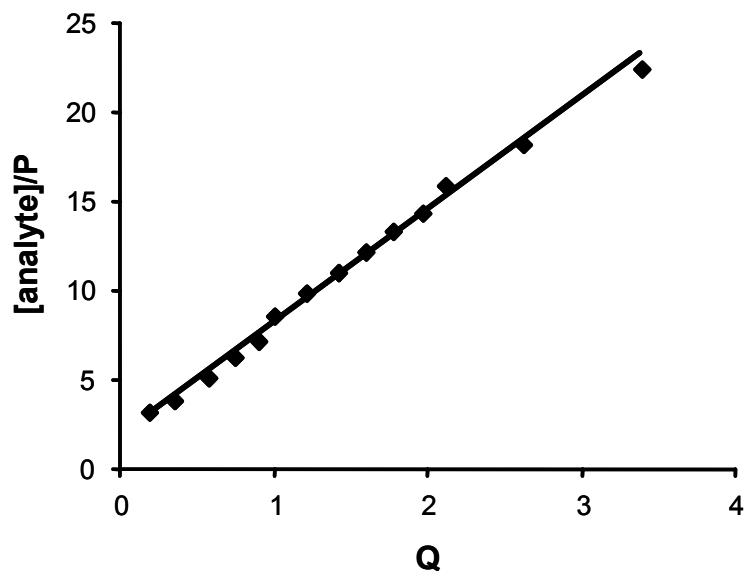
FIGURE 2.10. DETERMINING ASSOCIATION CONSTANTS FOR COMPETITION ASSAY. Analysis of Eq. 2.7 for determining the binding constant of **2.1** to gallate using a competitive binding algorithm. The data was taken at 605 nm (75% methanol in water (v/v), 10 mM HEPES buffer, pH 7.4).

Other analytes tested using this sensing ensemble included the aforementioned ellagic acid (no K_a determined),[35] 3,4-dihyroxybenzoic acid ($4.5 \times 10^3 \text{ M}^{-1}$), caffeic acid ($3.9 \times 10^3 \text{ M}^{-1}$), and 4-hydroxycinnamic acid ($<1 \times 10^2 \text{ M}^{-1}$), along with fructose ($4.0 \times 10^2 \text{ M}^{-1}$), and acetate ($<1 \times 10^2 \text{ M}^{-1}$). Some of their calibration curves are shown in Figure 2.11. The sensing ensemble shows selectivity for the analytes that possess both diols and carboxylates, but shows

little response to fructose, 4-hydroxycinnamic acid, and acetate. Looking at the affinity constants more closely, when one hydroxyl group is removed from gallate (3,4-dihydroxybenzoate) the affinity constant only drops by a factor of two. If the analyte is increased in length, 3,4-dihydroxybenzoate versus caffeic acid, the affinity constant essentially remains the same. The polyol fructose had a higher affinity than the mono-hydroxycinnamic acid, showing the importance of the diol interaction with the boronic acids. Due to the receptor's varied affinities for the entire class of analytes, it was determined that the sensing ensemble would not be able to quantify one particular analyte in the presence of similar analytes, but would bind the entire class of analytes.
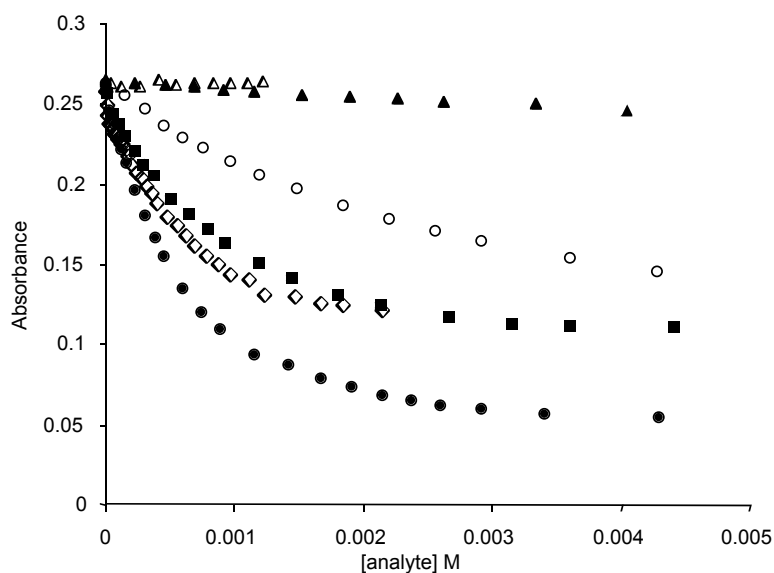
FIGURE 2.11. UV/VIS CALIBRATION CURVES WITH THE 2.1 SENSING ENSEMBLE The change in absorbance of the ensemble **2.1** (0.26 mM) and **2.24** (0.06 mM) upon addition of the analytes: gallate (●), 3,4-dihydroxybenzoic acid (◇), 3,4-dihydroxycinnamic acid (■), 4-hydroxycinnamic acid (Δ), fructose (○), and acetate (▲). (25% water in methanol (v/v), 10 mM HEPES, pH 7.0).

99

2.4   SCOTCH WHISKEY AND TEA ANALYSIS

The sensing ensemble **2.1-2.24** was used to evaluate several different scotch whiskies that had been aged between 5 and 16 years. In order to have the scotch whiskies as similar as possible in regards to production and materials, Islay scotches were chosen. Islay refers to a Scottish island. It was expected that the sensor response would correlate with the age of the scotch whiskey due to an overall response to the aforementioned class of compounds that contain diols and carboxylates.   Upon addition of microliter quantities of scotch whiskey, a "response number" was determined from the single calibration curve of gallate

TABLE 2.1. SENSING ENSEMBLE (2.1-2.24) ANALYSIS AND HPLC ANALYSIS OF SCOTCHES.

Single Islay Malt Whiskies	Age Years	UV/Vis Analysis "response number" (mM)	HPLC Analysis gallate only (mM)
Vintage Islay®	5	0.69	0.03
Caol Ila®	7	0.89	0.02
Laphroaig®	10	1.85	0.04
Macallan®	12	2.5	0.09
Lagavulin®	16	3.23	0.06

(Table 2.1). This means the response of the sensing ensemble to the class of similar analytes was correlated as if the entire response was from gallate, which is not the case. Hence, our "response number" should be much higher than the real gallate concentration.

Indeed, as the age of the scotch whiskey increased, there was an increase in the "response number." To show that the concentration obtained was more than just gallate, HPLC analysis[36] was performed to quantify gallate. As expected, the concentration of gallate was significantly lower than the "response" obtained through absorption analysis of the sensing ensemble. Either there are tannin hydrolysis products in much higher concentrations than gallate, or some which bind significantly better than gallate. Importantly, targeting the entire class of gallate analogs with our sensing ensemble shows a better correlation with age than quantifying gallate alone. It would be interesting to discover if the correlation holds for scotche whiskies from other regions of Scotland, and for blends.

An attempt was made to quantify gallate in herbal teas such as green tea and black tea. Gallate along with many polyphenols such as catechin, epicatechin, epigallocatechin gallate (EGCg), epicatechin gallate (ECg), and epigallocatechin (EGC) are present in the tea leaves and have been widely studied due to their antioxidant activity.[37] The association constants of **2.1** to each of these analytes were determined. They are shown under their structures. Since the guests were not charged, most of the binding was between the boronic acids and catechol functionalities (discussed in detail in Chapter 3). Also, since the guests

were considerably larger than gallate the binding constants were anticipated to be lower due to the size differences between the host and guest. When the diastereomers catechin and epicatechin were investigated, their affinities with **2.1** were determined to be 5×10^2 M^{-1} for both of them. This is about two orders of magnitude less than the association of gallate and **2.1**. Upon testing an analyte with one more hydroxyl group, EGC, the affinity constant doubled due to the increased interactions with the boronic acids. The last two analytes investigated, ECg and EGCg, had an affinity constant with **2.1** that was similar to gallate's. This increase in association constants relative to catechin or EGC could be due to the increased number of interactions with the boronic acids. Once the binding studies were completed, the concentration of gallate was determined in the teas through HPLC analysis. Next, an attempt to quantify gallate with the sensing ensemble **2.24-2.1** was performed. Problems were encountered with the assay, which resulted in the determination of inaccurate concentrations, therefore quantification was deemed impossible. Part of the problem was the background absorbance of the tea was interfering. Subtracting the raw absorbance of the tea still did not result in the correct concentration of gallate.

catechin
5.7×10^2 M^{-1}

epicatechin
5.5×10^2 M^{-1}

epigallocatechin
1.2×10^3 M^{-1}

epigallocatechin gallate
5.2×10^3 M^{-1}

epicatechin gallate
8.4×10^3 M^{-1}
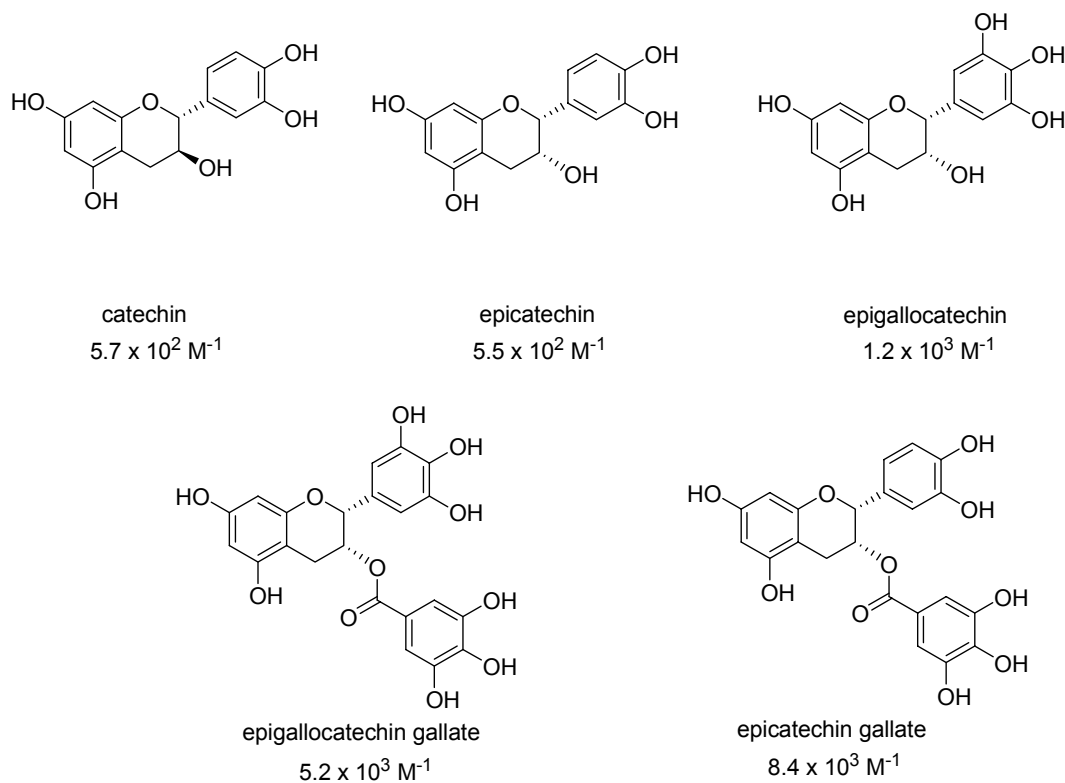
We have shown that a sensing ensemble of **2.1** and **2.24** was able to correlate an increase in the age of scotche whiskies to a class of compounds that increase in concentration during the maturation process. This shows that the inherent low selectivities of some synthetic systems can actually be an advantage for certain applications, and that such applications can be attractive targets for supramolecular and analytical chemists to contemplate. Perhaps this "low selectivity" can be used for other applications that require differential sensing as was discussed in Chapter 1.

103

2.5   SIMULTANEOUS QUANTIFICATION OF TARTRATE AND MALATE

In the first chapter, the drive to obtain highly selective synthetic receptors was discussed. Yet artificial receptors are inherently much simpler than their biological counterparts. Therefore, it is difficult to obtain a high degree of selectivity for complex guests. For example, one may expect it to be difficult using a synthetic receptor to distinguish between two structurally similar guests such as tartrate and malate, which differ by only one hydroxyl.

tartrate   malate
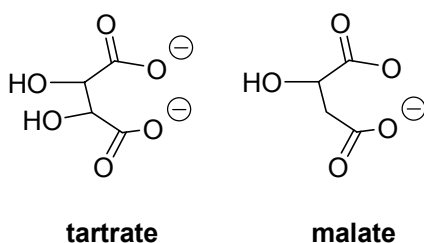
Mother Nature uses "differential" receptors to achieve our sense of taste and smell (Chapter 1, Section 1.7.1).[38] This is accomplished through the use of an array of cross reactive receptors. The response from each of these receptors for a particular mixture of stimuli creates a pattern that is stored in the brain. Upon introduction of that mixture again, the pattern is recalled to identify the taste or smell. We have proposed that the combination of pattern recognition and synthetic differential receptors can be advantageous in a sensing application.[39] When colorimetric sensors are used, several wavelengths in a UV/visible spectrum can be the "array" and the absorbance at each wavelength is the "pattern." In the particular application described, we have demonstrated that

using multiple hosts in combination with pattern recognition allows one to achieve a high degree of selectivity. This allows one to distinguish between and/or perform the simultaneous quantification of very structurally similar guests.

2.5.1 Two Hosts and Two Indicators

Two hosts with affinities for tartrate and malate were chosen for this study, which was a collaboration with John T. McDevitt's group.[40] The hosts (**1.34** and **2.1**) have each been discussed previously in regards to their design and their selectivities. Boronic acids impart affinity to vicinal diols,[14,41] while guanidinium groups impart affinity to carboxylates. Receptor **1.34** was previously found to have a similar affinity for tartrate and malate (Chapter 1, Section 1.6.4.6).[16] While for receptor **2.1**, the combination of two boronic acids and one guanidinium was determined to have a greater affinity for tartrate over malate (Chapter 3, Table 3.1).[42] We postulated that the differential responses that these two receptors have to the two analytes would allow pattern recognition to determine their concentrations.

1.34   **2.1**
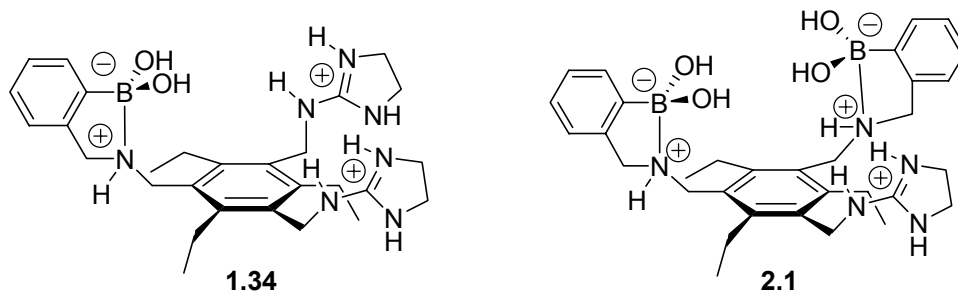
The previously reported synthesis[16,43] of **1.34** was accomplished (Scheme 2.11) from the mono BOC protected bis amine compound **2.25**, which is another product from the protection of **2.7** shown in Scheme 2.3. Guanidiniums were formed through a solid melt, coupling 2-methylthio-2-imidazole and the acetate salts of **2.25** to obtain **2.26**. The amine was deprotected with trifluoroacetic acid and the anions were exchanged to acetates using an ion exchange column (**2.27**). A reductive amination of **2.14** and **2.27** resulted in the final boronic acid/guanidinium receptor in moderate yields.

Scheme 2.11
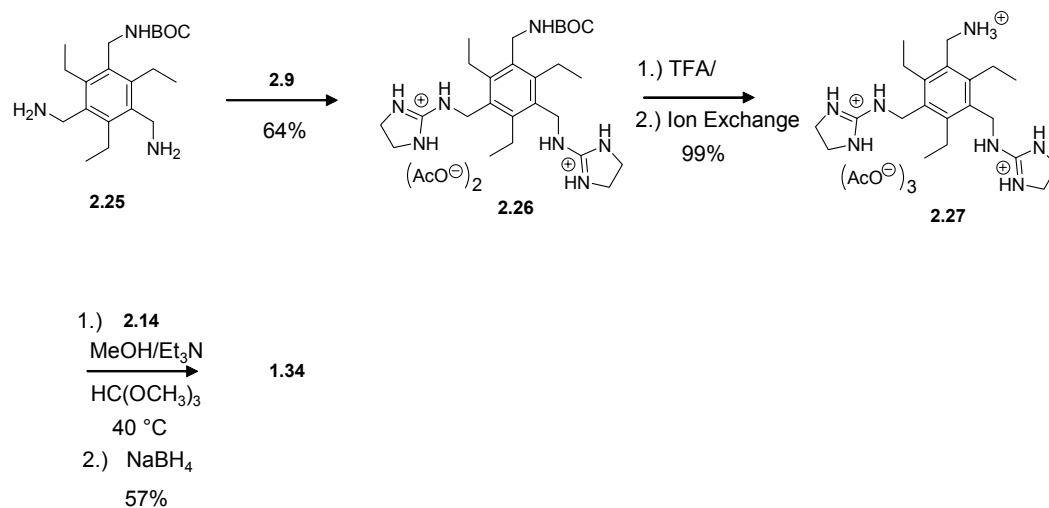
A signaling protocol was needed for this study. Again an indicator displacement assay was incorporated into this sensing system.[17] To further exploit the different characteristics of **1.34** and **2.1**, two indicators with different affinities for **1.34** and **2.1** were chosen. In addition, large differences in their

wavelength maximums were desirable so that the spectral response would be spread over a large wavelength axis. The two indicators chosen were bromopyrogallol red (**2.23**) (λ_{max} = 567 nm) and pyrocatechol violet (**2.24**) (λ_{max} = 445 nm). Figure 2.12 shows the change in absorbance of a mixture of **2.24** and **2.23** as increasing amounts of **2.1** are added (75% methanol in water (v/v)). A similar, but reproducibly different response is found upon addition of **1.34**. The combination of pyrocatechol violet (**2.24**) and alizarin complexone (**1.35**) was also investigated (Figure 2.13), but the change in absorbance upon addition of **2.1** was not as impressive because there were not large differences in their wavelength maximums. In essence, the two indicators have the opposite change in absorbance, where **2.24** is yellow and becomes maroon in the bound state, while **1.35** is maroon when free and yellow when bound.
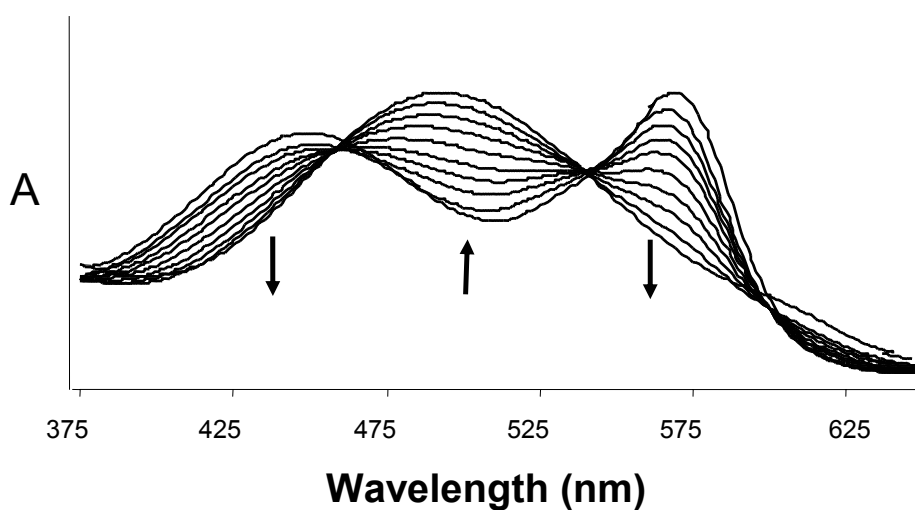
FIGURE 2.12. THE UV/VISIBLE SPECTRA OF 2.23 (30 μM) AND 2.24 (60 μM) upon addition of increasing amounts of **2.1** (75% methanol in water (v/v), pH 7.4, 10 mM HEPES buffer).

107
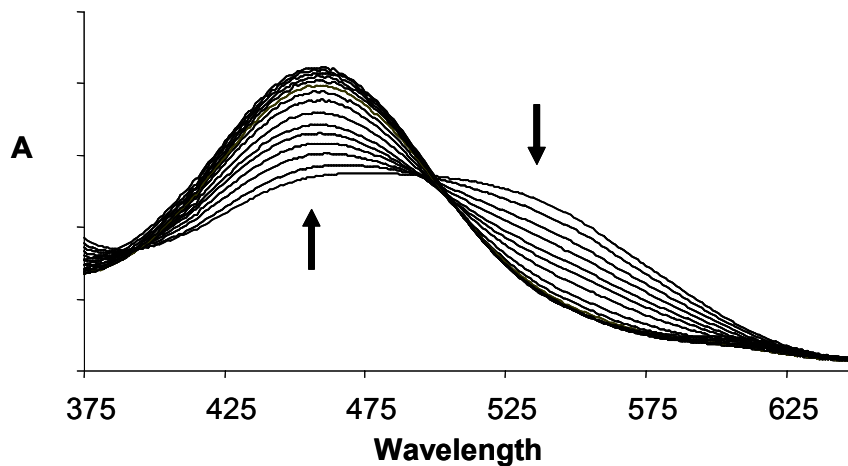
FIGURE 2.13. THE CHANGE IN ABSORBANCE OF A MIXTURE OF 2.24 (60 μM) AND 1.35 (180 μM) UPON ADDITION OF 2.1 (75% methanol in water (v/v), pH 7.4, 10 mM HEPES buffer).

2.5.2 The Experiment

The calibration for analysis of tartrate and malate was comprised of a four component ensemble of hosts and indicators in solution (150 μM of **1.34**, 150 μM of **2.1**, 30 μM of **2.23**, and 60 μM of **2.24**). UV/visible spectra were obtained upon addition of various amounts of tartrate and malate, keeping the concentrations of the hosts and indicators constant. The concentration of tartrate and malate were altered in increments of 0.2 mM ranging between 0 and 1.2 mM, resulting in 49 spectra (Figure 2.14 shows a schematic of the matrix of scans). One representative example of the differences between the binding of tartrate and malate to the two receptors is given in Figure 2.15. The UV/visible spectra shown are both taken at a total analyte concentration of 0.8 mM, but for one spectrum the

108

concentration of tartrate is greater than in the other. These two UV/visible traces demonstrate that the combination of two differential receptors differentiates tartrate and malate, and even mixtures of these two analytes. The reproducible variation in absorbance found for the pure samples and various mixtures of tartrate and malate is the data used as the training set for the artificial neural network (ANN)[44-46] pattern recognition algorithm.
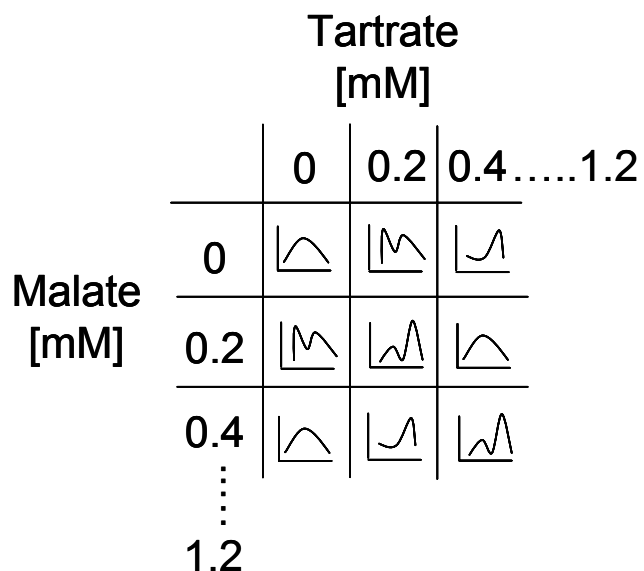
FIGURE 2.14. **A REPRESENTATION OF ONE TWO HOST/TWO DYE EXPERIMENT PERFORMED**, where spectrum were obtained at various concentrations of tartrate and malate.
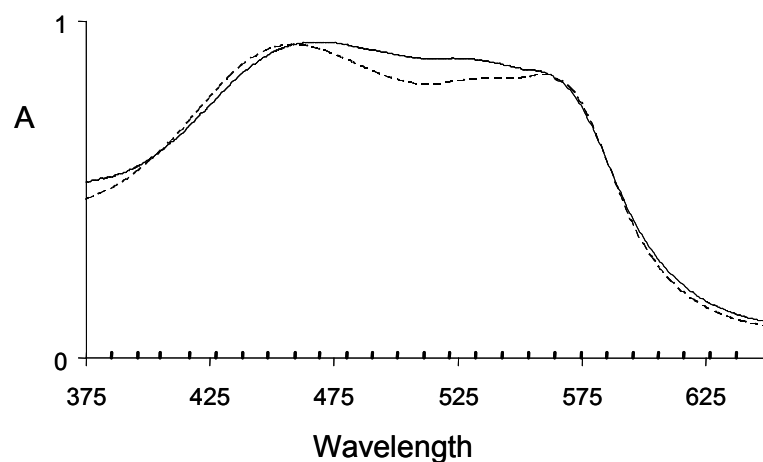
FIGURE 2.15. **VARYING TARTRATE AND MALATE CONCENTRATIONS IN SENSING ENSEMBLE.** The UV/visible spectra of the dye displacement assays formed from the mixture of the indicators **2.23** (30 μM) and **2.24** (60 μM) and the receptors **1.34** (150 μM) and **2.1** (150 μM) upon the addition of tartrate and malate in various concentrations [(-----) Tartrate (0.6 mM) and malate (0.2 mM)] and [(——) Tartrate (0.2 mM) and malate (0.6 mM)] (75% methanol in water (v/v), pH 7.4, 10 mM HEPES buffer). The inside ticks are representative of the 27 wavelengths chosen for analysis.

2.5.3   Pattern Recognition Analysis (Artificial Neural Network)

An artificial neural network (ANN) was chosen to analyze the data for this experiment. The next few sections describes ANN's in detail and how they work. ANN's are computer programs designed for pattern recognition, and are patterned after how the human brain processes information.   The idea of simulating biological neural networks has been around well before the introduction of

110

computers. The first artificial neuron was made in 1943 by the neurophysiologist Warren McCulloch and the logician Walter Pits,[47] but without the aid of computers, there was little they could achieve with this idea. Over the years, and a series of ups and downs, the technology has evolved such that neural networks are now used in numerous applications,[48] including voice and handwriting recognition. One exploit, analogous to that reported herein, trains the program to determine the concentrations of multiple metals in electroplating solutions using spectral data.[49]

2.5.3.1 Neurons

There is still much that is unknown about how the brain works and learns, but the basic idea is that the human brain is comprised of millions of neurons (Figure 2.16) through which electrical energy is transmitted.[46] Dendrites collect
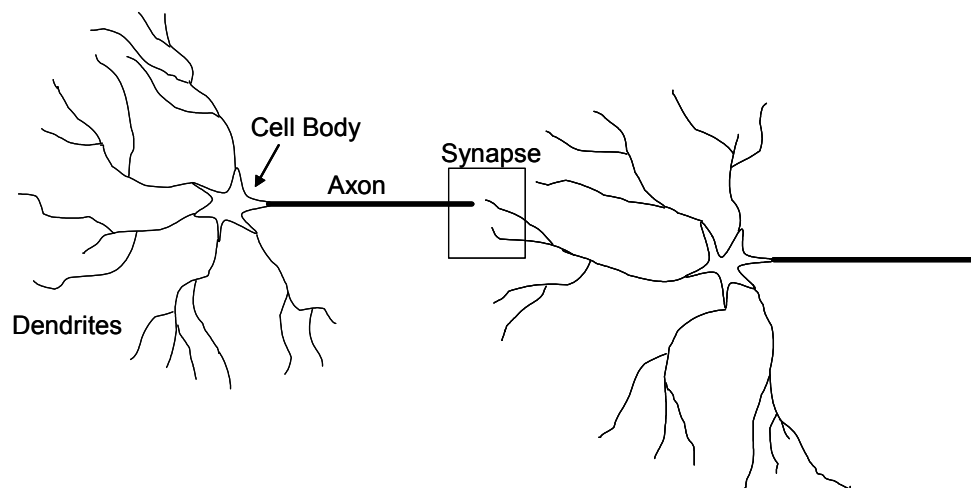
FIGURE 2.16. COMPONENTS OF A NEURON AND HOW IT WORKS.

111

signals from other neurons, where the signals are shuttled to the cell body to be stored. Once a certain number of signals are received or a threshold is reached, the neuron then sends an output signal down the axon. At the end of the axon, the signal is passed on to other connected neurons, and this junction is called the synapse. A simplification of this can be seen in Figure 2.17, where there are inputs and outputs, with a summation in the cell body.[50]
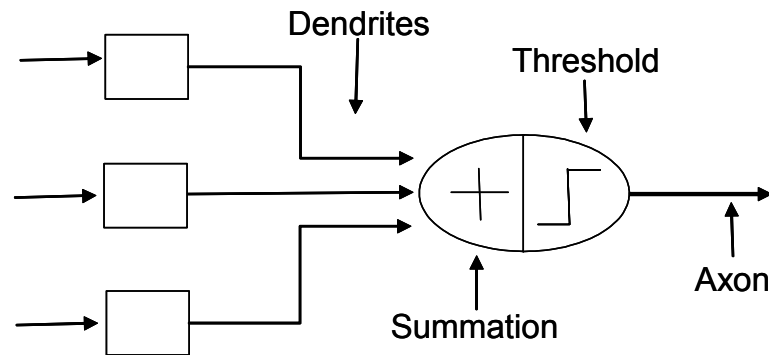
FIGURE 2.17. A SIMPLIFICATION OF A NEURON.

Neural networks work in a similar manner to the simplification seen in Figure 2.17, where the computer program is comprised of an input layer, neuron layer, and an output layer. The neuron layer is where most of the work is done with regards to the learning and usage functions. The following sections will be used to show how each of these layers work. Examples will be shown, starting with the very simple to the more complicated program setup.

112

2.5.3.2 Applications

There are many uses for ANN's, but their primary use is to create relationships between data. Some of the tasks that they are designed to perform include image, voice, and handwriting recognition. For example, the US Post Office uses these programs for the sorting of mail by recognizing handwritten zip codes.[51] This technology is also employed on train and airplane engines where the noises in the engine are recorded as a training set for neural network algorithms such that a different pattern in the noise can be detected. Scientists have also used the programs for spectra identification. The advantage of using these programs over other conventional computer programs is that they are able to deal with noisy or missing data and they can handle non-linear data. Conventional computer programs need to follow a specific set of instructions, hence if a step is missing; the program can not complete its task. Neural networks learn by example or absorbing experience. They have the ability to "spontaneously" learn from training samples, and therefore train themselves.

2.5.3.3 A Simple Neural Network

If we develop a simple artificial neuron[52] similar to the simplified one in Figure 2.17, a schematic of it might look like Figure 2.18A. This schematic shows the main three layers of neural networks: the input, the output, and the hidden layer. The hidden layer is where most of the work is done, which mostly

consists of the learning process. A simplified example of the learning process is shown in Figure 2.18B, where a basic form of pattern recognition is depicted. Four known inputs are entered into the system (in the light gray area), which consist of ones and zeros in different combinations in the blocks X1, X2, and X3. For the combinations 111 or 101, the output is going to be 1. When the input is 000 or 001, the output is 0. These are shown in columns A-D. The columns E-H represent the rest of the combinations of zeros and ones that could be inputs, where the output could either be a zero or a one (top chart). The neural network works by looking for patterns in the data. The program takes the data that it does not know an output for, and finds the data it is most similar to. For example, in order to find the output for column E, we need to look at similarities of E to the columns A-D. Column E has a pattern of 010. When compared to each of the known input columns A-D, column E differs from column A by one (X2), column B by two (X2 and X3), column C by two (X1 and X3), and column D by all three. Therefore E is related closely to A, which has an output of 0, therefore the network will also assign a 0 for the output of E (bottom chart). The same inspection is continued for each of the last three columns. The bottom chart reveals the outputs obtained after the inspection. When there is a similarity between two answers, and there is no more information to work from, the program may provide two answers as an output. When comparing F to the known inputs/outputs, it differs by one number for two columns, B and C, which have outputs of 0 and 1 respectively. Therefore, the output is both a 0 and a 1.

A. A Simple Neuron Input Layer

X_1

X_2 Hidden

⋮   Output Layer

X_n
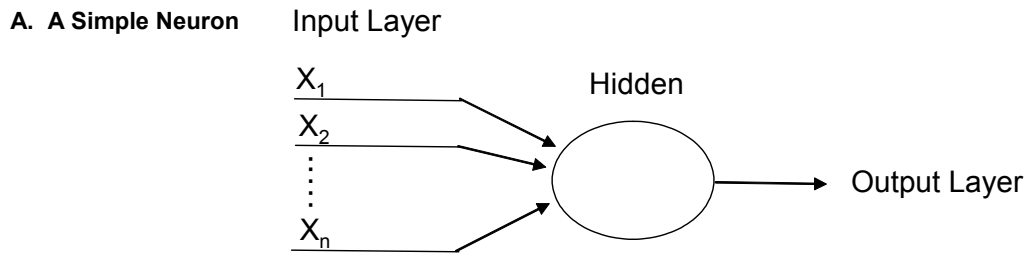
B. The Learning Process

Knowns: Output 1 when X1, X2, X3 is 111 or 101
Output 0 when X1, X2, X3 is 000 or 001

	A	B	C	D	E	F	G	H
X1	0	0	1	1	0	0	1	1
X2	0	0	1	0	1	1	0	1
X3	0	1	1	1	0	1	0	0
Out	0	0	1	1	0/1	0/1	0/1	0/1

	A	B	C	D	E	F	G	H
X1	0	0	1	1	0	0	1	1
X2	0	0	1	0	1	1	0	1
X3	0	1	1	1	0	1	0	0
Out	0	0	1	1	0	0/1	0/1	1

FIGURE 2.18. A SIMPLE SCHEMATIC OF AN ARTIFICIAL NEURAL NETWORK. A. The neuron consists of three layers, an input, an output, and a hidden layer. **B.** A simple example of the way the neuron processes data. There are four known inputs with known outputs. These are shown in the light gray area of the top chart. The last four columns show the rest of the combinations of ones and zeros. All of the unknown inputs could have outputs of one or zero (top chart). The bottom chart shows the outputs of the last four columns after looking at the light gray columns and finding the pattern that is the closest to its own.

2.5.3.4 Pattern Recognition in a Feedforward Network

Now that we have examined a simple neuron, the next step is to move to a more complicated example (Figure 2.19A).[52] This new model has nine inputs, three neurons in the hidden layer, and three outputs. Here blocks of gray and white are the patterns, where gray blocks represent zeros and white blocks represent ones. In part B of Figure 2.19, the known input and output values or patterns are shown. These patterns are translated into numbers in part C, so the top line of the cube with three gray blocks is translated to 000 for blocks X11, X12, and X13 respectively. The second pattern for X11, X12, and X13 was determined to be 010. The rest of the blocks are incorporated into the charts, and the knowns are shown as the light gray columns. The next step is to determine the outputs for the rest of the chart, which is done in the same manner as the example above, looking for similarities between knowns and unknowns. Once the patterns are determined, unknown inputs can be introduced into the system. Part D represents that process, where the first cube has an input of 001 (X11, X12, X13), 101 (X21, X22, X23), and 101 (X31, X32, X33). The outputs were determined to be 000 from the chart in part C. The second example works in a similar manner, but the third set of inputs is a little more complicated. The outputs for X10's and X30's are straight forward, while the X20's give two outputs, hence there are two output patterns given.

A. A More Complicated Neuron

X11	X12	X13
X21	X22	X23
X31	X32	X33

B. The Known Input and Output Values

0
0
0

1
1
1
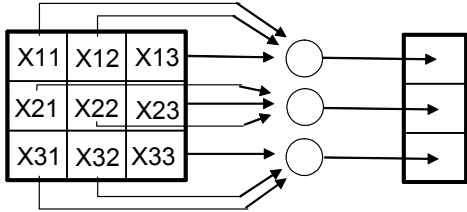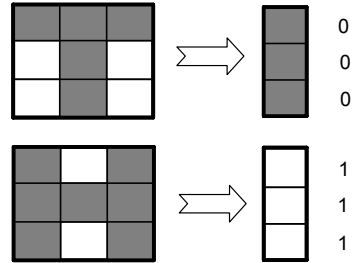
C. Pattern Recognition

X11	0	0	0	0	1	1	1	1
X12	0	0	1	1	0	0	1	1
X13	0	1	0	1	0	1	0	1
Out	0	0	1	1	0	0	1	1

X11	0	0	0	0	1	1	1	1
X12	0	0	1	1	0	0	1	1
X13	0	1	0	1	0	1	0	1
Out	1	0/1	1	0/1	0/1	0	0/1	0

X11	0	0	0	0	1	1	1	1
X12	0	0	1	1	0	0	1	1
X13	0	1	0	1	0	1	0	1
Out	1	0	1	1	0	0	1	0

D. Testing the Pattern Recognition Program

or
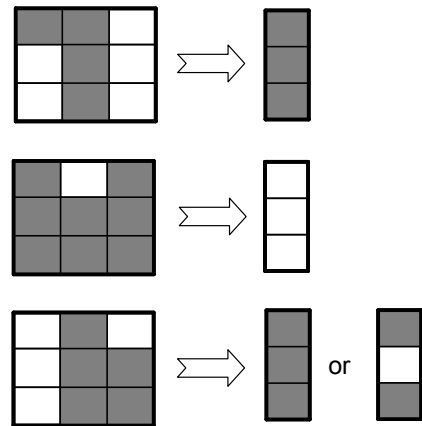
FIGURE 2.19. AN EXAMPLE OF A MORE COMPLICATED NEURON, WITH MORE INPUTS, OUTPUTS, AND HIDDEN NEURONS. **A.** Each row feeds into one neuron, that has one output. **B**. The known input and outputs for training the neural network. The zeros represent gray blocks, and the ones represent white blocks. **C**. With the help of the known inputs and outputs, the neural network is trained and the result is shown in the tables, with the knowns shown in light gray. **D**. The trained data set is then subjected to unknown inputs to obtain the outputs shown on the right. The third set of inputs has multiple outputs due to the similarity of the inputs to multiple patterns.

117

2.5.3.5 How the Network Learns

The phrase, the neural network is "learning", has been used a few times, but what does it really mean? The neural network is patterned after the human brain, where there are neurons and connections between them. It is not clearly known how the brain physically learns, but one widely held belief is that the connections between the neurons change, hence when something is learned the connection grows stronger.[50] Just the opposite happens when something is forgotten; the connection grows weaker. Neural network programs can not physically change the connections between the neurons, therefore, the learning is done through a series of weights that connect the inputs to the hidden layer (Figure 2.20).[46,52] These weights are a series of real numbers that are randomly chosen to start and the correct final weights are found through an iterative search. Each input is multiplied by a weight, and all the products are summed (Eq. 2.8) where I is the input and W is the weight.

$$I_1 W_1 + I_2 W_2 + ... I_n W_n = X \qquad\qquad \text{Eq. 2.8}$$

The neuron "fires" an output when the sum reaches a set threshold or the total X is greater than the threshold. The learning is continued, by comparison of the known output to the output obtained by the program. An iterative process is continued, by a continuous changing of the weights until the predicted output matches the expected output. The weights are changed through the delta learning

rule (Eq. 2.9), which changes the weight by taking the difference of outputs and multiplying it by the input (X) and the learning rate (R). The learning rate affects the magnitude of the weight change, and usually decreases during the learning process. This process continues until ΔW_i equals zero.

$$\Delta W_i = X_i (Output_{known} - Output_{ANN})R \qquad \text{Eq 2.9}$$

When the output is already known, this is considered supervised learning.[53] The "imaginary supervisor" looks at the error and changes the weights accordingly.

Input Layer
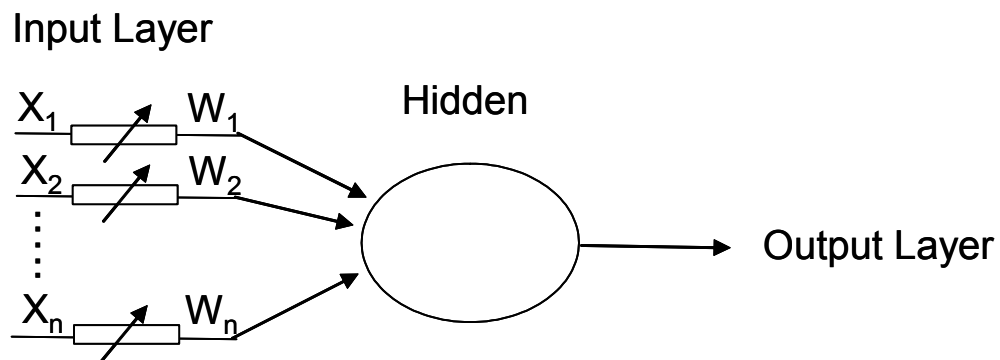
FIGURE 2.20. A SCHEMATIC OF A SIMPLE NEURON, WHERE WEIGHTS HAVE BEEN ADDED in order to improve the learning process. This follows the McCulloch and Pitts Model (MCP).

2.5.3.6 Perceptron

A very simple example of an ANN is the perceptron, which is a single layer, feedforward network (Figure 2.21).[53] This type of system only has an input

and an output layer, no hidden layer. Every input layer is connected to every output layer, and all the connections are weighted. The feedforward term states that neurons in the same layer can not be connected. The activation of the neuron is defined by a hard limiter function, which means the neuron only fires when a specific set of values are obtained. For example, the hard limiter might be set so the neuron fires a zero when $X \leq 0$ (Eq. 2.8) and a one is fired when $X \geq 1$. The training of the network is supervised, and the weights are adjusted through the delta learning rule.

Input Values

Input Layer

Weighted Matrix

Output Layer

Output Values
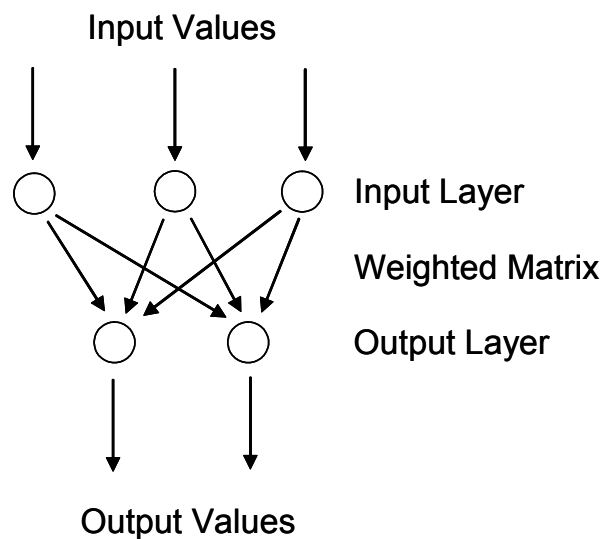
FIGURE 2.21. A PERCEPTRON NEURAL NETWORK. This feed forward network is the simplest example, with only an input and an output layer. Its activation function is defined by a hard limiter function, and learning is accomplished through the delta learning rule.

2.5.3.7 Multi-Layer Perceptron

The Multi-Layer Perceptron network (Figure 2.22) is an extension of the perceptron feedforward network, but has more options associated with the layers, the learning algorithm, and the activation function. This type of network still has input and output layers, plus one or more hidden layers, and the connections are associated with weights. For example, let's look at the connection between neurons in layer i and neurons in layer j. In order to get an input for neuron j (net_j), the neurons in layer i must fire outputs ($output_i$) and that is defined by Eq. 2.10, where w_{ij} is the weight between neuron i and j.

$$net_j = \sum_i w_{ij} output_i \qquad \text{Eq.2.10}$$

The activation function is the function that produces an output for the neuron. This output can be dictated through two options, the hard limiter, discussed previously, and the sigmoid. The sigmoidal function[45] compresses a wide range of inputs into a limited number of outputs. This is done through taking a weighted sum of the inputs at each neuron and "squashing" it using Eq. 2.11.

$$output_j = \frac{1}{1 + e^{-net_j}} \qquad \text{Eq. 2.11}$$

The output that is obtained is then passed on to the next layer as the input for that layer using Eq. 2.10. The learning process is supervised and the weights can be adjusted through the delta learning rule (Eq. 2.9) or through back propagation.

Input Values
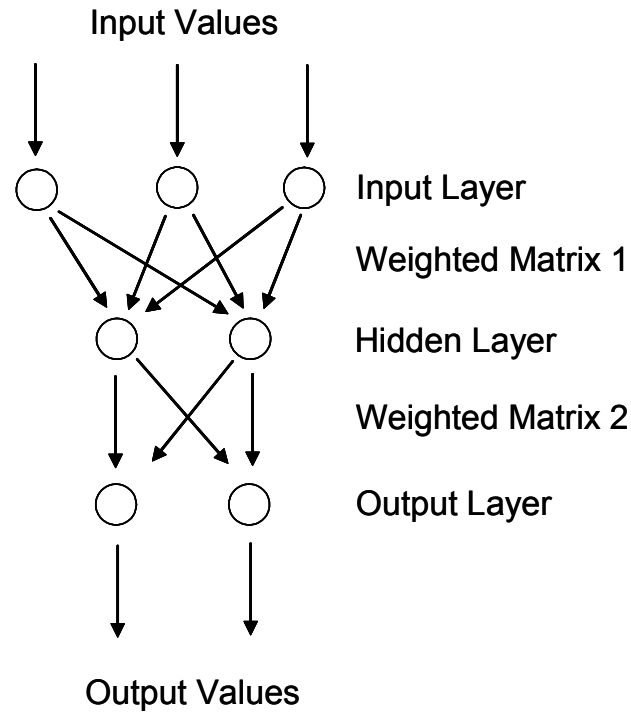
FIGURE 2.22. A SCHEMATIC OF THE MULTI-LAYER PERCEPTRON. It is at least a three layer, feedforward network, with weighted connections.

2.5.3.8 Back Propagation

Back propagation (BP)[45,54] is an algorithm for training the neural network, through reducing the error between the actual and expected results by determining how the error depends on the outputs, inputs, and weights. The algorithm works

in the opposite direction of the activity of the network. In other words, it starts with the output layer and works backwards, hence the term back propagation. This can become complicated with the increased number of weights as more layers are added as seen in Figure 2.22. The knowledge of how the final error is affected when each weight is slightly increased or decreased is needed, because the output of one layer affects the outputs of all layers to which it is connected.

An example with how the back propagation algorithm computes the error derivative of the weights is shown here. Once the ANN has gone through its first feedforward calculations, the error can be computed. The error for neuron j can be calculated from Eq. 2.12. The BP algorithm can then compute the rate at which the error changes as the activity of the output unit changes (Eq. 2.13). This we will term the EA, which is the difference between the calculated and known outputs for the output units.

$$E = \frac{1}{2}\sum_{j}(Output_{jANN} - Output_{jknown})^2 \qquad \text{Eq. 2.12}$$

$$EA_j = \frac{\partial E}{\partial Output_{jANN}} = Output_{jANN} - Output_{jknown} \qquad \text{Eq. 2.13}$$

Next, the dependence of the output on the activation and the weights is determined (Eq. 2.14). This comes from a combination of Eq.2.10 and 2.11 where $Output_i$ is essentially the output from the previous layer or the input for neuron j.

$$\frac{\partial Output_j}{\partial w_{ij}} = \frac{\partial Output_j}{\partial net_j} \frac{\partial net_j}{\partial w_{ij}} = Output_j(1-Output_j)Output_i \quad \text{Eq. 2.14}$$

The error associated with the output, which is associated with the changes in the weights, is shown in Eq. 2.15, which is essentially the product of Eq. 2.13 and 2.14.

$$\frac{\partial E}{\partial w_{ij}} = \frac{\partial E}{\partial Output_j} \frac{\partial Output_j}{\partial w_{ij}} = EA*Output_{jANN}(1-Output_{jANN})Output_i \quad \text{Eq. 2.15}$$

Through Eq. 2.15, the weight's contribution to the error of the network is obtained and the weight can be changed accordingly through Eq. 2.16 by multiplying the error times a constant η (the learning rate). If the learning rate is low it may take a long time for the algorithm to determine the correct weights, or it may get stuck in a local minima. If the learning rate is too high there is a chance of never converging on the correct set of weights.

$$\Delta w_{ij} = -\eta \frac{\partial E}{\partial w_{ij}} \quad\quad\quad \text{Eq. 2.16}$$

Now that the weights of the last layer have been adjusted, the process continues for each of the previous layers in the network until the weights are adjusted such that the desired output matches the output that the ANN derives.

2.5.4 Outputs for the Two Host/Two Indicator Experiment

The ANN employed was based on a Multilayer Perceptron architecture with a back propagation algorithm[55] for training, performed by Dr. Pierre N. Floriano. In Section 2.5.2, it was discussed that the change in absorbance was measured for the two host/two indicator system as the concentration of tartrate and malate were altered in small increments resulting in 49 spectra. Of the 49 spectra obtained, 45 were used to train the data set using 27 points or wavelengths from each spectrum, while the other 4 were left out as "unknowns." When the absorbances for the 27 wavelengths (shown as ticks in Figure 2.15) were entered for the four unknowns, an absolute error between 1 and 6% was obtained for the output concentrations of tartrate and malate (Table 2.2).

TABLE 2.2. THE PREDICTED CONCENTRATION VALUES OBTAINED FROM THE ANN COMPARED TO THE REAL CONCENTRATIONS OF TARTRATE AND MALATE (MM).

Training NN1	Real [malate]	Pred. [malate]	Real [tartrate]	Pred. [tartrate]
Val. case # 1	0.00	0.0731	1.00	0.9711 (3%)
Val. case # 2	0.59	0.568 (3%)	0.80	0.7911 (1%)
Val. case # 3	0.99	1.0340 (4%)	0.22	0.2119 (5%)
Val. case # 4	1.19	1.1362 (5%)	1.00	1.0126 (1%)
Training NN2	[malate]		Real [tartrate]	Pred. [tartrate]
Val. case # 1	0.2	-------	1.00	0.995 (0.6 %)
Val. case # 2	0.2	-------	0.53	0.527 (0.0 %)
Val. case # 3	0.2	-------	0.24	0.238 (1.3%)

Although we felt this level of error was very good for our first trial, we wanted to discover if the incorporation of more training data could further reduce

the error. In a second round of data collection, the concentration of malate was held constant (0.2 mM), and the concentration of tartrate was varied between 0 and 1.2 mM moving in increments of 0.05 mM. To test the ability of the data set to determine the concentration of tartrate, three spectra were held back from the training set to use as "unknowns." With this training set, the error in the calculated concentration was reduced to less than 2% for all unknowns (Table 2.2).

Next, three different wines were chosen in an attempt to use the multiple host and indicator sensing ensemble to determine the concentration of tartrate and malate in the grape beverages. The wines consisted of a Rioja (Marqués de Cáceres 1998), a Merlot (Fontana Candida 2000), and a Chardonnay (Rabbit Ridge 2000). The concentrations of tartrate and malate were determined in each of the wines by ^{1}H NMR analysis, by lyophilizing the wines, redissolving them in deuterated water, and adding a standard in known concentrations. Next, small aliquots of the wines were added to the sensing ensemble mixture and the resulting absorbances were run through a trained ANN. However, due to the interfering absorbance of the wine, an accurate concentration of the two analytes could not be obtained. In order to obtain these concentrations in the wine, the neural network would need a training set of the sensing ensembles with the wines at different concentrations. This would help to alleviate the interfering absorbances.

2.5.5   Expanding the Scope of the Project

To push the limits of the technique, the differential response of citrate to the two receptors **2.1** and **1.34** in the presence of the indicators **2.24** and **2.23** was investigated. The change in absorbance is shown in Figure 2.23 upon addition of citrate, tartrate, and malate to the sensing ensemble mixture. The plots shown (absorbance versus analyte concentration) are different than normal calibration curves due to the presence of two indicators and the mixed equilibrium that must
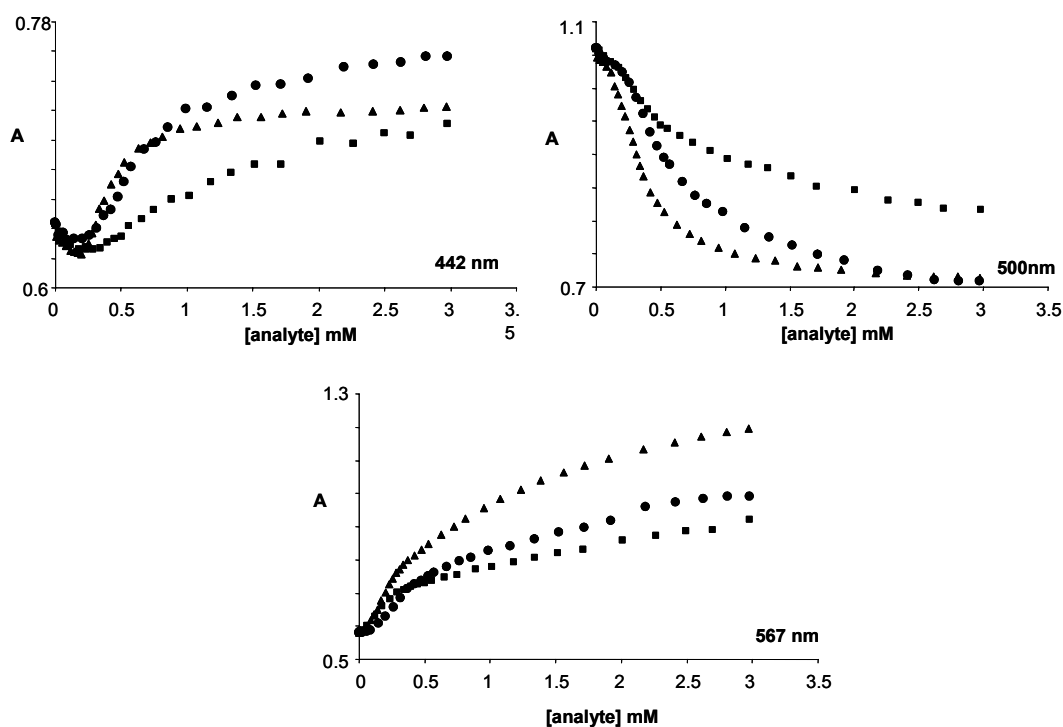
FIGURE 2.23.   THE CHANGE IN ABSORBANCE OF THE SENSING MIXTURE ENSEMBLE 2.1 (0.15 MM), 1.34 (0.16 MM), 2.24 (0.06 MM), AND 2.23 (0.03 MM) UPON ADDITION OF THREE DIFFERENT ANALYTES. Shows the differential response of **2.1** and **1.34** to tartrate (●), malate (■), and citrate (▲) (10 mM HEPES, 75% methanol in water, pH 7.4).

127

exist. Both receptors have an affinity for citrate, and indeed the response does show a differential response to citrate over tartrate and malate. The next step would involve developing a training set for the neural network program varying the concentration of the three analytes in an attempt to simultaneously quantify three analytes in solution.

Another approach in expanding this application would be the incorporation of more indicators and receptors in order to target more analytes. Figure 2.24 shows the initial investigation of a three indicator experiment.
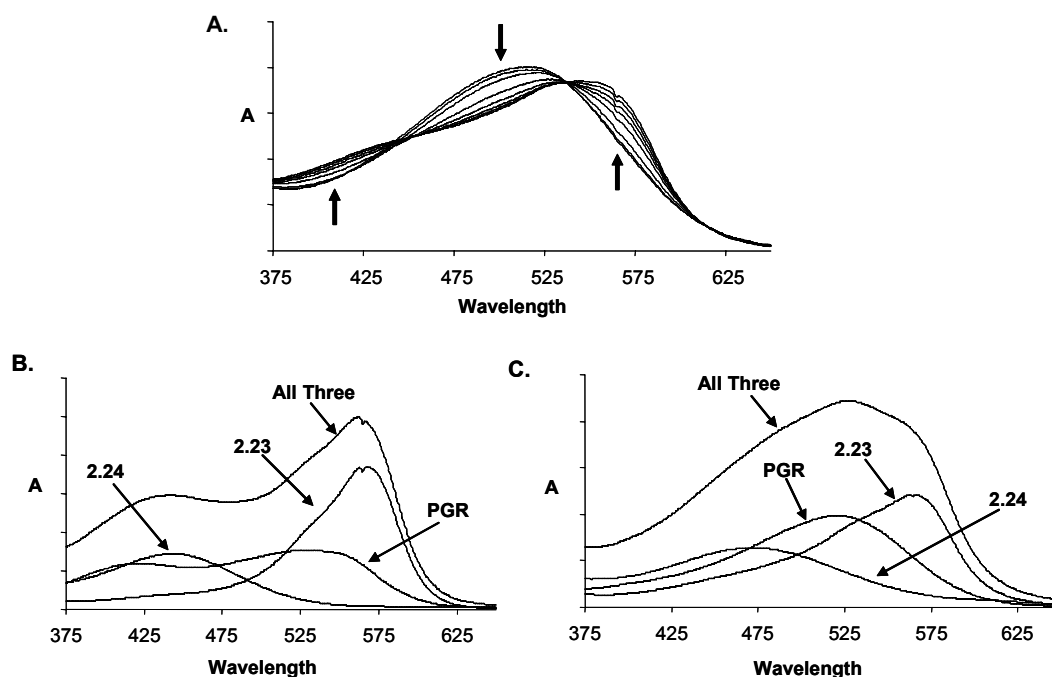
FIGURE 2.22. **THE INVESTIGATION OF THREE INDICATORS AND TWO RECEPTORS.** A. The change in absorbance of **2.24**, **2.23**, and **PGR** in the presence of **2.1** and **1.34** upon addition of tartrate. B. The absorbance of the three indicators, alone and together. C. The absorbance of the three indicators bound to **2.1** (10 mM HEPES, 75% methanol in water, pH 7.4).

128

Pyrogallol red (**PGR**) was included along with **2.24** and **2.23**. At first thought one would think that the increased number of indicators would increase the sensitivity of the technique, and this may very well be true in some systems. Yet looking at the change in absorbance of **2.24**, **2.23**, and **PGR** in the presence of **2.1** and **1.34** upon addition of tartrate (Figure 2.24) the change is very similar to the two indicator experiment (Figure 2.12). The free absorbances of the indicators are shown in Figure 2.24B along with the absorbance of the indicators bound to **2.1** (Figure 2.24C). PGR's absorbance is between the absorbances of **2.24** and **2.23** in both the bound and unbound state, which results in a decrease in sensitivity. This does not preclude the use of more than two indicators, but our prediction that one needs to use indicators with large absorbance maximum differences is enforced.

Here we have shown that using differential receptors in parallel can create a powerful method to differentiate between very structurally similar guests, and even render a method of simultaneous quantification. The key to this quantification lies with the use of pattern recognition, and with hosts that have differential responses to each of the guests, similar in theory to the sense of taste. This study shows that differential sensors in solution coupled with pattern recognition is a simplified example of a sensor array.

2.6   INCORPORATING THE HOST INTO A SOLID PHASE SENSOR ARRAY

Throughout this chapter the use of receptor **2.1** has been discussed in a couple of different sensing applications. It has been utilized as a differential sensor to detect a class of analytes in scotch whiskies, and in conjunction with another sensing ensemble to detect two analytes simultaneously through pattern recognition. Even though both have been shown to be powerful tools, both are limited in their usefulness. For example, in order to increase the number of analytes detected, more receptors need to be incorporated into the sensing ensemble. With the multiple hosts and indicators project, there will ultimately be a limit to the number of species that can be detected within one cuvette. One of the main disadvantages will be the limit to the number of indicators that can be incorporated. If too many indicators are present, a spectral response would be hard to visualize. Therefore, the next goal is to incorporate receptors into a sensor array platform, where many sensors are present, yet confined to their own spatially addressable positions. Such a goal can take many forms, yet the approach taken at UT requires that the sensor be immobilized on a resin bead to use the platform discussed in Chapter 1, Section 1.7.2. An analog of receptor **2.1** was incorporated into a solid phase resin (**2.28**), in preparation for its incorporation into a sensor array.

2.28
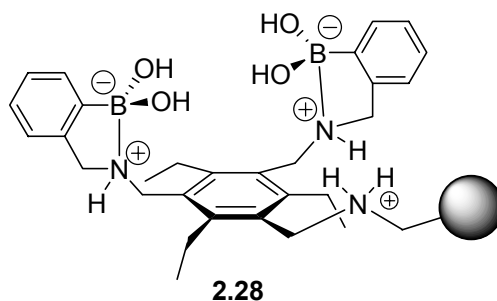
One of the first arrays that the receptor will be utilized in is a project that is in collaboration with the groups of Dr. Jason Shear and Dr. John T. McDevitt. The goal of the project is to have an artificial sensor and an enzyme sensing ensemble working simultaneously on the same chip. The chip would be used to quantify tartrate and malate, where malate dehydrogenase (MDH) will be used for the detection of malate, while receptor **2.28** will be used to quantify tartrate. Malate will be detected through the formation of a formazon dye through a series of reductions and oxidations with NAD/NADH, an electron mediator, and a tetrazolium indicator. The detection of tartrate with **2.28** will work in a similar manner to receptor **2.1**, with an indicator displacement assay as the signaling motif. Again, pyrocatechol violet (**2.24**) was the indicator of choice. The idea being that the indicator will associate with the resin bound host and upon addition of an analyte that binds the receptor, the indicator will be displaced and washed away, decreasing the light absorbed.

2.6.1 Synthesis

In an attempt to achieve the same selectivity for tartrate over malate, receptor **2.28** was designed to be very similar to receptor **2.1**. Therefore, upon the same hexa-substituted benzene scaffold was appended two boronic acids and an ammonium. The difference in the two receptors lies in the incorporation of an ammonium (**2.28**) for charge pairing and hydrogen bonding rather than a guanidinium as in **2.1**. This replacement was made to make the receptor's attachment to the resin facile.

In order to synthesize receptor **2.28** (Scheme 2.12), the scheme was started with the mono BOC protected compound **2.25**. Reductive amination of **2.25** with two equivalents of 2-formyl benzene boronic acid (**2.14**) gave the protected boronic acid compound **2.29**. The BOC group was cleaved with trifluoroacetic acid, and the resulting salt was ion exchanged to obtain the acetate salt **2.30**. Finally, the receptor was attached to two different solid supports to determine which matrix would work the best. The glyoxal activated 6% cross linked agarose beads (Scheme 2.12) was chosen for its water like interior. The host was attached through a reductive amination in a buffered solution by Dr. Anuradha Kachhar to obtain **2.28-Ag**. Tentagel MB FMP acid labile resin was the second resin that was investigated. Compound **2.30** was again reductively aminated to the aldehyde resin in dry methanol (Scheme 2.13) to give **2.28-TG**.[56]

Scheme 2.12
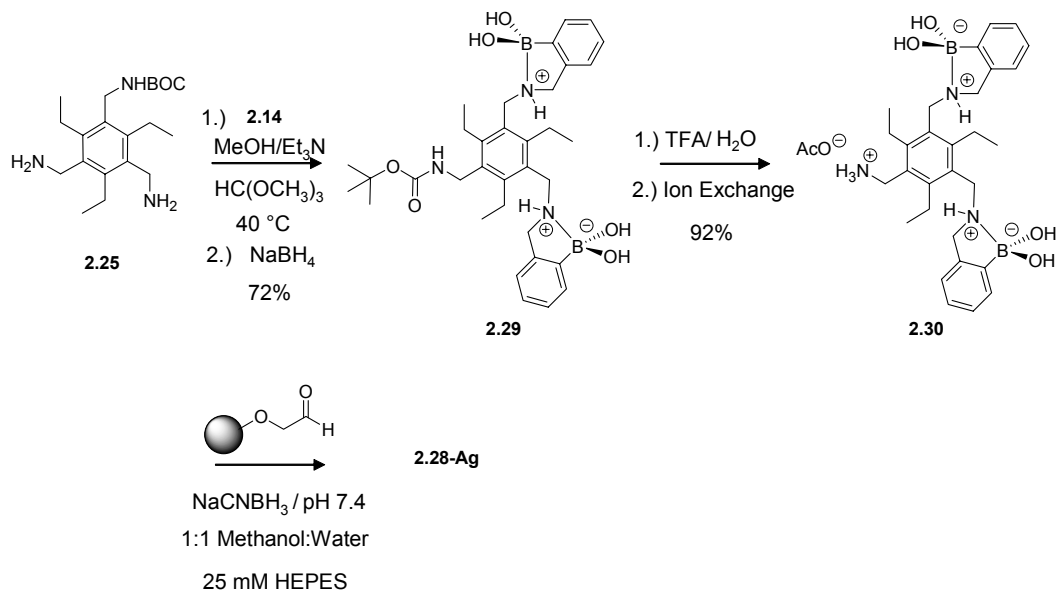
Scheme 2.13
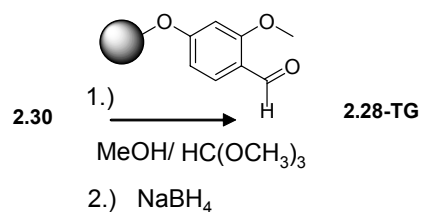
2.6.2 Platforms

Once the hosts were attached to the resins, the first item to be investigated was whether the receptors (**2.28-Ag** and **2.28-TG**) still bound the indicator (**2.24**), and whether the indicator still behaved in the same manner as in solution. Upon addition of a solution of **2.24** in 50% methanol in water (v/v), the yellow indicator

turned maroon upon binding **2.28-Ag** (Figure 2.25B) and **2.28-TG** (not shown). It is essential that the blank beads (Figure 2.25A) do not interact with any of the compounds introduced into the flow cell. In the case of the glyoxal activated agarose beads, the indicator easily washed out of the blank resin indicating that the color change associated with **2.28-Ag** is from the binding of the indicator to the host and not the beads. When the same test was performed on the Tentagel beads, the blank beads turned yellow upon addition of **2.24**, and the color remained over a series of several washes. Therefore, out of the two beads synthesized **2.28-Ag** were the ones that were used for further studies.

A   B   C
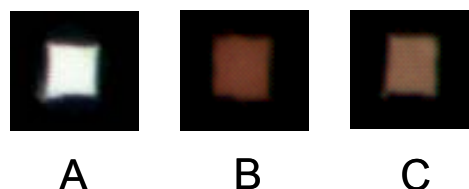
FIGURE 2.25. PICTURES OF RESIN BEADS (AGAROSE) IN ARRAY PLATFORM. A. Blank beads (no host). B. Resin **2.28-Ag** after **2.24** has been added. The indicator is originally yellow and upon binding the receptor turns maroon. C. The response of the sensing ensemble **2.28-Ag/2.24** upon addition of tartrate resulting in an increase in transmitted light.

The platform used for the sensing array was developed in the McDevitt group at the University of Texas at Austin. Figure 2.26 shows a schematic of the flow cell used to house the beads under investigation. The flow cell is designed to deliver the solvent to the top of the beads, force the solvent over the beads, and

Top View

delivery → waste

camera

Side View

threaded retainer

spacer

delivery → cover slip / solvent inlet

silicon chip / solvent outlet → waste

housing unit

light
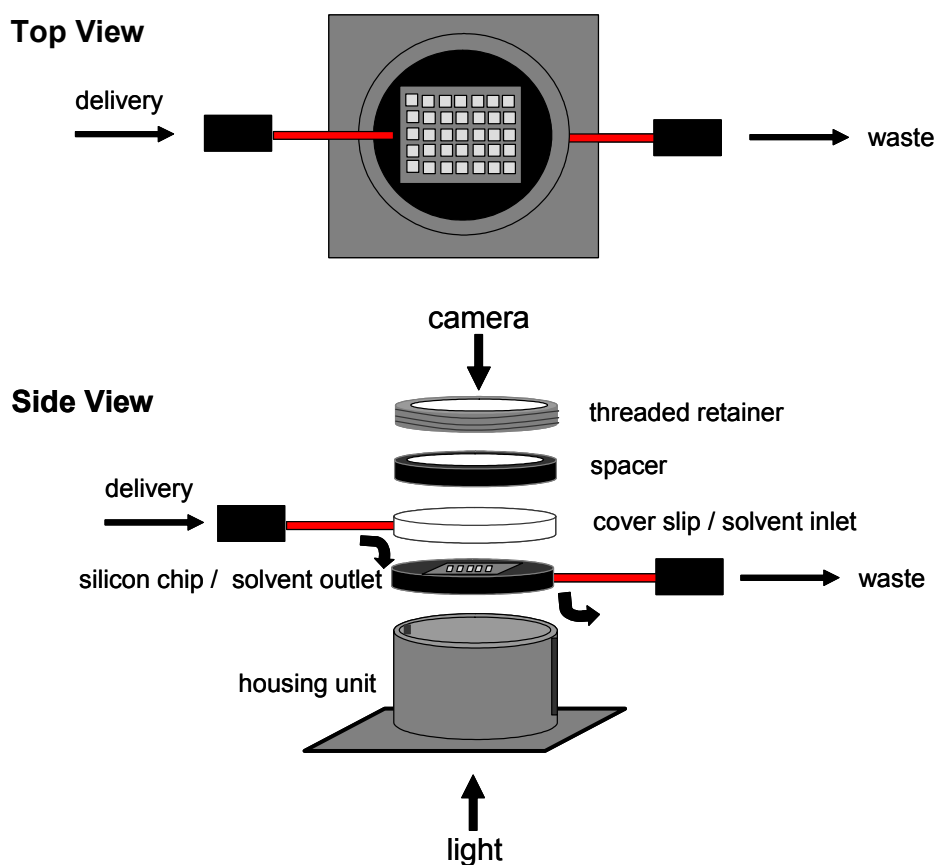
FIGURE 2.26. DRAWING OF THE SENSOR ARRAY FLOW CELL. The flow cell delivers the solvent over the top of the beads. The solvent is then forced down through the beads and it exits on the opposite side. The flow cell consists of multiple layers where the beads are housed in the silicon wafer, a clear cover slip through which the solvent is delivered, and spacers and a threaded retainer are used to seal the system together.

send the solvent to waste from the bottom. The beads sit in micromachined wells in a silicon wafer that is immobilized on a disc composed of PMMA (polymethylmethacrylate) plastic. PEEK tubing is imbedded in the disc for the solvent outlet. A second disc is placed on top of the first disc, acting as a cover slip. This also is imbedded with PEEK tubing for the solvent inlet. These two

plastic plates slip into a metal housing unit, and an internal threaded retainer is used to tighten everything down in order to compress the cover slip to the bottom disc, sealing the two together.

In order to flow a steady stream of solvent over the beads, an FPLC pump was incorporated for solvent delivery. The FPLC was also equipped with a sample injection valve with a 2 mL loop for delivery of indicator and analytes. The array platform was placed on a microscope with illumination from the bottom and red/green/blue (RGB) images were captured with an 8-bit CCD camera.

2.6.3   Studies

The beads were placed in the micromachined wells of the silicon chip in the pattern shown in Figure 2.27. Derivatized beads were placed in the first four rows of the chip, while the last row was reserved for blank beads. The

1	2	3	4	5	6	7
8	9	10	11	12	13	14
15	16	17	18	19	20	21
22	23	24	25	26	27	28
29	30	31	32	33	34	35

derivatized beads
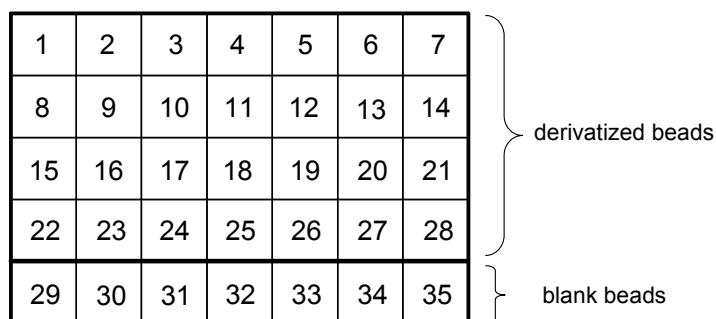
blank beads

FIGURE 2.27. LAYOUT OF THE SILICON WAFER AND BEAD PLACEMENT. The chip is micromachined with 35 wells. Derivatized beads are placed in the first four rows, while blanks beads are placed in the last row.

136

underivatized beads were used as a reference to the amount of light that is transmitted through the beads. Also, they are a good standard for determining if reagents are lingering in the beads.

Once the beads were locked in their wells, the selectivity of the beads needed to be investigated, and the signaling motif needed to be incorporated. The indicator **2.24** needed to be loaded into the beads for the receptors to bind. When a continuous flow of **2.24** (3.0 mM, 0.2 mL/min, 25 mM HEPES, 1:1 methanol:water, pH 7.4) was introduced to the beads, the yellow indicator turned maroon upon binding **2.28-Ag**, but over time the receptors in the beads bound so much indicator that the beads appeared black and no light was able to pass through. When a small aliquot of **2.24** was added (0.5 mM, 2 mL, 1.0 mL/min) instead of a continuous flow, the beads turned a level of maroon (Figure 2.25B) that appeared to be reproducible.

Upon addition of a concentrated aliquot of tartrate (14 mM, 2 mL, 0.5 mL/min, 1:1 methanol:water) to the sensing ensemble beads, the indicator was displaced and the color of the beads diminished (Figure 2.25C). When the same experiment was run in 100% water, the indicator was not displaced; hence the presence of methanol was needed for the assay to work. Further investigations should incorporate a study of the selectivity with the concentration of methanol. In between the addition of tartrate and loading the indicator again, the beads were washed to remove the excess tartrate and **2.24**. Washing with acidic solutions had no affect on the intensity of transmittance; therefore 2 mL injections of sodium hydroxide solutions were washed through the array. The color of the beads

137

diminished greatly, indicating that the sodium hydroxide solution was breaking up

the boronate esters. The change in transmitted light throughout this whole cycle

is shown in Figure 2.28, and the distinct changes upon the addition of each

reagent is illustrated. The first portion shows the addition of indicator with a
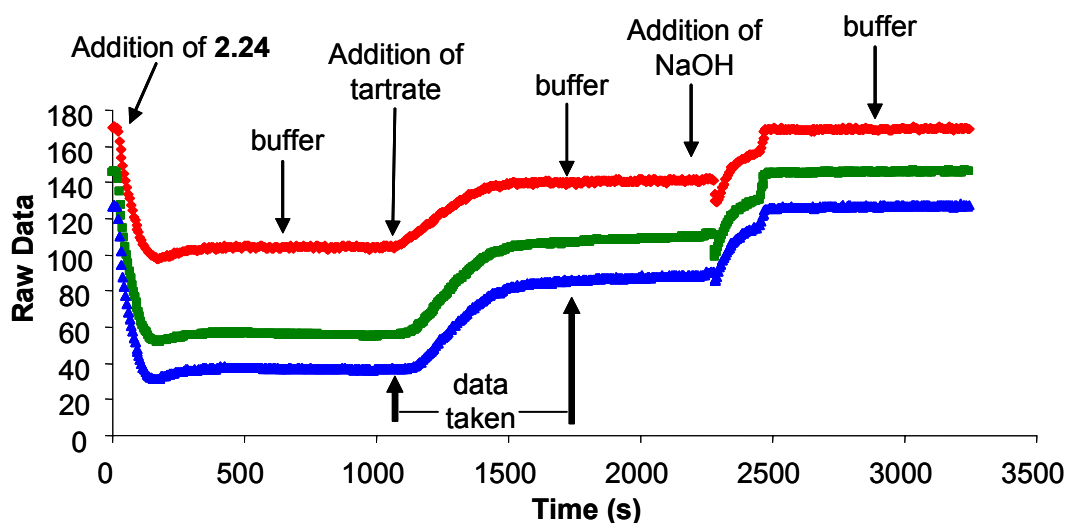
FIGURE 2.28. **THE CHANGE IN TRANSMITTED LIGHT OF ONE INDICATOR, TARTRATE, WASH CYCLE FOR 2.28-AG**. RGB is color coded. (0.5 mM **2.24**, 9.0 mM tartrate, 0.5 M NaOH, 25 mM HEPES, 1:1 methanol:water).

decrease in transmitted light as the indicator becomes bound to the receptor.

Upon addition of tartrate, the transmitted light increases as the indicator is

displaced and washed away, and a final wash with sodium hydroxide removes

tartrate and **2.24** from the resin, returning the transmitted light to the beginning

level, such that the cycle can be repeated.

The next step was to determine the selectivity of the sensing ensemble by introducing different concentrations of tartrate and recording the absorbance changes upon displacement of **2.24**. Figure 2.29 illustrates the RGB delta absorbance of **2.28-Ag-2.24** for one bead showing the change in absorbance in response to the varying concentrations of tartrate. Each bead is different, due to a high degree of bead to bead variance. The high end of the working concentration range is about 2 mM for this bead. The large delta absorbance at 5 mM appears to be due to human error since it is present in the other beads that were studied. Since every bead has a different loading of host and ultimately indicator, every bead requires its own calibration curve.
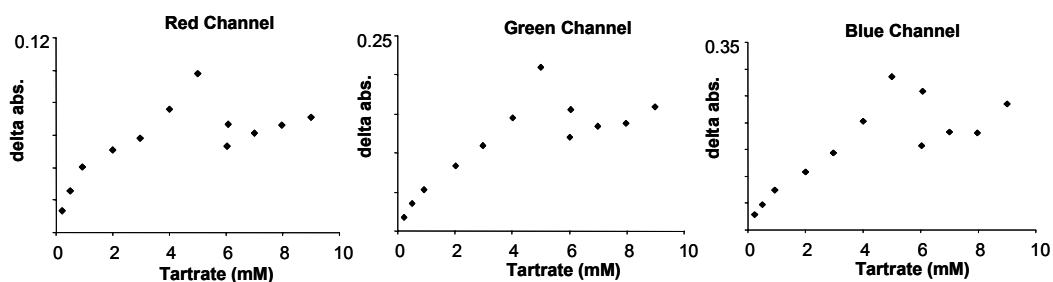
FIGURE 2.29. THE CHANGE IN ABSORBANCE OF 2.28-AG/2.24 UPON ADDITION OF TARTRATE. The calibration curves are shown in the separate RGB channels.

Receptor **2.1** was selective for tartrate over malate, and investigations were undertaken to determine if this same selectivity was true for **2.28-Ag**. Indeed upon addition of a couple of different concentrations of malate, the change in absorbance was significantly less (Figure 2.30) indicating that **2.28-Ag** has a higher affinity for tartrate over malate.

139
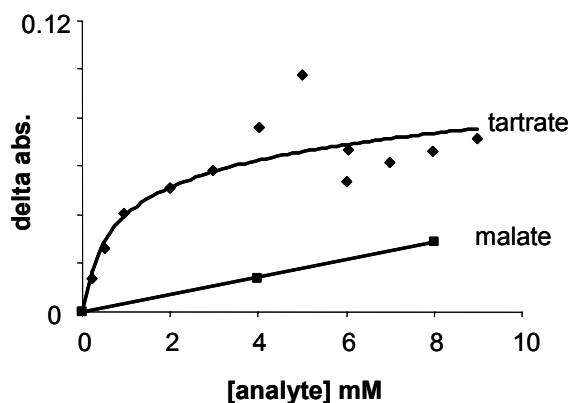
FIGURE 2.30. THE CHANGE IN ABSORBANCE IN THE RED CHANNEL IN RELATION TO TARTRATE AND MALATE for **2.28-Ag/2.24**.

Once it was determined that **2.28-Ag** was selective for tartrate over malate, we set out to develop a full calibration curve for tartrate and malate in order to quantify tartrate in some grape derived beverages. Figure 2.31 shows the change in absorbance in the red channel of one bead upon addition of various concentrations of tartrate and malate. Due to the length of each cycle, the experiment lasted for a series of days. Graph A in Figure 2.31 shows the calibration points obtained in day one for tartrate (blue). Despite some variance, the points lie in a line. During day two, both tartrate and malate were investigated with the system. These points from day two are shown in Figure 2.31B in the red. A distinct selectivity can be seen for the tartrate over the malate. On day three, more points were added to the malate calibration curve, shown in green in Figure 2.31C. Instead of lying on a line, the points appear to be random. This suggests that the beads or the receptor attached to them may be decomposing.

140
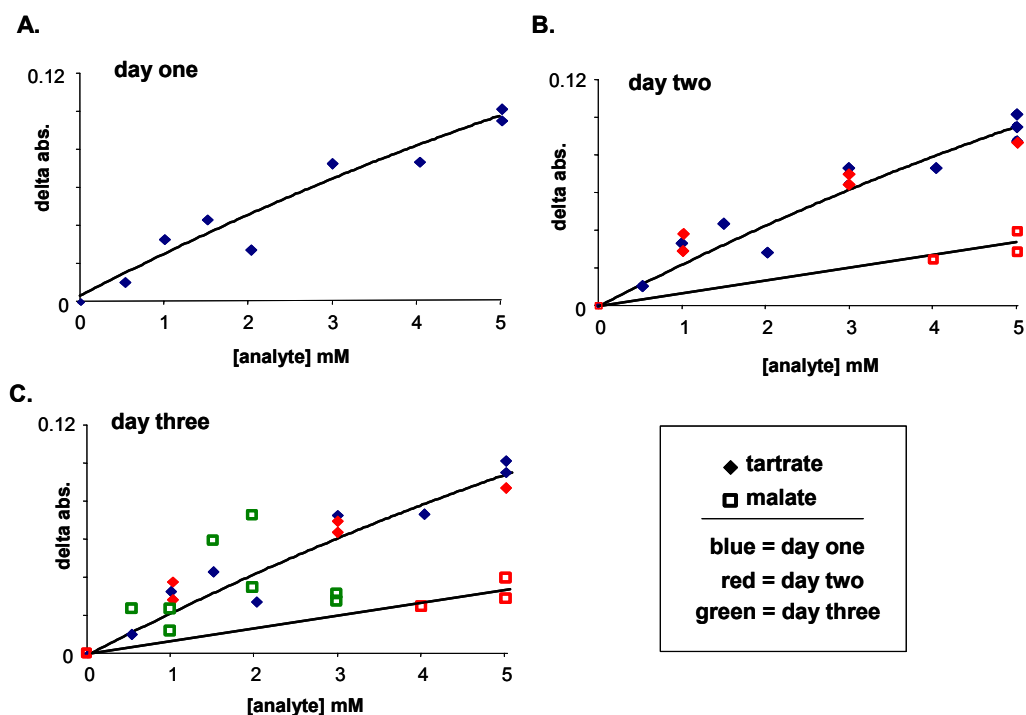
FIGURE 2.31. **CALIBRATION CURVES FOR ADDITION OF TARTRATE (♦) AND MALATE (□) TO 2.28-AG.** (Data taken in the red channel, difference between 1000 sec and 1700 sec) A. The calibration curve points taken on day one. B. The blue calibration points were taken day one; the red points were taken day two. C. The calibration curve from day two, plus calibration points from day three (green). Over time, the selectivity of the beads degrades.

2.6.4 Wines

Even though the calibration curves were not as expected, three different wines were examined with the platform anyway. The wines chosen were a Marqués de Caceras Rioja, a Rabbit Ridge Chardonnay, and a Rabbit Ridge Merlot. The concentrations of the tartrate and malate were determined through

141

analysis by ^{1}H NMR with a standard. The wines were buffered, the pH adjusted, and diluted till the concentration of the tartrate was around 2 mM. Two milliliter aliquots of wine were added to the sensing platform and the change in absorbance was determined. Each wine was run through the platform twice. Using each bead as its own calibration curve, the concentration of the tartrate was determined for each bead and the outcomes were averaged together (Table 2.3). For two out of three wines, there was an error of about 25% between the predicted and the actual value of tartrate. The concentration of the Rioja was the only one with a reasonable value. But due to the erratic behavior of the beads near the end of the experiment, it seems reasonable that the sensing ensemble was not able to quantify the concentration of tartrate.

TABLE 2.3. CONCENTRATIONS OF TARTRATE AND MALATE DETERMINED BY SENSOR ARRAY AND ^{1}H NMR.

	Tartrate (mM) **2.28-Ag-2.24**	Tartrate (mM) ^{1}H NMR	Malate (mM) ^{1}H NMR
Rioja	11.8	11.9	5.6
Merlot	9.7	13.2	12.3
Chardonnay	20.5	15.7	8.6

2.6.5 Future

Now that initial investigations are complete, efforts need to be put forth to improve the experiments. Items needing improvement are loading of the indicator, removal of the indicator, and the deterioration of the selectivity over time. In regards to loading the indicator, it is obvious that there is some variability in this process. Over the length of the aforementioned experiment, it became apparent that the absorbance of the beads increased slowly, indicating that more and more indicator was present in the resin. This could inevitably affect the amount of indicator that is displaced upon addition of analyte. It also became a problem with regards to such a small amount of transmitted light passing through the resin to the detector. There is a large error associated with the camera when the transmitted light is so low. This is mainly a factor in the blue channel. We had already learned that the loading of the indicator on the resin was not at maximum capacity. The concentration of the host on the resin is far in excess than what is needed, which could also affect the sensitivity. If there is a large concentration of host present within the resin not loaded with indicators, there are many free sites for tartrate to bind that will not illicit a colorimetric response from **2.24**. One way to alleviate this variability would be to reduce the number of receptors on the resin. In order to reduce the host concentration one could use an agarose resin with less activated sites. The resin used in this experiment was 6% activated. Perhaps a resin that was only 2% activated would be better. Also,

"capping" some of the aldehydes such that reductive amination with the host is reduced can be used in conjunction.

Another item that needs investigation is removal of tartrate and **2.24** from complexation with the boronic acids in the receptor. The studies shown within used a concentrated solution of sodium hydroxide to break up the boronate esters, but with such a strong basic solution the resins may be destroyed over time. One method might be a reverse competition assay, where the presence of excess indicator would displace tartrate from the binding pocket. In essence, we would be combining the "cleaning" step with loading the indicator. When the absorbance returned to the same level you would know the "cleaning" was complete. This was attempted previously, but due to the fact that the receptor was in such a large excess, one had no way of knowing if the tartrate was being removed. This might work better if the receptor was loaded on the resin at a lower concentration, such that when every receptor is loaded with indicator there is still a working amount of transmitted light.

In conclusion, we have transformed a solution based sensing ensemble to a solid phase sensing ensemble for the detection of tartrate. Further we have shown that the selectivity of tartrate over malate still holds true for the solid phase receptor. This new endeavor holds exciting opportunities in the area of differential sensing arrays. The first major effort will be focused on the simultaneous detection of tartrate and malate with the incorporation of the enzyme based sensing ensemble along side the synthetic sensing ensemble.

2.7   CONCLUSIONS

Throughout the last two chapters the idea has been put forth that synthetic receptors/sensors do not need to be highly selective to be useful to the scientific community.   Just as our sense of taste and smell are based on differential receptors and pattern recognition, these methods can also be used with synthetic receptors.   We have also shown that receptors that are sensitive to classes of analytes can be a useful endeavor.   Receptor **2.1** was used in a sensing ensemble to determine the age of scotch whiskies by responding to a class of age related analytes.   This was proven to be more effective than just determining the concentration of one of the age related analytes.   The next differential sensing project focused on the receptor's selectivity for tartrate over malate.   Due to this selectivity, differential sensing in solution was examined by placing two receptors (**2.1** and **1.34**) and two indicators in one cuvette.   Since the receptors displayed differential responses to tartrate and malate and to the indicators, a neural network algorithm was trained to simultaneously determine the concentrations of the two structurally similar analytes.   Finally, initial efforts were put forth to incorporate receptor **2.1** into a sensing array.   An analogous receptor was synthesized on a solid support and the selectivity of the receptor was examined for tartrate and malate.   Even though there is still much work to be done, initial studies show that the receptor does have a higher affinity for tartrate over malate.   All of these experiments have contributed to the advancement of differential sensing in supramolecular chemistry.   In order to have a differential sensor, the "tongue"

145

platform is not absolutely necessary. We have shown that through UV/visible absorption differential sensing arrays are possible in solution.

2.8   EXPERIMENTAL

General. The chemicals were obtained from Aldrich, and no further purification was done unless otherwise noted. Methyl alcohol was distilled from magnesium, and triethylamine was distilled from calcium hydride when noted. Products were placed under high vacuum for at least 12 hours before spectra were obtained. ^{1}H and ^{13}C NMR spectra were obtained on a Varian Unity Plus 300 MHz spectrometer. ^{11}B NMR spectra were obtained on a Bruker AMX-500 spectrometer. A Finnigan VG analytical ZAB2-E spectrometer was used to obtain high resolution mass spectra. UV/Visible spectra were collected on a Beckman DU640 spectrophotometer. Potentiometric measurements were taken with an Orion 720A pH meter.

UV/Visible titrations of indicator and receptor:

All solutions were buffered at pH 7.4 with HEPES buffer (10 mM) in 75% methanol in water (v/v). A solution of **2.24** (60 μM) was prepared in the cuvette and into this was titrated a stock solution of **2.1** (1.2 mM) and **2.24** (60 μM) keeping the indicator concentration constant. The data was collected at 510 nm to determine the association constant.

UV/Visible titrations of receptor/indicator ensemble and guests:

All solutions were buffered at pH 7.4 with HEPES buffer (10 mM) in 75% methanol in water (v/v). A solution of indicator (**2.24**, 60 µM) and receptor (**2.1**, 260 µM) was prepared in the cuvette and into this was titrated a stock solution of indicator, host, and guest, keeping the indicator and host concentrations constant. The data was collected at 605 nm to determine the association constant. The guest concentration in the stock solution varies between 5-80 times the concentration of host.

UV/visible titrations of receptor/indicator ensembles with scotch whiskies:

The solvent of 30 mL scotch whiskey was removed under reduced pressure and the resulting solid was redissolved to 10 mL in 75% methanol in water and buffered at pH 7.4 (10 mM HEPES). A stock solution of scotch (0.96 mL of aforementioned solution) was prepared which included pyrocatechol violet (0.023 mL, 0.06 mM) and **2.1** (0.017 mL, 0.26 mM). In the cuvette, a solution of **2.24** and **2.1** was prepared at the same concentrations. The change in absorbance of the sensing ensemble was measured upon addition of small aliquots of the stock solution of scotch. The identical titration was performed a second time, with the same concentrations minus the indicator. The absorbance of the scotch/host ensemble was subtracted from the absorbance of the sensing ensemble, and the "response number" was read off of a gallate calibration curve with the resulting absorbance.

HPLC analysis of scotch whiskies.

To determine the concentration of gallate in the scotch whiskies, the solvent of 10 mL of scotch was removed, and through a series of dilutions the scotch was diluted 20 times with a result of 2% methanol. The diluted scotch and the gallate standard were run through a reverse phase HPLC column, with a flow rate of 0.25 mL/min. The separation was run with a gradient starting with 20 minutes at 80% acidic water (1.5 mL trifluoroacetic acid and 498.5 mL water) and 20% methanol. The next 20 minutes was a gradient over to 100% methanol, with the final 20 minutes at pure methanol.

^{1}H NMR of wines:

The concentrations of tartrate and malate were determined by taking 10 mL of each of the wines, removing the solvent, and lyophilizing the samples. Each of the dehydrated wines was dissolved into 10 mL of D_2O and the pH was adjusted to 7.0. Samples of tartrate and malate were made in the same solvent conditions and pH, to be used as a reference. The final NMR samples were comprised of 0.9 mL of wine and 0.05 mL of a concentrated solution of dichloroacetic acid as a reference. Around 1000 scans were collected, the peaks were integrated, and concentrations of tartrate and malate were calculated.

^{11}B NMR Titrations.

Solutions of **2.18** and **2.19** were prepared in protic water with 10% deuterated methanol ranging in concentration between 20-40 mM. Sodium chloride was

added as the electrolyte and the pH of the solutions were adjusted between 1.6 and 12 with aqueous sodium hydroxide and hydrochloric acid. Quartz NMR tubes were used to limit background noise, but some residual noise was still present from the glass in the probe.

pH Titrations:

Solutions of **2.18** and **2.19** were made in water (4.5 mM) in the presence of 0.15 M NaCl and 0.1 M NaOH. Perchloric acid (0.1 M) was titrated into the solution in 50 μL aliquots. Potentiometric studies were conducted with a Brinkmann Titrino 702 autotitrator. A Metrohm combined pH glass electrode (Ag/AgCl) with 3 M NaCl internal filling solution was used. Measurements were taken at 25°C under nitrogen. About 100 data points were collected for each titration and the analysis was carried out as described by Martell,[21] and equilibrium constants were calculated using the program BEST. All constants were determined using at least two independent titrations.

1,3-Bis[(2-benzeneboronic acid)aminomethyl]-5-(4,5-dihydro-1H-imidazol-2-yl)aminomethyl-2,4,6-triethylbenzene (2.1)
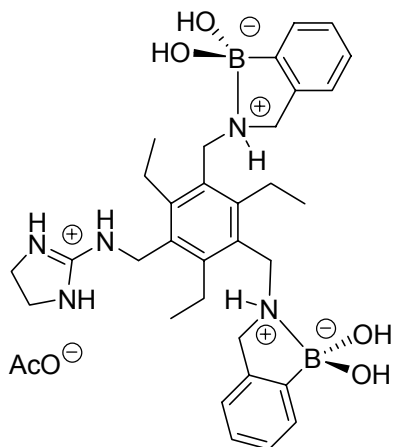
Dry triethylamine (1.0 mL) and 2-formylbenzene boronic acid (0.37 g, 2.44 mmol) was added to a solution of **2.11** (0.58 g, 0.16 mmol) in dry methanol over 3Å molecular sieves in an inert atmosphere. The reaction was heated to 30-40 °C for 4 hours. Sodium borohydride (0.11 g, 2.78 mmol) was then added and the mixture was filtered through celite. The solvent was removed and the resulting solid was put under vacuum for two days. The solid was then dissolved in water and filtered through celite again, and lyophilized. To dispose of any unwanted salts, the compound was dissolved in 9:1 ethyl acetate:methanol (v/v) and filtered through celite. Solvent removal and lyophilization resulted in a white fluffy powder. (0.61 g, 82%). M.P. = 190 °C (decomp.), ^{1}H NMR (300MHz, CD$_3$OD): δ 7.48 (d, 2H, Ph), 7.20 (m, 4H, Ph), 7.10 (d, 2H, Ph), 4.43 (s, 2H, CH$_2$), 4.14(s, 4H, CH$_2$), 3.95 (s, 4H, CH$_2$), 3.79 (s, 4H, CH$_2$), 2.85 (q, 6H, CH$_2$), 1.16 (t, 9H, CH$_3$); ^{13}C NMR (75MHz, CD$_3$OD): 161.16, 147.30, 146.71, 142.40, 131.82, 131.33, 131.00, 128.37, 127.77, 124.57, 53.75, 44.40, 44.19, 42.04, 24.24, 16.74,

16.63; HRMS-FAB$^+$ m/z: calcd for $C_{38}H_{54}B_2N_5O_6$ (Glycerol matrix): 698.426; obsd: 698.426: ^{11}B NMR (160MHz, CD$_3$OD, ref. BF$_3$-Et$_2$O 0.0 ppm): δ 10.16.

1,3,5-Tris(chloromethyl)-2,4,6-triethylbenzene (2.6)
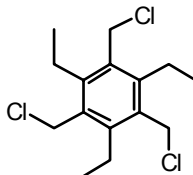
Into a 3-neck 200 mL round bottom flask, equipped with a condenser, dispersion tube, and a septum, 35 mL carbon disulfide and 1,3,5-triethylbenzene (**2.2**) (6.52g, 40.25 mmol) was added and nitrogen was bubbled through for 30 minutes. The dispersion tube was removed and under an inert atmosphere tin tetrachloride (99%) (12 mL, 102.54 mmol) was added along with chloromethylmethyl ether (29 mL, 381.82 mmol). The reaction was stirred for two hours. The mixture was poured over ice and aqueous sodium bicarbonate was added to neutralize the solution. The precipitant was filtered off and the carbon disulfide layer was separated from the aqueous layer and the solvent was removed. Purification was accomplished by loading the impure compound on silica gel (50 g) and the silica gel was placed in a fritted funnel and washed with a 3:1 hexanes:dichloromethane mixture. The solvent of the filtrate was removed, and the resulting solid was washed with ethanol to obtain the final purified compound. (9.7g, 78%). M.P. 130 ˚C. ^{1}H NMR (300 MHz, CDCl$_3$): δ 4.69 (s, 6H, CH$_2$), 2.92 (q, 6H, CH$_2$), 1.31 (t, 9H, CH$_3$); ^{13}C NMR (75 MHz, CDCl$_3$): δ 145.7, 130.3, 41.3, 23.4, 16.8; HRMS-EI$^+$ m/z: calcd for $C_{15}H_{21}Cl_3$: 306.071; obsd: 306.072

151

1,3-Bis[[(1,1-Dimethylethoxy)carbonyl]aminomethyl]-5-aminomethyl-2,4,6-triethylbenzene (2.8)
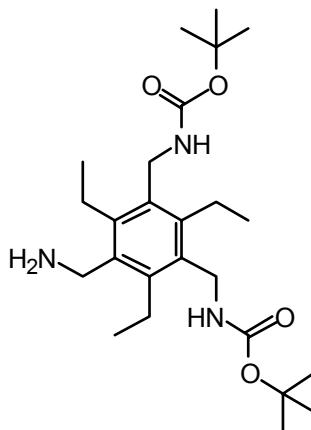
A solution of di-tert-butyl dicarbonate (1.74 g, 7.8 mmol) in chloroform was added dropwise to **2.7** (2.48 g, 10.0 mmol) in chloroform. The mixture was allowed to stir for 12 hours. The solvent was removed and separation was performed by column chromatography (silica gel, gradient of 1-20% ammonia sat. methanol in CH_2Cl_2 (v/v)). (1.25 g, 28%) M.P. = 150-154 °C; ^1H NMR (300MHz, CD_3OD): δ 4.27 (s, 4H), 3.84 (s, 2H), 2.75 (q, 6H), 1.45 (s, 18H), 1.16 (t, 9H); ^{13}C NMR (75MHz, $CDCl_3$): δ 156.17, 143.41, 138.08, 133.03, 80.17, 40.19, 39.57, 29.17, 23.49, 17.42; HRMS-CI$^+$ m/z: calcd for $C_{25}H_{43}N_3O_4$: 450.333; obsd: 450.332

1,3-Bis[[(1,1-dimethylethoxy)carbonyl]aminomethyl]-5-(4,5-dihydro-1H-imidazol-2-yl)aminomethyl-2,4,6-triethylbenzene hydroacetate (2.10)
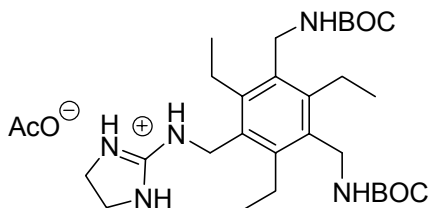
Aqueous acetic acid (5 %) was used to dissolve **2.8** (0.305 g, 0.678 mmol) and the solution was lyophilized twice to give the ammonium salt. This was ground together with free based 2-methylthio-2-imidazoline (0.294 g, 1.2 mmol) and the resulting sticky solid was packed in a conical vial, sealed, and heated to 100°C for 3 days. The vial was cooled to room temperature and dissolved in 5% acetic acid (aq.) and lyophilized. Purification was done by FPLC (reversed phase resin RP 18; C18 modified silica gel; particle size 55-105μm) and eluted with an NH$_4$Ac/CH$_3$CN gradient from 25 mM NH$_4$Ac to neat CH$_3$CN. (0.120 g, 32%) M.P. = 250 °C (decomp.); ^{1}H NMR (300MHz, CDCl$_3$): δ 4.39 (s, 2H, CH$_2$), 4.30 (s, 4H, CH$_2$), 3.76 (s, 4H, CH$_2$), 2.74 (q, 6H, CH$_2$), 1.85 (s, 3H, CH$_3$), 1.44 (s, 18H, CH$_3$), 1.17 (t, 9H, CH$_3$); ^{13}C NMR (75MHz, CDCl$_3$): 161.04, 158.03, 146.06, 144.95, 133.69, 130.49, 80.31, 44.17, 42.04, 39.64, 28.81, 23.85, 16.64, 16.57; HRMS-CI$^+$ m/z: calcd for C$_{28}$H$_{48}$N$_5$O$_4$: 518.370; obsd: 518.369

1-(4,5-Dihydro-1H-imidazol-2-yl)aminomethyl-3,5-bis(aminomethyl)-2,4,6-triethylbenzene trihydrotriacetate(2.11)
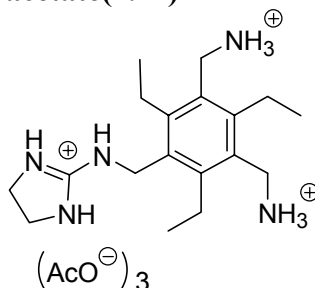
To a solution of **2.10** (0.767 g, 1.24 mmol) in dichloromethane, 15 mL of trifluoroacetic acid was added and the solution was allowed to stir for 2 hours. The solvent was removed and the anions were exchanged with an anion exchange resin to acetates. The water solution was then lyophilized to yield a white solid. (0.610 g, 98%) M.P. = 250 °C (decomp.), ^{1}H NMR (300MHz, CD$_3$OD): δ 4.46 (s, 2H), 4.26 (s, 4H), 3.78 (s, 4H), 2.80 (q, 6H), 1.84 (s, 9H), 1.21 (t, 9H); ^{13}C NMR (75MHz, CDCl$_3$): 180.20, 161.42, 147.14, 146.63, 131.83, 130.58, 44.16, 41.86, 37.69, 24.28, 24.12, 16.40; HRMS-CI$^+$ m/z: calcd for C$_{18}$H$_{32}$N$_5$: 318.266; obsd: 318.266.

N-(**1,1-Dimethylethoxycarbonyl**)-2-**methylthio**-2-**imidazole (2.12)**
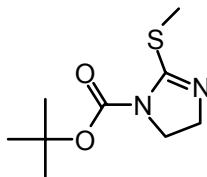
Into a 50 mL RBF, **2.9** (4.6 g, 18.96 mmol) and triethylamine (2.8 mL, 20.1 mmol) was dissolved in 15 mL dichloromethane and cooled to 0^0 C. Through an

addition funnel di-tert-butyl dicarbonate (4.6 g, 21.01 mmol) dissolved in 5 mL dichloromethane was slowly added to the mixture. After completion, the mixture was allowed to warmed to room temperature and stirred for 24 hours. The solvent was removed and residue was dissolved in ethyl acetate and filtered through celite to remove the insoluble salts. Separation was performed by column chromatography (silica gel, 1-2% ammonia sat. methanol in CH_2Cl_2 (v/v)) to yield white crystals. (3.9 g, 99%) M.P. 33-37 °C; ^{1}H NMR (CDCl$_3$, 300 MHz) δ 3.82 (s, 4H, CH$_2$), 2.36 (s, 3H, CH$_3$), 1.48 (s, 9H, CH$_3$); ^{13}C NMR (CDCl$_3$, 75 MHz) δ 151.09, 82.87, 53.64, 47.87, 28.38, 15.35; HRMS-CI$^+$ m/z: calcd for C$_9$H$_{17}$N$_2$O$_2$S$_1$: 217.101; obsd: 217.101

1,3-Bis[[(1,1-dimethylethoxy)carbonyl]aminomethyl]-5-(4,5-dihydro-N-(1,1-dimethylethoxy)carbonyl-imidazol-2-yl)aminomethyl-2,4,6-triethylbenzene (2.13)
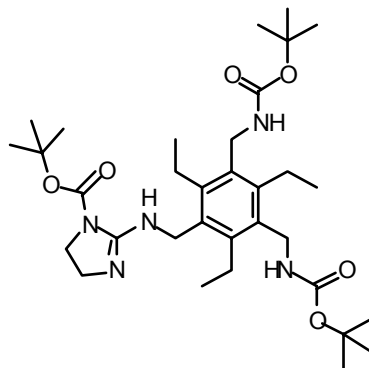
To a solution of **2.8 (**1.10 g, 2.5 mmol) in 20 mL ethanol and 2.5 mL glacial acetic acid, **2.12** (0.72 g, 3.3 mmol) was added. The mixture was heated to 60^0 C for 10 hours, then allowed to cool to room temperature for additional 10 hours.

155

After removal of the solvent, the mixture was purified by column chromatography (silica gel, 1-4% NH_3 sat. methanol in dichloromethane (v/v)). An impurity was still present with the compound, so recrystallization was performed with dichloromethane. (0.77 g, 51 %) M.P. = 165-167 °C, ^{1}H NMR (300MHz, CDCl$_3$): δ 6.70 (broad s, 1H), 4.44 (s, 2H), 4.40 (broad s, 2H), 4.32 (s, 4H), 3.84 (m, 4H), 2.70 (q, 6H), 1.43 (s, 27H), 1.17 (t, 9H); ^{13}C NMR (75MHz, CDCl$_3$): δ 155.64, 153.9, 153.3, 144.2, 132.54, 82.80, 48.19, 46.93, 41.37, 39.01, 28.41, 23.21, 16.74; HRMS-CI$^+$ m/z: calcd for $C_{33}H_{56}N_5O_6$: 618.423; obsd: 618.423

Synthesis of receptor 2.28 on the tentagel resin (2.28-PS)

To a solid phase reaction shaker was added dry methanol, trimethylortho formate, **2.30** (0.017 g, 0.03 mmol), and 200-250 μm Tentagel MB FMP acid labile resin (0.054 g, 0.015 mmol by a loading of 0.28 mmol/g). This was allowed to shake for 4 hours. Sodium borohydride (0.0095 g, 0.25 mmol) was added and the mixture shook overnight. The methanol was removed, and the resin was washed three more times with methanol. Upon addition of **2.24** to a small amount of the beads they turned pink, indicating that the resin was present.

1,3-Bis[(2-benzeneboronic acid)aminomethyl]-5-[[(1,1-dimethylethoxy) carbonyl] aminomethyl]-2,4,6-triethylbenzene (2.29)
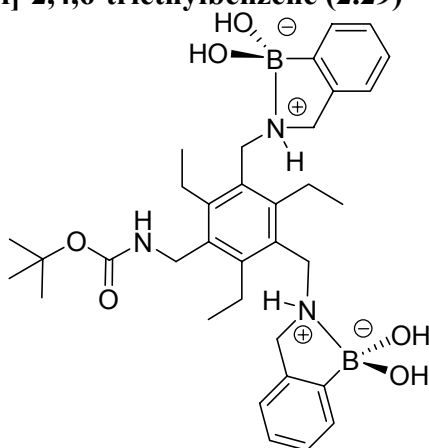
Dry methanol was added to a flame dried round bottom flask with sieves. To this was added 2.25 (0.202 g, 0.58 mmol), 2.14 (0.191 g, 1.27 mmol), triethylamine (dry) (1.0 mL, 7.2 mmol), and trimethylorthoformate. The reaction mixture was heated to 40° C under argon and was allowed to stir slowly for 3 hours. Sodium borohydride (0.06 g, 1.59 mmol) was then added. The mixture was filtered through celite and the methanol was removed. To dispose of any unwanted salts, the compound was dissolved in 9:1 ethyl acetate:methanol (v/v) and filtered through celite. The solvent was removed from the filtrate and the resulting solid was loaded onto a silica gel column. The column was run with 1.) 100 mL 9:1 ethyl acetate: NH_3 sat. methanol, 2.) 100 mL 8:2 ethyl acetate: NH_3 sat. methanol, and finally 3.) 200 mL1:1 ethyl acetate: NH_3 sat. methanol. The silica gel that was present with the product as a result of being dissolved in the conditions used was precipitated out of solution by dissolving the solid in a small amount 9:1 ethyl acetate:methanol. The precipitant was filtered off. The final product after lyophilization was a white fluffy solid. (0.257 g, 72 %). M.P. decomp.; ^{1}H NMR

(CD$_3$OD, 300 MHz) δ 7.49 (m, 2H), 7.21 (m, 4H), 7.11 (m, 2H), 4.31 (s, 2H), 4.07 (s, 4H), 3.90 (s, 4H), 2.80 (m, 6H), 1.44 (s, 9H), 1.12 (t, 6H), 1.05 (t, 3H); ^{13}C NMR (75MHz, CD$_3$OD): δ 157.06, 147.46, 146.96, 143.14, 132.72, 131.61, 129.18, 128.62, 125.47, 80.30, 45.30, 29.67, 24.94, 22.94, 17.52;. ^{11}B NMR (CD$_3$OD, 160 MHz, 25°C) δ 11.0; HRMS-FAB$^+$ m/z: calcd for C$_{40}$H$_{58}$B$_2$N$_3$O$_8$ (glycerol matrix): 730.441; obsd: 730.440.

1,3-Bis[(2-benzeneboronic acid)aminomethyl]-5-aminomethyl]-2,4,6-triethylbenzene hydroacetate (2.30)
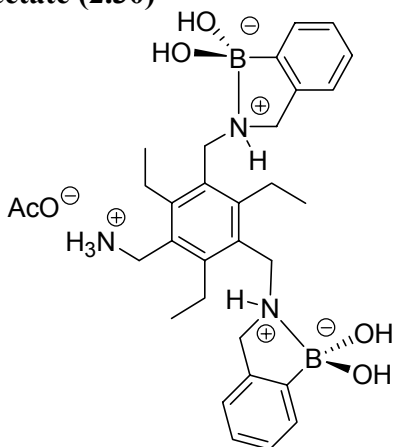
Trifluoroacetic acid was added to a solution of 2.29 (0.133 g, 0.22 mmol) in water and the mixture was allowed to stir for five hours. The solvent was subsequently removed and the counterions were exchanged to acetates by ion exchange chromatography. The aqueous solution of 2.30 was lyophilized to give a fluffy white powder. (0.114 g, 7292 %). M.P. decomp.; ^{1}H NMR (CD$_3$OD, 300 MHz) δ 7.47 (m, 2H), 7.19 (m, 4H), 7.11 (m, 2H), 4.17 (s, 6H), 3.98 (s, 4H), 2.91 (m, 6H), 1.92 (s, 3H), 1.16 (m, 9H); ^{13}C NMR (75MHz, CD$_3$OD): δ 149.61, 137.17, 136.80, 134.01, 132.56, 131.03, 129.18, 45.66, 38.52, 25.87, 16.99;. ^{11}B NMR

(CD$_3$OD, 160 MHz, 25°C) δ 9.97; HRMS-FAB$^+$ m/z: calcd for C$_{35}$H$_{50}$B$_2$N$_3$O$_6$ (glycerol matrix): 630.389; obsd: 630.389.

X-Ray crystal structure determination for C$_{33}$H$_{37}$B$_2$N$_7$O$_4$ (2.17): Crystals grew as pale yellow needles by slow evaporation in deuterated methanol. The data crystal was a long needle that was broken from a cluster of crystals and had approximate dimensions; 0.46 x 0.10 x 0.10 mm. The data were collected on a Nonius Kappa CCD diffractometer using a graphite monochromator with MoKα radiation (λ = 0.71073Å). A total of 192 frames of data were collected using ω-scans with a scan range of 2° and a counting time of 324 seconds per frame. The data was collected at -150 °C using an Oxford Cryostream low temperature device. Details of crystal data, data collection and structure refinement are listed in Table 1. Data reduction was performed using DENZO-SMN.[57] The structure was solved by direct methods using SIR92[58] and refined by full-matrix least-squares on F^2 with anisotropic displacement parameters for the non-H atoms using SHELXL-97.[59] The hydrogen atom positions were observed in a ΔF map and refined with isotropic displacement parameters. The function, Σw(|F$_o$|^2 - |F$_c$|^2)^2, was minimized, where w = 1/[((F$_o$))^2 + (0.0469*P)^2 + (1.8623*P)] and P = (|F$_o$|^2 + 2|F$_c$|^2)/3. R$_w$(F^2) refined to 0.119, with R(F) equal to 0.0549 and a goodness of fit, S, = 1.050. Definitions used for calculating R(F),R$_w$(F^2) and the goodness of fit, S, are given below.[60] Neutral atom scattering factors and values used to calculate the linear absorption coefficient are from the International Tables for X-ray Crystallography (1992). All figures were generated using

159

SHELXTL/PC. Tables of positional and thermal parameters, bond lengths and angles, figures and lists of observed and calculated structure factors are located in Tables 1 through 6.

X-Ray crystal structure determination for $C_{16}H_{20}BNO_2$ (2.18): Crystals grew as large colorless prisms by crystallization from methanol. The data crystal was cut from a much larger crystal and had approximate dimensions; 0.1x0.1x0.1 mm. The data were collected on a Nonius Kappa CCD diffractometer using a graphite monochromator with MoKα radiation (λ = 0.71073Å). A total of 298 frames of data were collected using ω-scans with a scan range of 1° and a counting time of 51 seconds per frame. The data were collected at 153 K using an Oxford Cryostream low temperature device. Details of crystal data, data collection and structure refinement are listed in Table 1. Data reduction were performed using DENZO-SMN.[57] The structure was solved by direct methods using SIR92[61] and refined by full-matrix least-squares on F^2 with anisotropic displacement parameters for the non-H atoms using SHELXL-97.[59] The hydrogen atoms on carbon were calculated in ideal positions with isotropic displacement parameters set to 1.2xUeq of the attached atom (1.5xUeq for methyl hydrogen atoms). The hydrogen atom bound to the nitrogen atom was found in a ΔF map and refined with an isotropic displacement parameter. The function, $\Sigma w(|F_o|^2 - |F_c|^2)^2$, was minimized, where $w = 1/[(\sigma(F_o))^2 + (0.0537*P)^2 + (0.4446*P)]$ and $P = (|F_o|^2 + 2|F_c|^2)/3$. $R_w(F^2)$ refined to 0.119, with R(F) equal to 0.0446 and a goodness of fit, S, = 1.01. Definitions used for calculating R(F),$R_w(F^2)$ and the goodness of

fit, S, are given below.[62]   The data were corrected for secondary extinction effects.   The correction takes the form: $F_{corr} = kF_c/[1 + (1.7(4)x10^{-5})* F_c^2 \lambda^3/(\sin2\theta)]^{0.25}$ where k is the overall scale factor.   Neutral atom scattering factors and values used to calculate the linear absorption coefficient are from the International Tables for X-ray Crystallography (1992).[63]   All figures were generated using SHELXTL/PC.[59]   Tables of positional and thermal parameters, bond lengths and angles, torsion angles, figures and lists of observed and calculated structure factors are located in tables 1 through 7.

2.9   REFERENCES AND NOTES

(1)   Antonisse, M. M. G.; Reinhoudt, D. N. Neutral Anion Receptors: Design
         and Application. *Chem. Commun.* **1998**, 443-448; Linton, B.; Hamilton,
         A. D. Formation of Artificial Receptors by Metal-Templated Self
         Assembly. *Chem. Rev.* **1997***, 97*, 1669-1680; Reichenback-Klinke, R.;
         Konig, B. Metal Complexes of Azacrown Ethers in Molecular
         Recognition and Catalysis. *J. Chem. Soc., Dalton Trans.* **2002**, 121-130;
         Sanders, J. K. M. Adventures in Molecular Recognition. The Ins and Outs
         of Templating. *Pure Appl. Chem.* **2000***, 72*, 2265-2274; Schneider, H.-J.
         Mechanisms of Molecular Recognition: Investigations of Organic Host-
         Guest Complexes. *Angew. Chem., Int. Ed.* **1991***, 30*, 1417-1436; Snowden,
         T. S.; Anslyn, E. V. Anion Recognition: Synthetic Receptors for Anions
         and Their Application in Sensors. *Curr. Opin. Chem. Biol.* **1999***, 3*, 740-
         746.

(2)   Bell, T. W.; Hou, Z.; Luo, Y.; Drew, M. G. B.; Chapoteau, E.; Czech, B.
         P.; Kumar, A. Detection of Creatinine by a Designed Receptor. *Science*
         1995*, 269*, 671-674; Bell, T. W.; Hou, Z. A Hydrogen-Bonding Receptor
         That Binds Urea with High Affinity. *Angew. Chem., Int. Ed.* **1997***, 36*,
         1536-1538; Chen, C.-T.; Huang, W.-P. A Highly Selective Fluorescent
         Chemosensor for Lead Ions. *J. Am. Chem. Soc.* **2002***, 124*, 6246-6247;
         Cheng, Y.; Suenaga, T.; Still, W. C. Sequence-Selective Peptide Binding
         with a Peptido-A,B-trans-steroidal Receptor Selected from an Encoded
         Combinatorial Receptor Library. *J. Am. Chem. Soc.* **1996***, 118*, 1813-
         1814; Chin, J.; Walsdorff, C.; Stranix, B.; Oh, J.; Chung, H. J.; Park, S.-
         M.; Kim, K. A Rational Approach to Selective Recognition of NH4+ over
         K+. *Angew. Chem., Int. Ed.* **1999***, 38*, 2756-2759; Haino, T.; Rudkevich,
         D. M.; Shivanyuk, A.; Rissanen, K.; Rebek, J. J. Induced-Fit Molecular
         Recognition with Water-Soluble Cavitands. *Chem. Eur. J.* **2000***, 6*, 3797-
         3805; Hirano, T.; Kikuchi, K.; Urano, Y.; Higuchi, T.; Nagano, T. Highly
         Zinc-Selective Fluorescent Sensor Molecules Suitable for Biological
         Applications. *J. Am. Chem. Soc.* **2000***, 122*, 12399-12400; Inouye, M.;
         Hashimoto, K.; Isagawa, K. Nondestructive Detection of Acetylcholine in
         Protic Media: Artificial-Signaling Acetylcholine Receptors. *J. Am. Chem.
         Soc.* **1994***, 116*, 5517-5518; James, T. D.; Sandanayake, K. R. A. S.;
         Shinkai, S. Chiral discrimination of monosaccharides using a fluorescent
         molecular sensor. *Nature* **1995***, 374*, 345-347; Kin, S.-G.; Ahn, K. H.
         Novel Artificial Receptors for Alkylammonium Ions with Remarkable
         Selectivity and Affinity. *Chem. Eur. J.* **2000***, 6*, 3399-3403.

(3)   Niikura, K.; Metzger, A.; Anslyn, E. V. Chemosensor Ensemble with Selectivity for Inositol-Trisphosphate. *J. Am. Chem. Soc.* **1998***, 120*, 8533-8534.

(4)   Metzger, A.; Lynch, V. M.; Anslyn, E. V. A synthetic receptor selective for citrate. *Angew. Chem., Int. Ed.* **1997***, 36*, 862-865.

(5)   Wiskur, S. L.; Anslyn, E. V. Using a Synthetic Receptor to Create an Optical-Sensing Ensemble for a Class of Analytes: A Colorimetric Assay for the Aging of Scotch. *J. Am. Chem. Soc.* **2001***, 123*, 10109-10110.

(6)   Iverson, D. J.; Hunter, G.; Blount, J. F.; Damewood, J. R., Jr.; Mislow, K. Static and dynamic stereochemistry of hexaethylbenzene and of its tricarbonylchromium, tricarbonylmolybdenum, and dicarbonyl(triphenylphosphine)chromium complexes. *J. Am. Chem. Soc.* **1981***, 103*, 6073-6083; Kilway, K. V.; Siegel, J. S. Effect of transition-metal complexation on the stereodynamics of persubstituted arenes. Evidence for steric complementarity between arene and metal tripod. *J. Am. Chem. Soc.* **1992***, 114*, 255-261; Marx, H.-W.; Moulines, F.; Wagner, T.; Astruc, D. Hexakis(3-butynyl)benzene. *Angew. Chem., Int. Ed.* **1996***, 35*, 1701-1704; Stack, T. D. P.; Hou, Z.; Raymond, K. N. Rational reduction of the conformational space of a siderophore analog through nonbonded interactions: the role of entropy in enterobactin. *J. Am. Chem. Soc.* **1993***, 115*, 6466-6467.

(7)   Wulff, G. Selective binding to polymers via covalent bonds. The construction of chiral cavities as specific receptor sites. *Pure Appl. Chem.* **1982***, 54*, 2093-2102.

(8)   Linton, B. R.; Goodman, M. S.; Fan, E.; Van Arman, S. A.; Hamilton, A. D. Thermodynamic Aspects of Dicarboxylate Recognition by Simple Artificial Receptors. *J. Org. Chem.* **2001***, 66*, 7313-7319; Berger, M.; Schmidtchen, F. P. Zwitterionic Guanidinium Compounds Serve as Electroneutral Anion Hosts. *J. Am. Chem. Soc.* **1999***, 121*, 9986-9993.

(9)   Hanes, R. E., Jr.; Lavigne, J. J.; Anslyn, E. V. *Org. Syn.* **2002**, In preparation.

(10)   Staudinger; Meyer *Helv. Chim. Acta* **1919***, 2*, 635.

(11)   Mundla, S. R.; Wilson, L. J.; Klopfenstein, S. R.; Seibel, W. L.; Nikolaides, N. N. A novel method for the efficient synthesis of 2-arylamino-2-imidazolines. *Tetrahedron Let.* **2000***, 41*, 6563-6566.

163

(12)   Juillard, J.; Geugue, N. C. R. Sur La Dissociation de Quelques Acides Arylboriques en Solvants Mixtes Eau-Methanol. *Acad. Paris C* **1967**, *264*, 259-261.

(13)   James, T. D.; Sandanayake, K. R. A. S.; Shinkai, S. Novel photoinduced electron-transfer sensor for saccharides based on the interaction of boronic acid and amine. *J. Chem. Soc., Chem. Commun.* **1994**, 477-478.

(14)   Ward, C. J.; Ashton, P. R.; James, T. D.; Patel, P. A molecular colour sensor for monosaccharides. *Chem. Commun.* **2000**, 229-230.

(15)   Ait Haddou, H.; Anslyn, E. V. University of Texas at Austin, Austin, TX. Unpublished Work,. **2002**.

(16)   Lavigne, J. J.; Anslyn, E. V. Teaching old indicators new tricks: a colorimetric chenosensing ensemble for tartrate/malate in beverages. *Angew. Chem., Int. Ed.* **1999**, *38*, 3666-3669.

(17)   Wiskur, S. L.; Ait-Haddou, H.; Lavigne, J. J.; Anslyn, E. V. Teaching old indicators new tricks. *Acc. Chem. Res.* **2001**, *34*, 963-972.

(18)   Lavigne, J. J.; Anslyn, E. V. Unpublished work. **2002**; Hawkins, R. T.; Snyder, H. R. Arylboronic Acids. VI. Aminoboronic Anhydrides and a New Heterocycle Containing Boron. *J. Am. Chem. Soc.* **1960**, *82*, 3863-3866; Hawkins, R. T.; Blackham, A. U. Reaction of o-(bromomethyl)benzeneboronic anhydride with primary amines. *J. Org. Chem.* **1967**, *32*, 597-600.

(19)   James, T. D.; Sandanayake, K. R. A. S.; Shinkai, S. A glucose-specific molecular fluorescence sensor. *Ang. Chem.* **1994**, *106*, 2287-2289; James, T. D.; Sandanayake, K. R. A. S.; Iguchi, R.; Shinkai, S. Novel Saccharide-Photoinduced Electron Transfer Sensors Based on the Interaction of Boronic Acid and Amine. *J. Am. Chem. Soc.* **1995**, *117*, 8982-8987.

(20)   Lavigne, J. J. Molecular Recognition and Molecular Sensing: Single Analyte Analysis and Multi-Component Sensor Arrays for the Simultaneous Detection of a Plethora of Analytes.; University of Texas at Austin: Austin, 2000.

(21)   Martell, A. E.; Motekaitis, R. J. *Determination and Use of Stability Constants*; VCH Publishers, Inc.: New York, 1992.

(22)   Potentiometric studies were conducted with a Brinkmann Titrino 702 autotitrator. A Metrohm combined pH glass electrode (Ag/AgCl) with 3 M NaCl internal filling solution was used. Measurements were taken at 25°C under nitrogen. About 100 data points were collected for each titration and the analysis was carried out as described by Martell (ref. below), and equilibrium constants were calculated using the program BEST. All constants were determined using at least two independent titrations. Martell, A. E.; Motekaitis, R. J. "Determination and Use of Stability Constants," VCH Publishers, Inc., New York, 1992.

(23)   11B NMR spectra was obtained with a Bruker AMX-500 spectrometer. Quartz NMR tubes were used to limit background noise. The pH of the solutions were adjusted between 1.6 and 11 and measured with an Orion 720A pH meter.

(24)   Noth, H.; Wrackmeyer, B. Nuclear Magnetic Resonance Spectroscopy of Boron Compounds. In *NMR Basic Principles and Progress*; Diehl, P., Fluck, E., Kosfeld, R. Eds.; Springer-Verlag: New York, 1978; pp 5-14, 287.

(25)   Wiskur, S. L.; Lavigne, J. J.; Ait-Haddou, H.; Lynch, V.; Chiu, Y. H.; Canary, J. W.; Anslyn, E. V. pKa Values and Geometries of Secondary and Tertiary Amines Complexed to Boronic Acids-Implications for Sensor Design. *Org. Lett.* **2001***, 3*, 1311-1314.

(26)   Toyota, S.; Futawaka, T.; Asakura, M.; Ikeda, H.; Oki, M. Experimental and Theoretical Evidence of an SN2-Type Mechanism for Dissociation of B-N Coordination Bonds in 2,6-Bis((dimethylamino)methyl)phenylborane Derivatives. *Organomet.* **1998***, 17*, 4155-4163.

(27)   Crystal Data for 2.19. C33H37B2N7O4, M = 617.32, Monoclinic, space group C2/c (No. 15), a = 21.7733(9), b = 16.3103(9), c = 8.9580(3)Å, = 99.049(3)°, V = 3141.7(2)Å3, Z = 4, Dc = 1.30g/cc, = 0.087 mm-1. Data were collected at 123(2)K on a Nonius Kappa CCD using graphite monochromatized Mo K radiation (0.71073Å). A total of 5976 reflections were collected, 3535 were unique (Rint = 0.028). The structures were refined on F2 to a wR2 = 0.119 with an R1 [for 2497 reflections with Fo > 4((Fo))] = 0.0549 and a goodness of fit = 1.05. The molecule lies on a crystallographic two-fold rotation axis passing through the central pyridine ring. Full X-ray experimental details are located in the Supplementary data.

(28)   Bissel, R. A.; de Silva, A. P.; Gunaratne, H. Q. N.; Lynch, P. L. M.;
         Maguire, G. E. M.; McCoy, C. P.; Sandanayake, K. R. A. S. Fluorescent
         PET (Photoinduced Electron Transfer) Sensors. *Top. Curr. Chem.* **1993**,
         168, 223-264.

(29)   Goldberg, D. M.; Hoffman, B.; Yang, J.; Soleas, G. J. Phenolic
         constituents, furans, and total antioxidant status of distilled spirits. *J.
         Agric. Food Chem.* **1999**, *47*, 3978-3985; Bronze, M. R.; Vilas Boas, L.
         F.; Belchior, A. P. Analysis of old brandy and oak extracts by capillary
         electrophoresis. *J. Chrom. A* **1997**, *768*, 143-152.

(30)   Ng, L. K.; Lafontaine, P.; Harnois, J. Gas chromatographic-mass
         spectrometric analysis of acids and phenols in distilled alcohol beverages.
         Application of anion-exchange disk extraction combined with in-vial
         elution and silylation. *J. Chrom. A* **2000**, *873*, 29-38.

(31)   Leonard, M. A.; West, T. S. Chelating Reactions of 1,2-
         Dihydroxyanthraquinon-3-ylmethyl-amine-N,N-diacetic Acid with Metal
         Cations in Aqueous Media. *J. Chem. Soc., Dalton Trans.* **1960**, 4477-
         4485; Belcher, R.; Leonard, M. A.; West, T. S. The Preparation and
         Analytical Properties of N,N-Di(carboxy-methyl)aminomethyl Derivatives
         of Some Hydroxyanthraquinones. *J. Chem. Soc.* **1958**, 2390-2393.

(32)   Herrington, J.; Steed, K. C. Spectrophotometric Determination of the Rare
         Earths Yttrium and Cerium by Bromopyrogallol Red. *Anal. Chim. Acta*
         1960, *22*, 180-184.

(33)   Hughes, D. E.; Cardone, M. J. Simultaneous titrimetric determination of
         bismuth ion and free nitric acid concentrations. *Anal. Chem.* **1980**, *52*,
         940-942; Corbin, H. B. Rapid and selective pyrocatechol violet method for
         tin. *Anal. Chem.* **1973**, *45*, 534-537.

(34)   Connors, K. A. *Binding Constants, The Measurement of Molecular
         Stability*; Wiley: New York, 1987.

(35)   Due to low solubility in the solvent system, a binding constant was not
         determined.

(36)   Mangas, J.; Rodríguez, R.; Moreno, J.; Suárez, B.; Blanco, D. Evolution
         of Aromatic and Furanic Congeners in the Maturation of Cider Brandy: A
         Contribution to Its Characterization. *J. Agric. Food Chem.* **1996**, *44*, 3303-
         3307.

(37)   Lin, J.-K.; Lin, C.-L.; Liang, Y.-C.; Lin-Shiau, S.-Y.; Juan, I.-M. Survey of Catechins, Gallic Acid, and Methylxanthines in Green, Oolong, Pu-erh, and Black Teas. *J. Agric. Food Chem.* **1998***, 46*, 3635-3642; Aucamp, J. P.; Hara, Y.; Apostolides, Z. Simultaneous Analysis of Tea Catechins, Caffeine, Gallic Acid, Theanine, and Ascorbic Acid by Micellar Electrokinetic Capillary Chromatography. *J. Chrom. A* **2000***, 876*, 235-242.

(38)   Margolskee, R. F. Receptor Mechanisms in Gustation. In *Handbook of Olfaction and Gustation*; Doty, R. L. Ed.; Marcel Dekker: New York, 1995; pp 575-595; Mierson, S. Transduction of Taste Stimuli by Receptor Cells in the Gustatory System. In *Handbook of Olfaction and Gustation*; Doty, R. L. Ed.; Marcel Dekker: New York, 1995; pp 597-610; Miller, I. J., Jr. Anatomy of the Peripheral Taste System. In *Handbook of Olfaction and Gustation*; Doty, R. L. Ed.; Marcel Dekker: New York, 1995; pp 521-547.

(39)   Lavigne, J. J.; Anslyn, E. V. Sensing a paradigm shift in the field of molecular recognition: from selective to differential receptors. *Angew. Chem., Int. Ed.* **2001***, 40*, 3118-3130.

(40)   Wiskur, S. L.; Floriano, P. N.; Anslyn, E. V.; McDevitt, J. T. A Multi Component Sensing Ensemble in Solution: Differentiation Between very Structurally Similar Analytes. *Nature* **2002**, Submitted.

(41)   Sandanayake, K. R. A.; Shinkai, S. Novel molecular sensors for saccharides based on the interaction of boronic acid and amines: saccharide sensing in neutral water. *J. Chem. Soc., Chem. Commun.* **1994**, 1083-1084; Yoon, J.; Czarnik, A. W. Fluorescent Chemosensors of Carbohydrates. A Means of Chemically Communicating the Binding of Polyols in Water Based on Chelation-Enhanced Quenching. *J. Am. Chem. Soc.* **1992***, 114*, 5874-5875.

(42)   Wiskur, S. L.; Lavigne, J. J.; Metzger, A.; Tobey, S. L.; Lynch, V.; Anlsyn, E. V. Thermodynamic Analysis of Guanidinium/Boronic Acid Based Receptors for the Complexation of Carboxylates and Diols: Driving force for Binding and Cooperativity. *J. Am. Chem. Soc.* **2002**, submitted.

(43)   Lavigne, J. J. Molecular Recognition and Molecular Sensing: Single Analyte Analysis and Multi-Component Sensor Arrays for the Simultaneous Detection of a Plethra of Analytes. In *Department of Chemistry and Biochemistry*; University of Texas at Austin: Austin, 2000.

(44) Burns, J. A.; Whitesides, G. M. Feed-forward neural networks in chemistry: mathematical systems for classification and pattern recognition. *Chem. Rev.* **1993***, 93*, 2583-2601; Kateman, G.; Smits, J. R. M. Colored information from a black box? Validation and evaluation of neural networks. *Anal. Chim. Acta* **1993***, 277*, 179-188.

(45) Jansson, P. A. Neural Networks: An Overview. *Anal. Chem.* **1991***, 63*, 357A-362A.

(46) Zupan, J.; Gasteiger, J. Neural networks: a new method for solving chemical problems or just a passing phase? *Anal. Chim. Acta* **1991***, 248*, 1-30.

(47) McCulloch, W. S.; Pitts, W. A Logical Calculus of the Ideas Imminent in Nervous Activity. *Bull. Math.Biophys.* **1943***, 5*, 115.

(48) Sukhaswami, M. B.; Seetharamulu, P.; Pujari, A. K. Recognition of Telugu characters using neural networks. *Inter. J. Neural Sys. Field* **1995***, 6*, 317-357; Meiler, J.; Meusinger, R.; Will, M. Fast Determination of 13C NMR Chemical Shifts Using Artificial Neural Networks. *J. Chem. Inf. Comput. Sci.* **2000***, 40*, 1169-1176; Kurogi, S. Speech recognition by an artificial neural network using findings on the afferent auditory system. *Biol. Cyber. Field* **1991***, 64*, 243-249.

(49) Ni, Y.; Chen, S.; Kokot, S. Spectrophotometric Determination of Metal Ions in Electroplating Solutions in the Presence of EDTA with the Aid of Multivariate Calibration and Artificial Neural Networks. *Anal. Chim. Acta* **2002***, 463*, 305-316.

(50) Levitan, I. B.; Kaczmarek, L. K. *The Neuron*; Oxford University Press: New York, 1997.

(51) LeCun, Y.; Boser, B.; Denker, J. S.; Henderson, D.; Howard, R. E.; Hubbard, W.; Jackel, L. D. Back Propagation Applied to Handwritten Zip Code Recognition. *Neur. Comp.* **1989***, 1*, 541-551.

(52) Stergiou, C.; Siganos, D. Neural Networks. http://www.doc.ic.ac.uk/%7End/surprise_96/journal/vol4/cs11/report.html . Accessed:Dec. 2002.

(53) Fröhlich, J. Neural Net Overview. http://rfhs8012.fh-regensburg.de/~saj39122/jfroehl/diplom/e-1.html. Accessed:Dec. 2002.

(54) Gershenson, C. Artificial Neural Networks for Beginners.
      http://www.cogs.susx.ac.uk/users/carlos/doc/FCS-ANN-tutorial.htm.
      Accessed:Dec. 2002.

(55) Saha, A. *NNinExcel - Prediction tool and NNinExcel -Classification tool*;
      Personal.

(56) The attachment of the receptor to a resin was also investigated through a
      biotin/avidin approach, but the synthesis of a linker to 2.32 proved
      difficult due to arduous task of purifying boronic acids.

(57) Otwinowski, Z.; Minor, W. Macromolecular crystallography. *Methods in
      Enzymology*; Academic Press: San Diego, 1997; pp 307-326.

(58) Altomare, A.; Cascarano, G.; Giacovazzo, C.; Guagliardi, A. *J. Appl.
      Cryst.* **1993***, 26*, 343-350.

(59) Sheldrick, G. M. *SHELXL-97*; 5.03 ed.; Siemans Analytical X-Ray
      Instruments, Inc.: Madison, Wisconsin.

(60) Rw(F2) = { w(|Fo|2 - |Fc|2)2/ w(|Fo|)4}1/2 where w is the weight given
      each reflection. R(F) = (|Fo| - |Fc|)/ |Fo|} for reflections with Fo > 4(
      (Fo)). S = [w(|Fo|2 - |Fc|2)2/(n - p)]1/2, where n is the number of
      reflections and p is the number of refined parameters.

(61) Altomare, A.; Cascarano, G.; Giacovazzo, C.; Guagliardi, A. Completion
      and Refinement of Crystal Structures SIR92. *J. Appl. Cryst.* **1993***, 26*,
      343-350.

(62) Rw(F2) = { w(|Fo|2 - |Fc|2)2/ w(|Fo|)4}1/2 where w is the weight given
      each reflection. R(F) =   (|Fo| - |Fc|)/ |Fo|} for reflections with Fo > 4(
      (Fo)). S = [w(|Fo|2 - |Fc|2)2/(n - p)]1/2, where n is the number of
      reflections and p is the number of refined parameters.

(63) *International Tables for X-ray Crystallography*; Kluwer Academic Press:
      Boston, 1992; Tables 4.2.6.8 and 6.1.1.4.

Chapter 3: Thermodynamic Analysis of Guanidinium/Boronic Acid Based Receptors for the Complexation of Carboxylates and Diols

3.0   INTRODUCTION

Due to the prevalence of natural products that contain carboxylates and diols, our group has developed a series of receptors that target these types of analytes. Examples of these receptors have been discussed in Chapters 1 and 2, in which many of them possess guanidiniums[1] and/or boronic acids.[2] To further understand the binding selectivities and the thermodynamics of the guanidinium[3] and boronic acid groups, three of these previous receptors were stinvestigated, along with a new one. The first receptor **1.26,** a tris-guanidinium host, was designed to bind citrate (Chapter 1, Section 1.6.4.2), a tris-carboxylate anion found in citrus fruits and beverages.[4,5] The second receptor (**1.34**) contained a boronic acid and two guanidiniums and was designed to selectively bind tartrate in grape derived beverages (Chapter 1, Section 1.6.4.6), yet it also had a high affinity for the structurally similar analyte malate.[6,7] The third receptor (**2.1**) incorporated two boronic acids and one guanidinium to bind a class of age related analytes found in scotch whiskies[8,9] (Chapter 2, Section 2.3-2.4). In order to have a series of receptors that contain all the possible combinations of guanidinium and boronic acid groups, the fourth receptor (**3.1**) was synthesized which contained three boronic acids. The binding constants of a large variety of guests with these

170

1.26

1.34

2.1

3.1
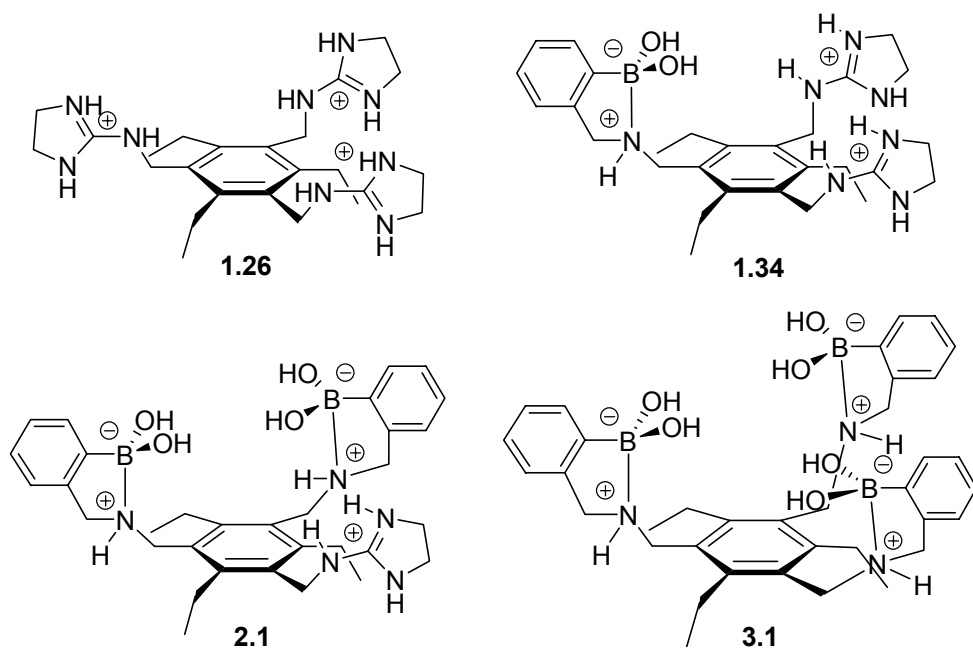
hosts were determined to show the selectivity of each of these. The guests chosen for this experiment all contained a variety of carboxylates and diols. Cooperativity of two of the hosts with tartrate was also investigated from the UV/vis data, along with ITC analysis to determine the components of the Gibbs free energy of binding. The selectivity of boronic acids for more than just diols was investigated. A variety of compounds were tested such as amino acids, α-hydroxycarboxylates, and dicarboxylates with a simplified boronic acid compound (**2.18**).[10] From the ITC data, an entropy/enthalpy compensation effect is found for all the hosts and guests. The data is combined to present a unified picture of how the four hosts recognize and bind diol/carboxylate containing guests.

2.18
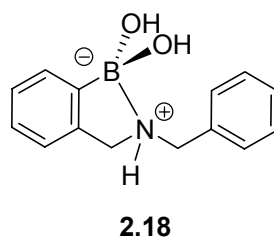
3.1 DESIGN AND SYNTHESIS OF RECEPTORS

All of the receptors used in this study are based on the 1,3,5-trisubstituted-2,4,6-triethylbenzene scaffold seen throughout the previous two chapters, where the groups attached to the methylene groups alternate up and down around the ring, allowing the binding sites to be preorganized on one face of the benzene ring.[11] This preorganization of the binding sites forms a binding pocket which helps to increase association constants.

Since the synthesis of **1.34** (Chapter 2, Section 2.5.1),[6] **2.1** (Chapter 2, Section 2.1.2), and **2.18** (Chapter 2, Section 2.2.1) have been discussed already, only the synthesis of **1.26** and **3.1** will be discussed here. Receptor **1.26** was synthesized by our previously reported procedure (Scheme 3.1),[5] by coupling 2-methylthio-2-imidazoline with the acetate salt of **2.7** in a solid melt to obtain the final compound. The tris-boronic acid compound **3.1** was synthesized by reductive amination of **2.7** with 2-formylbenzene boronic acid (**2.14**) (Scheme 3.2)

172

Scheme 3.1

2.7

2.9

80 °C

66%

1.26

Scheme 3.2

2.7

1.) **2.14**

MeOH/Et₃N

HC(OCH₃)₃

40 °C

2.) NaBH₄

28%

3.1
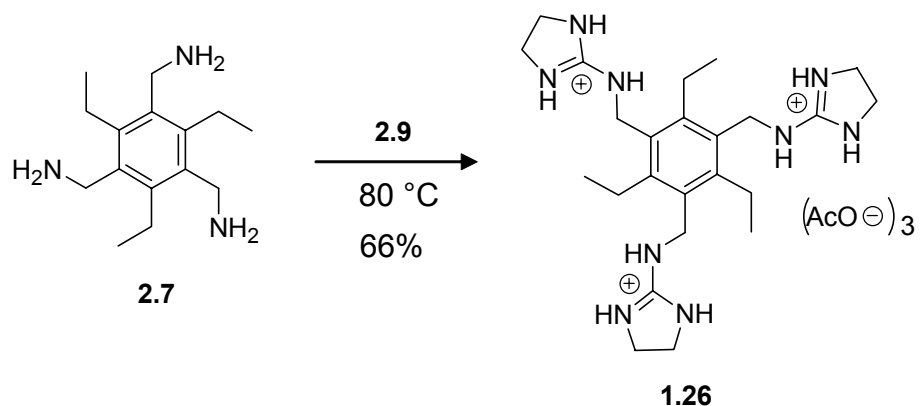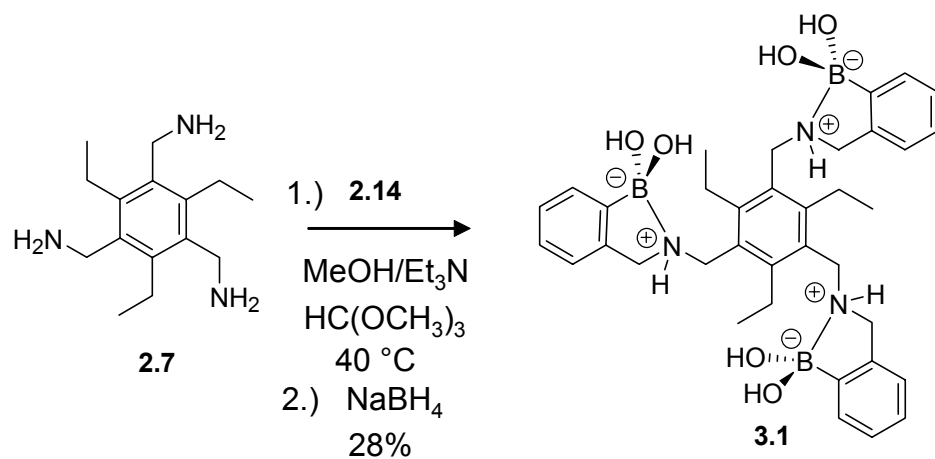
3.2   BINDING AND STRUCTURAL STUDIES

To determine binding constants, a mechanism to signal the binding, such as the modulation of spectroscopic properties of a chromophore or fluorophore, is needed. Since dye displacement assays[12] have been proven to work with three of

the four receptors, this method was chosen for determining association constants with the guests. The same pH sensitive indicators were used with the hosts that they have been proven to work with.[4,7,8] Therefore **1.26** was paired with 5-carboxyfluorescein (**1.27**), **1.34** was used with alizarin complexone (**1.35**), and pyrocatechol violet (**2.24**) was used with **2.1**. Receptor **3.1** was originally tested with pyrogallol red (**3.2**), but due to the instability of the indicator, alizarin complexone was finally chosen. All of the indicator/host affinity constants were determined in 75% methanol in water buffered with HEPES (4-(2-hydroxyethyl)-1-piperazineethane-sulfonic acid) buffer at pH 7.4 with a 1:1 binding algorithm.[13] The binding affinities were determined to be: 4.7×10^3 M^{-1} between **1.26** and **1.27**, 2.7×10^4 M^{-1} between **1.34** and **1.35**, 6.2×10^4 M^{-1} between **2.1** and **2.24**, and 4.6×10^4 M^{-1} for the association of **3.1** and **1.35**.
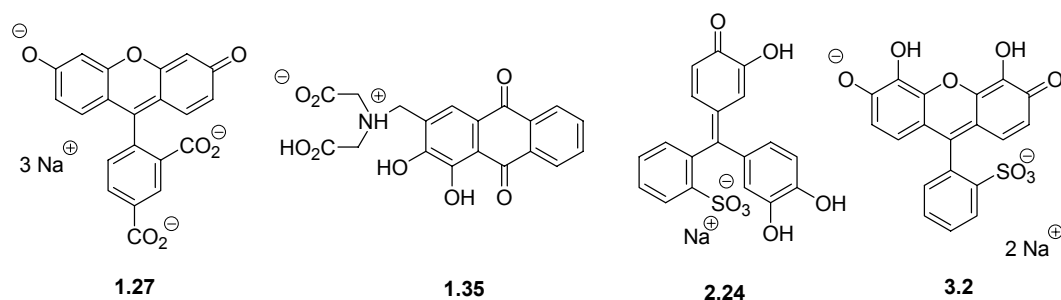
3.2.1 Binding Studies of 1.26

A competition assay was used to determine the binding constant of the guests to the receptors. Each of the hosts **1.26, 1.34**, **2.1**, and **3.1** were tested with a variety of guests (Figure 3.1) using the indicator displacement method. The

174
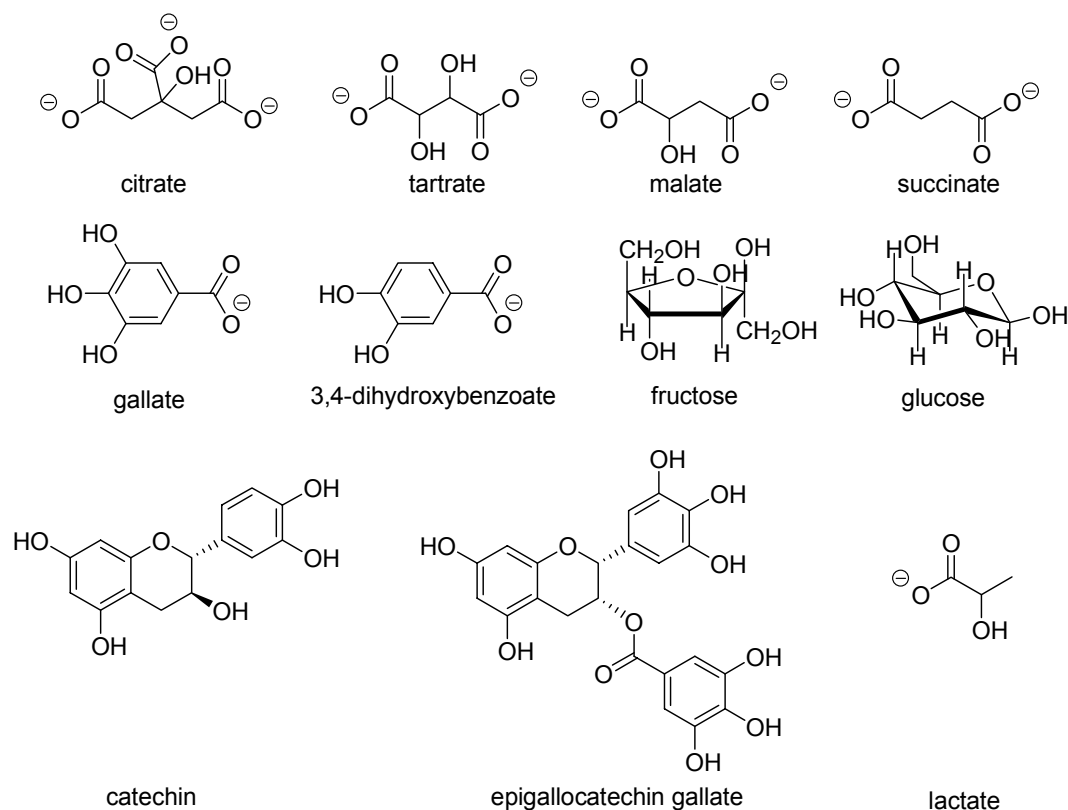
FIGURE 3.1. GUESTS TESTED FOR AFFINITIES WITH RECEPTORS 1.26, 1.34, 2.1, AND 3.1.

work was completed through a combined effort by Dr. Axel Metzger, Dr. John Lavigne, and myself. All of the binding constants, determined with a competitive binding algorithm,[13] are listed in Table 3.1. Due to the design of **1.26**, it was expected that the guests that were highly anionic would give the strongest interactions and the guests that were neutral would not bind. It was found that citrate, which has three carboxylates, was the guest with the highest binding constant. Scheme 3.4 depicts one possible binding motif (**A**), which was observed in the crystal structure obtained,[5] where all three carboxylates of citrate

175

TABLE 3.1. THE BINDING CONSTANTS (M-1) DETERMINED FOR RECEPTORS 1.26, 1.34, 2.1, AND 3.1, using the competition assay. (75% methanol in water, 5-10 mM HEPES, pH 7.4)

	1.26	1.34	2.1	3.1
Citrate	6.2×10^4	2.0×10^5	1.8×10^5	2.7×10^4
Tartrate	1.7×10^4	5.5×10^4	1.4×10^5	4.0×10^4
Malate	1.3×10^4	4.8×10^4	1.5×10^4	8.5×10^3
Succinate	3.6×10^3	3.5×10^2	$<1.4 \times 10^2$	No Binding
Gallate	<100	2.0×10^4	1.0×10^4	1.0×10^4
3,4-Dihydroxybenzoate	<100	1.0×10^4	4.5×10^3	9.0×10^3
Lactate	Not 1:1	5.0×10^2	5.0×10^2	1.1×10^3
Glucose	No Binding	1.6×10^2	1.4×10^2	9.0×10^2
Fructose	No Binding	3.0×10^2	4.0×10^2	6.0×10^2
Catechin	No Binding	8.0×10^2	5.7×10^2	5.0×10^2
EGCg	No Binding	4.5×10^3	5.2×10^3	6.0×10^3

are hydrogen bonded to the guanidiniums of **1.26**. Guests that have two carboxylates, such as tartrate, malate, and succinate were also strong binders with **1.26**, where tartrate, which also possesses a vicinal diol functional group, and malate, a mono alcohol, had 3 to 4 times smaller binding constants than the three carboxylate counterpart. Succinate, which has no hydroxyl groups, had a binding constant with **1.26** that was over an order of magnitude less than citrate. The binding affinities of **1.26** with mono carboxylate containing guests such as 3,4-dihydroxybenzoate and gallate were so low that they were estimated to be less

than 100 M^{-1}. The other mono carboxylate guest, lactate, was determined to bind **1.26** with a higher stoichiometry, where more than one guest bound in the cavity. Other analytes that only contain hydroxyl or catechol functionalities were not expected to bind to **1.26**, such as fructose, glucose, catechin, and epigallocatechin gallate (EGCg), and they indeed had no detectable binding interactions.

SCHEME 3.4.

A
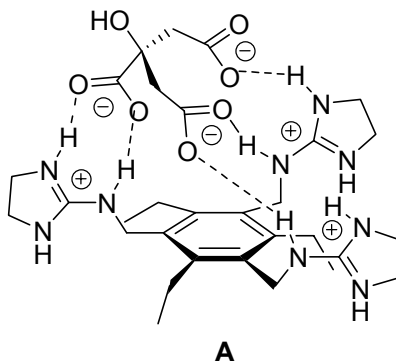
3.2.2   Determining the Selectivity of 1.34

With receptor **1.34** it was expected that guests that possess two carboxylates and one diol would show optimum binding. Tartrate was the guest of choice, which indeed bound strongly to the receptor. But malate, which is similar in structure to tartrate, minus one hydroxyl group, had an affinity to the receptor that was almost identical. Citrate bound **1.34** with an affinity that was almost 4 times stronger than tartrate, indicating that the carboxylates of citrate were interacting with the boronic acid. Succinate, the malate equivalent minus a

single hydroxyl group, had a significantly decreased affinity for **1.34**, by almost two orders of magnitude. This indicated that the α-hydroxycarboxylate functionality has a greater affinity for boronic acids[14] than 1,2-alkane diols. Possible conformations for binding are depicted in Scheme 3.5. Here the binding of the α-hydroxycarboxylate of tartrate to the boronic acid of **1.34** (**B**) is depicted in equilibrium with the formation of the boronate ester between the boronic acid and the diol (**C**). The fact that tartrate and malate have very similar binding constants with **1.34**, gives evidence for **B** being a more favorable binding motif for tartrate. However, it is likely that both binding modes exist in solution. Structure **D** is proposed for malate bound to **1.34** in solution.

SCHEME 3.5.
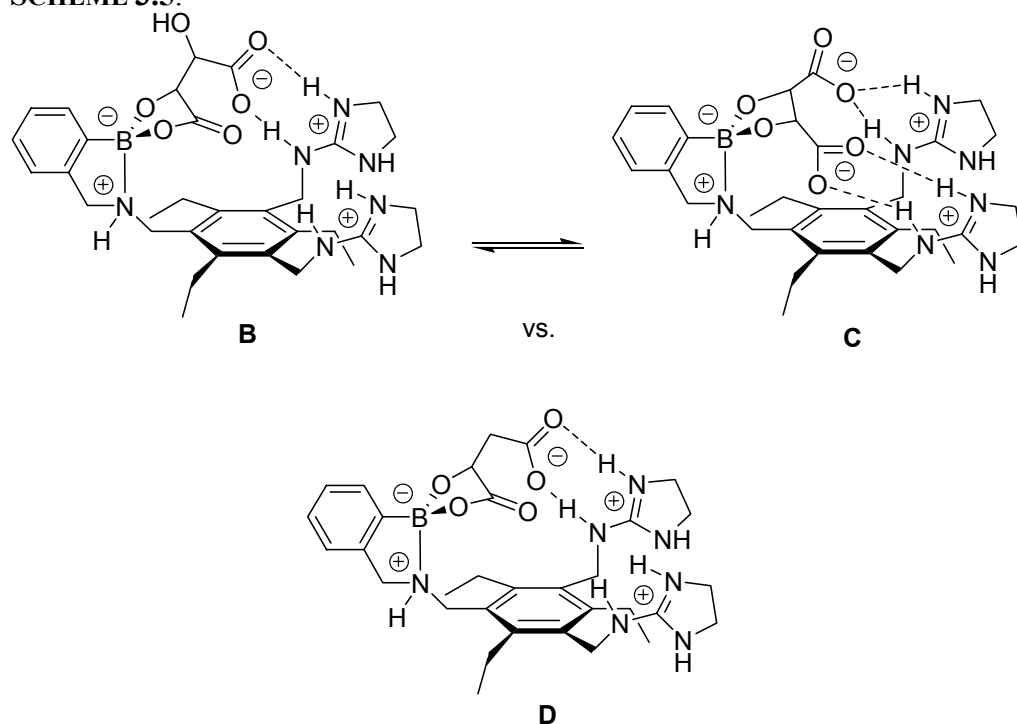
The binding constants of gallate and 3,4-dihydroxybenzoate with receptor **1.34** were also on the same order of magnitude as tartrate and malate. This is due to the catechol/boronic acid interactions, which are know to be stronger than vicinal diols.[15] The larger neutral catechol containing guests (catechin and EGCg) had binding affinities with **1.34** that were decreased by an order of magnitude over the aromatic carboxylates. Simple sugars such as fructose and glucose bound with even lower binding constants, since the main interaction with the receptor is with the boronic acid.

3.2.3 Binding Investigations of 2.1

Receptor **2.1** was tested with all the same guests. Both citrate and tartrate had the strongest affinities for the receptor, while malate's affinity was an order of magnitude less. Again, this indicates that the boronic acids are preferentially interacting with the α-hydroxycarboxylates. This can be seen in Scheme 3.6, where the binding of tartrate and malate with **2.1** is depicted. With tartrate, two α-hydroxycarboxylate interactions can be drawn with the two boronic acids (**E**), along with a structure in equilibrium that possesses a boronate ester (**F**). With malate's interaction (**G**) only one α-hydroxycarboxylate interaction with a boronic acid can be formed, which results in the lower binding affinity with **2.1**.

SCHEME 3.6.
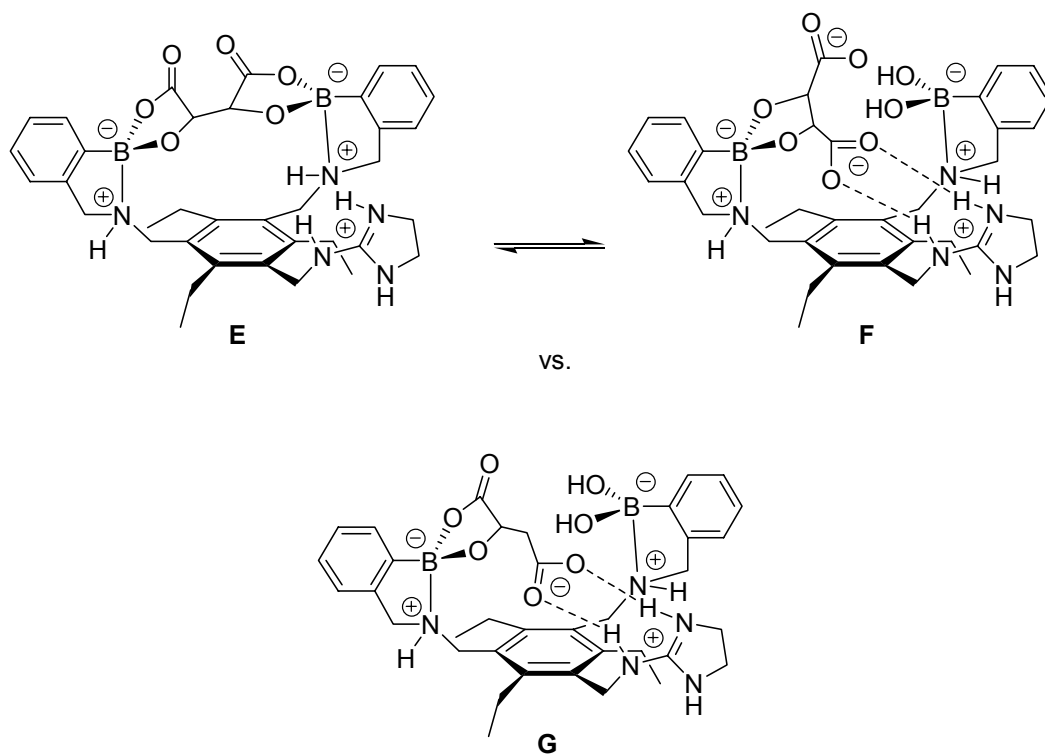
Gallate bound **2.1** with an affinity on the same order of magnitude as malate, showing the large role the 1,2-hydroxyphenyl groups play over the 1,2-alkane diols since the association of **2.1** with simple sugars were much lower. When testing a guest with one less hydroxyl group, 3,4-dihydroxybenzoate, the binding affinity of **2.1** for the guest dropped by a factor of 2, indicating the third hydroxyl is also involved in binding to the second boronic acid. EGCg was an order of magnitude higher in its binding constant with **2.1** over catechin and epicatechin (Figure 3.2), presumably due to the increased number of hydroxyl groups. Once again, we postulate that this increase in affinities is related to an increase in hydroxyl groups through comparison of epicatechin and

epigallocatechin (EGC) bound to **2.1**. The association constant of EGC was double that of epicatechin by the addition of one hydroxyl group. Receptor **2.1** had similar affinities for epicatechin gallate (ECg) and ECG due to the structural similarities of the two guests. EGCg's similar binding affinity to 3,4-dihydroxybenzoate again shows the importance of the catechol functionalities, where the affinities of glucose and fructose were an order of magnitude less. This can be attributed to the geometry of the two boronic acids around the binding pocket, which is not conducive for binding poly alkane diols. Finally, guests that were not expected to bind such as caffeine and sorbate showed no affinity for **2.1**.

epicatechin
5.5×10^2 M^{-1}

epigallocatechin
1.2×10^3 M^{-1}

epicatechin gallate
8.4×10^3 M^{-1}
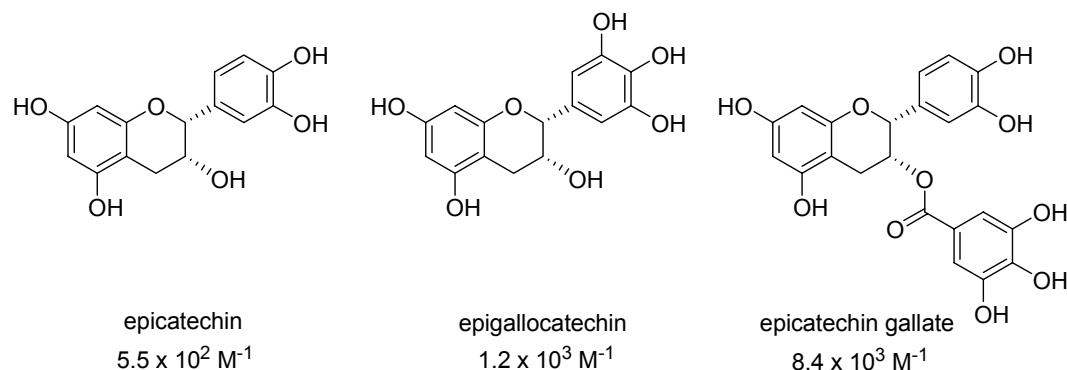
FIGURE 3.2. ADDITIONAL ANALYTES TESTED WITH 2.1.

3.2.4   Binding Studies of 3.1

Receptor **3.1** which has three boronic acids, again showed selectivity for the guests with α-hydroxycarboxylates, such as tartrate. Citrate, which only has one α-hydroxycarboxylate, had a comparable binding constant with **3.1**, which was attributed to the added interactions of the other two carboxylates with the

181

other boronic acid and the guanidinium. The affinity of **3.1** to malate was five times less than **3.1** to tartrate, due to the one less hydroxyl group. The possible binding modes of tartrate are illustrated in Scheme 3.7, showing the formation of a boronate ester (**I**) versus the binding of the α-hydroxycarboxylates (**H**). A similar binding mode for malate as in Schemes 3.5 and 3.6 can be assumed, highlighting the increased number of favorable binding interactions for tartrate. Importantly, upon removal of the alcohols (succinate), no binding could be detected to the receptor suggesting that the di-carboxylates are not interacting with the boronic acids.

SCHEME 3.7.
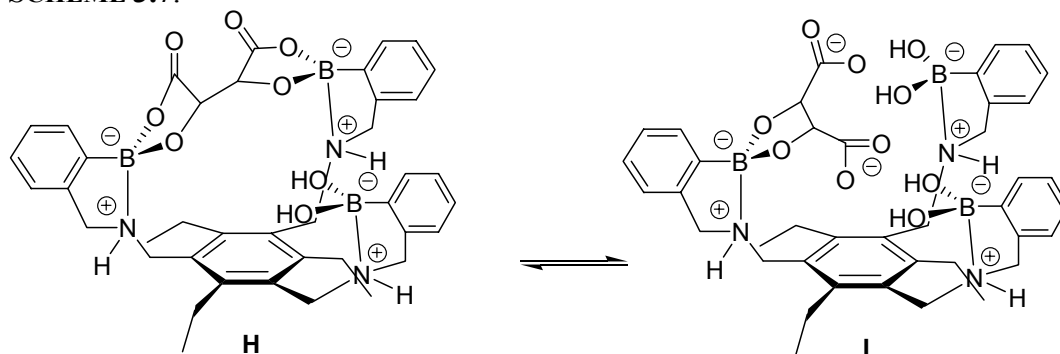
Both gallate and 3,4-dihydroxybenzoate had affinity constants with **3.1** that were on the same order of magnitude as malate, showing the strong interactions of the boronic acids with the catechols. The simple alkane diols (glucose and fructose) had the lowest affinities with **3.1**, while EGCg had a binding constant that was almost seven times as strong.

3.2.5 Binding Studies with the Boronic Acid Model

Upon analyzing all of these binding constants, it became clear that the boronic acids were playing more of a role than just binding vicinal diols.[14] Therefore, we turned our attention more closely on the role of the boronic acids. After analyzing the guests that were tested with hosts **1.34**, **2.1**, and **3.1**, a series of simpler guests (Figure 3.3) were analyzed with a simplified boronic acid compound (**2.18**). Since **2.18** does not possess a signaling site, the competition assay was also employed, using **1.35** as the indicator. The binding constants that were determined are shown in Table 3.2, along with the binding constant of **2.18** with **1.35**. Aliphatic diols have been widely examined with boronic acids, but catechols have not been as widely tested,[15] so this was our starting point. Catechol proved to be one of the stronger binding guests, which is part of the functionality present in alizarin complexone. Since **1.35** bound so strongly with
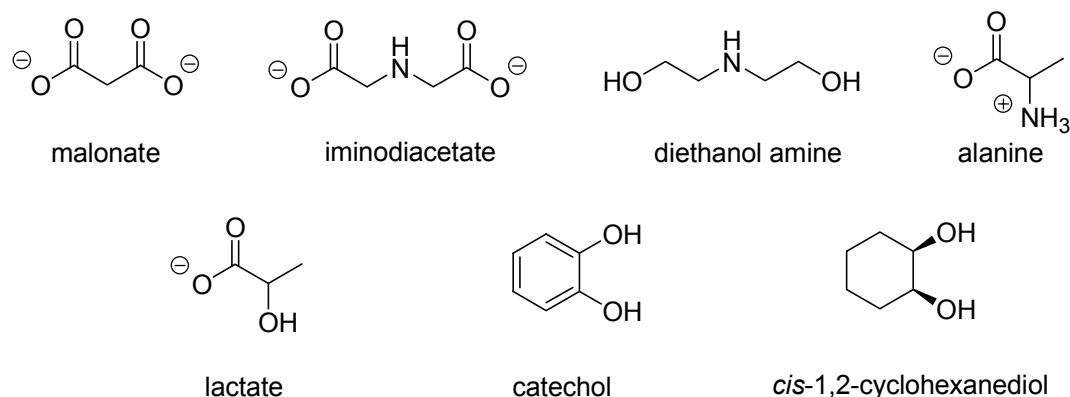
FIGURE 3.3. GUESTS TESTED FOR AFFINITY TO RECEPTOR **2.18**.

2.18, the iminodiacetate[16] functionality was tested to see if the boronic acid was binding through the catechol or the side arm of **1.35**. However, the binding of this guest with **2.18** was too weak to be determined. Diethanolamine, the alcohol equivalent to iminodiacetate was also tested, but also had weak binding. Because citrate bound hosts **1.34**, **2.1**, and **3.1** better than expected, the interaction of lactate, an α-hydroxycarboxylate was tested. It was shown to have an excellent binding affinity for the boronic acid of **2.18**. The amino acid[17] equivalent alanine, had very little affinity with the receptor, showing the alcohol is required over an amine. Malonate also showed a strong affinity for **2.18**, indicating that binding was also possible through the two carboxylates,[18] forming a six membered ring. When any simple aliphatic diols were attempted such as ethylene glycol, *cis*-1,2-

TABLE 3.2. THE BINDING CONSTANTS (M-1) DETERMINED FOR 2.18, by using the competition assay with the indicator alizarin complexone. (75% methanol in water, 10 mM HEPES, pH 7.4)

	2.18
alizarin complexone (**1.35**)	4.4×10^3
malonate	8.6×10^2
lactate	3.1×10^2
alanine	< 50
iminodiacetate	< 50
catechol	4.0×10^2
cis-1,2-cyclohexanediol	No Binding
diethanol amine	75

cyclohexane diol, *trans*-1,2-cyclohexane diol, or neopentyl glycol, binding was always too low to be determined. Therefore, it was determined that a simple boronic acid (**2.18**) has high affinities for α-hydroxycarboxylates, catechols, and di-carboxylates that can form 6-membered rings, over amino acids and simple 1,2-alkane diols.

3.3 ENTHALPY AND ENTROPY

Given that the selectivities of the hosts were determined, along with some structural insight, we were interested in the driving force for binding of hosts **1.26**, **1.34**, **2.1**, **3.1**, and **2.18**. The Gibbs free energy of binding can be calculated from the K_a's, but in order to divide ΔG^o into its parts, enthalpy and entropy, isothermal titration calorimetry (ITC) was used. This method measures the heat evolved or absorbed upon binding, and in a single experiment derives K_a, ΔG^o, ΔH^o, and ΔS^o.[19] The instrument measures the change in heat of a system upon addition of an aliquot of guest into a solution of host. This is shown in the top part of Figure 3.4 for the addition of tartrate into a solution of **1.34** at pH 7.4 (100% water, 50 mM HEPES buffer, 25 ^{o}C). Integration of the exothermic peaks leads to the binding curve shown in the bottom part of Figure 3.4. Using a one-site binding model to fit the data, leads to the values shown in Table 3.3. The association constant between tartrate and **1.34** has dropped significantly from the one reported in Table 3.1. This can be attributed to performing the ITC experiments in 100% water compared to performing the UV/visible studies in

75% methanol in water. Ion-pairing interactions are reduced in pure water, and in addition the increased buffer concentration can lower binding interactions.
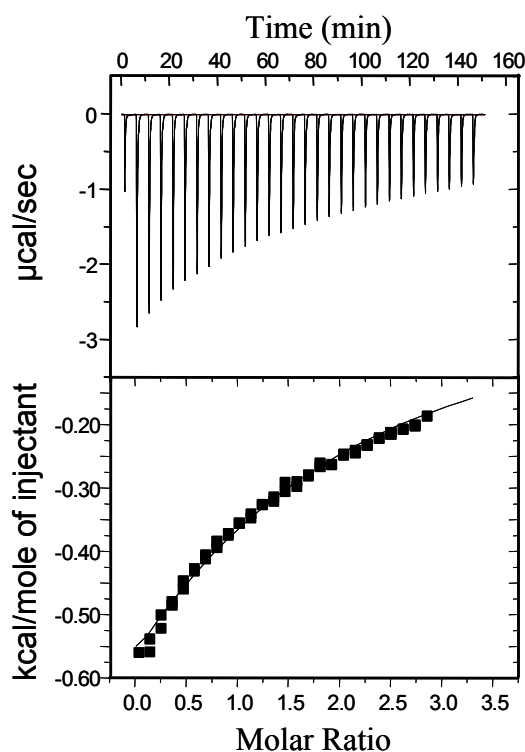
FIGURE 3.4. ITC ANALYSIS OF 1.34 WITH TARTRATE (100% water, 50 mM HEPES buffer, pH 7.4).

The data shows that binding is driven by a combination of entropy and enthalpy, both being favorable. In many systems, enthalpy that is exothermic is associated with charge pairing interactions or tight binding interactions that result in structural tightening, while positive entropy is generally associated with a release of solvent into bulk solution. Negative entropy can result from the cost of freezing intermolecular motion.[20] When looking at the binding of **1.26** and citrate

in pure water, with a phosphate buffer, the majority of the driving force is derived from entropic contributions.[21] This indicates a large release of solvent upon **1.26** binding citrate. Also, the use of phosphate as a buffer can reduce the carboxylate/guanidinium interactions due to competition for the binding site.[5]

TABLE 3.3. ITC ANALYSIS of **1.26** (100% water, pH 7.4, 103 mM phosphate buffer),[21] **1.34**, **2.1**, and **3.1** (100% water, pH 7.4, 50 mM HEPES) and **2.18** (100% water, pH 7.4, 250 mM HEPES).

	1.26 and Citrate	**1.34** and Tartrate	**2.1** and Tartrate	**3.1** and Tartrate	**2.18**•and Catechol	**2.18**•and Malonate
ΔH^o (kcal/mol)	-0.2	-1.6	-2.9	-1.5	-1.4	0.02
$T\Delta S^o$ (kcal/mol)	3.3	2.1	0.6	1.8	1.8	4.2
ΔG^o (kcal/mol)	-3.6	-3.7	-3.5	-3.3	-3.2	-4.2
K_a (M^{-1})	4.4×10^2	5.2×10^2	3.7×10^2	2.6×10^2	2.2×10^2	1.2×10^3

The binding between **1.34** and tartrate was determined to be exothermic with positive entropy. The increase in the enthalpic component versus **1.26** binding citrate indicates stronger interactions between **1.34** and tartrate. The covalent bonds between the boronic acid and tartrate (Scheme 3.5, **B** and **C**) could impart this added rigidity over the hydrogen bonding and charge pairing interactions of **1.26**. Further, the entropic component is still present with **1.34**, which could result from the release of solvent from the binding pocket and the

guest. The binding of the carboxylates of tartrate to the guanidiniums of **1.34** displace water into bulk solvent. Further, two water molecules are released for each boronate ester formed (Eq. 3.1) from either the diol or the α-hydroxycarboxylates.
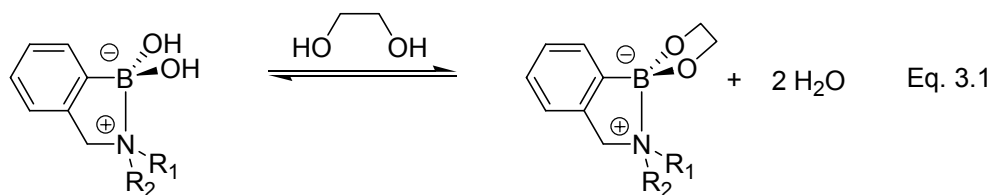
A large enthalpic component with a small entropic component was determined for the binding of **2.1** to tartrate. This receptor is now comprised of two boronic acids and one guanidinium. The possibility of forming four reversible, covalent bonds to tartrate exists (Scheme 3.6, **E**) making the complexation exothermic, but results in a rigid host/guest complex, which is less disordered, resulting in lower entropy of binding relative to **1.26** and **1.34**. The rigidity of the host/guest complex induces the loss of translational and rotational entropy, which may out weigh the increased entropy from the displacement of solvent from the binding cavity, lowering the overall entropy.

The binding of **3.1** with tartrate had a similar driving force to receptor **1.34** binding tartrate, where the enthalpy and entropy were both favorable. Scheme 3.6 shows **3.1** binding tartrate (Complex **H**) in a similar orientation as **2.1** (Scheme 3.6, **E**), yet the exothermicity with **3.1** has decreased and there is more entropy. Perhaps, the rigidity in the binding of tartrate to **3.1** is not as pronounced as tartrate to **2.1**, due to subtle size and shape differences of the binding cavity.

Without the increase in rigidity, not as much entropy is lost and the displacement of solvent into bulk solution has a more pronounced effect.

Using the boronic acid model compound **2.18**, the association of catechol, malonate, and lactate were all analyzed by ITC. Catechol was both entropy and enthalpy driven, with exothermic binding and positive entropy. Malonate on the other hand was primarily entropy driven (positive), with enthalpy being slightly endothermic. Looking at these two studies from the point of rigidity, it would appear that the formation of the boronate ester with catechol results in a more rigid complex than malonate binding **2.18**. This rigidity reduces the entropy of the system, even though two solvent molecules are being released for each boronate ester formed. Lactate was not reported due to the fact that an accurate association constant could not be measured due to small changes in the heat of the system, which means that the binding is primarily entropy driven.

When the entropy and enthalpy for each of the receptors are plotted together (Figure 3.5), a straight line is the result. This phenomenon is termed enthalpy/entropy compensation (EEC),[20,22,23] and is an effect that reflects how increasing favorable enthalpy is offset by a change in entropy or vice versa, resulting in a small change in free energy. For example, as the rigidity of the host/guest complexes increase, the disorder of the complexes decreases, resulting in a compensation of the entropy. This can be seen in receptors **1.26**, **1.34**, and **2.1**, as the binding sites of the receptors change from three guanidiniums to two boronic acids and one guanidinium. The slope of the EEC graph is determined to be 0.8, which means that the free energy of binding is more sensitive to changes is

189

entropy.[23,24] A slope less than one suggests that by rationally designing a receptor that is a tight binder to an guest, the exothermicity of the receptor (-ΔH°) would eventually be defeated by the compensating entropy (TΔS°).

It is interesting that receptors containing both boronic acids and guanidinium groups lie on the same plot, having the same slope. This means the extent to which the increased enthalpy of binding is offset by lower entropy is identical for the two molecular recognition motifs. Ion pairing a carboxylate with a guanidinium and the reversible binding of α-hydroxycarboxylates with boronic acids act similarly in this regard, at least in the series of receptors studied. More work is required to see if this is a general phenomenon.
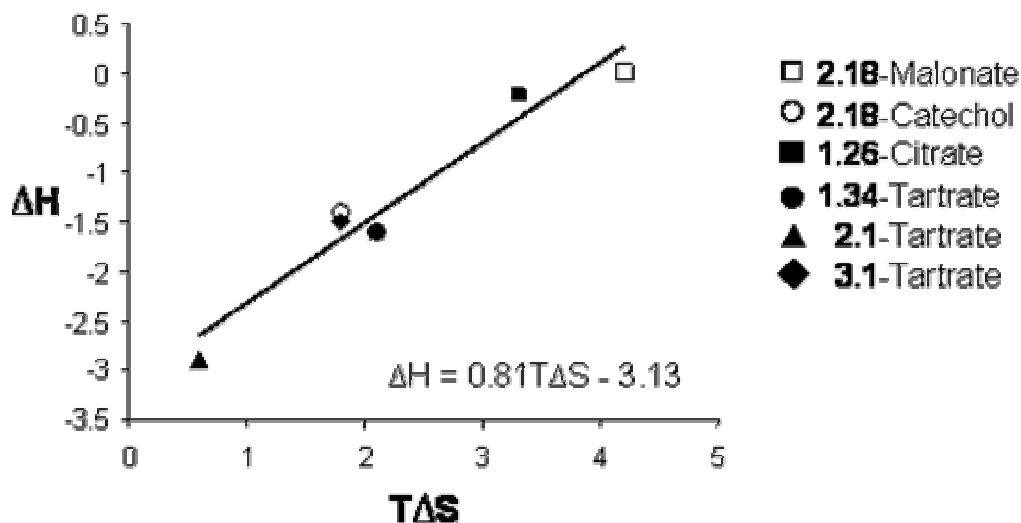
FIGURE 3.5. ENTROPY (TΔS) VS. ENTHALPY (ΔH) COMPENSATION PLOT for hosts **1.26**, **1.34**, **2.1**, **3.1**, and **2.18**, binding different guests.

190

3.4   COOPERATIVITY

Studies were done to explore the cooperativity of receptors **1.34** and **2.1** in binding various guests. Cooperativity in the case of receptor **1.34** is defined as enhanced or diminished binding interactions of the boronic acid and the two guanidiniums to the diol and carboxylates of tartrate, respectively. The method proposed by Jencks[25] was used to analyze the two receptors. The guest to be studied is divided into parts A and B where the receptor can independently bind both of these, such that the parts can be compared to the whole to determine if the binding is cooperative when they are connected. Here, the Gibbs free energy of connection (ΔG_s°) is defined as the change that results from the connection of A and B, and can be determined from the difference between the Gibbs free energy of the parts minus the Gibbs free energy of the whole (Eq. 3.2) or the binding constants (Eq. 3.3). Positive cooperativity would be shown by a positive ΔG_s°, which is a gain in free energy from binding AB vs. binding A and B separately. The opposite is true with a value for ΔG_s° that is negative.

$$\Delta G_s^\circ = \Delta G_A^\circ + \Delta G_B^\circ - \Delta G_{AB}^\circ \qquad\qquad \text{Eq. 3.2}$$

$$\Delta G_s^\circ = RT \ln \frac{K_{AB}}{K_A K_B} \qquad\qquad \text{Eq. 3.3}$$

For receptors **1.34** and **2.1**, the binding of tartrate was studied. The study of the parts of tartrate was performed two different ways. Glucose and succinate

were chosen as one break down of tartrate, separating the boronic acid/diol interactions from the guanidinium/carboxylate interactions. Two lactates were chosen for the second study to investigate the α-hydroxycarboxylate interactions with the boronic acids and the guanidiniums. The binding constants of **1.34** with glucose and succinate were 160 M^{-1} and 350 M^{-1}, respectively. Using Eq. 3.3, the ΔG_s° was determined to be -0.1 kcal/mol, which is indicative of negative cooperativity, but close to no cooperativity. Lactate's binding constant with **1.34** was determined to be 500 M^{-1}, which gave a ΔG_s° of -0.9 kcal/mol, which is also indicative of negative cooperativity.

The cooperativity of binding with regards to receptor **2.1** and tartrate was also analyzed, using the two different methods just discussed for **1.34**. The complex **2.1** with glucose had an affinity constant of 140 M^{-1}, and succinate's affinity to **2.1** was so low that a binding constant of less than 140 M^{-1} was estimated. The ΔG_s° for this scenario was determined to be +1.2 kcal/mol, which indicates positive cooperativity between the boronic acids and the guanidinium. This represents a significant gain in free energy due to the connection of the binding sites. However, when tartrate is broken down into two lactates, the association constant between **2.1** and lactate was determined to be 500 M^{-1}, which resulted in a ΔG_s° of -0.3 kcal/mol, negative but close to no cooperativity.

We interpret these results to further show the favorable interactions of boronic acids with α-hydroxycarboxylates over alkane diols. The positive cooperativity determined from comparing the diol/carboxylate interactions with tartrate is likely false because the assumed binding geometry is for boronate ester

formation and guanidinium/carboxylate ion pairing. It is actually very rare using the Jencks method of determining cooperativity to achieve positive cooperativity.[26] One must remember that both negative and positive cooperativity, both can give enhancements in the binding affinities. Negative cooperativity merely suggests that the enhancement was not as large as could have been achieved. In this example, the two experiments are comparing two different interactions of the guests with the host. Our earlier analysis showed that tartrate is most likely binding through α-hydroxycarboxylates to the boronic acids, and therefore using two lactates as the parts is a better model. The fact that there is only a small negative cooperativity in free energy with the lactate as the parts, suggests equal enthalpic interactions from each of the α-hydroxycarboxylates of the lactate, when binding to **2.1**, which is accompanied by a loss in entropy by tethering the parts. Hence, this cooperativity study is in agreement with the ΔH^o and ΔS^o evaluation of tartrate binding **2.1** given above.

3.5   CONCLUSIONS

Guanidiniums and boronic acids have been widely investigated in their role of binding carboxylates and diols, respectively. We have analyzed four receptors (**1.26**, **1.34**, **2.1**, and **3.1**) that incorporate these functionalities by themselves and together, examining the thermodynamics of binding, selectivities, and cooperativity. The tris-guanidinium receptor (**1.26**) gave a predictable selectivity for highly anionic guests. However, receptors **1.34**, **2.1**, and **3.1**, which

incorporated boronic acids, displayed high affinities for guests that possessed α-hydroxycarboxylates and catechol functionalities over simple alkane 1,2-diols. Due to this, a mono boronic acid compound **2.18** was studied to further investigate the role that boronic acids play in binding guests other than diols, confirming high affinity for α-hydroxycarboxylates and catechols. Isothermal titration calorimetry revealed that the binding of citrate and tartrate with all the hosts was exothermic, with positive entropy. The boronic acids appear to add an enthalpic component to the thermodynamics of binding along with an entropy component due to the release of water. However, the binding with the boronic acids also leads to tighter bound complexes, while the complexes with guanidiniums are looser and also have a larger entropic component related to solvent release. An enthalpy/entropy compensation phenomenon was determined to exist between the guanidinium and boronic acid hosts. This indicated that the offset of enthalpy for losses in entropy for guanidiniums and boronic acids were essentially the same for our hosts. The cooperativity of tartrate binding to **1.34** and **2.1** was also investigated. It was determined that **2.1** had a binding pocket that was complimentary for the binding of tartrate, only showing small negative cooperativity.

3.6   EXPERIMENTAL

General. The chemicals were obtained from Aldrich, and no further purification was done unless otherwise noted. Methanol was distilled from

magnesium, and triethylamine was distilled from calcium hydride when noted. Products were placed under high vacuum for at least 12 hours before spectra were obtained. ^{1}H and ^{13}C NMR spectra were obtained on a Varian Unity Plus 300 MHz spectrometer. ^{11}B NMR spectra were obtained on a Bruker AMX-500 spectrometer. A Finnigan VG analytical ZAB2-E spectrometer was used to obtain high resolution mass spectra. UV/Visible spectra were collected on a Beckman DU640 spectrophotometer. Isothermal titration calorimetry was performed on a VP-ITC MicroCalorimeter instrument by MicroCal.

UV/Visible titrations of indicator and receptor:

All solutions were buffered at pH 7.4 with HEPES buffer (5 mM) in 75% methanol in water (v/v). A solution of 5-carboxyfluorescein (23 μM) was prepared in the cuvette and into this was titrated a stock solution of **1.26** (500 μM) and 5-carboxyfluorescein (23 μM) keeping the indicator concentration constant. The data was taken at 498 nm to determine the association constant. The rest of the host/indicator association constants were determined in a similar manner with differences in concentrations. Alizarin complexone-**1.34** (10 mM HEPES, 150 μM of indicator, 1.6 mM of **1.34**, 525 nm); pyrocatechol violet-**2.1** (10 mM HEPES, 60 μM of indicator, 1.2 mM of **2.1**, 510 nm); alizarin complexone-**3.1** (10 mM HEPES, 150 μM of indicator, 1.2 mM of **3.1**, 525 nm); and alizarin complexone-**2.18** (10 mM HEPES, 150 μM of indicator, 2.8 mM of **2.18**, 525 nm)

UV/Visible titrations of receptor/indicator ensemble and guests:

All solutions were buffered at pH 7.4 with HEPES buffer (5-10 mM) in 75% methanol in water (v/v). A solution of indicator (**1.27**, 14 µM) and receptor (**1.26**, 74 µM) was prepared in the cuvette and into this was titrated a stock solution of indicator, host, and guest, keeping the indicator and host concentrations constant. The data was taken at the appropriate wavelength to determine the association constant. The guest concentration in the stock solution varies between 5-80 times the concentration of host. Alizarin complexone-**1.34** (10 mM HEPES, 150 µM of indicator, 170 µM of **1.34**, 525 nm); pyrocatechol violet-**2.1** (10 mM HEPES, 60 µM of indicator, 260 µM of **2.1**, 510 or 605 nm); alizarin complexone-**3.1** (10 mM HEPES, 150 µM of indicator, 185 µM of **3.1**, 525 nm); and alizarin complexone-**2.18** (10 mM HEPES, 150 µM of indicator, 470 µM of **2.18**, 525 nm).

Isothermal titration calorimetry of receptors 1.34, 2.1, and 3.1 with tartrate:

All solutions were buffered at pH 7.4 with HEPES buffer (50 mM) in 100% water. The calorimetry cell contained the receptor (1.0 mM), and tartrate (21.4 mM) was titrated into the cell. A total of 30 injections were made at a volume of 6 µL per injection and a spacing of 300 seconds between injections. The solution is constantly stirred and kept at 25 °C. The heat of dilution is measured by titrating the tartrate solution, in the same experiment as above into a solution of just buffer. The heat of dilution data is subtracted from the raw titration data to produce the final binding curve. The data was fit with a one-site binding model

using the Origin software Version 5.0. The other ITC experiments were all performed in a similar manner, with variations in buffers and concentrations.

1,3,5-Tris[(2-benzeneboronic acid)aminomethyl]-2,4,6-triethylbenzene. (3.1)
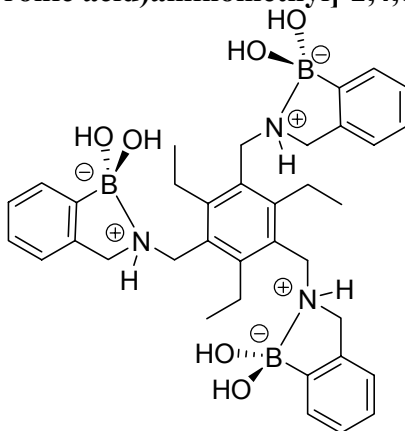
Dry triethylamine (1.0 mL) and 2-formylbenzene boronic acid (0.33 g, 2.19 mmol) was added to a solution of **2.7** (0.16 g, 0.63 mmol) in dry methanol over 3Å molecular sieves in an inert atmosphere. The reaction was heated to 45 °C for 6 hours. Sodium borohydride (0.18 g, 4.76 mmol) was added and the reaction was cooled to room temperature. The mixture was filtered through celite and the solvent was removed. The solid was dissolved in water, filtered through celite, and lyophilized. Trimethylorthoformate (2 mL) and dry methanol were then added and stirred for 2 hours, and the resulting residue was placed under vacuum for an additional 24 hours. The final purification step involved dissolving the solid with a mixture of 9:1 ethyl acetate:methanol (v/v) and filtering through celite. The solvent was removed to yield a white solid. (0.12 g, 28%) M.P. = 230 °C (decomp.); ^{1}H NMR (CD$_3$OD, 300 MHz) δ 7.49 (d, 3H), 7.1-7.2 (m, 9H,, 4.05 (s, 6H), 4.02 (s, 6H), 2.98 (q, 6H), 1.07 (t, 9H); ^{13}C NMR

(CD$_3$OD, 75 MHz) δ 157.1, 148.2, 143.2, 132.7, 129.2, 128.7, 125.6, 54.8, 45.3, 25.3, 17.6; ^{11}B NMR (CD$_3$OD, 160 MHz, 25°C) δ 10.0; HRMS-CI$^+$ m/z calcd. for C$_{39}$H$_{48}$B$_3$N$_3$O$_3$: 639.399, obsd.:639.397 (dehydrated methoxy form)

3.7 REFERENCES

(1)   Fitzmaurice, R. J.; Kyne, G. M.; Douheret, D.; Kilburn, J. D. Synthetic receptors for carboxylic acids and carboxylates. *J. Chem.Soc., Perkin Trans. 1* **2002**, 841-864; Hannon, C. L.; Anslyn, E. V. The guanidinium group: its biological role and synthetic analogs. *Bioorg. Chem. Front.* **1993***, 3*, 193-255.

(2)   Sandanayake, K. R. A.; Shinkai, S. Novel molecular sensors for saccharides based on the interaction of boronic acid and amines: saccharide sensing in neutral water. *J. Chem. Soc., Chem. Commun.* **1994**, 1083-1084; Springsteen, G.; Wang, B. Alizarin Red S. as a general optical reporter for studying the binding of boronic acids with carbohydrates. *Chem. Commun.* **2001**, 1608-1609; Ward, C. J.; Ashton, P. R.; James, T. D.; Patel, P. A molecular colour sensor for monosaccharides. *Chem. Commun.* **2000**, 229-230; Deetz, M. J.; Smith, B. D. Heteroditopic ruthenium(II) bipyridyl receptor with adjacent saccharide and phosphate binding sites. *Tetrahedron Lett.* **1998***, 39*, 6841-6844; Norrild, J. C.; Eggert, H. Boronic acids as fructose sensors. Structure determination of the complexes involved using 1JCC coupling constants. *J. Chem. Soc., Perkin Trans. 2* **1996**, 2583-2588.

(3)   Metzger, A.; Gloe, K.; Stephan, H.; Schmidtchen, F. P. Molecular Recognition and Phase Transfer of Underivatized Amino Acids by a Foldable Artificial Host. *J. Org. Chem.* **1996***, 61*, 2051-2055; Berger, M.; Schmidtchen, F. P. Zwitterionic Guanidinium Compounds Serve as Electroneutral Anion Hosts. *J. Am. Chem. Soc.* **1999***, 121*, 9986-9993; Schiessl, P.; Schmidtchen, F. P. Abiotic molecular recognition of dicarboxylic anions in methanol. *Tetrahedron Lett.* **1993***, 34*, 2449-2452; Sukharevsky, A. P.; Read, I.; Linton, B.; Hamilton, A. D.; Waldeck, D. H. Experimental Measurements of Low-Frequency Intermolecular Host-Guest Dynamics. *J. Phys. Chem. B* **1998***, 102*, 5394-5403; Linton, B.; Hamilton, A. D. Calorimetric investigation of guanidinium-carboxylate interactions. *Tetrahedron* **1999***, 55*, 6027-6038.

(4)   Metzger, A.; Anslyn, E. V. A chemosensor for citrate in beverages. *Angew. Chem., Int. Ed.* **1998***, 37*, 649-652.

(5)   Metzger, A.; Lynch, V. M.; Anslyn, E. V. A synthetic receptor selective for citrate. *Angew. Chem., Int. Ed.* **1997***, 36*, 862-865.

(6)   Lavigne, J. J. Molecular Recognition and Molecular Sensing: Single Analyte Analysis and Multi-Component Sensor Arrays for the Simultaneous Detection of a Plethra of Analytes. In *Department of Chemistry and Biochemistry*; University of Texas at Austin: Austin, 2000.

(7)   Lavigne, J. J.; Anslyn, E. V. Teaching old indicators new tricks: a colorimetric chenosensing ensemble for tartrate/malate in beverages. *Angew. Chem., Int. Ed.* **1999***, 38*, 3666-3669.

(8)   Wiskur, S. L.; Anslyn, E. V. Using a Synthetic Receptor to Create an Optical-Sensing Ensemble for a Class of Analytes: A Colorimetric Assay for the Aging of Scotch. *J. Am. Chem. Soc.* **2001***, 123*, 10109-10110.

(9)   Ng, L. K.; Lafontaine, P.; Harnois, J. Gas chromatographic-mass spectrometric analysis of acids and phenols in distilled alcohol beverages. Application of anion-exchange disk extraction combined with in-vial elution and silylation. *J. Chrom., A* **2000***, 873*, 29-38.

(10)   Wiskur, S. L.; Lavigne, J. J.; Ait-Haddou, H.; Lynch, V.; Chiu, Y. H.; Canary, J. W.; Anslyn, E. V. pKa Values and Geometries of Secondary and Tertiary Amines Complexed to Boronic Acids-Implications for Sensor Design. *Org. Lett.* **2001***, 3*, 1311-1314.

(11)   Iverson, D. J.; Hunter, G.; Blount, J. F.; Damewood, J. R., Jr.; Mislow, K. Static and dynamic stereochemistry of hexaethylbenzene and of its tricarbonylchromium, tricarbonylmolybdenum, and dicarbonyl(triphenylphosphine)chromium complexes. *J. Am. Chem. Soc.* **1981***, 103*, 6073-6083; Kilway, K. V.; Siegel, J. S. Effect of transition-metal complexation on the stereodynamics of persubstituted arenes. Evidence for steric complementarity between arene and metal tripod. *J. Am. Chem. Soc.* **1992***, 114*, 255-261; Marx, H.-W.; Moulines, F.; Wagner, T.; Astruc, D. Hexakis(3-butynyl)benzene. *Angew. Chem., Int. Ed.* **1996***, 35*, 1701-1704; Stack, T. D. P.; Hou, Z.; Raymond, K. N. Rational reduction of the conformational space of a siderophore analog through nonbonded interactions: the role of entropy in enterobactin. *J. Am. Chem. Soc.* **1993***, 115*, 6466-6467.

(12)   Ohyoshi, E. Spectrophotometric Study of Complexation Equilibria Involving a Metal and Colored and Buffer Ligands by the Competitive Effect of the Two Ligands. *Anal. Chem.* **1985***, 57*, 446-448; Klotz, I. M. Spectrophotometric Investigations of the Interactions of Proteins with Organic Anions. *J. Am. Chem. Soc.* **1946***, 68*, 2299-2304.

(13)   Connors, K. A. *Binding Constants, The Measurement of Molecular Stability*; Wiley: New York, 1987.

(14)   Friedman, S.; Pace, B.; Pizer, R. Complexation of phenylboronic acid with lactic acid. Stability constant and reaction kinetics. *J. Am. Chem. Soc.* **1974***, 96*, 5381-5384; Katzin, L. I.; Gulyas, E. Optical rotatory dispersion studies on the borotartrate complexes and remarks on the aqueous chemistry of boric acid. *J. Am. Chem. Soc.* **1966***, 88*, 5209-5212; Kustin, K.; Pizer, R. Temperature-jump study of the rate and mechanism of the boric acid-tartaric acid complexation. *J. Amer. Chem. Soc.* **1969***, 91*, 317-322; Gray, C. W., Jr.; Houston, T. A. Boronic Acid Receptors for .alpha.-Hydroxycarboxylates: High Affinity of Shinkai's Glucose Receptor for Tartrate. *J. Org. Chem.* **2002***, 67*, 5426-5428.

(15)   Lorand, J. P.; Edwards, J. O. Polyol complexes and structure of the benzeneboronate ion. *J. Org. Chem.* **1959***, 24*, 769-774; Springsteen, G.; Wang, B. A detailed examination of boronic acid-diol complexation. *Tetrahedron* **2002***, 58*, 5291-5300.

(16)   Mancilla, T.; Contreras, R.; Wrackmeyer, B. New bicyclic organylboronic esters derived from iminodiacetic acids. *J. Organomet. Chem.* **1986***, 307*, 1-6.

(17)   Mohler, L. K.; Czarnik, A. W. .alpha.-Amino acid chelative complexation by an arylboronic acid. *J. Am. Chem. Soc.* **1993***, 115*, 7037-7038.

(18)   Friedman, S.; Pizer, R. Mechanism of the complexation of phenylboronic acid with oxalic acid. Reaction which requires ligand donor atom protonation. *J. Am. Chem. Soc.* **1975***, 97*, 6059-6062.

(19)   Wadsoe, I. Trends in isothermal microcalorimetry. *Chem. Soc. Rev.* **1997***, 26*, 79-86; Stoedeman, M.; Wadsoe, I. Scope of microcalorimetry in the area of macrocyclic chemistry. *Pure Appl. Chem.* **1995***, 67*, 1059-1068.

(20)   Calderone, C. T.; Williams, D. H. An Enthalpic Component in Cooperativity: The Relationship between Enthalpy, Entropy, and Noncovalent Structure in Weak Associations. *J. Am. Chem. Soc.* **2001***, 123*, 6262-6267.

(21)   Rekharsky, M.; Inoue, Y.; Tobey, S. L.; Metzger, A.; Anslyn, E. V. Ion-Pairing Molecular Recognition in Water: Aggregation at Low Concentrations That is Entropy Driven. *J. Am. Chem. Soc.* **2002**, Accepted.

201

(22)   Swaminathan, C. P.; Surolia, N.; Surolia, A. Role of Water in the Specific Binding of Mannose and Mannooligosaccharides to Concanavalin A. *J. Am. Chem. Soc.* **1998**, *120*, 5153-5159; Liu, L.; Guo, Q.-X. The Driving Forces in the Inclusion Complexation of Cyclodextrins. *J. Incl. Phenom.* **2002**, *42*, 1-14.

(23)   Sun, S.; Fazal, M. A.; Roy, B. C.; Chandra, B.; Mallik, S. Thermodynamic Studies on the Recognition of Flexible Peptides by Transition-Metal Complexes. *Inorg. Chem.* **2002**, *41*, 1584-1590.

(24)   Hegde, S. S.; Dam, T. K.; Brewer, C. F.; Blanchard, J. S. Thermodynamics of Aminoglycoside and Acyl-Coenzyme A Binding to the Salmonella enterica AAC(6')-Iy Aminoglycoside N-Acetyltransferase. *Biochem.* **2002**, *41*, 7519-7527.

(25)   Jencks, W. P. On the attribution and additivity of binding energies. *Proc. Natl. Acad. Sci. U. S. A.* **1981**, *78*, 4046-4050.

(26)   Bell, D. A.; Diaz, S. G.; Lynch, V. M.; Anslyn, E. V. An alcohol recognition motif: clear evidence of binding site cooperativity in the complexation of cyclohexanediols by neutral polyaza-clefts. *Tetrahedron Lett.* **1995**, *36*, 4155-4158.

Chapter 4: Siderophores

4.0   INTRODUCTION

The binding of catechol functionalities was described in Chapters 2 and 3 using receptors functionalized with boronic acids. In this chapter we set out to develop a new sensor for catchol containing compounds through complexation by a metal center. Receptors **4.1** and **4.2** were designed to detect the presence of simple catechol compounds. The two hosts are modeled after siderophores, where iron(III) is complexed by three catecholates. Our design incorporates the same iron(III) center, but with two catecholates and one 2,4-pentanedione (acac) ligand. The idea being that in the presence of a catechol containing guest, the acac would be replaced by the diol. An ammonium was incoroporated into **4.1** and a guanidinium into **4.2** for charge pairing and hydrogen bonding to any anion containing guests.
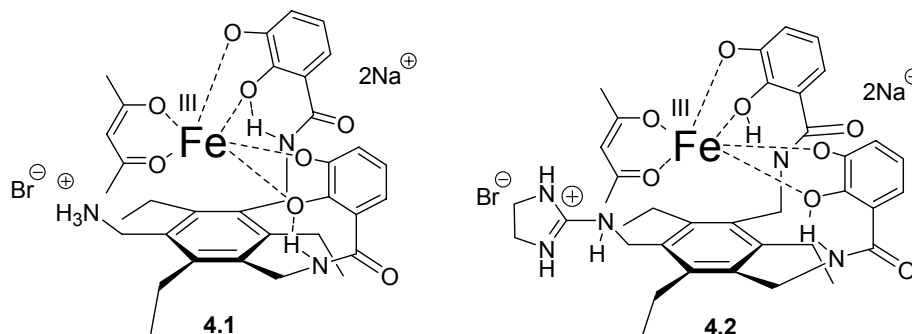
4.1 PHENOLIC COMPOUNDS

One important class of analytes found in red wines are phenolic compounds. Their concentration in the beverage affects many characteristics such as appearance, taste, and fragrance, and they are derived from a combination of the grapes, the vines, and the wood casks they are fermented in.[1] The two major groups present are flavanoids and nonflavanoids. Examples of nonflavanoids are caffeic acid and gallic acid, while flavanoid examples consist of catechin and leucoanthocyanidin (shown below). Flavanoids are found in monomeric and polymeric forms, making a very diverse family of compounds.

gallic acid

caffeic acid

catechin

leucoanthocyanidin
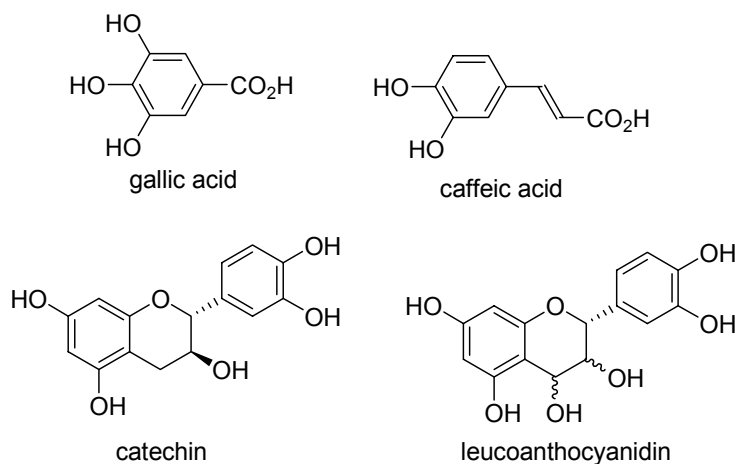
Therefore due to their assorted presence in wines, the development of a sensor array to detect and quantify these compounds would be an interesting endeavor. In order to do this, a sensor that is selective for the catechol functionality must be developed. Even though receptors **2.1** and **1.34** bind catechols, they bind tartrate

and malate with a high affinity, which is also in high concentrations in these grape derived beverages.

4.2   SIDEROPHORES

Natural siderophores are low molecular weight compounds that microorganisms have developed to aid in the solubilization and transport of iron(III) into cells.[2]   The microorganism produces these compounds when it is iron deprived, due to the siderophore's abilities to form strong complexes with the metal.   Enterobactin (**4.3**) is one of the most effective iron chelating agents with an association constant of around 10^{49} M^{-1}, and upon absorption of the complex into the cell the iron is removed from the ligand, possibly through hydrolysis of the ligand.[3]   Many synthetic iron sequestering agents have been designed[4] due to the need to detect trace amounts of iron in complex systems or in medicine for the treatment of iron overload.[5]   Raymond and coworkers developed receptor **4.4**, which actually rivals the binding affinity of enterobactin[6] with a K_a of 10^{47} M^{-1} for the ligand to iron.   The receptor was designed with the 1,3,5-trisubstituted-2,4,6-triethylbenzene scaffold that the Anslyn group is familiar with,[7] which preorganizes the catecholate binding sites to one face of the benzene ring.

4.3

4.4

3 cations
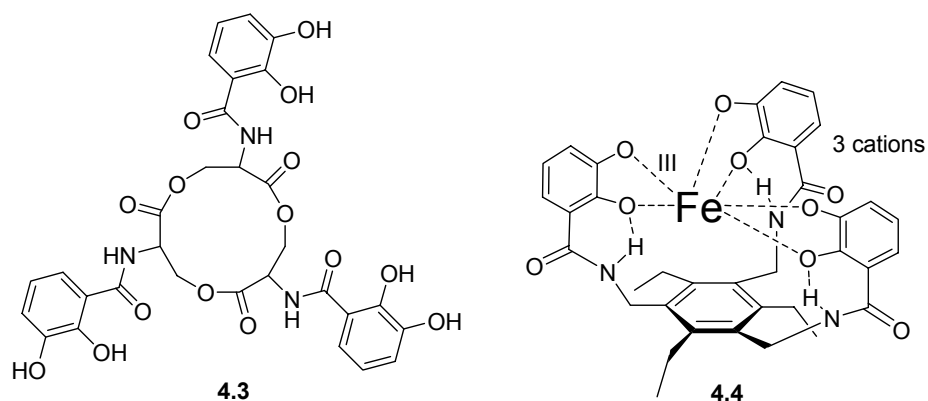
4.3 SYNTHESIS

The design of our receptors **4.1** and **4.2** are based on Raymond's iron receptor (**4.4**) with the idea of leaving off one of the catecholate arms in order to leave a binding site for our catechol containing guests. An ammonium and a guanidinium was incorporated in place of the catecholate to aid in binding guests such as 2,3-dihydroxybenzoate or gallate.

The synthesis of ligand **4.5** (Scheme 4.1) begins with amide formation between bis-amine/mono-BOC protected compound **2.26** and 2,3-dihydroxybenzoic acid (**4.3**) with 1,3-dicyclohexylcarbodiimide (DCC) to obtain compound **4.4**. Purifying **4.4** was completed through column chromatography, followed by a series of crystallizations to remove the urea byproduct of the DCC that coeluted. A final crystallization produced the product with only a fifty percent yield. The protecting group of **4.4** was subsequently cleaved with trifluoroacetic acid to obtain the TFA salt of **4.5**. When an attempt was made to perform this synthesis again, the product **4.4** was never obtainable in a yield that

was reasonable. Problems accrued with regards to the amide formation and the purification resulting in little to no yields of **4.4**. Even though the product was forming and could be seen by TLC, the isolation proved to be difficult due to decomposition on the column. Other coupling agents were tested in an attempt to obtain the bis-amide product in near quantitative yields in order to avoid the purification through chromatography, but the result was always a mixture of products. Therefore, a new route was chosen, shown in Scheme 4.2.

Scheme 4.1
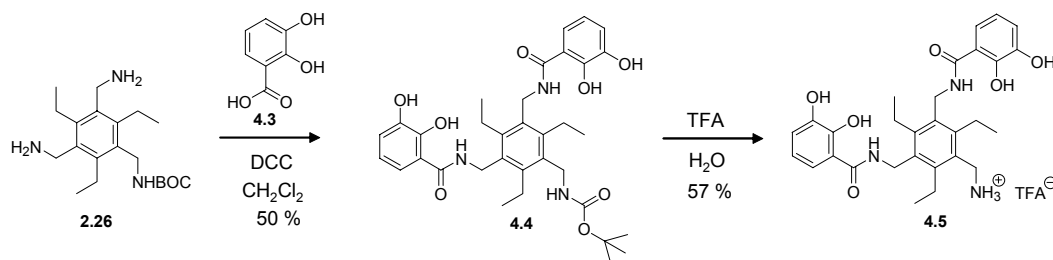
Due to the apparent instability of the catechol functionality, a route was chosen that protected them as methyl ethers similar to literature precedures.[8,9] Therefore, the purchasable 2,3-dimethoxybenzoic acid (**4.6**) was coupled to **2.26** with DCC. The carbamate of the resulting compound **4.7** was deprotected with trifluoroacetic acid.   This deprotection was performed even though the deprotection of both the catechols and the amine could have been accomplished in one step with the boron tribromide. With the free amine, a final attempt to purify the compound and remove any excess DCU was performed before the ethers were

cleaved. Finally, boron tribromide in dry dichloromethane[9,10] was added to a solution of **4.8** to obtain the bromide salt of the ammonium compound **4.5**.

Scheme 4.2
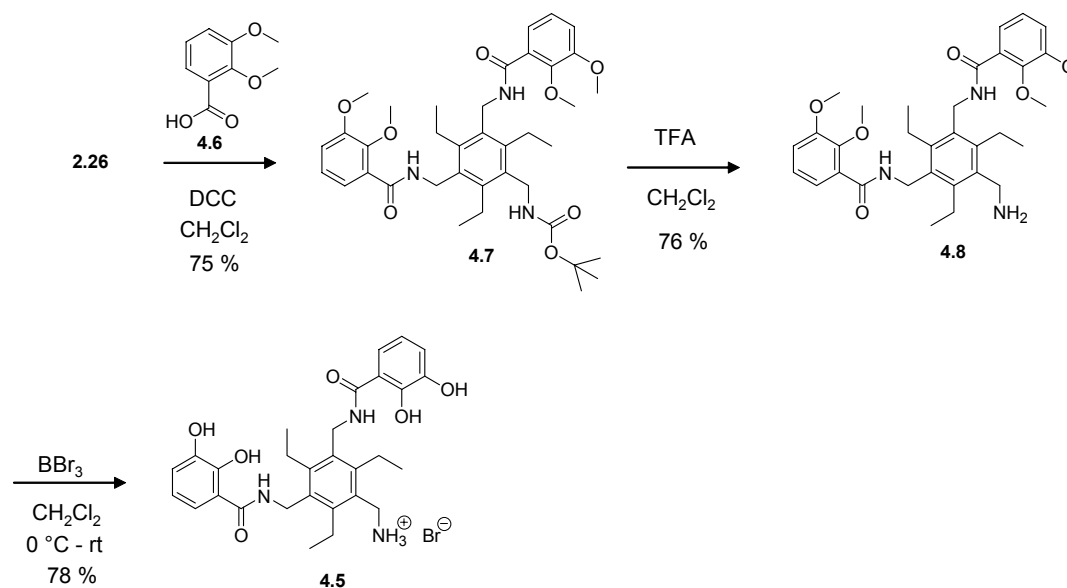
To form the guanidinium receptor **4.2**, compound **4.8** was coupled with the *N*-BOC protected 2-methylthioimidazoline derivative[11] in an acetic acid/ethanol solution to obtain **4.9**. Both the BOC protecting group and the methyl ethers were cleaved by the addition of boron tribromide to obtain guanidinium product **4.10**.

Scheme 4.3
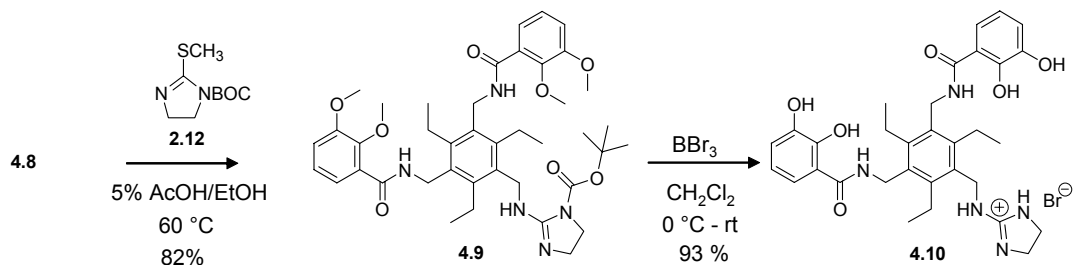
4.4   FORMATION OF THE IRON-LIGAND COMPLEX

After the ligands were synthesized, the iron ligand complexes needed to be formed. In order to determine the stoichiometry of the iron/ligand complex, it was necessary to titrate the iron into a solution of the ligand. When an attempt was made to adjust the pH of $FeCl_3$ and $Fe(NO_3)_3$ solutions in the presence of HEPES (75% methanol in water) a precipitate immediately formed due to hydrolysis. When a solution of pure $FeCl_3$ (no pH adjustment) was titrated into a buffered solution of ligand the complex **4.1** formed, but the pH of the solution was altered due to the unbuffered iron. Therefore, an iron species that is more stable in aqueous solutions was chosen, iron(III) acetylacetonate $(Fe(acac)_3)$.[9] Upon addition of $Fe(acac)_3$ to a solution of **4.5**, there was a strong increase in absorbance with a wavelength maximum at 575 nm (Figure 4.1A). This results in a deep purple colored solution. The mole ratio plot (Figure 4.1B) shows a distinct break in the delta absorbance at one, indicating a 1:1 complex formation. From the data, an association constant of iron to **4.5** was determined to be near 10^7 M^{-1}

using a 1:1 binding algorithm.[12] Two other metals were investigated, titanium(IV) oxide bis(2,4-pentanedionate) and vanadium(IV) oxide bis(2,4-pentanedionate),[9] but neither one showed binding to **4.5** through a spectral change.

The stoichiometry of the binding of ligand **4.10** to iron was also investigated. Under the same conditions, a very similar absorbance and mole ratio plot was obtained. The association constant was again determined to be 10^7 M^{-1} for **4.2**.
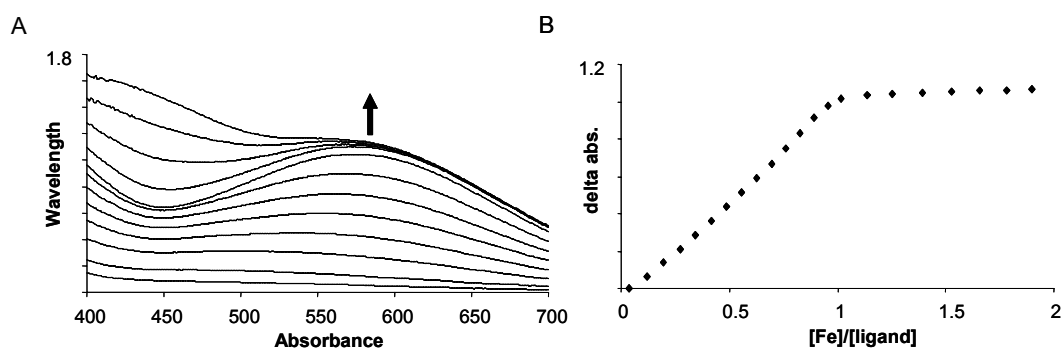
FIGURE 4.1. THE CHANGE IN ABSORBANCE AS LIGAND 4.5 BINDS IRON. A. The increase in absorbance as Fe(acac)$_3$ is added to a solution of **4.5**. B. The mole ratio of the formation of **4.1** shows that a 1:1 complex is formed (75% methanol in water, 10 mM HEPES buffer, pH 7.4).

4.5   BINDING STUDIES

Now that we have investigated the formation of the iron/ligand complexes, the next step was to determine if the hosts were selective for any particular guests.

The group of guests that were investigated (shown below) were comprised of catechol, 2,3-dihydroxybenzoic acid, 3,4-dihydroxybenzoic acid, and gallic acid. We were interested in developing a receptor that worked in water, but due to the limited solubility of the host in water, the solvent system chosen was 25% methanol in water. The stoichiometry of the iron/ligand complex was also determined to be 1:1 in the new solvent system. Therefore, the guests were titrated into a solution of **4.1** (10 mM HEPES, 25% methanol in water, pH 7.4), in which a small spectral change resulted. Initial studies indicated that binding was occurring, yet further examination yielded results that were not reproducible. For example, Figure 4.2A shows the change in absorbance of **4.1** upon addition of 2,3-dihydroxybenzoate. The color of the solution changes from a deep purple to a reddish purple. Figure 4.2B shows the data fit to a 1:1 binding algorithm at 580 nm. The affinity constant for this experiment was determined to be $1.6 \times 10^3 \text{ M}^{-1}$, yet when the experiment was repeated, the resulting K_a was calculated to be $1.0 \times 10^4 \text{ M}^{-1}$. In a third experiment, the changes in absorbance appeared to be random, where no binding curve was obtained. This pattern was repeated for all the analytes, where the association constants and the change in absorbance varied. Similar results were obtained with the titration of **4.2** with the same analytes.

catechol   2,3-dihydroxybenzoate   3,4-dihydroxybenzoate   gallate
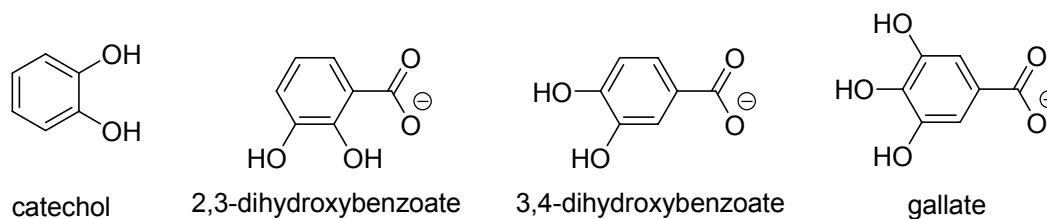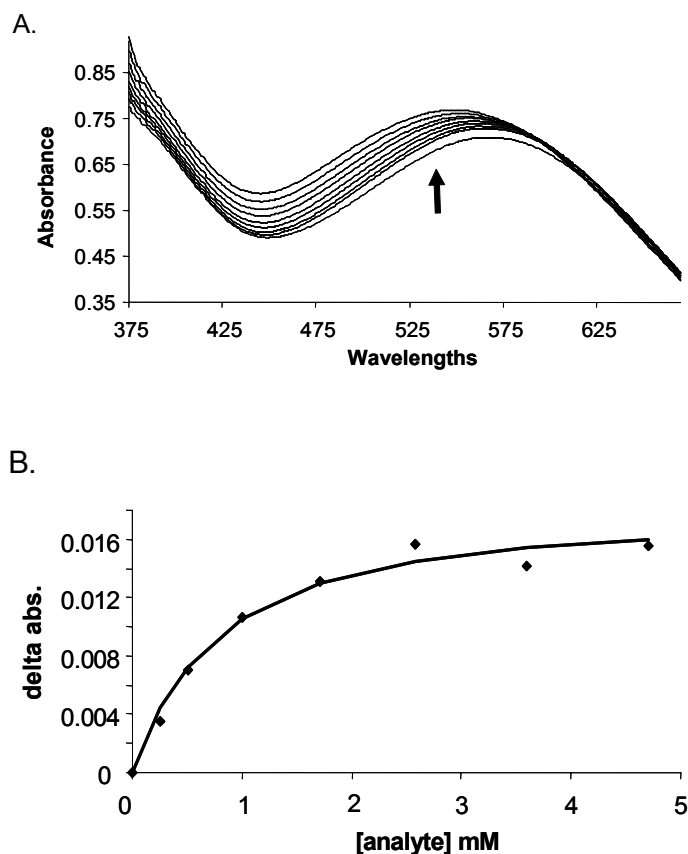
FIGURE 4.2. **CHANGE IN ABSORBANCE OF 4.1** (240 µM) upon addition of 2,3-dihydroxybenzoic acid. A. The UV/vis spectra at different concentrations of 2,3-dihydroxybenzoic acid. B. The binding curve at 580 nm fit with a 1:1 binding algorithm.

Investigations were next undertaken to try to determine what was occuring in solution. First, we knew what the spectra of the bis-catecholate host **4.1** looked like, but we wanted to know what the spectra looked like with three catecholates bound to the iron in our solvent system. Therefore, the synthesis of Raymond's iron/ligand complex (**4.4**) was undertaken (Scheme 4.4). The tris amine

compound **2.7** is coupled to **4.6** three times with DCC in methylene chloride to give **4.11**. The methyl protecting groups are subsequently removed with boron tribromide to obtain **4.12**. One equivalent of Fe(acac)$_3$ was added to a solution of **4.12** in 25% methanol in water and a UV/vis spectrum was obtained. This spectrum was compared with the one taken of **4.1** (Figure 4.3). When another catecholate is complexed to the iron, the result is a hypsochromic shift in the absorbance. This suggests that the complexation of 2,3-dihydroxybenzoic acid to **4.1** is a similar to the complexation of the three catecholates of **4.4** to iron, due to the similar absorbance shift of **4.1** upon addition of the guest. This has also been confirmed by Raymond and coworkers where they observed a typical red complex when three catecholates were bound to iron, versus a blue complex typical of ferric bis(catecholate).[3]

Scheme 4.4.
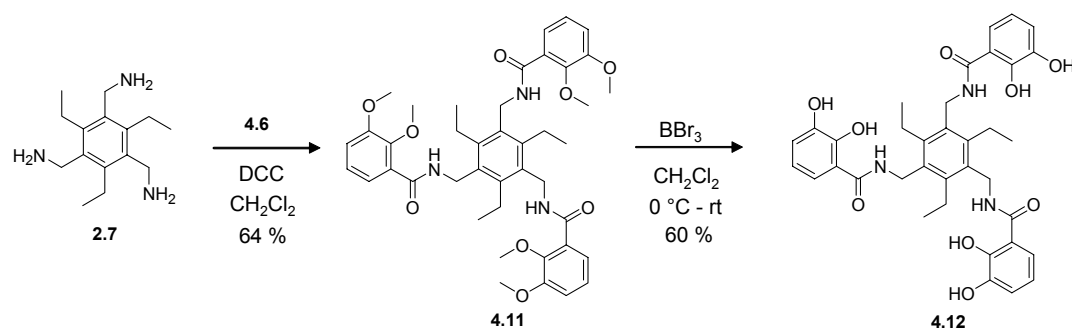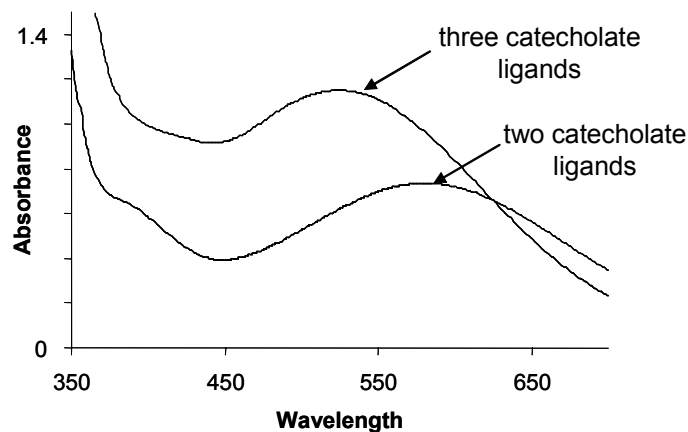
FIGURE 4.3. THE UV/VIS SPECTRA OF 4.1 AND 4.4. This shows the difference in the absorbance of three catecholates around iron versus two.

In order to confidently confirm this binding motif, a crystal structure was needed, but all attempts to obtain crystallographic quality crystals of **4.1** and **4.1** bound to guests failed. The solvent systems were selected based on past precedent of growing crystals of other siderophore compounds.[9,13] At first an attempt was made to form the iron/ligand complex directly in the chosen solvent system by adding the ligand to the Fe(acac)$_3$. The problem is that upon formation of **4.1**, two equivalents of 2,4-pentanedione are released. This creates an impure environment to attempt to grow crystals in. Another approach focused on forming the complex **4.1**, isolating it, then attempting to recrystallize it from a pure environment. Upon attempting to redissolve the isolated complex problems in solubility occurred. Even though it was evident that some of the complex was going into solution, a fine powder was also present. Even though the precipitant was removed, no crystals were obtained from this batch either. The problem of identifying the complex was also approached with the idea of using mass

214

spectroscopy. The complex **4.1** that was isolated was submitted for analysis along with a sample in a buffered solution. But neither sample resulted in a peak corresponding to the molecular weight of the complex.

4.13
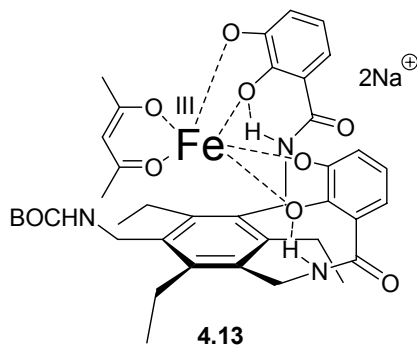
In an effort to simplify what is happening in solution, a BOC protected version of **4.1** was synthesized (**4.13**). Therefore, we investigated the catechol/iron binding interactions without being concerned about how the ammonium comes into play. The synthesis involved taking the mono amine bis catecholate compound **4.5** and protecting the amine with di-*t*-butyl dicarbonate to obtain **4.4** (Scheme 4.5).

Scheme 4.5.

4.4
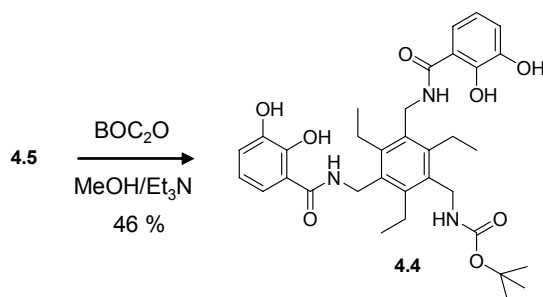
Complex **4.13** was formed in the same manner discussed above by titrating Fe(acac)$_3$ into a solution of **4.4** which indicated a binding stoichiometry of 1:1. In order to help confirm this, appropriate UV/vis spectra were obtained for the creation of a Job plot,[12] which also indicated the formation of a 1:1 complex (Figure 4.4). The complex **4.13** was seen in an electrospray ionization mass spectrum, where the solvent was buffered at pH 7.4. There were also peaks indicating higher molecular weight species, but their source was never determined. Since the complex had been characterized, binding studies were undertaken. Yet, upon titrating guests into solutions of **4.13** the absorption spectra did not show a reproducible response. Any spectral change was very small and appeared random rather than forming a binding isotherm. The difference between **4.1** and **4.13** was the protected amine. One hypothesis might be that the BOC group was sterically hindering the binding of the guests.
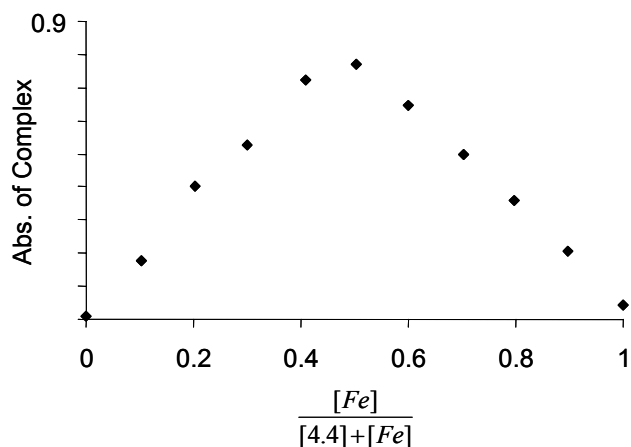
FIGURE 4.4. JOB PLOT OF 4.4 AND FE(ACAC)3.

216

Due to the small and irreproducible spectral response of **4.1** upon addition of guests, another method of signaling their binding was explored. Indicator displacement assays have been discussed frequently throughout Chapters 1, 2, and 3, and recently there has been evidence from the Anslyn group that it also works with metallated hosts.[14] The two indicators that were investigated were pyrocatechol violet (**2.24**) and bromopyrogallol red (**2.23**). They were chosen because they both possess catechol functionalities. When $Fe(acac)_3$ was added to a solution of **2.24**, the indicator changed color from yellow to blue, but when **4.1** was added to the same indicator, there essentially was no color change. This indicated that the indicator was not binding to the host. The next indicator investigated, **2.23**, displayed a detectable color change upon addition of **4.1**. The indicator turned from a pink to a purple upon complexation of the host. But upon addition of an analyte such as 2,3-dihydroxybenzoate to the complex, the indicator was never displaced.

As discussed above, it was known from earlier titrations that **4.1** was binding the guests, but the change in absorbance was not consistent and reproducible. Attempts were made in obtaining a crystal structure with the guest bound to the host using similar strategies shown earlier, but all of these attempts failed. Therefore, again the formation of a Job plot was attempted to investigate the binding of 2,3-dihydroxybenzoate to **4.1**. This is shown in Figure 4.5, but this data was actually manipulated so it is hard to tell if this is a true 1:1 complex. In a Job plot only the absorbance of the host/guest is to be plotted on the y-axis, but in this case the host itself has a strong absorbance. In order to only plot the

absorbance of the complex, we took the association constant that was determined earlier and calculated the amount of free host at each point, and subtracted its absorbance. Due to all of these assumptions, the indication of 1:1 binding cannot be trusted.
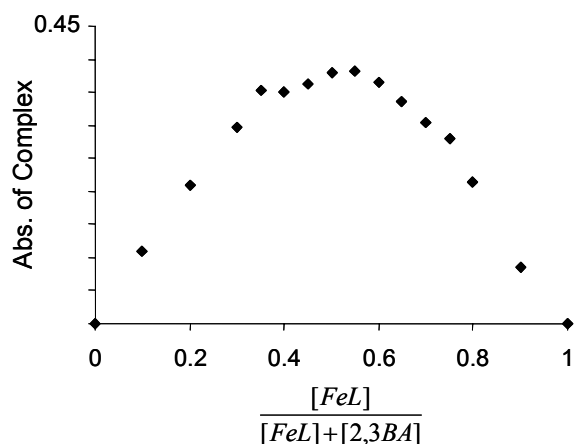
FIGURE 4.5. JOB PLOT OF THE ASSOCIATION OF 4.1 AND 2,3-BA.

4.6   CONCLUSION

The development of a receptor for the detection of catechol containing compounds was attempted. But due to the inherent low changes in absorbance and the irreproducibility of the data, binding constants were not obtainable. Many of the experiments resulted in conflicting conclusions as to the stoichiometry and the form of the iron/ligand complex. Titrating the iron into a solution of the ligand suggested a 1:1 complex, but this complex was not evident in the mass spectrum obtained. There were, however, peaks corresponding to higher

molecular weight complexes present. Also, when the iron/ligand complex was formed, the species that was formed was highly insoluble even in dimethylformamide. Without a crystal structure, it is difficult to know what is actually happening. Perhaps due to the strong association constants related to siderophore formation, oligomer type complexes are forming. In conclusion, after many investigations into the binding of host **4.1** to catechol related analytes, there is still an uncertainty present as to what is happening.

4.7   EXPERIMENTAL

General. The chemicals were obtained from Aldrich, and no further purification was done unless otherwise noted. Dichloromethane was distilled from calcium hydride when noted, and triethylamine was run down a plug of alumina. Products were placed under high vacuum for at least 12 hours before spectra were obtained. ^{1}H and ^{13}C NMR spectra were obtained on a Varian Unity Plus 300 or 400 MHz spectrometer. A Finnigan VG analytical ZAB2-E spectrometer was used to obtain high resolution mass spectra. UV/Visible spectra were collected on a Beckman DU640 spectrophotometer.

1-[[(1,1-dimethylethoxy)carbonyl]aminomethyl]-3,5-N,N'-Bis(2,3-hydroxybenzoyl)aminomethyl-2,4,6-triethylbenzene (4.4)
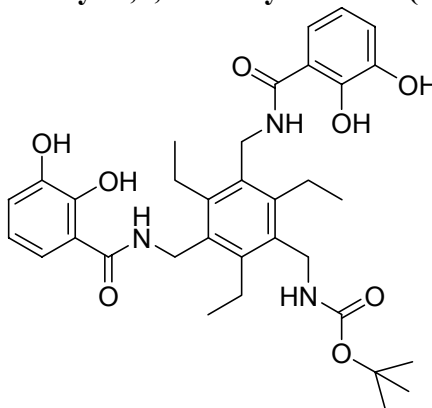
From 2.26:

A solution of dry dichloromethane, **2.26** (0.1035 g, 0.296 mmol), and **4.3** (0.0905 g, 0.587 mmol) was cooled to 0 °C. To this was added dicyclohexylcarbodiimide (DCC) (0.1387 g, 0.672 mmol) and 1-hydroxybenzotriazole hydrate (HOBt) (0.1364 g, 1.009 mmol). The mixture was stirred for one hour at 0 °C, then it was allowed to warm to room temperature to stir an additional 12 hours. The solvent was removed and an attempt was made to purify the product through silica gel column chromatography (3-10% methanol in dichloromethane with a few drops acetic acid). Some of the first fractions contained the product plus dicylcohexylurea. The product was then recrystallized from dichloromethane. (0.091 g, 50%)

From 4.5:

To a solution of **4.5** (0.034 g, 0.057 mmol) in methanol was added triethylamine (0.008 mL, 0.058 mmol) and (BOC)$_2$O (0.012 g, 0.055 mmol). The mixture was

stirred at room temperature for two hours, the solvent was subsequently removed and purification was obtained through recrystallization from dichloromethane. (0.016 g, 46%). ^{1}H NMR (300MHz, CD$_3$OD): δ 7.26 (d, 2H, Ar), 6.90 (d, 2H, Ar), 6.68 (t, 2H, Ar), 4.67 (s, 4H, CH$_2$), 4.34 (s, 2H, CH$_2$), 2.83 (q, 4H, CH$_3$), 1.44 (s, 9H, CH$_3$), 1.20 (t, 9H, CH$_3$); ^{13}C NMR (75MHz, CD$_3$OD): 169.70, 157.06, 149.50, 147.59, 145.78, 133.66, 129.37, 119.78, 119.31, 117.43, 80.31, 38.98, 28.81, 24.93, 24.01, 16.44; HRMS-CI$^+$ m/z: calcd for C$_{34}$H$_{43}$N$_3$O$_8$: 621.305; obsd: 621.305

1-aminomethyl-3,5-N,N'-Bis(2,3-hydroxybenzoyl)aminomethyl-2,4,6-triethylbenzene hydroanion (4.5)
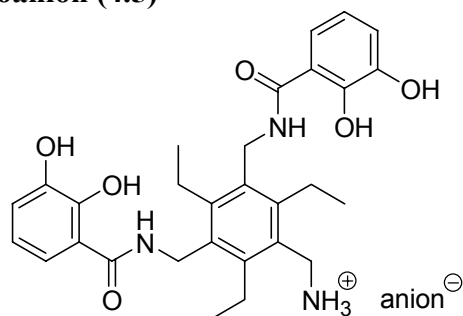
From 4.4:

Trifluoroacetic acid (2 mL) was added to a solution of 4.4 (0.09 g, 0.145 mmol) in dichloromethane (5 mL). The reaction was allowed to stir for two hours and the solvent was removed. The resulting solid was still contaminated with DCU from the previous coupling reaction, so it was recrystallized from methanol to yield the product. (0.052 g, 57 %)

From 4.8:

To a solution of **4.8** (0.09 g, 0.156 mmol) in dry dichloromethane (0 °C) under argon was added boron tribromide in dichloromethane (4.0 mL, 4.0 mmol, 6.4 eq. per methoxy). The mixture was allowed to warm to room temperature and the reaction was allowed to proceed for 15 hours. Methanol was added to quench the reaction. The solvent was removed and methanol was added three more times in an attempt to remove $B(OCH_3)_3$. The resulting solid was washed by adding water and dichloromethane. The solid did not dissolve, but remained mostly in the water layer, such that the organic layer could be removed. The water layer was brought to a boil and cooled to room temperature, and the resulting precipitate was collected. (0.073 g, 78%). ^{1}H NMR (300MHz, CD$_3$OD): δ 7.29 (d, 2H, Ar), 6.90 (d, 2H, Ar), 6.70 (t, 2H, Ar), 4.72 (s, 4H, CH$_2$), 4.25 (s, 2H, CH$_2$), 2.97 (q, 2H, CH$_3$), 2.87 (q, 4H, CH$_3$), 1.22 (m, 9H, CH$_3$); ^{13}C NMR (75MHz, CD$_3$OD): 170.34, 149.61, 147.62, 145.84, 133.72, 129.42, 119.85, 119.38, 117.49, 39.02, 37.96, 24.07, 16.50; HRMS-CI$^+$ m/z: calcd for C$_{29}$H$_{36}$N$_3$O$_6$: 522.260; obsd: 522.260

1-[[(1,1-dimethylethoxy)carbonyl]aminomethyl]-3,5-N,N'-Bis(2,3-dimethoxybenzoyl)aminomethyl-2,4,6-triethylbenzene (4.7)
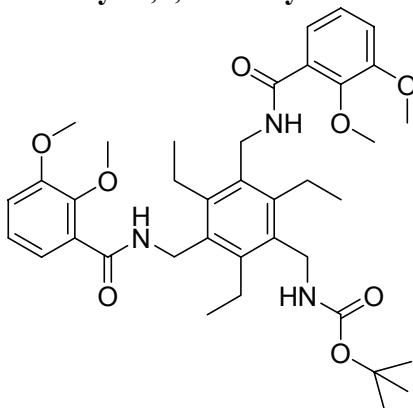
Dry dichloromethane (1 mL) was used to dissolve **2.26** (0.1544 g, 0.442 mmol) and **4.6** (0.17 g, 0.933 mmol). Note: DCC was purified with dichloromethane. DCC is soluble in CH_2Cl_2, but the urea is not. A solution of DCC (0.1905 g, 0.923 mmol) in dry dichloromethane (1 mL) was added dropwise and the resulting solution quickly turned cloudy and stirring was continued for 12 hours. A few drops of acetic acid were added at the end and after 20 minutes the precipitate was filtered off (DCU). The filtrate's solvent was removed and a second cropping of DCU was removed through precipitation with dichloromethane. After the solvent was again removed from the filtrate, the resulting solid was purified by column chromatography (silica gel, elutant: gradient 1-10% ammonia saturated methanol in dichloromethane).). (0.223 g, 75%) ^{1}H NMR (300MHz, CDCl$_3$): δ 7.77 (broad s, 2H, NH), 7.69 (d, 2H, Ar), 7.15 (t, 2H, Ar), 7.01 (d, 2H, Ar), 4.67 (s, 4H, CH$_2$), 4.36 (s, 2H, CH$_2$), 3.84 (s, 6H, CH$_3$), 3.71 (s, 6H, CH$_3$), 2.78 (q, 6H, CH$_3$), 1.43 (s, 9H, CH3$_2$), 1.22 (t, 9H, CH$_3$); ^{13}C NMR (75MHz, CDCl$_3$): 165.05, 157.48, 152.80, 147.54, 144.04,

132.77, 132.55, 126.92, 124.81, 122.92, 115.56, 79.77, 61.51, 56.28, 38.59, 28.65, 23.18, 16.75; HRMS-CI$^+$ m/z: calcd for $C_{38}H_{52}N_3O_8$: 678.375; obsd: 678.375

1-aminomethyl-3,5-N,N'-Bis(2,3-dimethoxybenzoyl)aminomethyl-2,4,6-triethylbenzene (4.8)
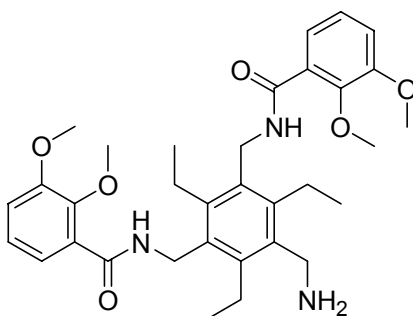
To a solution of **4.7** (0.087 g, 0.13 mmol) in 2 mL dichloromethane was added 2 mL trifluoroacetic acid, and the mixture was stirred at room temperature of two hours. The resulting salt was free based with a solution of sodium hydroxide (1 M) and the dichloromethane layer was dried with sodium sulfate. Upon solvent removal, the resulting solid was purified from any excess DCU present by running it through a silica gel column (1-2% ammonia saturated methanol in dichloromethane). (0.69 g, 93%) ^{1}H NMR (400MHz, CDCl$_3$): δ 7.77 (broad s, 2H, NH), 7.67 (d, 2H, Ar), 7.11 (t, 2H, Ar), 6.99 (d, 2H, Ar), 4.67 (s, 4H, CH$_2$), 3.89 (s, 2H, CH$_2$), 3.83 (s, 6H, CH$_3$), 3.69 (s, 6H, CH$_3$), 2.81 (m, 6H, CH$_3$), 1.59 (broad s, 2H, NH$_2$), 1.24 (m, 9H, CH$_3$); ^{13}C NMR (75MHz, CDCl$_3$): 165.05, 152.82, 147.59, 142.99, 137.86, 132.37, 127.03, 124.75, 122.92, 115.55, 61.48, 56.28, 39.88, 38.64, 23.03, 16.91; HRMS-CI$^+$ m/z: calcd for $C_{33}H_{44}N_3O_6$: 578.323; obsd: 578.323

1-(4,5-dihydro-N-(1,1-dimethylethoxy)carbonyl-imidazol-2-yl)aminomethyl-3,5-N,N'-Bis(2,3-dimethoxybenzoyl)aminomethyl-2,4,6-triethylbenzene (4.9)
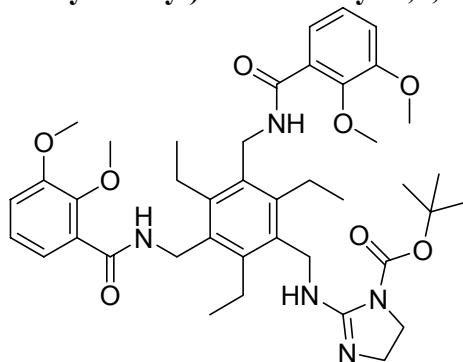
To a solution of **4.8** (0.067 g, 0.12 mmol) in ethanol (0.9 mL) was added 0.1 mL acetic acid and **2.12** (0.049 g, 0.228 mmol) and the mixture was heated to 60 °C for 10 hours. The solvent was removed and purification was accomplished by silica gel chromatography. (1-2% ammonia saturated methanol in dichloromethane). (0.071 g, 82%) ^{1}H NMR (300MHz, CDCl$_3$): δ 7.83 (broad s, 2H, NH), 7.66 (d, 2H, Ar), 7.11 (t, 2H, Ar), 6.99 (d, 2H, Ar), 4.66 (s, 4H, CH$_2$), 4.43 (s, 2H, CH$_2$), 3.80 (s, 6H, CH$_3$), 3.72 (m, 4H, CH$_2$), 3.66 (s, 6H, CH$_3$), 2.77 (q, 6H, CH$_3$), 1.41 (s, 9H, CH$_3$), 1.21 (t, 9H, CH$_3$); ^{13}C NMR (75MHz, CDCl$_3$): 165.07, 153.74, 152.83, 147.71, 144.20, 132.78, 132.49, 126.84, 124.65, 122.89, 115.66, 82.24, 61.41, 56.27, 48.91, 46.95, 41.11, 38.59, 28.38, 23.21, 16.77; HRMS-CI$^+$ m/z: calcd for C$_{41}$H$_{56}$N$_5$O$_8$: 746.413; obsd: 746.413

1-(4,5-dihydro-imidazol-2-yl)aminomethyl-3,5-N,N'-Bis(2,3-dihydroxybenzoyl)aminomethyl-2,4,6-triethylbenzene hydrobromide (4.10)
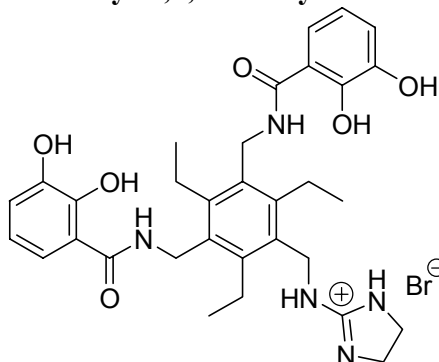
To a solution of **4.9** (0.071 g, 0.095 mmol) in dry dichloromethane (0 °C) was added boron tribromide in dichloromethane (2.5 mL, 2.5 mmol, 4.4 eq. per methoxy). The mixture was allowed to warm to room temperature and the reaction was allowed to proceed for 15 hours. Methanol was added to quench the reaction. The solvent was removed and methanol was added three more times in an attempt to remove $B(OCH_3)_3$. The resulting solid was washed by adding water and dichloromethane. The solid did not dissolve, but remained mostly in the water layer, such that the organic layer could be removed. The water layer was brought to a boil and cooled to room temperature, and the resulting precipitate was collected. (0.056 g, 93%). ^1H NMR (300MHz, CD_3OD): δ 8.14 (broad s, 2H, NH), 7.31 (d, 2H, Ar), 6.91 (d, 2H, Ar), 6.69 (t, 2H, Ar), 4.70 (s, 4H, CH_2), 4.46 (s, 2H, CH_2), 3.76 (s, 4H, CH_2), 2.93 (q, 2H, CH_3), 2.82 (q, 4H, CH_3), 1.22 (t, 9H, CH_3); ^{13}C NMR (75MHz, CD_3OD): 169.09, 159.69, 155.06, 147.97, 145.98, 144.53, 132.25, 129.67, 118.73, 118.42, 116.33, 43.03, 41.00, 37.93, 22.84, 15.45; HRMS-CI$^+$ m/z: calcd for $C_{32}H_{40}N_5O_6$: 590.298; obsd: 590.299

4.8 REFERENCES

(1)   Jackson, R. S. *Wine Science: Principles and Applications*; Academic Press: San Diego, 1994; Zoecklein, B. W.; Fugelsang, K. C.; Gump, B. H.; Nury, F. S. *Wine Analysis and Production*; Chapman and Hall: New York, 1995.

(2)   Palanché, T.; Marmolle, F.; Abdallah, M. A.; Shanzer, A.; Albrecht-Gary, A.-M. Fluorescent Siderophore-based Chemosensors: Iron(III) Quantitative Determinations. *J. Biol. Inorg. Chem.* **1999***, 4*, 188-198.

(3)   Scarrow, R. C.; Ecker, D. J.; Ng, C.; Liu, S.; Raymond, K. N. Iron(III) Coordination Chemistry of Linear Dihydroxyserine Compounds Derived from Enterobactin. *Inorg. Chem.* **1991***, 30*, 900-906.

(4)   Matsumoto, K.; Suzuki, N.; Ozawa, T.; Jitsukawa, K.; Masuda, H. Crystal Structure and Solution Behavior of the Iron(III) Complex of the Artificial Trihydroxamate Siderophore with a Tris(3-aminopropyl)amine Backbone. *Eur. J. Inorg. Chem.* **2001**, 2481-2484; Imbert, D.; Thomas, F.; Baret, P.; Serratrice, G.; Gaude, D.; Pierre, J.-L.; Laulhere, J.-P. Synthesis and iron(III) complexing ability of CacCAM, a new analog of enterobactin possessing a free carboxylic anchor arm. Comparative studies with TRENCAM. *New Journal of Chemistry* **2000***, 24*, 281-288.

(5)   Fages, F.; Bodenant, B.; Weil, T. Fluorescent, Siderophore-Based Chelators. Design and Synthesis of a Trispyrenyl Trishydroxamate Ligand, an Intramolecular Excimer-Forming Sensing Molecule Which Responds to Iron(III) and Gallium(III) Metal Cations. *J. Org. Chem.* **1996***, 61*, 3956-3961; Rodgers, S. J.; Ng, C. Y.; Raymond, K. N. High-Dilution Synthesis of Macrocyclic Polycatecholates. *J. Am. Chem. Soc.* **1985***, 107*, 4094-4095.

(6)   Stack, T. D. P.; Hou, Z.; Raymond, K. N. Rational Reduction of the Conformational Space of a Siderophore Analog through Nonbonded Interactions: The Role of Entropy in Enterobactin. *J. Am. Chem. Soc.* **1993***, 115*, 6466-6467.

(7)   Niikura, K.; Metzger, A.; Anslyn, E. V. Chemosensor Ensemble with Selectivity for Inositol-Trisphosphate. *J. Am. Chem. Soc.* **1998***, 120*, 8533-8534; Metzger, A.; Lynch, V. M.; Anslyn, E. V. A synthetic receptor

selective for citrate. *Angew. Chem., Int. Ed.* **1997***, 36*, 862-865; Lavigne, J. J.; Anslyn, E. V. Teaching old indicators new tricks: a colorimetric chenosensing ensemble for tartrate/malate in beverages. *Angew. Chem., Int. Ed.* **1999***, 38*, 3666-3669.

(8)   Albrecht, M.; Napp, M.; Schneider, M. The Synthesis of Amino Acid Bridged Dicatechol Derivatives. *Synthesis* **2001***, 3*, 468-472.

(9)   Karpishin, T. B.; Stack, T. D. P.; Raymond, K. N. Octahedral vs. Trigonal Prismatic Geometry in a Series of Catechol Macrobicyclic Ligand-Metal Complexes. *J. Am. Chem. Soc.* **1993***, 115*, 182-192.

(10)   Clauder, D. L.; Brückner, C.; Powers, R. E.; König, S.; Parac, T. N.; Leary, J. A.; Raymond, K. N. Design, Formation and Properties of Tetrahedral M4L4 and M4L6 Supramolecular Clusters. *J. Am. Chem. Soc.* **2001***, 123*, 8923-8938.

(11)   Mundla, S. R.; Wilson, L. J.; Klopfenstein, S. R.; Seibel, W. L.; Nikolaides, N. N. A novel method for the efficient synthesis of 2-arylamino-2-imidazolines. *Tetrahedron Lett.* **2000***, 41*, 6563-6566.

(12)   Connors, K. A. *Binding Constants, The Measurement of Molecular Stability*; Wiley: New York, 1987.

(13)   Hou, Z.; Stack, T. D. P.; Sunderland, C. J.; Raymond, K. N. Enhanced Iron(III) Chelation through Ligand Predisposition: Syntheses, Structures, and Stability of Tris-catecholate Enterobactin Analogs. *Inorg. Chim. Acta* **1997***, 263*, 341-355.

(14)   Aiet-Haddou, H.; Wiskur, S. L.; Lynch, V. M.; Anslyn, E. V. Achieving large color changes in response to the presence of amino acids: a molecular sensing ensemble with selectivity for aspartate. *Journal of the American Chemical Society* **2001***, 123*, 11296-11297; Zhong, Z.; Anslyn, E. V. Controlling the Oxygenation Level of Hemoglobin using a Synthetic Receptor for 2,3-Bisphosphoglycerate. *Nature* **2002**, Submitted.

Bibliography

Ait-Haddou H., Wiskur S. L., Lynch V. M., and Anslyn E. V. (2001) Achieving large color changes in response to the presence of amino acids: a molecular sensing ensemble with selectivity for aspartate. *J. Am. Chem. Soc.* **123**(45), 11296-11297.

Albrecht M., Napp M., and Schneider M. (2001) The Synthesis of Amino Acid Bridged Dicatechol Derivatives. *Synthesis* **3**, 468-472.

Altomare A., Cascarano G., Giacovazzo C., and Guagliardi A. (1993) Completion and Refinement of Crystal Structures SIR92. *J. Appl. Cryst.* **26**, 343-350.

Amendola V., Bastianello E., Fabbrizzi L., Mangano C., Pallavicini P., Perotti A., Lanfredi A. M., and Ugozzoli F. (2000) Halide-ion encapsulation by a flexible dicopper(II) bis-tren cryptate. *Angew. Chem., Int. Ed.* **39**(16), 2917-2920.

Antonisse M. M. G. and Reinhoudt D. N. (1998) Neutral Anion Receptors: Design and Application. *Chem. Commun.*, 443-448.

Aoyagi T., Nakamura A., Ikeda H., Ikeda T., Mihara H., and Ueno A. (1997) Alizarin Yellow-Modified -Cyclodextrin as a Guest-Responsive Absorption Change Sensor. *Anal. Chem.* **69**, 659-663.

Arimori S., Bell M. L., Oh C. S., and James T. D. (2002) A Modular Fluorescence Intramolecular Energy Transfer Saccharide Sensor. *Org. Lett.* **4**, 4249-4251.

Aucamp J. P., Hara Y., and Apostolides Z. (2000) Simultaneous Analysis of Tea Catechins, Caffeine, Gallic Acid, Theanine, and Ascorbic Acid by Micellar Electrokinetic Capillary Chromatography. *J. Chrom. A* **876**, 235-242.

Beer P. D. and Gale P. A. (2001) Anion Recognition and Sensing: The State of the Art and Future Perspectives. *Angew. Chem., Int. Ed.* **40**, 486-516.

229

Belcher R., Leonard M. A., and West T. S. (1958) The Preparation and Analytical Properties of N,N-Di(carboxy-methyl)aminomethyl Derivatives of Some Hydroxyanthraquinones. *J. Chem. Soc.*, 2390-2393.

Bell D. A., Diaz S. G., Lynch V. M., and Anslyn E. V. (1995a) An alcohol recognition motif: clear evidence of binding site cooperativity in the complexation of cyclohexanediols by neutral polyaza-clefts. *Tetrahedron Lett.* **36**(24), 4155-4158.

Bell T. W., Cragg P. J., Firestone A., Kwok A. D. I., Liu J., Ludwig R., and Sodoma A. (1998) Molecular Architecture 2. Synthesis and Metal Complexation of Heptacyclic Terpyridyl Molecular Clefts. *J. Org. Chem.* **63**(7), 2232-2243.

Bell T. W. and Hou Z. (1997) A Hydrogen-Bonding Receptor That Binds Urea with High Affinity. *Angew. Chem. Int. Ed.* **36**, 1536-1538.

Bell T. W., Hou Z., Luo Y., Drew M. G. B., Chapoteau E., Czech B. P., and Kumar A. (1995b) Detection of Creatinine by a Designed Receptor. *Science* **269**, 671-674.

Berger M. and Schmidtchen F. P. (1999) Zwitterionic Guanidinium Compounds Serve as Electroneutral Anion Hosts. *J. Am. Chem. Soc.* **121**(43), 9986-9993.

Berridge M. J. (1993) Inositol Trisphosphate and Calcium Signaling. *Nature* **361**, 315-325.

Bissell R. A., de Silva A. P., Gunaratne H. Q. N., Lynch P. L. M., Maguire G. E. M., McCoy C. P., and Sandanayake K. R. A. S. (1993) Fluorescent PET (Photoinduced Electron Transfer) Sensors. *Top. Curr. Chem.* **168**, 223-264.

Bissell R. A., de Silva A. P., Gunaratne H. Q. N., Lynch P. L. M., Maguire G. E. M., and Sandanayake K. R. A. S. (1992) Molecular Fluorescent Signaling with 'Fluor-Spacer-Receptor' Systems: Approaches to Sensing and Switching Devices via Supramolecular Photophysics. *Chem. Soc. Rev.* **21**, 187-195.

Bisson A. P., Lynch V. M., Monahan M.-K. C., and Anslyn E. V. (1997) Recognition of anions through NH-.pi. hydrogen bonds in a bicyclic cyclophane- selectivity for nitrate. *Angew. Chem., Int. Ed.* **36**(21), 2340-2342.

Bramhall J., Hofmann J., DeGuzman R., Montestruque S., and Schell R. (1987) Temperature Dependence of Membrane Ion Conductance Analyzed by Using the Amphiphilic Anion 5/6-Carboxyfluorescein. *Biochem.* **26**, 6330-6340.

Breslow R. and Zhang B. (1996) Cholesterol Recognition and Binding by Cyclodextrin Dimers. *J. Am. Chem. Soc.* **118**(35), 8495-8496.

Bronze M. R., Vilas Boas L. F., and Belchior A. P. (1997) Analysis of old brandy and oak extracts by capillary electrophoresis. *J. Chrom. A* **768**(1), 143-152.

Cabell L. A., Monahan M.-K., and Anslyn E. V. (1999) A competition assay for determining glucose-6-phosphate concentration with a Tris-boronic acid receptor. *Tetrahedron Lett.* **40**(44), 7753-7756.

Calderone C. T. and Williams D. H. (2001) An Enthalpic Component in Cooperativity: The Relationship between Enthalpy, Entropy, and Noncovalent Structure in Weak Associations. *J. Am. Chem. Soc.* **123**, 6262-6267.

Chen C.-T. and Huang W.-P. (2002) A Highly Selective Fluorescent Chemosensor for Lead Ions. *J. Am. Chem. Soc.* **124**, 6246-6247.

Cheng Y., Suenaga T., and Still W. C. (1996) Sequence-Selective Peptide Binding with a Peptido-A,B-trans-steroidal Receptor Selected from an Encoded Combinatorial Receptor Library. *J. Am. Chem. Soc.* **118**, 1813-1814.

Chin J., Walsdorff C., Stranix B., Oh J., Chung H. J., Park S.-M., and Kim K. (1999) A Rational Approach to Selective Recognition of NH4+ over K+. *Angew. Chem., Int. Ed.* **38**(18), 2756-2759.

Choi K. and Hamilton A. D. (2001) Selective Anion Binding by a Macrocycle with Convergent Hydrogen Bonding Functionality. *J. Am. Chem. Soc.* **123**, 2456 - 2457.

Clauder D. L., Brückner C., Powers R. E., König S., Parac T. N., Leary J. A., and Raymond K. N. (2001) Design, Formation and Properties of Tetrahedral M4L4 and M4L6 Supramolecular Clusters. *J. Am. Chem. Soc.* **123**, 8923-8938.

231

Connors K. A. (1987) *Binding Constants, The Measurement of Molecular Stability*. Wiley.

Corbin H. B. (1973) Rapid and selective pyrocatechol violet method for tin. *Anal. Chem.* **45**(3), 534-537.

Coteron J. M., Vicent C., Bosso C., and Penades S. (1993) Glycophanes, cyclodextrin-cyclophane hybrid receptors for apolar binding in aqueous solutions. A stereoselective carbohydrate-carbohydrate interaction in water. *J. Am. Chem. Soc.* **115**(22), 10066-10076.

Cram D. J. (1983) Cavitands: Organic Hosts with Enforced Cavities. *Science* **219**, 1177-1183.

Cram D. J. (1988) The Design of Molecular Hosts, Guests, and Their Complexes. *Science* **240**, 760-767.

Czarnik A. W. (1993) Supramolecular Chemistry, Fluorescence, and Sensing. In *Fluorescent Chemosensors for Ion and Molecule Recognition* (ed. A. W. Czarnik). American Chemical Society.

Czarnik A. W. (1994) Chemical Communication in Water using Fluorescent Chemosensors. *Acc. Chem. Res.* **27**, 302-308.

Davis A. P., Gilmer J. F., and Perry J. J. (1996) A steroid-based cryptand for halide anions. *Angew. Chem., Int. Ed.* **35**(12), 1312-1315.

Davis A. P. and Wareham R. S. (1999) Carbohydrate Recognition through Noncovalent Interactions: A Challenge for Biomimetic and Supramolecular Chemistry. *Angew. Chem., Int. Ed.* **38**, 2978-2996.

de Silva A. P., Gunaratne H. Q. N., Gunnlaugsson T., Huxley A. J. M., McCoy C. P., Rademacher J. T., and Rice T. E. (1997) Signaling Recognition Events with Fluorescent Sensors and Switches. *Chem. Rev.* **97**, 1515-1566.

Deetz M. J. and Smith B. D. (1998) Heteroditopic ruthenium(II) bipyridyl receptor with adjacent saccharide and phosphate binding sites. *Tetrahedron Lett.* **39**(38), 6841-6844.

Dietrich B., Fyles D. L., Fyles T. M., and Lehn J.-M. (1979) Anion Coordination Chemistry: Polyguanidinium Salts as Anion Complexones. *Helv. Chim. Acta* **62**, 2763-2787.

232

Dietrich B., Fyles T. M., Lehn J.-M., Pease L. G., and Fyles D. L. (1978) Anion Receptor Molecules. Synthesis and Some Anion Binding Properties of Macrocyclic Guanidinium Salts. *J. Chem. Soc., Chem. Commun.*, 934-936.

Easton C. J. and Lincoln S. F. (1999) *Modified Cyclodextrins, Scaffolds and Templates for Supramolecular Chemistry*. Imperial College Press.

Fabrizzi L., Leone A., and Taglietti A. (2001) A Chemosensing Ensemble for Selective Carbonate Detection in Water Based on Metal-Ligand Interactions. *Angew. Chem., Int. Ed.* **40**, 3066-3069.

Fages F., Bodenant B., and Weil T. (1996) Fluorescent, Siderophore-Based Chelators. Design and Synthesis of a Trispyrenyl Trishydroxamate Ligand, an Intramolecular Excimer-Forming Sensing Molecule Which Responds to Iron(III) and Gallium(III) Metal Cations. *J. Org. Chem.* **61**, 3956-3961.

Fitzmaurice R. J., Kyne G. M., Douheret D., and Kilburn J. D. (2002) Synthetic receptors for carboxylic acids and carboxylates. *J. Chem. Soc., Perkin Trans. 1*(7), 841-864.

Friedman S., Pace B., and Pizer R. (1974) Complexation of phenylboronic acid with lactic acid. Stability constant and reaction kinetics. *J. Am. Chem. Soc.* **96**(17), 5381-5384.

Friedman S. and Pizer R. (1975) Mechanism of the complexation of phenylboronic acid with oxalic acid. Reaction which requires ligand donor atom protonation. *J. Am. Chem. Soc.* **97**(21), 6059-6062.

Fröhlich J. (1999) Neural Net Overview, Vol. 2002.

Fujimoto T., Shimizu C., Hayashida O., and Aoyama Y. (1997) Solution-to-Surface Molecular-Delivery System Using a Macrocyclic Sugar Cluster. Sugar-Directed Adsorption of Guests in Water on Polar Solid Surfaces. *J. Am. Chem. Soc.* **119**(28), 6676-6677.

Furka A., Sebestyên F., Asgedom M., and Dibó G. (1991) General method for rapid synthesis of multicomponent peptide mixtures. *Int. J. Peptide Protein Res.* **37**, 487-493.

Gale P. A., Twyman L. J., Handlin C. I., and Sessler J. L. (1999) A Colourimetric Calix[4]pyrrole-4-nitrophenolate Based Anion Sensor. *Chem. Commun.*, 1851-1852.

Gershenson C. Artificial Neural Networks for Beginners, Vol. 2002. University of Sussex.

Goldberg D. M., Hoffman B., Yang J., and Soleas G. J. (1999) Phenolic constituents, furans, and total antioxidant status of distilled spirits. *J. Agric. Food Chem.* **47**(10), 3978-3985.

Gonzalez A. G., Herrador M. A., and Asuero A. G. (1991) Acid-Base Behavior of Some Substituted Azo Dyes in Aqueous N,N-dimethylformamide Mixtures. *Anal. Chim. Acta* **246**, 429-434.

Goodman M. S., Jubian V., Linton B., and Hamilton A. D. (1995) A Combinatorial Library Approach to Artificial Receptor Design. *J. Am. Chem. Soc.* **117**, 11610-11611.

Graber M. L., DiLillo D. C., Friedman B. L., and Pastoriza-Munoz E. (1986) Characteristics of Fluoroprobes for Measuring Intracellular pH. *Anal. Biochem* **156**, 202-212.

Gray C. W., Jr. and Houston T. A. (2002) Boronic Acid Receptors for .alpha.-Hydroxycarboxylates: High Affinity of Shinkai's Glucose Receptor for Tartrate. *J. Org. Chem.* **67**(15), 5426-5428.

Gunnlaugsson T., Bichell B., and Nolan C. (2002) A novel fluorescent photoinduced electron transfer (PET) sensor for lithium. *Tetrahedron Lett.* **43**(28), 4989-4992.

Haino T., Rudkevich D. M., Shivanyuk A., Rissanen K., and Rebek J. J. (2000) Induced-Fit Molecular Recognition with Water-Soluble Cavitands. *Chem. Eur. J.* **6**, 3797-3805.

Hanes R. E., Jr., Lavigne J. J., and Anslyn E. V. (2002) *Org. Syn.*, In preparation.

Hannon C. L. and Anslyn E. V. (1993) The guanidinium group: its biological role and synthetic analogs. *Bioorg. Chem. Front.* **3**, 193-255.

Hawkins R. T. and Blackham A. U. (1967) Reaction of o-(bromomethyl)benzeneboronic anhydride with primary amines. *J. Org. Chem.* **32**, 597-600.

Hawkins R. T. and Snyder H. R. (1960) Arylboronic Acids. VI. Aminoboronic Anhydrides and a New Heterocycle Containing Boron. *J. Am. Chem. Soc.* **82**, 3863-3866.

Hegde S. S., Dam T. K., Brewer C. F., and Blanchard J. S. (2002) Thermodynamics of Aminoglycoside and Acyl-Coenzyme A Binding to the Salmonella enterica AAC(6')-Iy Aminoglycoside N-Acetyltransferase. *Biochem.* **41**, 7519-7527.

Herrington J. and Steed K. C. (1960) Spectrophotometric Determination of the Rare Earths Yttrium and Cerium by Bromopyrogallol Red. *Anal. Chim. Acta* **22**, 180-184.

Hirano T., Kikuchi K., Urano Y., Higuchi T., and Nagano T. (2000) Highly Zinc-Selective Fluorescent Sensor Molecules Suitable for Biological Applications. *J. Am. Chem. Soc.* **122**, 12399-12400.

Hiratsuka T., 7442, 496. (1983) New ribose-modified fluorescent analogs of adenine and guanine nucleotides available as substrates for various enzymes. *Biochem. Biophys. Acta.* **742**, 496-508.

Hou Z., Stack T. D. P., Sunderland C. J., and Raymond K. N. (1997) Enhanced Iron(III) Chelation through Ligand Predisposition: Syntheses, Structures, and Stability of Tris-catecholate Enterobactin Analogs. *Inorg. Chim. Acta* **263**, 341-355.

Hubbard R. D., Horner S. R., and Miller B. L. (2001) Highly substituted ter-cyclopentanes as receptors for lipid A. *J. Am. Chem. Soc.* **123**(24), 5810-5811.

Hughes D. E. and Cardone M. J. (1980) Simultaneous titrimetric determination of bismuth ion and free nitric acid concentrations. *Anal. Chem.* **52**(6), 940-942.

Imbert D., Thomas F., Baret P., Serratrice G., Gaude D., Pierre J.-L., and Laulhere J.-P. (2000) Synthesis and iron(III) complexing ability of CacCAM, a new analog of enterobactin possessing a free carboxylic anchor arm. Comparative studies with TRENCAM. *New J. Chem.* **24**(5), 281-288.

Inouye M., Chiba J., and Nakazumi H. (1999) Glucopyranoside Recognition by Polypyridine-Macrocyclic Receptors Possessing a Wide Cavity with a Flexible Linkage. *J. Org. Chem.* **64**(22), 8170-8176.

Inouye M., Hashimoto K., and Isagawa K. (1994) Nondestructive Detection of Acetylcholine in Protic Media: Artificial-Signaling Acetylcholine Receptors. *J. Am. Chem. Soc.* **116**, 5517-5518.

Inouye M., Miyake T., Furusyo M., and Nakazumi H. (1995) Molecular Recognition of .beta.-Ribofuranosides by Synthetic Polypyridine-Macrocyclic Receptors. *J. Am. Chem. Soc.* **117**(50), 12416-12425.

Issa I. M., Issa R. M., Temerk Y. M., and Mahmoud M. R. (1973) Reduction of Azo-Compounds-I. Polarographic Behavior of Some 4-Hydroxy-monoazo Compounds at the Dropping Mercury Electrode. *Electrochim. Acta* **18**, 139-144.

Iverson D. J., Hunter G., Blount J. F., Damewood J. R., Jr., and Mislow K. (1981) Static and dynamic stereochemistry of hexaethylbenzene and of its tricarbonylchromium, tricarbonylmolybdenum, and dicarbonyl(triphenylphosphine)chromium complexes. *J. Am. Chem. Soc.* **103**(20), 6073-6083.

Jackson R. S. (1994) *Wine Science: Principles and Applications*. Academic Press.

James T. D., Sandanayake K. R. A. S., Iguchi R., and Shinkai S. (1995a) Novel Saccharide-Photoinduced Electron Transfer Sensors Based on the Interaction of Boronic Acid and Amine. *J. Am. Chem. Soc.* **117**(35), 8982-8987.

James T. D., Sandanayake K. R. A. S., and Shinkai S. (1994a) A glucose-specific molecular fluorescence sensor. *Angew. Chem.* **106**(21), 2287-2289.

James T. D., Sandanayake K. R. A. S., and Shinkai S. (1994b) Novel photoinduced electron-transfer sensor for saccharides based on the interaction of boronic acid and amine. *J. Chem. Soc., Chem. Commun.*(4), 477-478.

James T. D., Sandanayake K. R. A. S., and Shinkai S. (1995b) Chiral discrimination of monosaccharides using a fluorescent molecular sensor. *Nature* **374**, 345-347.

Jansson P. A. (1991) Neural Networks: An Overview. *Anal. Chem.* **63**, 357A-362A.

Jencks W. P. (1981) On the attribution and additivity of binding energies. *Proc. Natl. Acad. Sci.* **78**(7), 4046-4050.

Juillard J. and Geugue N. C. R. (1967) Sur La Dissociation de Quelques Acides Arylboriques en Solvants Mixtes Eau-Methanol. *Acad. Paris C* **264**, 259-261.

Karpishin T. B., Stack T. D. P., and Raymond K. N. (1993) Octahedral vs. Trigonal Prismatic Geometry in a Series of Catechol Macrobicyclic Ligand-Metal Complexes. *J. Am. Chem. Soc.* **115**, 182-192.

Katzin L. I. and Gulyas E. (1966) Optical rotatory dispersion studies on the borotartrate complexes and remarks on the aqueous chemistry of boric acid. *J. Am. Chem. Soc.* **88**(22), 5209-5212.

Kessler G. and Wolfman M. (1964) An Automated Procedure for the Simultaneous Determination of Calcium and Phosphorus. *Clin. Chem.* **10**, 686-703.

Kilway K. V. and Siegel J. S. (1992) Effects of Transition-Metal Complexation on the Stereodynamics of Persubstituted Arenes. Evidence for Steric Complementarity between Arene and Metal Tripod. *J. Am. Chem. Soc.* **114**, 255-261.

Kimura E., Sakonaka A., Yatsunami T., and Kodama M. (1981) Macromonocyclic polyamines as specific receptors for tricarboxylate-cycle anions. *J. Am. Chem. Soc.* **103**(3041-3045).

Kin S.-G. and Ahn K. H. (2000) Novel Artificial Receptors for Alkylammonium Ions with Remarkable Selectivity and Affinity. *Chem. Eur. J.* **6**, 3399-3403.

Klotz I. M. (1946) Spectrophotometric Investigations of the Interactions of Proteins with Organic Anions. *J. Am. Chem. Soc.* **68**, 2299-2304.

Klotz I. M., Triwush H., and Walker F. M. (1948) The Binding of Organic Ions by Proteins. Competition Phenomena and Denaturation Effects. *J. Am. Chem. Soc.* **70**, 2935-2941.

Koh K. N., Araki K., Ikeda A., Otsuka H., and Shinkai S. (1996) Reinvestigation of Calixarene-Based Artificial-Signaling Acetylcholine Receptors Useful in Neutral Aqueous (Water/Methanol) Solution. *J. Am. Chem. Soc.* **118**(4), 755-758.

Kral V., Rusin O., and Schmidtchen F. P. (2001) Novel Porphyrin-Cryptand Cyclic Systems: Receptors for Saccharide Recognition in Water. *Org. Lett.* **3**(6), 873-876.

Kustin K. and Pizer R. (1969) Temperature-jump study of the rate and mechanism of the boric acid-tartaric acid complexation. *J. Amer. Chem. Soc.* **91**(2), 317-322.

Lakowicz J. R. (1983) *Principles of Fluorescence Spectroscopy.* Plenum Press.

Lavigne J. J. (2000) Molecular Recognition and Molecular Sensing: Single Analyte Analysis and Multi-Component Sensor Arrays for the Simultaneous Detection of a Plethra of Analytes, University of Texas at Austin.

Lavigne J. J. and Anslyn E. V. (1999) Teaching old indicators new tricks: a colorimetric chenosensing ensemble for tartrate/malate in beverages. *Angew. Chem., Int. Ed.* **38**(24), 3666-3669.

Lavigne J. J., Savoy S., Clevenger M. B., Ritchie J. E., McDoniel B., Yoo S.-J., Anslyn E. V., McDevitt J. T., Shear J. B., and Neikirk D. (1998) Solution-Based Analysis of Multiple Analytes by a Sensor Array: Toward the Development of an \"Electronic Tongue\". *J. Am. Chem. Soc.* **120**(25), 6429-6430.

LeCun Y., Boser B., Denker J. S., Henderson D., Howard R. E., Hubbard W., and Jackel L. D. (1989) Back Propagation Applied to Handwritten Zip Code Recognition. *Neur. Comp.* **1**, 541-551.

Lehn J. M. (1988) Supramolecular Chemistry-Scope and Perspectives: Molecules - Supermolecules - Molecular Devices. *J. Incl. Phenom.* **6**, 351-396.

Lehn J.-M. (1978) Cryptates: The Chemistry of Macropolycyclic Inclusion Complexes. *Acc. Chem. Res.* **11**, 49-57.

Leonard M. A. and West T. S. (1960) Chelating Reactions of 1,2-Dihydroxyanthraquinon-3-ylmethyl-amine-N,N-diacetic Acid with Metal Cations in Aqueous Media. *J. Chem. Soc., Dalton Trans.*, 4477-4485.

Leucke H. and Quiocho F. A. (1990) High Specificity of a Phosphate Transport Protein Determined by Hydrogen Bonds. *Nature* **347**, 402-406.

Levitan I. B. and Kaczmarek L. K. (1997) *The Neuron.* Oxford University Press.

Lewis P. T., Davis C. J., Cabell L. A., He M., Read M. W., McCarroll M. E., and Strongin R. M. (2000) Visual sensing of saccharides promoted by resorcinol condensation products. *Org. Lett.* **2**(5), 589-592.

Lin J.-K., Lin C.-L., Liang Y.-C., Lin-Shiau S.-Y., and Juan I.-M. (1998) Survey of Catechins, Gallic Acid, and Methylxanthines in Green, Oolong, Pu-erh, and Black Teas. *J. Agric. Food Chem.* **46**, 3635-3642.

Linton B. and Hamilton A. D. (1997) Formation of Artificial Receptors by Metal-Templated Self Assembly. *Chem. Rev.* **97**, 1669-1680.

Linton B. and Hamilton A. D. (1999) Calorimetric investigation of guanidinium-carboxylate interactions. *Tetrahedron* **55**(19), 6027-6038.

Linton B. R., Goodman M. S., Fan E., Van Arman S. A., and Hamilton A. D. (2001) Thermodynamic Aspects of Dicarboxylate Recognition by Simple Artificial Receptors. *J. Org. Chem.* **66**(22), 7313-7319.

Liu L. and Guo Q.-X. (2002) The Driving Forces in the Inclusion Complexation of Cyclodextrins. *J. Incl. Phenom.* **42**, 1-14.

Lorand J. P. and Edwards J. O. (1959) Polyol complexes and structure of the benzeneboronate ion. *J. Org. Chem.* **24**, 769-774.

Mancilla T., Contreras R., and Wrackmeyer B. (1986) New bicyclic organylboronic esters derived from iminodiacetic acids. *J. Organomet. Chem.* **307**(1), 1-6.

Mangas J., Rodríguez R., Moreno J., Suárez B., and Blanco D. (1996) Evolution of Aromatic and Furanic Congeners in the Maturation of Cider Brandy: A Contribution to Its Characterization. *J. Agric. Food Chem.* **44**, 3303-3307.

Margolskee R. F. (1995) Receptor Mechanisms in Gustation. In *Handbook of Olfaction and Gustation* (ed. R. L. Doty), pp. 575-595. Marcel Dekker.

Martell A. E. and Motekaitis R. J. (1992) *Determination and Use of Stability Constants*. VCH Publishers, Inc.

Marx H.-W., Moulines F., Wagner T., and Astruc D. (1996) Hexakis(3-butynyl)benzene. *Angew. Chem., Int. Ed.* **35**(15), 1701-1704.

Matsumoto K., Suzuki N., Ozawa T., Jitsukawa K., and Masuda H. (2001) Crystal Structure and Solution Behavior of the Iron(III) Complex of the Artificial Trihydroxamate Siderophore with a Tris(3-aminopropyl)amine Backbone. *Eur. J. Inorg. Chem.*, 2481-2484.

McCulloch W. S. and Pitts W. (1943) A Logical Calculus of the Ideas Imminent in Nervous Activity. *Bull. Math.Biophys.* **5**, 115.

Metzger A. and Anslyn E. V. (1998) A chemosensor for citrate in beverages. *Angew. Chem., Int. Ed.* **37**(5), 649-652.

Metzger A., Gloe K., Stephan H., and Schmidtchen F. P. (1996) Molecular Recognition and Phase Transfer of Underivatized Amino Acids by a Foldable Artificial Host. *J. Org. Chem.* **61**(6), 2051-2055.

Metzger A., Lynch V. M., and Anslyn E. V. (1997) A synthetic receptor selective for citrate. *Angew. Chem., Int. Ed.* **36**(8), 862-865.

Mierson S. (1995) Transduction of Taste Stimuli by Receptor Cells in the Gustatory System. In *Handbook of Olfaction and Gustation* (ed. R. L. Doty), pp. 597-610. Marcel Dekker.

Miller I. J., Jr. (1995) Anatomy of the Peripheral Taste System. In *Handbook of Olfaction and Gustation* (ed. R. L. Doty), pp. 521-547. Marcel Dekker.

Mohler L. K. and Czarnik A. W. (1993).alpha.-Amino acid chelative complexation by an arylboronic acid. *J. Am. Chem. Soc.* **115**(15), 7037-7038.

Morales J. C., Zurita D., and Penades S. (1998) Carbohydrate-Carbohydrate Interactions in Water with Glycophanes as Model Systems. *J. Org. Chem.* **63**(25), 9212-9222.

Mundla S. R., Wilson L. J., Klopfenstein S. R., Seibel W. L., and Nikolaides N. N. (2000) A novel method for the efficient synthesis of 2-arylamino-2-imidazolines. *Tetrahedron Lett.* **41**(34), 6563-6566.

Nakatani H., Morita T., and Hiromi K. (1978) Substituent Effect on the Elementary Processes of the Interaction between Several Benzeneboronic Acids and Substilisin BPN. *Biochim. Biophys. Acta* **525**, 423-428.

Ng L. K., Lafontaine P., and Harnois J. (2000) Gas chromatographic-mass spectrometric analysis of acids and phenols in distilled alcohol beverages. Application of anion-exchange disk extraction combined with in-vial elution and silylation. *J. Chrom. A* **873**(1), 29-38.

Niikura K., Bisson A. P., and Anslyn E. V. (1999) Optical sensing of inorganic anions employing a synthetic receptor and ionic colorimetric dyes. *J. Chem. Soc., Perkin Trans. 2*(6), 1111-1114.

Niikura K., Metzger A., and Anslyn E. V. (1998) Chemosensor Ensemble with Selectivity for Inositol-Trisphosphate. *J. Am. Chem. Soc.* **120**(33), 8533-8534.

Norrild J. C. and Eggert H. (1996) Boronic acids as fructose sensors. Structure determination of the complexes involved using 1JCC coupling constants. *J. Chem. Soc., Perkin Trans. 2*(12), 2583-2588.

Noth H. and Wrackmeyer B. (1978) Nuclear Magnetic Resonance Spectroscopy of Boron Compounds. In *NMR Basic Principles and Progress*, Vol. 14 (ed. P. Diehl, E. Fluck, and R. Kosfeld), pp. 5-14, 287. Springer-Verlag.

Ohyoshi E. (1985) Spectrophotometric Study of Complexation Equilibria Involving a Metal and Colored and Buffer Ligands by the Competitive Effect of the Two Ligands. *Anal. Chem.* **57**, 446-448.

Otwinowski Z. and Minor W. (1997) Macromolecular crystallography. In *Methods in Enzymology*, Vol. 276 (ed. C. W. Carter and R. M. Sweet), pp. 307-326. Academic Press.

Palanché T., Marmolle F., Abdallah M. A., Shanzer A., and Albrecht-Gary A.-M. (1999) Fluorescent Siderophore-based Chemosensors: Iron(III) Quantitative Determinations. *J. Biol. Inorg. Chem.* **4**, 188-198.

Pedersen C. J. (1988) The Discovery of Crown Ethers. *Science* **241**, 536-540.

Perry M. J. (1995) The Role of Monoclonal Antibodies in the Advancement of Immunoassay Technology. In *Monoclonal Antibodies: Principles and Applications* (ed. J. R. Birch and E. S. Lennox), pp. 107-120. Wiley-Liss.

Pflugrath J. W. and Quiocho F. A. (1985) Sulphate Sequestered in the Sulphate-Binding Protein of Salmonella Typhimurium is Bound Solely by Hydrogen Bonds. *Nature* **314**, 257-260.

Potter B. V. L. and Lampe D. (1995) Chemistry of Inositol Lipid Mediated Cellular Signaling. *Angew. Chem., Int. Ed.* **34**, 1933-1972.

Raposo C., Mussons M. L., Caballero M. C., and Morán J. R. (1994) Readily Available Chromenone Receptors for Carboxylates. *Tetrahedron Lett.* **35**, 3409-3410.

Ray Sakar B. C. and Chauhan U. P. S. (1967) A New Method for Determining Micro Quantities of Calcium in Biological Materials. *Anal. Biochem.* **20**, 155-166.

Reichenback-Klinke R. and Konig B. (2002) Metal Complexes of Azacrown Ethers in Molecular Recognition and Catalysis. *J. Chem. Soc., Dalton Trans.*, 121-130.

Rekharsky M., Inoue Y., Tobey S. L., Metzger A., and Anslyn E. V. (2002) Ion-Pairing Molecular Recognition in Water: Aggregation at Low Concentrations That is Entropy Driven. *J. Am. Chem. Soc.*, Accepted.

Rodgers S. J., Ng C. Y., and Raymond K. N. (1985) High-Dilution Synthesis of Macrocyclic Polycatecholates. *J. Am. Chem. Soc.* **107**, 4094-4095.

Sandanayake K. R. A. and Shinkai S. (1994) Novel molecular sensors for saccharides based on the interaction of boronic acid and amines: saccharide sensing in neutral water. *J. Chem. Soc., Chem. Commun.*(9), 1083-1084.

Sanders J. K. M. (2000) Adventures in Molecular Recognition. The Ins and Outs of Templating. *Pure Appl. Chem.* **72**, 2265-2274.

Scarrow R. C., Ecker D. J., Ng C., Liu S., and Raymond K. N. (1991) Iron(III) Coordination Chemistry of Linear Dihydroxyserine Compounds Derived from Enterobactin. *Inorg. Chem.* **30**, 900-906.

Schauer C. L., Steemers F. J., and Walt D. R. (2001) A Cross-Reactive, Class Selective Enzymatic Array Assay. *J. Am. Chem. Soc.* **123**, 9443-9444.

Schiessl P. and Schmidtchen F. P. (1993) Abiotic molecular recognition of dicarboxylic anions in methanol. *Tetrahedron Lett.* **34**(15), 2449-2452.

Schmidtchen F. P. and Berger M. (1997) Artificial Organic Host Molecules for Anions. *Chem. Rev.* **97**, 1609-1646.

Schneider H.-J. (1991) Mechanisms of Molecular Recognition: Investigations of Organic Host-Guest Complexes. *Angew. Chem., Int. Ed.* **30**, 1417-1436.

Schneider S. E., O'Neil S. N., and Anslyn E. V. (2000) Coupling Rational Design with Libraries Leads to the Production of an ATP Selective Chemosensor. *J. Am. Chem. Soc.* **122**(3), 542-543.

Sebo L., Schweizer B., and Diederich F. (2000) Cleft-type diamidinium receptors for dicarboxylate binding in protic solvents. *Helv. Chim. Acta* **83**(1), 80-92.

Shallenberger R. S. (1993). In *Taste Chemistry*, pp. Chapter 1. Blankie Academic and Professional.

Snowden T. S. and Anslyn E. V. (1999) Anion Recognition: Synthetic Receptors for Anions and Their Application in Sensors. *Curr. Opin. Chem. Biol.* **3**, 740-746.

Spielman A. I., Brand J. G., and Kare M. R. (1991) *Encycl. Human Biol.*

Springsteen G. and Wang B. (2001) Alizarin Red S. as a general optical reporter for studying the binding of boronic acids with carbohydrates. *Chem. Commun.*(17), 1608-1609.

Springsteen G. and Wang B. (2002) A detailed examination of boronic acid-diol complexation. *Tetrahedron* **58**(26), 5291-5300.

Stack T. D. P., Hou Z., and Raymond K. N. (1993) Rational reduction of the conformational space of a siderophore analog through nonbonded interactions: the role of entropy in enterobactin. *J. Am. Chem. Soc.* **115**(14), 6466-6467.

Staudinger and Meyer. (1919) *Helv. Chim. Acta* **2**, 635.

Stergiou C. and Siganos D. Neural Networks, Vol. 2002. Imperial College, London.

Stoedeman M. and Wadsoe I. (1995) Scope of microcalorimetry in the area of macrocyclic chemistry. *Pure Appl. Chem.* **67**(7), 1059-1068.

Sukharevsky A. P., Read I., Linton B., Hamilton A. D., and Waldeck D. H. (1998) Experimental Measurements of Low-Frequency Intermolecular Host-Guest Dynamics. *J. Phy. Chem. B* **102**(27), 5394-5403.

Sun S., Fazal M. A., Roy B. C., Chandra B., and Mallik S. (2002) Thermodynamic Studies on the Recognition of Flexible Peptides by Transition-Metal Complexes. *Inorg. Chem.* **41**, 1584-1590.

Swaminathan C. P., Surolia N., and Surolia A. (1998) Role of Water in the Specific Binding of Mannose and Mannooligosaccharides to Concanavalin A. *J. Am. Chem. Soc.* **120**, 5153-5159.

Szejtli J. (1982) *Cyclodextrins and Their Inclusion Complexes*. Akadémiai Kiadó.

Takakusa H., Kikuchi K., Urano Y., Sakamoto S., Yamaguchi K., and Nagano T. (2002) Design and Synthesis of an Enzyme-Cleavable Sensor Molecule for Phosphodiesterase Activity Based on Fluorescence Resonance Energy Transfer. *J. Am. Chem. Soc.* **124**(8), 1653-1657.

Toyota S., Futawaka T., Asakura M., Ikeda H., and Oki M. (1998) Experimental and Theoretical Evidence of an SN2-Type Mechanism for Dissociation of B-N Coordination Bonds in 2,6-Bis((dimethylamino)methyl)phenylborane Derivatives. *Organomet.* **17**, 4155-4163.

Ueyama H., Takagi M., and Takenaka S. (2002) A Novel Potassium Sensing in Aqueous Media with a Synthetic Oligonucleotide Derivative. Fluorescence Resonance Energy Transfer Associated with Guanine Quartet-Potassium Ion Complex Formation. *J. Am. Chem. Soc.* **124**, ASAP.

Unob F., Asfari Z., and Vicens J. (1998) An anthracene-based fluorescent sensor for transition metal ions derived from calix[4]arene. *Tetrahedron Lett.* **39**(19), 2951-2954.

Wadsoe I. (1997) Trends in isothermal microcalorimetry. *Chem. Soc. Rev.* **26**(2), 79-86.

Wang W., Springsteen G., Gao S., and Wang B. (2000) The First Fluorescent Sensor for Boronic Acids and Boric Acids with Sensitivity at Sub-Micromolar Concentrations. *Chem. Commun.*, 1283-1284.

Ward C. J., Ashton P. R., James T. D., and Patel P. (2000) A molecular colour sensor for monosaccharides. *Chem. Commun.*(3), 229-230.

Wenz G. (1994) Cyclodextrins as Building Blocks for Supramolecular Structures and Functional Units. *Angew. Chem., Int. Ed.* **33**, 803-822.

Wiskur S. L., Ait-Haddou H., Lavigne J. J., and Anslyn E. V. (2001a) Teaching old indicators new tricks. *Acc. Chem. Res.* **34**(12), 963-972.

Wiskur S. L. and Anslyn E. V. (2001) Using a Synthetic Receptor to Create an Optical-Sensing Ensemble for a Class of Analytes: A Colorimetric Assay for the Aging of Scotch. *J. Am. Chem. Soc.* **123**(41), 10109-10110.

Wiskur S. L., Floriano P. N., Anslyn E. V., and McDevitt J. T. (2002) A Multi Component Sensing Ensemble in Solution: Differentiation Between very Structurally Similar Analytes. *Nature*, Submitted.

Wiskur S. L., Lavigne J. J., Ait-Haddou H., Lynch V., Chiu Y. H., Canary J. W., and Anslyn E. V. (2001b) pKa Values and Geometries of Secondary and Tertiary Amines Complexed to Boronic Acids-Implications for Sensor Design. *Org. Lett.* **3**(9), 1311-1314.

Wulff G. (1982) Selective binding to polymers via covalent bonds. The construction of chiral cavities as specific receptor sites. *Pure Appl. Chem.* **54**(11), 2093-2102.

Yoo S.-J., Lavigne J. J., Savoy S., McDoniel J. B., Anslyn E. V., McDevitt J. T., Neikirk D. P., and Shear J. B. (1997) Micromachined storage wells for chemical sensing beads in an "artificial tongue". *SPIEs Micromachining and Microfabrication 1996 Symposium: Micromachined Devices and Components III*.

Yoon J. and Czarnik A. W. (1992) Fluorescent Chemosensors of Carbohydrates. A Means of Chemically Communicating the Binding of Polyols in Water Based on Chelation-Enhanced Quenching. *J. Am. Chem. Soc.* **114**, 5874-5875.

Zhong Z. and Anslyn E. V. (2002) Controlling the Oxygenation Level of Hemoglobin using a Synthetic Receptor for 2,3-Bisphosphoglycerate. *Nature*, Submitted.

Zimmerman S. C. and Zeng Z. (1990) Improved binding of adenine by a synthetic receptor. *J. Org. Chem.* **55**(16), 4789-4791.

Zoecklein B. W., Fugelsang K. C., Gump B. H., and Nury F. S. (1995) *Wine Analysis and Production*. Chapman and Hall.

Zupan J. and Gasteiger J. (1991) Neural networks: a new method for solving chemical problems or just a passing phase? *Anal. Chim. Acta* **248**(1), 1-30.

Vita

Sheryl Lynn Wiskur was born in Flint, Michigan on April 8, 1974 to Mary Ann and Dale Wiskur. She lived her first twenty years in Columbiaville, Michigan and graduated LakeVille Memorial High School in 1992, fourth in her class. After high school, she entered college at the University of Michigan at Flint as part of the honors college. After the summer of 1994, she transferred to Arizona State University to complete her bachelors of science in chemistry in 1997 and became a member of the chemical fraternity Alpha Chi Sigma while there. During the next year she continued to do research at ASU, before entering graduate school at the University of Texas at Austin in the fall of 1998.

Permanent Address: 20410 HWY 1806, Ft. Pierre, South Dakota 57532

This dissertation was typed by Sheryl L. Wiskur.